

# The development of simplistic and cost-effective methods for the evaluation of tray and packed column efficiencies

*by*

Johannes Hendrik Lamprecht

Thesis presented in partial fulfilment  
of the requirements for the Degree



in the Faculty of Engineering  
at Stellenbosch University

*Supervisor*

Professor A.J Burger

March 2017



---

# DECLARATION

By submitting this thesis electronically, I declare that the entirety of the work contained therein is my own, original work, that I am the sole author thereof (save to the extent explicitly otherwise stated), that reproduction and publication thereof by Stellenbosch University will not infringe any third party rights and that I have not previously in its entirety or in part submitted it for obtaining any qualification.

DATE

*March 2017*



---

# ABSTRACT

Phase contacting column internals are manufactured through a series of punching, die moulding and bending. Although cost-effective on a large scale, this process is considered unfavourable for prototyping, as it is both time-consuming and expensive. This limits designer creativity and introduces extended waiting periods between the design, fabrication and evaluation phases. This translates into development timelines in excess of two years.

During the evaluation stage, efficiencies are conventionally measured using hydrocarbons system at total reflux. This introduces notable constraints on the prototype packing and tray material, due to the high temperatures and pressures required for these tests. Therefore, this research project focused on the development and experimental validation of two simplistic and cost effective methods that can be used to quantify column internal efficiency. The ADIBAA (aqueous desorption of isobutyl acetate in air) and HA (Humidification of air) methods are hereby proposed for efficiency measurements in packed and tray columns respectively. For validation of both methods, two separate pilot plant facilities were designed and constructed, one at Stellenbosch University and one at an industrial research laboratory.

The ADIBAA-method involved using a liquid phase limiting system to isolate the performance parameters in the liquid phase. The combination of the method and experimental setup offered rapid quantification, while remaining cost-effective and environmentally friendly. The ADIBAA-method was experimentally validated in a 400mm diameter stainless steel packed column, with a bed height of 1.1 metre. Such validation entailed (a) experimental measurement of isobutyl acetate concentrations, (b) calculation of volumetric liquid phase mass transfer coefficients and (c) comparison of these calculated coefficients with predictions by four independent correlations from literature. Agreement between the literature correlations and the newly-determined experimental data was found to be within 10%.

The applicability of the ADIBAA-method, in evaluating column internal efficiencies, was confirmed through comparison of 1.5' FlexiRings® and the equivalent Intalox® Ultra™. A quantifiable improvement of 15% was recorded in the preloading regime, in favour of the Intalox® Ultra™. Further justification of the ADIBAA-method was presented in the evaluation of 2.5' Intalox® Ultra™ packing.

The HA-method, proposed to use for tray columns, focused on the evaluation of Murphree tray efficiencies. This method offered large improvements over the constant reflux method in terms of environmental and safety considerations, while also reducing the experimental time by an order of magnitude. A rectangular tray column with respective weir and flow path lengths of 762mm and 870mm was used in the experimental evaluation.

The HA-method was found to adequately quantify hydrodynamic variations in both weeping and vapour bypass. The comparative ability of the method was experimentally verified by relating a 12% open area

sieve tray with two separate prototypes. The method enabled rapid evaluation and quantitatively illustrated difference in efficiencies between the prototypes.

From this research, it follows that the ADIBAA- and HA- methods can indeed be used as cost-effective, simple and time-efficient methods to evaluate prospective designs of random packing and trays.

---

# SAMEVATTING

Distillasie-kolomme word industrieel vervaardig deur 'n kombinasie van buig- en ponsgreedskap. Alhoewel hierdie metodes koste-effektief is vir grootskaalse produksie, bied dit struikelblokke vir die ontwerpproses. Dit is onder meer omdat die ontwikkeling van die gereedskap en produksielyn beide tydrowend en kapitaalintensief is. Die beperkende vervaardigingstegnieke is daarvolgens geïdentifiseer as 'n moontlike knelpunt in die ontwikkeling van nuwe plate en pakking.

Massa-oordrageffektiwiteit word tradisioneel geëvalueer met behulp van koolwaterstof-oplossings in 'n konstante-terugvloei-distillasiekolom. Dié metingsmetode vereis hoë temperatuur en druk, tesame met die gebruik van gevaarlike oplosmiddels. Daarvolgens word die gebruik van moderne en versnelde vervaardigingstegnieke grootliks ingekamp. Hierdie navorsingsprojek het dus gefokus op die ontwikkeling en eksperimentele validering van vereenvoudigde en bekostigbare alternatiewe metingsmetodes vir beide gepakte- en plaatkolomme. Die ADIBAA- (selektiewe verdamping van isobutielasetaat in lug) en die HA-metodes (verdamping van water in lug) is gevolglik ontwikkel vir gebruik in onderskeidelik gepakte- en plaatkolomme.

Die ADIBAA metode fokus op die kwantifisering van vloeistoffase-mass-oordrag-koëffisiënte. Dié metode word voorgestel in stede van tradisionele konstante-terugvloei-distillasie weens spoedige kwantifisering, kostebesparings en omgewingsvriendelikhed. Die ADIBAA-metode is eksperimenteel gevalideer in 'n 400 mm-deursneekolom met 'n gepakte bedhoogte van 1,1 m. Die ooreenstemming tussen literatuur- en eksperimentele waardes was in die orde van 10%.

Die bruikbaarheid van die ADIBAA-metode is bevestig deur die vergelyking van 1.5' FlexiRings® met die ooreenstemmende Intalox® Ultra™ pakking. Daarvolgens is kwantifiseerbare verbeterings in die orde van 15% opgemerk, ten gunste van die laasgenoemde.

In die geval van die plaatkolom is die isotermiese verdamping van water in lug gebruik ter kwantifisering van Murphree-plaat-effektiwiteite. Eksperimentele data is daarvolgens ingesamel in 'n reghoekige kolom met dimensies van 762 mm by 870 mm. Die voordele van dié metode sluit onder meer koste- en tydbesparing sowel as aansienlik verminderde veiligheidsrisiko's in.

Ter vergelyking van verskillende ontwerpe op grond van die metode, is bevind dat genoemde onderskeid in Murphree-plaat -effektieweite gesien kon word. Kwantitatief is verbeteringe tot en met 10% waargeneem gedurende die eksperimentele vergelyking van 'n 12% oop-area-sifplaat en 'n alternatiewe prototipe.

In die lig van dié bevindinge word beide die ADIBAA- en die HA-metodes voorgestel vir gebruik tydens die aanvanklike ontwerpproses waar spoedige resultate benodig word. Die gebruik daarvan belooft om die ontwerpproses aansienlik te verkort, aangesien die prototipes nie meer aan die tradisionele vervaardigingstechnieke onderhewig is nie.



---

# TABLE OF CONTENTS

<b>Declaration .....</b>	<b>iii</b>
<b>Abstract .....</b>	<b>v</b>
<b>List of Figures .....</b>	<b>xiii</b>
<b>List of Tables.....</b>	<b>xix</b>
<b>Glossary .....</b>	<b>xxi</b>
Greek Symbols.....	xxv
Dimensionless Numbers .....	xxv
Column Flow Definitions .....	xxvi
<b>CHAPTER 1: Introduction and Project Outline.....</b>	<b>1</b>
1.1. Mass Transfer in Column Design.....	1
1.2. Efficiency Quantification .....	2
1.3. Industrial Relevance of Proposed Work.....	2
1.4. Aims of this Study .....	3
<b>CHAPTER 2: Background on Column Internals.....</b>	<b>5</b>
2.1. Tray Columns .....	5
2.1.1. Tray Types.....	6
2.2. Packed Columns .....	7
2.2.1. Random Packing.....	7
2.2.2. Structured Packing.....	8
2.3. Trays versus Packing.....	9
<b>CHAPTER 3: Mass Transfer Literature.....</b>	<b>11</b>
3.1. Gas-Liquid Mass Transfer .....	12
3.2. Summary.....	14
<b>CHAPTER 4: Packed Column Mass Transfer Literature .....</b>	<b>15</b>
4.1. Predictive Correlations .....	15
4.1.1. Volumetric Mass Transfer Coefficient in the Liquid Phase .....	15
4.1.2. Liquid Side Mass Transfer Correlations and Effective Interfacial Area .....	17
4.1.3. Models chosen for validation .....	20

4.2.	Historic Experimental Evaluation of the Volumetric Liquid Mass Transfer Coefficient.....	21
4.3.	Translating the Liquid Mass Transfer Coefficient into Packed Column Efficiency .....	22
4.3.1.	Transfer Unit Approach (NTU).....	22
4.3.2.	Column Efficiency.....	25
4.4.	Concluding Remarks on Liquid Phase Volumetric Mass Transfer Measurements .....	26
<b>CHAPTER 5: Tray Column Literature .....</b>		<b>29</b>
5.1.	Liquid versus Vapour Mass Transfer Limiting .....	29
5.2.	Vapour Phase Predictive Correlations .....	30
5.2.1.	Vapour NTU Models.....	30
5.2.2.	Vapour Side Mass Transfer and Effective interfacial Area Correlations .....	32
5.2.3.	Concluding remarks on the predictive correlations .....	36
5.3.	Historic Experimental Evaluation of Mass Transfer in Tray Columns .....	37
5.4.	Tray Column NTU Method .....	38
5.5.	Tray Column Efficiency .....	39
5.5.1.	Relating Murphree Point Efficiencies to NTU Approach .....	40
5.5.2.	Relating Point Efficiencies to Colum Design.....	43
5.6.	Concluding Remarks on Tray Column Literature .....	45
<b>CHAPTER 6: Materials and Methods.....</b>		<b>49</b>
6.1.	Liquid Phase Mass Transfer: Method development .....	49
6.1.1.	Solute Considerations .....	49
6.1.2.	Liquid Phase Quantification .....	51
6.2.	Vapour Mass Transfer: Method development .....	51
6.3.	Method Procedures .....	52
6.4.	Design Considerations.....	55
6.4.1.	Packed Column.....	55
6.4.2.	Tray Column.....	55
6.5.	Experimental Setup .....	57
6.5.1.	Packed Column.....	57
6.5.2.	Tray Column.....	63

6.6.	Experimental Design .....	68
6.6.1.	Random Packed Column .....	68
6.6.2.	Tray Column.....	69
6.7.	Error Analysis.....	69
6.7.1.	Variability in Composition Quantification: Packed Column.....	70
6.7.2.	Variability in Composition Quantification: Tray Column.....	71
6.7.3.	Hydrodynamic and Atmospheric Variability: Packed Column .....	71
6.7.4.	Hydrodynamic and Atmospheric Variability: Tray Column .....	71
<b>CHAPTER 7: Results and Discussion .....</b>		<b>74</b>
7.1.	Packed Column Liquid Phase Evaluation .....	74
7.1.1.	Method Validation.....	74
7.1.2.	Repeatability.....	75
7.1.3.	Comparing Column Internals on Liquid Phase Mass Transfer.....	76
7.1.4.	Evaluation of Mass Transfer Coefficients .....	86
7.1.5.	Concluding Remarks on the ADIBAA-Method .....	88
7.2.	Tray Column Vapour Phase Evaluation .....	89
7.2.1.	Validation of HA-Method .....	89
7.2.2.	Predictive Correlations: Point efficiency.....	94
7.2.3.	Using the HA-Method in Tray Prototyping.....	97
7.2.4.	Extending the HA-method to Column Design.....	105
<b>CHAPTER 8: Conclusion and Recommendations .....</b>		<b>114</b>
8.1.	Packed Column Efficiency Alternative: ADIBAA-Method.....	114
8.2.	Tray Column Efficiency Alternative: HA-Method.....	116
8.3.	Final Conclusions .....	117
8.4.	Recommendations for future work.....	117
8.4.1.	Packed Columns .....	117
8.4.2.	Tray Columns .....	118
<b>References .....</b>		<b>120</b>
<b>CHAPTER 9: Appendices .....</b>		<b>142</b>

9.1.	Packed Columns .....	142
9.1.1.	Correlation Discussion: Volumetric Liquid Mass Transfer Coefficient.....	142
9.1.2.	Correlation Discussion: The Liquid Mass Transfer Coefficient.....	143
9.1.3.	Summary of Evaluated Literature: Volumetric Liquid Mass Transfer Coefficient.....	145
9.1.4.	Chemical Regression .....	148
9.1.5.	Packed Column Design: Mechanical Design .....	160
9.1.6.	Packed Venturi Calibration .....	165
9.1.7.	Bed Pressure Drop Validation .....	167
9.1.8.	UV Quantification .....	168
9.1.9.	Packed Column Results in Vapour flow factors.....	173
9.2.	Appendix B: Tray Columns.....	178
9.2.1.	Concentration Profiles Below the Test Tray .....	178
9.2.2.	Tray column Design: Bubble Promotor Schematic .....	179
9.3.	Appendix C: Supplementary Considerations .....	180
9.3.1.	Hofhuis and Zuiderweg [6] Graphical Illustration (redrawn from original paper).....	180
9.3.2.	Theoretical Considerations Related to the Mass Transfer Coefficient .....	181
9.3.3.	Tray Column $K_L a$ Correlations.....	182

---

# LIST OF FIGURES

Figure 3.1: Schematic of mass transfer from the bulk liquid to the vapour. redrawn from Henley [4].....	12
Figure 4.1: Graphical illustration of the number of transfer units .....	23
Figure 4.2: Differential packed column analysis (redrawn from Cussler [24]).....	23
Figure 5.1: Percentage liquid phase resistance in tray columns redrawn from Lockett [16].....	29
Figure 5.2: Differential schematic for a tray column redrawn from Lockett [18].....	38
Figure 5.3: Schematic of different efficiencies. 5.3A Depicts the Murphree tray efficiencies. 5.3B Presents Murphree point efficiencies. adapted from Lockett [18] .....	39
Figure 5.4: Models relating point efficiencies to NTU.....	42
Figure 5.5: Effect of interfacial area on point efficiencies. ....	42
Figure 5.6: Lewis case representation, illustrating the concentration profiles above and below the evaluated trays.....	43
Figure 5.7: Comparison between AIChE model and Ashley data.....	46
Figure 5.8: Sensitivity analysis of operating temperature. ....	47
Figure 6.1: Regression flow diagram. ....	50
Figure 6.2: ADIBAA - Method flow diagram and calculation procedure.....	53
Figure 6.3: HA – Method flow diagram and calculation procedure.....	54
Figure 6.4: Packed column design: Inventor model.....	56
Figure 6.5: Random packing experimental setup. ....	61
Figure 6.6: Isobutyl acetate spectrum scan using the UV-VIS spectrophotometer. ....	62
Figure 6.7: Schematic of tray column parameters .....	65
Figure 6.8: Experimental setup for tray column.....	67
Figure 6.9: Isobutyl acetate error scan using UV-VIS spectrophotometer.....	70
Figure 7.1: Packed column experimental verification: literature model comparison with own Data.....	74

Figure 7.2: Verification of experimental data with the Onda [19] model. ....	75
Figure 7.3: Experimental repeatability of the packed column data across varying liquid flow rates. ....	76
Figure 7.4: HETP comparison of 1.5' FlexiRings® and Intalox® Ultra™ (6 to 23.9 m <sup>3</sup> .m <sup>-2</sup> .h <sup>-1</sup> ). ....	77
Figure 7.5: HETP comparison of 1.5' FlexiRings® and Intalox® Ultra™ (36 to 47 m <sup>3</sup> .m <sup>-2</sup> .h <sup>-1</sup> ). ....	78
Figure 7.6: HETP comparison between 1.5' FlexiRings® and Intalox® Ultra™ (72 to 96 m <sup>3</sup> .m <sup>-2</sup> .h <sup>-1</sup> ). ....	78
Figure 7.7: HETP comparison of 1.5' and 2.5' Intalox® Ultra™ (6 m <sup>3</sup> .m <sup>-2</sup> .h <sup>-1</sup> ).....	79
Figure 7.8: HETP comparison of 1.5' and 2.5' Intalox® Ultra™ (11.9 m <sup>3</sup> .m <sup>-2</sup> .h <sup>-1</sup> ).....	80
Figure 7.9: HETP comparison of 1.5' and 2.5' Intalox® Ultra™ (23.9 m <sup>3</sup> .m <sup>-2</sup> .h <sup>-1</sup> ).....	80
Figure 7.10: HETP comparison of 1.5' and 2.5' Intalox® Ultra™ (36 m <sup>3</sup> .m <sup>-2</sup> .h <sup>-1</sup> ).....	81
Figure 7.11: HETP comparison of 1.5' and 2.5' Intalox® Ultra™ (47 m <sup>3</sup> .m <sup>-2</sup> .h <sup>-1</sup> ).....	81
Figure 7.12: HETP comparison of 1.5' and 2.5' Intalox® Ultra™ (72 m <sup>3</sup> .m <sup>-2</sup> .h <sup>-1</sup> ).....	82
Figure 7.13: Non-oscillatory behaviour.....	83
Figure 7.14: Oscillatory behaviour.....	83
Figure 7.15: HETP comparison of 1.5', 2' and 2.5' Intalox® Ultra™ (23.9 m <sup>3</sup> .m <sup>-2</sup> .h <sup>-1</sup> ), with reference to flooding velocity. ....	83
Figure 7.16: HETP comparison of 1.5' and 2.5' Intalox® Ultra™ (47 m <sup>3</sup> .m <sup>-2</sup> .h <sup>-1</sup> ), with reference to flooding velocity. ....	84
Figure 7.17: HETP comparison of 1.5' and 2.5' Intalox® Ultra™ (36 m <sup>3</sup> .m <sup>-2</sup> .h <sup>-1</sup> ), with reference to flooding velocity. ....	84
Figure 7.18: Volumetric liquid phase mass transfer coefficients for FlexiRing®; 1.5' vs. 2' .....	87
Figure 7.19: Volumetric liquid phase mass transfer coefficients for 1.5' Intalox® Ultra™ Packing vs 2' Flexiring®.....	87
Figure 7.20: Volumetric liquid phase mass transfer coefficients for 2.5' Intalox® Ultra™ Packing Vs. 2' Flexiring®.....	88

Figure 7.21: Sieve tray parameter clarification .....	90
Figure 7.22: Tray column repeatability, evaluated over 2 independent sieve tray runs at 122 m <sup>3</sup> .m <sup>-2</sup> .h <sup>-1</sup> . .....	91
Figure 7.23: Comparison of FRI data with sieve tray experimental data -61 m <sup>3</sup> .m <sup>-2</sup> .h <sup>-1</sup> over varying capacity factors.....	93
Figure 7.24: Comparison of FRI data with sieve tray experimental data -122 m <sup>3</sup> .m <sup>-2</sup> .h <sup>-1</sup> over varying capacity factors.....	93
Figure 7.25: Comparison of FRI data with sieve tray experimental data - 183 m <sup>3</sup> .m <sup>-2</sup> .h <sup>-1</sup> over varying capacity factors.....	94
Figure 7.26: Literature point efficiency models compared with own data (61 m <sup>3</sup> .m <sup>-2</sup> .h <sup>-1</sup> ) over varying capacity factors.....	95
Figure 7.27: Literature point efficiency models compared with own data (122 m <sup>3</sup> .m <sup>-2</sup> .h <sup>-1</sup> ) over varying capacity factors.....	96
Figure 7.28: Literature point efficiency models compared with own data (183 m <sup>3</sup> .m <sup>-2</sup> .h <sup>-1</sup> ) over varying capacity factors.....	96
Figure 7.29: Efficiency and weeping comparison of prototype ‘A’ with a 12% Open Sieve Tray; at 12 m <sup>3</sup> .m <sup>-2</sup> .h <sup>-1</sup> . over varying capacity factors.....	98
Figure 7.30: Positional weeping with increase vapour loading on a conventional sieve tray with a bubble promotor.....	99
Figure 7.31: Efficiency and Weeping comparison of prototype ‘B’ with a 12% Open Sieve Tray- at 61 m <sup>3</sup> .m <sup>-2</sup> .h <sup>-1</sup> over varying capacity factors.....	100
Figure 7.32: Efficiency and Weeping comparison of prototype ‘B’ with a 12% Open Sieve Tray- at 122 m <sup>3</sup> .m <sup>-2</sup> .h <sup>-1</sup> over varying capacity factors. ....	101
Figure 7.33: Efficiency and Weeping comparison of prototype ‘B’ with a 12% Open Sieve Tray- at 183 m <sup>3</sup> .m <sup>-2</sup> .h <sup>-1</sup> over varying capacity factors.....	101
Figure 7.34: Sieve trays vs valve trays under high vapour loads. ....	102
Figure 7.35: Efficiency comparison of Prototype B and sieve tray 61 m <sup>3</sup> .m <sup>-2</sup> .h <sup>-1</sup> vs. pressure drop.....	103

Figure 7.36: Efficiency comparison of Prototype B and sieve tray at $122 \text{ m}^3 \cdot \text{m}^{-2} \cdot \text{h}^{-1}$ vs. pressure Drop.....	104
Figure 7.37: Efficiency comparison of Prototype B and sieve tray $183 \text{ m}^3 \cdot \text{m}^{-2} \cdot \text{h}^{-1}$ vs. pressure drop.....	104
Figure 7.38: Effect of liquid Flow on vapour entrapment in a tray column .....	106
Figure 7.39: Concentration profiles above the testing tray for a liquid loading of $61 \text{ m}^3 \cdot \text{m}^{-2} \cdot \text{h}^{-1}$ .....	107
Figure 7.40: Concentration profiles above the testing tray for a liquid loading of $122 \text{ m}^3 \cdot \text{m}^{-2} \cdot \text{h}^{-1}$ .....	108
Figure 7.41: Concentration profiles above the testing tray for a liquid loading of $183 \text{ m}^3 \cdot \text{m}^{-2} \cdot \text{h}^{-1}$ .....	108
Figure 7.42: Hypothetical case 1; low liquid loading.....	109
Figure 7.43: Hypothetical case 2; medium liquid loading.....	109
Figure 7.44: Hypothetical case 3; high liquid loading.....	109
Figure 7.45: Parity evaluation of the Lewis approximation of point efficient and the experimental sieve tray data. ....	111
Figure 7.46: Parity evaluation of the Lewis approximation of point efficient and the experimental Prototype B data.....	111
Figure 9.1: Aqueous hood behaviour. ....	160
Figure 9.2: Chimney vapour distributor. ....	161
Figure 9.3: Liquid sampling. ....	161
Figure 9.4: Holdup-grid.....	162
Figure 9.5: Plc main screen. ....	164
Figure 9.6: Pitot tube pressure drop validation by way of water manometer.....	165
Figure 9.7: Pressure drop readings across a full pipe section.....	166
Figure 9.8: Bed Pressure Drop Validation.....	167
Figure 9.9: Calibration curve for cell 1. ....	168
Figure 9.10: Calibration curve for cell 2. ....	169



Figure 9.11: Inlet concentration; water baseline correction for 25.6°C-23°C.....	170
Figure 9.12: Inlet concentration: water baseline correction for 23°C-20.5°C.....	170
Figure 9.13: Inlet concentration: water baseline correction for 20.5°C-19°C.....	171
Figure 9.14: Outlet concentration: water baseline correction for 25°C-22°C.....	171
Figure 9.15: Outlet concentration: water baseline correction for 22°C-20.4°C.....	172
Figure 9.16: Outlet concentration: water baseline correction for 20.4°C-19.4°C.....	172
Figure 9.17: Figure 7.4 in terms of vapour flow factors.....	173
Figure 9.18: Figure 7.5 in terms of vapour flow factors.....	173
Figure 9.19: Figure 7.6 in terms of vapour flow factors.....	174
Figure 9.20: Figure 7.7 in terms of vapour flow factors.....	174
Figure 9.21: Figure 7.8 in terms of vapour flow factors.....	175
Figure 9.22: Figure 7.9 in terms of vapour flow factors.....	175
Figure 9.23: Figure 7.10 in terms of vapour flow factors.....	176
Figure 9.24: Figure 7.11 in terms of vapour flow factors.....	176
Figure 9.25: Figure 7.12 in terms of vapour flow factors.....	177
Figure 9.26: Concentration profile below the test tray .....	178
Figure 9.27: Example of a bubble promotor.....	179
Figure 9.28: Tray flow regimes (redrawn Hofhuis and Zuiderweg [6]).....	180



---

# LIST OF TABLES

Table 2.1: Random packings according to generation (Lamprecht [9] and Erasmus [3]) [7, 12].....	8
Table 2.2: Generational evaluation of structured packing [9] [3] [7, 12].....	9
Table 2.3: Considerations for choosing between trays or packing [14, 15]. .....	10
Table 4.1: Correlations for the estimation of the volumetric mass transfer coefficient in packed columns. ....	16
Table 4.2: Predictive correlations for the effective interfacial area and liquid side mass transfer coefficient. ....	18
Table 4.3: Perceived influence of surface tension. ....	20
Table 4.4: Literature systems experimentally evaluating liquid phase mass transfer coefficients.....	21
Table 4.5: Packings and materials of construction used in Table 4.4.....	22
Table 5.1: Correlations for the prediction vapour phase transfer units (NTU).....	31
Table 5.2: Predictive correlations for both vapour mass transfer coefficient and effective interfacial area within tray columns. ....	33
Table 5.3: historic Tray columns experimental evaluations. ....	37
Table 6.1: Tray column design detail. ....	64
Table 6.2: Packed column Liquid composition measurement variability (UV-Vis-spectrophotometer). ....	71
Table 6.3: Packed column normalized errors for hydrodynamic measurements.....	71
Table 6.4: Tray column normalized standard deviations for hydrodynamic measurements. ....	72
Table 7.1: Sieve Tray parameters. ....	89
Table 9.1: Summary of evaluated literature. ....	145
Table 9.2: Summary of evaluated literature continued.....	146
Table 9.3: Column internals related to the literature evaluations. ....	147
Table 9.4: Table 10.3 continued. ....	148

Table 9.5: Regression of systems experimentally proven to exhibit liquid phase mass transfer limiting behaviour. ....	150
Table 9.6: Evaluated chemicals. ....	152
Table 9.7: Open area grid modelling. ....	163
Table 9.8: Venturi friction coefficient. ....	167
Table 9.9: Theoretical evaluation of the liquid phase mass transfer coefficient. ....	181
Table 9.10: Correlations for the prediction of $k_{La}$ in tray columns. ....	182

# GLOSSARY

Symbol	Description	Units
<b>A</b>	Absorption factor	
<b>a<sub>e</sub></b>	Effective interfacial mass transfer area	m <sup>2</sup> or m <sup>2</sup> /m <sup>3</sup>
<b>a<sub>G</sub></b>	Effective vapour area	m <sup>2</sup> /m <sup>3</sup>
<b>a<sub>L</sub></b>	Effective liquid area	m <sup>2</sup> /m <sup>3</sup>
<b>a<sub>p</sub></b>	Geometric area of packing, as stated by manufacturers	m <sup>2</sup> /m <sup>3</sup>
<b>a<sub>w</sub></b>	Wetted geometric area of packing	m <sup>2</sup> /m <sup>3</sup>
<b>C<sub>1</sub></b>	Regressed packing specific parameter	
<b>C<sub>i,L</sub></b>	Concentration of component i in the liquid phase	mol /m <sup>3</sup>
<b>C<sub>i,I</sub></b>	Concentration of component i at the interface	mol /m <sup>3</sup>
<b>C<sub>i</sub><sup>*</sup></b>	Equilibrium concentration of component i	mol/m <sup>3</sup>
<b>c<sub>i,1</sub></b>	Concentration of solute at the inlet	g/m <sup>3</sup>
<b>c<sub>i,2</sub></b>	Concentration of solute at the outlet	g/m <sup>3</sup>
<b>d<sub>1</sub></b>	Regressed parameter for Linek equations	-
<b>d<sub>2</sub></b>	Regressed parameter for Linek equations	-
<b>d<sub>32L</sub></b>	Sauter mean bubble diameter of large bubbles	m
<b>d<sub>32S</sub></b>	Sauter mean bubble diameter of small bubbles	m
<b>De<sub>G</sub></b>	Eddie diffusivity of vapour mixing	m <sup>2</sup> /s
<b>d<sub>h</sub></b>	Hydraulic diameter of dumped packing	m
<b>D<sub>i,L</sub></b>	Liquid phase diffusivity of component i	m <sup>2</sup> /s
<b>d<sub>p</sub></b>	Diameter of packing	m
<b>E<sub>B</sub></b>	Point efficiency fraction due to bubbles	%
<b>E<sub>j</sub></b>	Point efficiency fraction due to jets	%
<b>E<sub>LB</sub></b>	Point efficiency due to large bubbles	%
<b>E<sub>ML</sub></b>	Murphree liquid efficiency	%
<b>E<sub>MV</sub></b>	Murphree vapour efficiency	%
<b>E<sub>O</sub></b>	Section efficiency	%
<b>E<sub>OG</sub></b>	Point efficiency	%
<b>E<sub>SB</sub></b>	Point efficiency from small bubbles	%
<b>f<sub>j</sub></b>	Fraction of vapour jetting	
<b>F<sub>s</sub></b>	F factor, product of the superficial gas velocity and square root of gas density	kg <sup>0.5</sup> m <sup>-0.5</sup> s <sup>-1</sup>
<b>F<sub>s</sub>'</b>	F factor, product of the superficial gas velocity and square root of gas density (Imperial Units)	lb <sub>m</sub> <sup>0.5</sup> .ft <sup>-0.5</sup> .s <sup>-1</sup>
<b>F<sub>SB</sub></b>	Fraction Small bubbles	
<b>FF</b>	Fraction of flooding F factor	
<b>g</b>	Gravity acceleration	m/s <sup>2</sup>

<b>Symbol</b>	<b>Description</b>	<b>Units</b>
<b>G</b>	Gas flow rate	kg/h
<b>G'</b>	Vapour flow rate per bubbling area	kmol.m <sup>-2</sup> .s <sup>-1</sup>
<b>G<sub>m</sub></b>	Gas molar flow rate	mol /h
<b>Ġ</b>	Gas loading rate	m <sup>3</sup> m <sup>-2</sup> h <sup>-1</sup>
<b>H</b>	Packed column height	m
<b>H<sub>c</sub></b>	Henry's constant (concentration definition)	
<b>h<sub>cl</sub></b>	Height of clear liquid in a tray column	m
<b>HETP</b>	Height equivalent of tray packing	m
<b>h<sub>f</sub></b>	Froth height in meters	m
<b>h<sub>f</sub>'</b>	Froth height in inches	inches
<b>h<sub>FL</sub></b>	Liquid holdup in a packed column at flooding	m <sup>3</sup> /m <sup>3</sup>
<b>h<sub>L</sub></b>	Liquid holdup in a packed column	m <sup>3</sup> /m <sup>3</sup>
<b>h<sub>LS</sub></b>	liquid holdup in a packed column at the onset of the loading point	m <sup>3</sup> /m <sup>3</sup>
<b>HTU<sub>G</sub></b>	Height of vapour transfer unit	m
<b>HTU<sub>OG</sub></b>	Height of overall vapour transfer unit	m
<b>HTU<sub>L</sub></b>	Height of liquid transfer unit	m
<b>HTU<sub>OL</sub></b>	Height of overall liquid transfer unit	m
<b>h<sub>w</sub></b>	Weir height	m
<b>h<sub>w</sub>'</b>	Weir height in inches	inches
<b>K</b>	Equilibrium K value(y/x)	
<b>k<sub>i</sub></b>	Rate constant	m/s
<b>k<sub>G</sub></b>	Vapour mass transfer mass transfer coefficient	m/s
<b>k<sub>L</sub></b>	Liquid mass transfer mass transfer coefficient	m/s
<b>k<sub>La</sub></b>	Volumetric liquid mass transfer coefficient	1/s
<b>k<sub>LLB</sub></b>	k <sub>L</sub> for large bubbles	1/s
<b>K<sub>OL</sub></b>	Overall liquid mass transfer coefficient	m/s
<b>K<sub>OL</sub>'</b>	Overall liquid mass transfer coefficient using mole fractions	mol.m <sup>-2</sup> .s <sup>-1</sup>
<b>K<sub>OGa</sub></b>	Volumetric overall vapour mass transfer coefficient	1/s
<b>K<sub>OG</sub></b>	Overall vapour mass transfer coefficient	m/s
<b>L</b>	Liquid flow rate	kg/h
<b>L'</b>	Liquid flow rate per bubbling area	kmol.m <sup>-2</sup> .s <sup>-1</sup>
<b>L<sub>f</sub></b>	Volumetric liquid flow rate per unit average flow width	m <sup>2</sup> /s
<b>L<sub>m</sub></b>	Liquid molar flow rate	mol/h
<b>Ī</b>	Partial pressure of component i at the phase interphase	Pa
<b>m<sub>i</sub></b>	Slope of the equilibrium line	mol/mol
<b>M<sub>G</sub></b>	Vapour mass flow rate	kg/s

<b>Symbol</b>	<b>Description</b>	<b>Units</b>
$N_i$	Specific absorption rate	mol/(m <sup>2</sup> .s)
$n_i$	Molar absorption rate of component i	mol/s
$N_{IB}$	Number of bubbles entering the froth	
$(N_i)_x$	Molar flux of component i, in direction x	Mol.m <sup>-2</sup> .s <sup>-1</sup>
$\bar{N}_f$	Number of large bubbles leaving the froth	
$\bar{N}_s$	Number of small bubbles leaving the froth	
$NTU_G$	Number of vapour mass transfer units	
$NTU_{OG}$	Number of overall vapour mass transfer units	
$NTU_{OL}$	Number of overall liquid mass transfer units	
$NTU_L$	Number of liquid mass transfer units	
$NTU_L'$	Number of liquid mass transfer units, with the assumption that liquid flows in as plug flow and that there is no vertical liquid mixing	
$p$	Hole Pitch in sieve trays	m
$P_{i,I}$	Partial pressure of component i at the phase interphase	Pa
$P_{i,G}$	Partial pressure of component i in the bulk gas phase	Pa
$P_i^*$	Partial Pressure in equilibrium	Pa
$P_T$	Total pressure	Pa
$Q_L$	Liquid flow rate	m <sup>3</sup> /s
$Q_{wl}'$	Load per weir length	Gpm/ft
$t_G$	Average vapour residence time	s
$t_{GLB}$	Average large bubble residence time	s
$t_L$	Average liquid residence time	s
$T_s$	Tray Spacing	m
$u_{V,fs}$	Superficial gas velocity the loading point	m/s
$u_g$	Superficial gas velocity	m/s
$u_h$	Velocity of vapour leaving perforations	m/s
$u_L$	Superficial liquid velocity	m/s
$u_{s,G}$	Superficial gas velocity in tray columns	m/s
$u_{v,FL}$	Superficial gas velocity at flooding	m/s
$V_G$	Vapour volumetric flow rate	m <sup>3</sup> /s
$V_L$	Liquid volumetric flow rate	m <sup>3</sup> /s
$V_{LB}$	Volume of large bubbles	m <sup>3</sup>
$V_{SB}$	Volume of small bubbles	m <sup>3</sup>
$W$	Weir length	m
$X$	Liquid mole ratio	Mol solute in the liquid per mol solvent free solvent

<b>Symbol</b>	<b>Description</b>	<b>Units</b>
$x_{i,L}$	Mole Fraction of component I in the liquid phase	Mol/mol
$x^*$	Equilibrium liquid mole fraction	mol/mol
$X^*$	Equilibrium liquid mole Ratio	Equilibrium mol solute in the liquid per mol solvent free solvent
$y$	Mole fraction in the vapour phase	Mol/mol
$Y$	Mole ratio of a set component in the vapour phase	Mol solute in the vapour per mol solvent free vapour
$\bar{y}_i$	Average mole fraction	
$y^*$	Mole fraction in the vapour in equilibrium with the liquid	Mol/mol
$z$	Directional variable	m
$dz$	Special vector	m
$Z$	Length of liquid flow path	m



## GREEK SYMBOLS

Symbol	Description	SI Units
$\alpha$	Liquid holdup volume fraction	$\text{m}^3/\text{m}^3$
$\beta$	Vapour holdup in froth	$\text{ft}^3/\text{ft}^2$
$\mu$	dynamic viscosity	$\text{kg}\cdot\text{m}^{-1}\cdot\text{s}^{-1}$
$\alpha_e$	Effective liquid volume fraction	
$\delta$	Film thickness	m
$\varepsilon$	Bed voidage	$\text{m}^3/\text{m}^3$
$\lambda$	Stripping factor	
$\nu_L$	Kinematic viscosity	$\text{m}^2/\text{s}$
$\rho_G$	Gas phase density	$\text{kg}/\text{m}^3$
$\rho_L$	Liquid phase density	$\text{kg}/\text{m}^3$
$\rho_{\text{Mol,L}}$	Molar density for liquid	$\text{kmol}/\text{m}^3$
$\rho_{\text{Mol,V}}$	Molar density for vapour	$\text{kmol}/\text{m}^3$
$\sigma$	Surface tension	N/m
$\sigma_{\text{crit}}$	Critical surface tension based on the packing	N/m
$\phi$	Fraction of perforated tray area (Free area)	
$\Gamma$	Foaming factor	

## DIMENSIONLESS NUMBERS

Symbol	Name and Physical Interpretation	Definition
<b>Ca</b>	<b>Capillary</b> ; Ratio of viscosity to surface tension	$\mu_L * \frac{u_L}{\sigma}$
<b>Fr</b>	<b>Froude</b> ; Ratio of inertia to gravity acceleration	$u_L^2 * \frac{a_p}{g}$
<b>Ga</b>	<b>Galileo</b> ; Ratio of buoyancy to viscosity	$dp_3 * g_p / u_L^2$
<b>k<math>\sigma</math></b>	Ratio of gravity to surface tension	$\rho_L * \frac{g}{a_p^2 * \sigma_L}$
<b>Re</b>	<b>Reynolds</b> ; Ratio of inertia to viscosity	$\frac{u_L}{a_p * \nu_L}$
<b>Sc</b>	<b>Schmidt</b> ; Ratio of momentum to diffusivity	$\frac{\mu_L}{\rho_L * D_{i,L}}$
<b>We</b>	<b>Weber</b> ; Ratio of inertia to surface tension	$u_L^2 * \frac{\rho_L}{\sigma_L * a_p}$
<b>Pe<sub>G</sub></b>	<b>Peclet</b> ; Ratio of axial dispersion by flow	$u_s * \frac{Z^2}{De_G(T_s - h_f)}$

## COLUMN FLOW DEFINITIONS

<b>Symbol</b>	<b>Name and Physical Interpretation</b>	<b>Definition</b>
<b>F<sub>s</sub></b>	<b>Vapour flow factor;</b> Based on superficial velocity	$u_s * \sqrt{\rho_v}$
<b>F<sub>a</sub></b>	<b>Vapour flow factor;</b> Based active area	$u_a * \sqrt{\rho_v}$
<b>F<sub>b</sub></b>	<b>Vapour flow factor;</b> Base on bubbling area	$u_b * \sqrt{\rho_v}$
<b>F<sub>h</sub></b>	<b>Vapour flow factor;</b> Base on hole area	$u_h * \sqrt{\rho_v}$
<b>FP</b>	<b>Flow parameter</b>	$\frac{\dot{M}_l}{\dot{M}_v} \sqrt{\frac{\rho_G}{\rho_L}}$
<b>C<sub>b</sub></b>	<b>Capacity factor according to the Glitsch correlation</b>	$u_b \sqrt{\frac{\rho_G}{\rho_L - \rho_G}}$
<b>C<sub>s</sub></b>	<b>Capacity factor according to superficial velocity</b>	$u_s \sqrt{\frac{\rho_G}{\rho_L - \rho_G}}$

---

# CHAPTER 1: INTRODUCTION AND PROJECT OUTLINE

The process of separating components through either selective condensation or evaporation is extensively exploited within the chemical industry. Examples thereof include distillation, absorption and stripping. Despite being considered thermodynamically inefficient, these separation processes are still thought invaluable [1]. Consequently, the need for improvement continues to exist, with daily crude oil distillation capacities exceeding  $2.14 \times 10^6 \text{ m}^3$  in USA alone [2].

## 1.1. MASS TRANSFER IN COLUMN DESIGN

Industrial gas-liquid contactors are historically designed based on the assumption of an equilibrium stage model (for example McCabe Thiele). Such a model divides a column into a number of discrete stages in thermodynamic equilibrium. As all streams leaving the respective stages are considered in equilibrium, this model fails to distinguish between column internals and their respective efficiencies [3, 4].

The limitations of the equilibrium models, motivated literature authors to develop of a rate-based approach. This historical approach is founded on the assumption that thermodynamic equilibrium is attained directly at the phase boundary, resulting in phase-based rate equations and constants. For the remainder of this project, the preceding rate constants are also referred to as mass transfer coefficients.

The resulting mass transfer coefficients play an indispensable role in column design, relating the rate of separation to the flow rates and concentration gradients of the respective phases. Although useful for design purposes, column internal performance is rarely compared on the basis of mass transfer coefficients. This is a result of the artificial fundament of transfer coefficients, failing to account for the extent to which a system approximates the thermodynamic best case scenario. The comparison of transfer coefficients, therefore, often leads to the misinterpretation that increased values are indicative of increased efficiency. This is, however, not always the case, with an example to follow.

The increase of transfer coefficients with an increase in liquid loading, is presented as a case in point for stripping applications in a liquid phase limited system. As liquid loadings increase, the effective contact time decreases. This produces a trade-off between the increase of the mass transfer coefficient due to interfacial turbulence and the decrease of effective contact time. Generally speaking, the latter is found to dominate, effectively decreasing the efficiency with increased liquid loading. For this reason, this project refrained from using mass transfer coefficients as a comparative tool. In order to bridge this perceived gap, performance comparisons were done using either tray efficiencies or the HETP (Height Equivalent of a Theoretical Tray) for packed columns. This thesis unconventionally chose HETP for liquid limited systems, as it provided easy comparison.

## 1.2. EFFICIENCY QUANTIFICATION

Constant reflux distillation (hydrocarbon  $C_6/C_7$ ) is widely received as the norm in evaluating column internal efficiencies. As this entails effectively equal liquid and vapour mass flow rates, variable pressure is required to influence densities and thereby vary volumetric flow rates. This efficiency evaluation method, therefore necessitates the use hazardous solvents in combination with high temperatures and pressures.

Constant reflux distillation therefore imposes various constraints on the physical and mechanical property requirements of column internals (trays and packing), creating a bottleneck in the prototyping process. Rather than attempting to alter the system mixture in favour of a less corrosive and hazardous solvent, this thesis evaluated alternative methods for quantifying efficiency. Motivation for the aforementioned decision is presented as follows:

- [1] Reboilers and condensers for industrially applicable sized columns are slow in reaching steady state. This translates into testing times of between 4 and 8 hours, depending on the internal type. The use of constant reflux in quantifying efficiency is thus both expensive and time-consuming.
- [2] The combination of high temperatures and pressure introduce an intrinsic risk. It is therefore preferable to minimize the risk of the efficiency quantification method, rather than employing additional safety measures and protocols.

Two independent alternatives were developed resulting from the need for simple and cost-effective efficiency quantification. Aqueous desorption of isobutyl acetate in air (ADIBAA-method) was chosen for quantifying the liquid phase resistance and thereby the efficiency in packed columns. The humidification of air (HA-method) was selected for the tray counterpart. For the remainder of this project, the preceding methods are referred to in acronym form.

In providing a simple and cost-effective approximation for internal efficiencies, both the ADIBAA- and HA- methods are expected to simplify the process of column internal prototyping.

## 1.3. INDUSTRIAL RELEVANCE OF PROPOSED WORK

Phase contacting column internals are industrially produced through a series of punching, die moulding and bending (and in rare cases welding). The process of designing and fabricating such a production line is both expensive and time-consuming. This notably limits the initial design of new internals, as physical prototypes are required for the various performance tests. Consequently, sizable capital investments are incurred, prior to the performance evaluation.

This hampers the freedom of designers to easily and quickly explore new ideas. The sizable cost and time-consuming nature of the prototyping process, is thus considered partly responsible for the relatively slow rate of column internal development. The aforementioned slow progression is illustrated in Section 2.2.1, suggesting that new packing generations are only produced every decade and a half. This is considered unacceptable when compared to modern technologies, and concepts such as Moore's law. The aforementioned law states that computational power is said to increase twofold within a period of 24 months [5]. This sizable discrepancy between improvement of computing power and progression of distillation product design illustrates the delays in development of mass transfer equipment.

Based on the financial benefits and enhanced designer freedom, the need for more rapid prototyping seems evident. It was therefore opted to focus on simplistic, cost-effective testing techniques, that limited the material restrictions of the column internals. This led this project in focusing on the development of both the ADIBAA- and HA-methods. The methods offered simplistic quantification of complex efficiencies, while remaining cost-effective.

#### 1.4. AIMS OF THIS STUDY

The overarching aim of this study was to streamline the prototyping of column internals, while eliminating the use of hazardous solvents and expanding the possible range of prototyping materials. As column internal performance is evaluated on the basis of efficiency, the main aim was to develop simplistic, cost-effective alternatives (ADIBAA-and HA-methods) to conventional constant reflux.

To identify possible alternatives, this study set out to evaluate the historical methods of measuring mass transfer, and their translation to efficiencies. The available literature methods were, however, ill-suited towards rapid prototyping, due to practical, environmental and economic reasons. The shortcomings of the existing methods and their proposed improvements are presented in the literature chapters (Sections 4.4 and 5.6). The historical method evaluation was therefore used to provide background knowledge for the development of both the ADIBAA-and HA-methods.

Motivated by literature, the project set out to evaluate tray column internals using Murphree tray efficiencies. The relevant efficiencies were calculated through the HA-method and therefore using a known vapour phase mass transfer limited system. The packed column efficiency evaluation was conducted using HETP (Height equivalent to a theoretical tray) with the ADIBAA-method focussing on the alternative liquid phase resistance.

The following objectives were identified, in accomplishing the main goal:

- [1] **Developing and experimentally verifying alternative methods** (ADIBAA- and HA-methods) for measuring **liquid and vapour phase mass transfer** coefficients (translated into efficiencies) in tray and randomly packed columns.

For industrial application, the proposed methods were required to

- a. Respectively measure either **liquid phase or vapour phase mass transfer coefficients** within a said confidence interval.
  - b. Satisfy **environmental** considerations.
  - c. Utilize **easy** and reliable **measurement techniques**.
  - d. Remain **cost-effective**.
  - e. Provide a time **optimized** design, in both **quantification and experimental times**.
  - f. **Limit the restrictions** on the prototype fabrication material and techniques.
- [2] **Design and construction** of two independent, industrially sized, pilot plants for the experimental validation of the ADIBAA- and HA-methods.
- [3] Evaluating the use of both of the developed methods in **differentiating** column internals based **on their efficiency**. This is critical in being able to quantify the improvements of one designed compared to another.
- [4] Evaluating the applicability of the ADIBAA- and HA-methods as **simplistic tools in comparing efficiencies during the initial design phase**.

---

# CHAPTER 2: BACKGROUND ON COLUMN INTERNALS

Column internals are conventionally categorized into either trays or packing (excluding distributors and collectors), with both functioning as a promoter for phase contact and interfacial area. Differences in column internal performance are attributed to hydrodynamic variations, intricately related to the design. This project, therefore, set out independently evaluate both tray and columns, due to their widely varying mechanisms of phase contact. A short description of the subsequent column operations is presented in the succeeding chapter.

## 2.1. TRAY COLUMNS

In tray columns, vapour-liquid contact originates from an upward flowing vapour phase, bubbling through a laterally moving liquid. As a result of the ratio between vapour - liquid loadings and the physical properties, four separately identifiable flow regimes are distinguished. According to Hofhuis and Zuiderweg [6], the regimes are noted as:

- [1] Free bubbling regime;
- [2] Mixed froth regime;
- [3] Emulsified regime;
- [4] Spray regime.

Historically, the mixed froth regime was considered the most advantageous. Under these operating conditions the vapour passes through the continuous liquid phase in a series of jets and bubbles, leading to increased holdup and froth height [4]. In later publications, however, Hofhuis and Zuiderweg [6] suggested significant applications for the spray regime under vacuum conditions, whilst the emulsion regime was considered preferable for high liquid-load absorption.

Commercially it has been opted not to work within the bubbling regime, as it is both inefficient and close to the dumping limit. This limit refers to the minimum vapour loading required to suspend the laterally flowing liquid. Vapour flow below this point, therefore, results in the liquid dropping through the perforations in the tray.

An illustration of the vapour - liquid flow ratios of the respective regimes is provided in Appendix C (Section 9.3.1, p 180 ), redrawn from Hofhuis and Zuiderweg (1979) [6] The capacity factors used in this analogy, are defined in the Glossary (p xxvi) . In addition to the relative flow rates, the regimes are also impacted by the tray design. This due to the specific nature of the momentum balance of the vapour and liquid on a set tray. The design of the perforations intricately affect the local vapour velocity and consequently the momentum forces. Section 2.1.1 therefore focusses on different tray designs.

### 2.1.1. TRAY TYPES

Tray types are roughly categorized within:

- [1] Bubble cap trays;
- [2] Sieve trays;
- [3] Valve trays.

Bubble cap trays were the first to be employed industrially and satisfied much of the market prior to 1960 [7]. The design consists of a flat perforated plate with gas risers extending upwards, around the perforations in a tube-like fashion. Caps are placed over the riser tops, inhibiting liquid dumping from the vertically acting gravity component. This leads to a high turndown ratio i.e. the ratio between the maximum and minimum liquid loading.

The gas risers are equipped with perforated sides through which the vertically flowing vapour escapes, bubbling into the liquid phase, hence the name *bubble cap tray*. Bubble cap trays are considered expensive in comparison to the other tray designs, mostly due to the complexity of the fabrication techniques [3]. As a result, they are rarely used in modern columns, with the exception of fine spirit distilleries [3].

The alternative, sieve trays being straightforward to fabricate, are considered inexpensive and established [8]. These tray, however, experience significant weeping behaviour at low gas rates, leading to low turndown ratios. In a bid to minimize this behaviour, bubble promotors were implemented in the early 1990's at the inlet weir of each tray. The inclusion of bubble promotors mitigate weeping at the start of the tray, shifting the weeping locus towards the middle where the expanded is liquid contracts. Sieve trays are still considered to saturate much of the market due to their established nature and the abundance of heuristic data. A schematic of a typical bubble promotor is provided in Appendix B in Figure 9.27.

Valve trays were historically developed in an attempt to combine the attributes of both sieve and bubble cap trays. The resulting valves equipped each perforation with a sliding cover. At high vapour flow rates the cover moves vertically upwards, exposing a higher effective area. The extent of upward mobility is limited by restrictive legs extending below the tray. The alternative holds for low vapour rates, at which the effective perforated area is decreased in a bid to limit weeping. On this account, valve trays are frequently preferred to sieve trays, justifying the increase in expenditure through larger turndown ratios and improved fouling characteristics.



## 2.2. PACKED COLUMNS

In packed columns, vapour-liquid contact originates as descending liquid coats individual packing rivulets. The liquid is counteracted by continuous vapour travelling upward. The resulting interaction on the packing rivulets, create surface area through a combination of specific area and droplet formation. Modern packings are divided into three classifications, namely:

- [1] Grid Packing;
- [2] Random Packing;
- [3] Structured Packing.

Random and structured packings are considered heavily susceptible to fouling and corrosion [9]. As such, in cases where regular column upsets are expected, grid packings are employed for their robustness [3]. Examples of such applications include heat transfer and wash or crude oil [3]. Due to their limited application, grid packings were not considered in this thesis.

### 2.2.1. RANDOM PACKING

In randomly packed columns, elements of a specific geometry are dumped into a column, forming a randomized structure and variable rivulet flowpath [3, 10] . During operations, both liquid and vapour flowpaths are constantly disrupted, increasing liquid hold up. The accompanied increase in pressure drop, is considered advantageous, as it increases both the contact time and mass transfer interfacial area [10].

Developed in four distinct generations, the progression of random packing is largely characterized through the evolution of rings and saddles to hybrid- and wave-based geometries [9]. The first and second generations largely focused on rings and saddles [9]. In doing so, the relative geometrical differences were exploited in increasing mass transfer and decreasing pressure drop.

The third-generation of packing opted to merge the attributes of both rings and saddles, to produce a hybrid [3]. Equipped with free tips, the hybrid geometry focussed on drop generation for increased interfacial area. The enhanced droplets produced a trade-off between interfacial area and entrainment [11]. Furthermore, the third generation saw the creation of rivulets with varying characteristic lengths depending on the viewing angle. One such example is the Koch Glitsch IMTP® Ring. This ring uses a design with a notably smaller size, depending on whether it was viewed from the top or the side. This shifts the centre of gravity of the packing, ultimately reducing the extent of randomness when dumped into a column. The aforementioned advance combined the cost-effectiveness of random packing with the organized nature of the structured counterpart. This notably decreased pressure drop.

The fourth-generation of packing attempted to do away with the hybrid approach, by developing a sinus wave-like geometry. This geometry is considered beneficial as it reduces excessive droplet formation,

while still increasing turbulent film flow and interfacial area [9]. A representation of modern packing progression is provided in Table 2.1, generated from Lamprecht [9] (2010) as well as Erasmus [3] (2004). Both authors drew inspiration from Kister [7] and Schultes [12].

TABLE 2.1: RANDOM PACKINGS ACCORDING TO GENERATION (LAMPRECHT [9] AND ERASMUS [3]) [7, 12].

<b>First-Generation (1895-1950's)</b>	<b>Second-Generation (1950-1970's)</b>	<b>Third-Generation (1970-1990's)</b>	<b>Fourth-Generation (1990's to present)</b>
Berl Saddle	Hy-Pak®	Cascade Mini Rings(CMR®)	Intalox® Ultra™
Lessing Ring	Intalox® Saddle	FlexiMac™	Raschig Super Ring
Raschig Ring	Pall® Ring	Hiflow® Ring	Sulzer NeXring™ (released 2016)
	Super Intalox® packing	Intalox® Snowflake®	
		IMTP®	
		Levapak	
		Nutter Rings™	

Random packing is extensively used in industry for small to medium sized columns, operated under both high pressures (>14 bar) and liquid loadings (> 45 m<sup>3</sup>m<sup>-2</sup>h<sup>-1</sup>) [7]. Various applications, however, warrant the purification of small quantities of high value components. In such cases, structured packings are industrially preferred, due to their high efficiencies and low pressure drop.

### 2.2.2. STRUCTURED PACKING

Structured packings were developed in response to the need for high efficiency, low-pressure drop alternatives. The subsequently developed packings, utilize modular corrugated sheets in creating two-phase flow channels. The ordered arrangement of the sheets, result in decreased pressure drop.

In similar fashion to the random packing, structured packings were also developed in four distinct generations; evolving from metal gauze to folded sheet-metal packings. The first and second generations largely consisted of wire gauze contactors. The resulting contactors offered notably decreased pressure drop, but were very expensive to equip [3].

The third generation was trademarked by the use of sheet-metal packing, leading to high efficiencies, low-pressure drops and decreased solids sensitivity. However, as mentioned Section 2.2.1, structured packings were not yet considered in cases of higher liquid loadings, as the sharp directional changes essentially caused flooding. This led to the development of the fourth generation, which employed larger flow channels and smooth directional changes [13]. A similar representation, as provided for random packings, is included in Table 2.2. This table was reproduced from both Erasmus [3] and Lamprecht [9] on inspiration from Kister [7] and Schultes [12].

TABLE 2.2: GENERATIONAL EVALUATION OF STRUCTURED PACKING [9] [3] [7, 12].

<b>First Generation (1940 -1950's)</b>	<b>Second Generation (1950-1970's)</b>	<b>Third Generation (1970-1990's)</b>	<b>Fourth Generation (1990's to present)</b>
Panapak	Goodloe®	Gempak®	Flexipac®S
	Hyperfil®	Koch Flexipac®	Flexipac®HC
	Sulzer, Koch BX and AX Wire Gauge Packing	Montzpak-B®	Intalox® High Capacity Packing
		Sulzer MellapakTM®	MellapakTMplus®
			Mellapak AYPlus DC Hybrid Packing
			Montz-PakM® Montz- PakA® Fabric
			Raschig Super-Pak

As a result of poor wetting characteristics, aqueous solutions are rarely fractionated by means of structured packings. In such cases, random packings are considered more advantageous, due to their constantly interrupted flowpaths, forcefully increasing the interfacial area [7, 3]. The combination of this knowledge with the aim of remaining both environmentally friendly and cost-effective (Section 1.4), led this thesis to focus on random packing.

## 2.3. TRAYS VERSUS PACKING

Although both tray and packed columns are widely employed, certain factors are used as rule of thumb in influencing the decision-making process between the two. Similar factors are used to influence the choice between random and structured packings. Table 2.3 is presented, summarizing the Kister evaluation between trays and packing [14, 15].

Industrial columns are consequently equipped on the basis of the considerations listed in Table 2.3. Resulting from these factors, random packing is preferentially employed in use of absorption and stripping applications, with limited applicability in industrial distillation [16]. This is due to distillation applications, favouring throughput (crude oil etc.) and the flexibility of side streams. This statement is motivated by Krummrich [17], who estimated that 90% of the world's distillation columns are equipped with trays.

TABLE 2.3: CONSIDERATIONS FOR CHOOSING BETWEEN TRAYS OR PACKING [14, 15].

Consideration	Trays	Packing
Vacuum applications		✓
Solids	✓	
Low pressure drops applications		✓
Small column diameters		✓
Large diameters columns	✓	
Foaming behaviour		✓
Low liquid hold-up requirements (decomposition or polymerization fears)		✓
High liquid loadings	✓	
High degree of uncertainty	✓	
Complex systems and orientations	✓	

Industrial randomly packed columns are therefore extensively used in absorption and stripping applications. The relevant systems include both vapour and liquid phase limited mass transfer (elaborated in Chapter 3). This thesis focused on latter, as it offered cost-effective testing and simplified quantification (discussed in Chapter 4).

Industrial examples of liquid phase limited systems include the absorption CO<sub>2</sub> in MEA (ethanolamine) [10] and the volatilization of hydrocarbons from wastewater [18, 19]. These applications are limited by the rate at which the solute component is transported, to or from, the liquid phase. This is as the systems are operated close to equilibrium in the liquid phase, while far removed (from equilibrium) in the vapour. The approach of equilibrium, subsequently slows down the rate of mass transfer, leading to the approximation that the system is limited in the liquid phase. Based on the presented knowledge and the current industrial drive for carbon capture [10, 20], this projected focused on liquid phase mass transfer limited systems. This directly resulted in the development of the ADIBAA-method (aqueous desorption of isobutyl acetate in air).

In the case of tray columns, applications were found dominated by distillation [21]. As distillation is conventionally overshadowed by vapour phase mass transfer resistance, it in turn offers applicability in evaluating the efficiency of tray column internals [4]. This led this thesis to focus on vapour limited systems during the development of the HA-method (humidification of air).

Although dissimilar in design, the overarching aim of the both trays and packing is to promote mass transfer by increasing residence time and interfacial area. This motivated the fundamental evaluation of mass transfer, presented in Chapter 3

---

# CHAPTER 3: MASS TRANSFER

## LITERATURE

Diffusion or mass transfer is the process by which molecules spontaneously migrate from regions of high to low concentrations [22]. The resulting transport phenomenon, present in systems removed from physical or chemical equilibrium, is conceptualized through two separate yet similar philosophies [22, 4].

The first viable mass transfer philosophy was developed in 1855 by Adolf Fick. [22]. His approach related mass flux to an electrical stream overcoming a resistance. Explicitly the analogy is presented as:

$$I = V \cdot R^{-1} \approx (\text{Flux}) = (\text{Driving force}) \cdot (\text{Resistance})^{-1}; \quad 3.1$$

$$I = \text{Current Flow} \approx \text{Mass transfer Flux}; \quad 3.2$$

$$V = \text{Potential difference} \approx \text{Mass Transfer Driving Force}; \quad 3.3$$

$$R = \text{Resistance} \approx \text{Resistance to Mass Transfer}. \quad 3.4$$

The resulting Fick's Law relationship is mathematically presented through Equation 3.5 (refer to glossary for annotation) [10].

$$(N_i)_x = D_{i,L} \cdot \left( \frac{dC_i}{dz} \right) \quad 3.5$$

This approach describes the use of diffusion coefficients as a fundamental basis for the estimation of mass flux [22]. Fick's Law, however, offers limited industrial applicability due to the complexity of evaluating the mass transfer spatial vector ( $dz$ ).

Mass transfer coefficients were, therefore, developed as an alternative philosophy. [1, 2]. The approach removed the mass transfer spatial vector from the concentration driving force and lumped it into a newly defined mass transfer coefficient [1]. A mathematical depiction of the approximation is included in Equation 3.6.

$$(N_i)_x = k_i \cdot (\Delta C_i) = \left( \frac{D_{i,L}}{\Delta z} \right) \cdot \Delta C_i \quad 3.6$$

Equation 3.6 still represented mass transfer in terms of mass flux (i.e. the rate of mass transfer per unit area), thus limiting its application. The final stage in the historic development of the mass transfer approach was subsequently to simplify the spatial vector as the area of phase contact (discussed in Section 3.1). The resulting equation is expressed as:

$$n_i = k_L a \cdot (\Delta C_i). \quad 3.7$$

The choice of appropriate philosophy in using either the mass transfer coefficient or Fick's law approach, is largely dependent on the available experimental resources and application. Resulting from the experimental difficulties in measuring the spatial vectors inside industrial mass transfer equipment, it was decided to base the bulk of this study on the mass transfer approach. Although not fundamental, this approach is still expected to provide sufficient accuracy when fitted to experimental data [22, 23, 4].

### 3.1. GAS-LIQUID MASS TRANSFER

Founded from the need for simplification, mass transfer coefficients are often employed as an approximation in streamlining multi-phase systems. The ensuing analysis is done through the assumption that compositional changes are limited to the small areas adjacent to the phase boundary, while turbulence is responsible for mixing in the bulk fluid [1]. The phase boundary inhibits adjacent flow motions, creating a stagnant layer where molecular diffusion governs mass transfer. As a result, mass transfer spatial vectors are approximated as the area of phase contact. A graphical illustration of the resulting concentration profile for desorption, is presented in Figure 3.1.

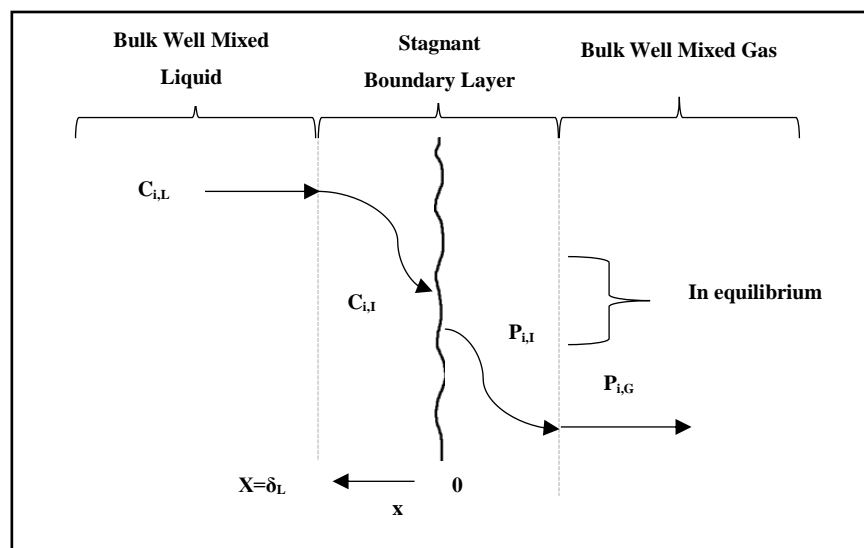


FIGURE 3.1: SCHEMATIC OF MASS TRANSFER FROM THE BULK LIQUID TO THE VAPOUR. REDRAWN FROM HENLEY [4]

Through the reasoning of a steady state assumption, the subsequent rate of diffusion is mathematically expressed as:

$$(N_i)_x = \frac{n_i}{a_e} = k_L(C_{i,L} - C_{i,I}) = k_G(P_{i,I} - P_{i,G}). \quad 3.8$$

As a result of the experimental intricacy in measuring compositional data at the phase boundary, it is considered common practise to eliminate the interfacial concentrations [24]. This is done through

considering the overall mass transfer coefficient as depicted in Equation 3.9. The depiction is based on the assumption of equilibrium at the interface.

$$(N_i)_x = \frac{n_i}{a_e} = K_{OL}(C_{i,L} - C_i^*) = \frac{K_{OL}}{H_c}(P_i^* - P_{i,L}) = K_{OG}(P_i^* - P_{i,G}) \quad 3.9$$

Various sources use different analogies in representing the mass transfer driving force, for example either fractions or concentrations. Thereby, the overall mass transfer coefficient has variable units, depending on the driving force. In an attempt to avoid ambiguity, the corresponding mole fraction mass transfer coefficients are indicated with an apostrophe in this thesis. The subsequent conversion is provided in Equation 3.10:

$$(N_i)_x = \frac{n_i}{a_e} = K_{OL}(C_{i,L} - C_i^*) = K_{OL} \cdot \rho_{Mol,L} (x_{i,L} - x_i^*) = K'_{OL}(x_{i,L} - x_i^*) \quad 3.10$$

Continuing on the analogy between diffusion and Ohm's law (presented by Fick in Equations 3.1 to 3.4), mass transfer resistance is represented as two resistances in series. Thus, through transposing Equation 3.10 the relationship between overall and local or phase dependent mass transfer coefficients is expressed as:

$$\frac{1}{K_{OL}} = \frac{1}{k_L} + \frac{1}{k_G \cdot H_c}; \quad 3.11$$

$$\frac{1}{K_{OG}} = \frac{1}{k_L} + \frac{H_c}{k_G}. \quad 3.12$$

where Henry's volatility constant is defined as the ratio between partial pressure and liquid phase concentration:

$$H_c = \frac{P_i}{C_{i,L}}. \quad 3.13$$

The relationships are provided for the consideration of a concentration driving force and therefore  $K_{OL}$ , not  $K'_{OL}$ . The alternate mole fraction relationship may be obtained by replacing the Henry's volatility constant with the equilibrium curve K-value ( $y/x$ ).

Equations 3.11 and 3.12, mathematically depict the importance of the gas solubility on the significance of the individual phase resistances. Subsequently, if the gas phase (or solute) is sparingly soluble in the liquid, such that the Henry's volatility constant is large, the principle resistance to mass transfer may be approximated to be in the liquid phase. This causes the concentration gradient on the liquid side of Figure 3.1 to become steeper while the gradient on the vapour phase flattens (between bulk phase and interface). For high gas phase solubilities, the reverse holds with system representing vapour phase limitations [24].

The relative significance of each resistance, as presented in the Equations 3.11 and 3.12, is both system and operating condition specific. This is reasoned as the Henry's volatility constant is dependent solely on the equilibrium conditions of the system. In contrast, the individual transfer coefficients are effected by a combination of the relative flow rates, diffusion properties and interfacial turbulence (see Appendix C, Table 9.9). This highlights the inapplicability of a generalised approach for both tray and packed columns, as different mechanisms of phase contact are exploited. This thesis therefore separately evaluated mass transfer in tray and packed columns (Chapters 4 and 5).

## 3.2. SUMMARY

Chapters 3 provided a short overview of phase based mass transfer coefficients and the influence of the equilibrium on the significance of each resistance. The analysis indicated that the transport of sparingly soluble and volatile solutes was limited by the liquid resistance, when operated far from the vapour equilibrium. This is as the vapour phase effectively approximates an infinite medium (maximizing the driving force), while collisions in the bulk liquid limit the transport of the solute at the effective interface. In contrast, the rate of transfer slows down as the system approaches the vapour equilibrium. This is due to collisions on the vapour side and is therefore considered to be vapour limited.

The ability of measuring the individual phase resistances, allows for the isolation of relative internal parameters and their effects on the respective phases. For this reason, this thesis considered systems that were either liquid or vapour phase limited and not a combination of both. This allows for parameter isolation within the respective phases.

Literature was used as the main consideration of phase resistance, in the respective tray and packed columns. Motivation for the liquid phase packed column analysis was hence found through various authors noting the impediment of packed column mass transfer by insufficient liquid interfacial turbulence [25, 26, 27, 28]. The resulting lack of turbulence, inhibits the renewal of the effective transfer surface thereby creating a bottleneck in the liquid phase.

This is pronounced in packed columns, as the descending liquid coats the individual packing rivulets with a thin film. The interfacial turbulence of the descending liquid is therefore constantly counteracted by the boundary layer of the liquid on packing itself. It was therefore suggested that packed column internals could be evaluated on the extent to which they overcome surface-renewal limitations on the liquid side. The influence of interfacial turbulence on the liquid phase mass transfer coefficient, is presented at the hand of the various surface refreshing theories presented in Table 9.9 of Appendix C.

Tray columns were in contrast considered limited by the vapour phase. This is due to the turbulence of the liquid in the froth promoting the corresponding surface renewal. It was therefore decided to base the tray column section on vapour phase mass transfer limiting systems.



---

# CHAPTER 4: PACKED COLUMN MASS TRANSFER LITERATURE

A detailed literature review was performed on liquid phase mass transfer in packed columns. The review included both correlations and experimental work, with the motivation as follows:

- [1] The study included an evaluation of the historical experimental setups used in quantifying the liquid phase mass transfer coefficient. This was included to highlight:
  - a. The conventional methods for the experimental measurement of liquid phase mass transfer (presented in Section 4.2 ).
  - b. Possible improvement of the methods, in terms of financial, practical and environmental considerations (presented in Section 4.4).
  - c. And finally, the applicability of liquid phase mass transfer as a simplistic and cost-effective measure packed column efficiency (presented in Section 4.4).
- [2] An evaluation of the predictive correlations found in literature was also conducted, to use as validation for the ADIBAA-method. As far as could be ascertained, this was the first evaluation of ADIBAA system and therefore no applicable experimental data was found, to which to compare the results.

## 4.1. PREDICTIVE CORRELATIONS

The liquid film transfer coefficient has been the centre of various studies over the past 80 years. As a result, a variety of attempts have been made to develop predictive correlations for both mass transfer and mass flux. An array of literature sources, however, mistakenly refer to the liquid side mass transfer coefficient as  $k_{La}$ . The actual liquid side mass transfer coefficient is represented by  $k_L$  with  $k_{La}$  depicting the volumetric mass transfer coefficient on the liquid side.

### 4.1.1. VOLUMETRIC MASS TRANSFER COEFFICIENT IN THE LIQUID PHASE

In the ensuing section, literature correlations are presented for the estimation of the volumetric liquid mass transfer coefficient. The correlations were developed through a combination of experimental and theoretical considerations (dimensionless evaluations), with the exception of the Linek model [29, 30, 18]. A chronological sequence was adopted to illustrate the progression of scientific knowledge.

The details of the experimental systems and column internals, are presented in Tables 9.1 to 9.4 of Appendix A. The purpose of this section, however, was not to explain the derivation of the correlations, but rather to the experimental setups, system choices and predictive capabilities of the models. This is as they are poised for use in validation of the experimental setup.

Table 4.1 is presented summarizing the relevant equations for the liquid side volumetric mass transfer coefficient. The core arguments of the resulting study are presented in the main body of thesis, with the full discussion in Section 9.1.1 of Appendix A.

**TABLE 4.1: CORRELATIONS FOR THE ESTIMATION OF THE VOLUMETRIC MASS TRANSFER COEFFICIENT IN PACKED COLUMNS.**

Source	Date	Equations	Equation ID
Sherwood and Holloway [31, 23, 24]	1940	$\frac{k_L a}{D_{i,L}} = C_1 \cdot \left(\frac{u_L}{v}\right)^{c_2} \cdot Sc_L^{0.5}$ Where $C_1$ is a function of the packing	4.1
Norman [32, 24]	1961	$\frac{k_L a}{D_{i,L}} = 530 \cdot \left(\rho_L \cdot \frac{u_L}{\mu_L}\right)^{0.75} \cdot Sc_L^{0.5}$	4.2
Mohunta et al [33, 34, 24]	1969 b	$k_L a \cdot \left(\frac{a_p \cdot u_L}{g}\right)^{\frac{2}{3}} \cdot \left(\frac{u_L}{g^2}\right)^{\frac{1}{9}} = 0.025 \left(\mu_L \cdot u_L^3 \cdot \frac{a_p^3}{\rho_L \cdot g^2}\right)^{\frac{1}{4}} \cdot Sc_L^{-\frac{1}{2}}$	4.3
Mangers and Ponter [35, 24]	1980	$\frac{k_L a}{D_{i,L}} = 2.03 \cdot \left(\frac{u_L}{v}\right)^{1.44} \cdot Sc^{0.5} \cdot Ga^{-0.183}$	4.4
Billet [36, 37, 24]	1983	$k_L a = \frac{1}{C_1} \cdot \left(\frac{\rho_L \cdot g}{\mu_L}\right)^{\frac{1}{6}} \cdot D_{i,L}^{0.5} \cdot a_p^{\frac{2}{3}} \cdot U_L^{\frac{1}{3}}$ where $C_1$ is a function of the packing	4.5
Schultes [24]	1990	$k_L a = C_1 \left(\frac{g}{\mu_L}\right)^{\frac{1}{6}} \cdot \left(\frac{D_{i,L}}{d_h}\right)^{0.5} \cdot a_p^{\frac{2}{3}} \cdot u_L^{\frac{1}{3}} \cdot \left(\frac{a_e}{a_p}\right)$	4.6
Linek <i>et al.</i> [26] [38, 18, 11]	2005	$k_L a = d_1 \cdot L^{d_2}$ where $d_1$ and $d_2$ are regressed constants	4.7

A number of the equations (4.1-4.3) presented in Table 4.1 are considered inapplicable for modern packings, as a result of the progression of column internals (Table 2.1). The relevant models were regressed on Berl saddles and Raschig Rings. These internals were part of the first and second packing generations and are now seldom used in industry.

Although the listed correlations offer applicability for the sake initial estimates (Section 9.1.1 of Appendix A), the predictive performance is estimated to be doubtful, especially in cases where changes in the physical properties are considered [24]. This stems from complex interactions between the liquid mass transfer coefficient, interfacial area and the physical properties of the system. In addition, all but one [31] of the correlations were regressed on oxygen-water or carbon dioxide-water desorption data. This suggests little variation in diffusion coefficients and therefore the possibility of unquantified interactions.

Further investigations into liquid phase mass transfer included independently evaluating the constants “ $k_L$ ” and “ $a_e$ ”. This increased fundamentality and predictive capability is discussed in Section 4.1.2.

#### 4.1.2. LIQUID SIDE MASS TRANSFER CORRELATIONS AND EFFECTIVE INTERFACIAL AREA

As a result of the absence of fundamental literature models, devoted to decomposing the volumetric mass transfer coefficient researchers saw fit to experimentally evaluate the separate parameters. Two methodologies are historically employed in segregating the volumetric mass transfer coefficient, namely:

- [1] Wetted wall evaluations,
- [2] Chemical absorption.

In wetted wall evaluations, the inside of a known diameter tube is coated with a thin layer of liquid. Using a known liquid phase mass transfer limiting system, a solute is either stripped or absorbed from the liquid, using counter current vapour. Quantifying the composition at the inlet and outlet yields the volumetric mass transfer coefficient. The liquid side mass transfer coefficient is therefore evaluated through division, as the interfacial contact area is approximated as the inner diameter of the tube. The calculated mass transfer coefficient is thereafter used in evaluating the effective interfacial area in column evaluations.

The chemical absorption methodology entails evaluating the liquid side volumetric mass transfer coefficient through absorption and near instantaneous chemical reaction in the liquid phase (for example reacting carbon dioxide with a caustic solution). As such, under conditions of negligible vapour phase resistance, the rate of absorption is limited by the chemical reaction. The liquid phase mass transfer coefficient ( $k_L$ ) is thereby calculated through reaction kinetic evaluations. Consequently, the effective area is evaluated through division of the results.

As a result of the experimental methodologies, an explicit dependence exists between correlations for the  $k_L$  and  $a_e$ , by each research group. Combination of models developed by different authors is therefore not advised. A summary of the correlations found in literature is presented in Table 4.2 with a discussion in Appendix A (Section 9.1.2). For the purpose of comparison between research groups, the correlations are presented in tabulated format.

Based on the discussion presented in Appendix A, the correlations presented by van Krevelen [39, 40], Semmelbauer [41] and Zech & Mersmann [42] are expected to inadequately represent experimental data. This was on the account of a combination between questionable experimental techniques and the assumptions made during the dimensionless analysis.

TABLE 4.2: PREDICTIVE CORRELATIONS FOR THE EFFECTIVE INTERFACIAL AREA AND LIQUID SIDE MASS TRANSFER COEFFICIENT.

Source	Liquid Phase Mass Transfer Coefficient	Equation ID	Source	Effective Interfacial Area	Equation ID
Van Krevelen and Hofstjizer (1947) [39, 40]	$\frac{k_L \cdot \delta_L^{\frac{1}{3}}}{D_{i,L}} = 0.015 \cdot \left( \frac{u_L}{a_w \cdot v_L} \right)^{\frac{2}{3}} \cdot Sc^{\frac{1}{3}} \cdot \frac{\delta_L \cdot \left( \frac{K}{D_{i,L}} \right)^{0.5}}{\tanh\left( \delta_L \left( \frac{K}{D_{i,L}} \right)^{0.5} \right)}$ <p>Where</p> $\delta_L = \frac{\mu_L^2}{\rho_L \cdot g}$	4.8	Krevelen and Hofstjizer (1947) [39, 40]	$a_e = a_p \cdot (1 - \exp(-5000 \cdot u_L))$	4.9
Semmelbauer (1967) [41]	$k_L \cdot \frac{d_p}{D_{i,L}} = C_1 \cdot (Re_L)^{0.5} \cdot Sc_L^{0.5} \cdot Ga_L^{0.17}$ <p>Where</p> $C_1 = \begin{cases} 0.32 & \text{for Raschig rings} \\ 0.25 & \text{for Berl Saddles} \end{cases}$	4.10	Semmelbauer (1967) [41]	$\frac{a_w}{a_p} = C_1 \cdot \left( u_L \cdot \frac{d_p}{v} \right)^{C_2} \cdot \left( \rho_L \cdot \frac{dp^2}{\sigma_L} \right)^{0.5}$	4.11
Onda <i>et al.</i> (1968) [43, 44, 19, 45, 46, 47]	$k_L \cdot \left( \frac{\rho_L}{g \cdot \mu_L} \right)^{\frac{1}{3}} = 0.0051 \left( \frac{L}{a_w \cdot \mu_L} \right)^{\frac{2}{3}} \cdot Sc^{-0.5} \cdot (a_p \cdot d_p)^{0.4}$	4.12	Onda <i>et al.</i> (1967) [43, 44, 19]	$\frac{a_w}{a_p} = 1 - \exp\left(-1.45 \left( \frac{\sigma_{crit}}{\sigma} \right)^{0.75} \cdot Re^{0.1} \cdot Fr^{-0.05} \cdot We^{0.2}\right)$	4.13
			Bravo and Fair (1982) [45, 46]	$\frac{a_w}{a_p} = 19.76 \left( Ca_L \cdot \frac{u_g \cdot \rho_G}{a_p \cdot v_G} \right)^{0.392} \cdot \sigma^{0.5} \cdot h^{-0.4}$ <p>Note that his equation was translated to SI units.</p>	
Kolev (1976) [48, 49]	$k_L \cdot \frac{d_s}{D_{i,L}} = 0.03 \cdot (4Re_L)^{0.5} \left( \frac{a_e}{a_p} \right)^{-0.5} \cdot Ga^{0.28} Sc^{0.5}$	4.14	Kolev (1976) [48, 49]	$\frac{a_e}{a_p} = 0.583 k_\sigma^{0.49} \cdot Fr^{0.196} \cdot (a_p \cdot d_p)^{0.42}$	4.15
Zech and Mersmann (1979) [42, 24]	$k_L = C_1^{-\frac{1}{3}} \left( \frac{6D_{i,L}}{\pi \cdot d_p} \right)^{\frac{1}{2}} \left( \frac{\rho_L \cdot g \cdot d_p}{\sigma} \right)^{-0.15} \left( \frac{u_L d_p g}{3} \right)^{\frac{1}{6}}$	4.16	Zech and Mersmann (1979) [42]	$\frac{a_w}{a_p} = C_1 \cdot Re^{0.5} \left( \rho_L \cdot g \cdot \frac{d_p^2}{\sigma} \right)^{0.45} \cdot (a_p \cdot d_p)^{-0.5}$ <p>Where <math>C_1 =</math>  0.0222 for Berl saddles  0.0155 for Raschig Rings  0.0085 for spheres</p>	4.17
Billet and Schultes (1993) [50, 47]	$k_L = C_L \cdot 12^{\frac{1}{6}} \cdot \left( \frac{\bar{u}_L \cdot D_{i,L}}{h_L \cdot d_h} \right)^{0.5}$ <p>Where</p> $dh = 4 \cdot \frac{\varepsilon}{d_p}$ $h_L = \left( 12 \cdot \frac{\mu_L}{g \cdot \rho_L} \cdot u_L \cdot a_p^2 \right)^{0.33}$ $\bar{u}_L = \frac{u_L}{h_L}$	4.18	Billet and Schultes (1993) [50, 47]	$\frac{a_w}{a_p} = 1.5 \cdot (a_p \cdot d_p)^{-0.5} \cdot \left( u_L \cdot \frac{d_h}{\mu_L} \right)^{-0.2} \cdot \left( \frac{u_L^2 \cdot \rho_L \cdot d_h}{\sigma} \right)^{0.75} \cdot \left( \frac{u_L^2}{g \cdot d_h} \right)^{-0.45}$ <p>Where</p> $dh = 4 \cdot \frac{\varepsilon}{d_p}$	4.19

TABLE 4.2 CONTINUED

Source	Liquid Phase Mass Transfer Coefficient	Equation ID	Source	Effective Interfacial Area	Equation ID
Billet and Schultes (1999) [50]	$k_L = C_L \cdot 12^{\frac{1}{6}} \cdot \left( \bar{u}_1 \cdot \frac{D_{i,L}}{h_L \cdot d_h} \right)^{0.5}$ $\bar{u}_1 = \left( \frac{g \cdot \rho_G \cdot u_V^2}{12 \cdot \mu_L \cdot a_e^2 \cdot \rho_L} \right)^{1/3} \cdot \left( \frac{L}{V} \right)^{\frac{2}{3}} \cdot \left( 1 - \left( \frac{u_v - u_{v,s}}{u_{v,FL} - u_{v,s}} \right)^2 \right)$	4.20	Billet and Schultes (1999) [50]	Considering working above the loading point $h_L = h_{L,s} + (h_{FL} - h_{L,s}) \left( \frac{u_v}{u_{v,FL}} \right)^{13}$ $h_{FL}^3 (3 \cdot h_{FL} - \epsilon) = \frac{6}{g} \cdot a_p^2 \cdot \epsilon \cdot \frac{\mu_L}{\rho_L} \cdot \frac{L}{V} \cdot \frac{\rho_V}{\rho_L} \cdot u_{v,FL}$ $\frac{a_e}{a_p} = \frac{a_{e,s}}{a_p} + (a_{e,FL} - A_{eL,s}) \left( \frac{u_v}{u_{v,FL}} \right)^{13}$ $\frac{a_{e,FL}}{a_e} = 10.5 \left( \frac{\sigma_L}{\sigma_W} \right)^{0.56} (a_p \cdot d_h)^{-0.5} \left( \frac{u_L d_H}{v_l} \right)^{-0.2} \left( u_1 \rho_L \cdot \frac{d_h}{\sigma_L} \right)^{0.75} \left( \frac{u_L^2}{g \cdot d_h} \right)^{-0.45}$	4.21

The models presented in Table 4.2 contain a high degree of uncertainty, although in contrast they are considered more applicable for predictive purposes than the equivalent volumetric mass transfer approximation (Section 4.1.1). The uncertainty originates from the experimentally unproven dimensionless analyses conducted by each research group.

Surface tension was found an example of such a parameter, as no source experimentally evaluated surface tensions below that of water. Consequently, the relevant effect was calculated through dimensionless modelling. The subsequent deviations resulting from the differing dimensionless analyses are presented in Table 4.3. Differing considerations regarding the exponent of the diffusion coefficient and liquid density is given as explanation for the wide spread of the approximations.

**TABLE 4.3: PERCEIVED INFLUENCE OF SURFACE TENSION.**

<b>Reference</b>	<b>Exponent Surface Tension in <math>a_e</math></b>
Krevelen and Hofjizer (1947) [39, 40]	0
Semmelbauer (1967) [41]	-0.5
Onda <i>et al.</i> (1968) [43, 44, 19, 45, 46, 47]	0
Kolev (1976) [48, 49]	-0.49
Zech and Mersmann (1979) [42, 24]	-0.45
Billet and Schultes (1993) [50, 47]	-0.75
Billet and Schultes (1999) [50]	-0.75
Average	-0.42
Standard Deviation	0.31

As illustrated in Table 4.3, largely contradicting thoughts are historically considered regarding the influence of surface tension. This suggest a large empirical component in the presented correlations, limiting their use.

#### 4.1.3. MODELS CHOSEN FOR VALIDATION

The models proposed for evaluation in Sections 4.1.1 and 4.1.2 were screened on the availability of regressed parameters for currently available packing. On this consideration, the following models were eliminated, as they were regressed on either Berl saddles or Raschig Rings:

- [1] Norman [32, 24],
- [2] Mohunta *et al.* [33, 34, 24],
- [3] Krevelen and Hofjizer [39, 40]
- [4] Zech and Mersmann (1979) [42, 24],
- [5] Semmelbauer [41]

The Mangers and Ponter [35] model was omitted from the experimental study, as it was regressed for very viscous liquids.

The following models were consequently identified for the validation of the ADIBAA-method. The choice of models was further justified by Rejl [27], suggesting a comparative fit between the selected models.

- [1] Linek [26] [38, 18, 11] - (Equation 4.7)
- [2] Onda [19] - (Equations 4.12 and 4.13)
- [3] Billet and Schultes [50, 47]- (Equations 4.18 and 4.19)
- [4] Bravo and Fair [45] - (Equations 4.12 and 4.13b)

## 4.2. HISTORIC EXPERIMENTAL EVALUATION OF THE VOLUMETRIC LIQUID MASS TRANSFER COEFFICIENT

A thorough literature study was performed on the historical experimental evaluation of the liquid phase volumetric mass transfer coefficient in packed columns. This was done through considering 39 independent experimental evaluations, 10 systems and 17 types of packing. A summary of the findings is presented in Tables 4.4 and 4.5. The full literature evaluation, with references, is presented in Section 9.1.3 of Appendix A (Tables 9.1 to 9.4).

**TABLE 4.4: LITERATURE SYSTEMS EXPERIMENTALLY EVALUATING LIQUID PHASE MASS TRANSFER COEFFICIENTS.**

<b>System</b>	<b>Absorption</b>	<b>Desorption</b>	<b>Chemical Absorption</b>
Carbon dioxide-water	11		
Aqueous Carbon dioxide-air		7	
Oxygen-water	2		
Aqueous Oxygen		6	
Aqueous Nitrogen; Helium; Hydrogen		2	
Organic solvents	1		
Viscosity alterations	2	2	
Chemical Methods			4
Organic Solutes		2	
Ammonia-water	1		
<b>Total Independent Evaluations</b>	<b>16</b>	<b>19</b>	<b>4</b>

On the account of the literature systems evaluation, presented in Table 4.4, the absorption/desorption of either oxygen or carbon dioxide into an aqueous solution was found historically preferred. This method was traditionally chosen in a bid to remain liquid side mass transfer limiting, while still being relatively easy to quantify the composition experimentally.

As illustrated in the Table 4.5, very little published data were found on modern column internals in terms of mass transfer efficiencies. As such, much room is provided for the evaluations of new generation column internals and subsequently improved sizing estimations. However, the shortage of evaluations

on the newer generation packings, also limited the internals upon which the ABIDAA-method could be validated. The predictive correlations of Section 4.1 where there used as validation on 2' Pall Rings.

TABLE 4.5: PACKINGS AND MATERIALS OF CONSTRUCTION USED IN TABLE 4.4.

<b>Material of Construction</b>								
	Total Number of Evaluations	# Ceramic	# Metal	#Plastic	#Glass	#Inox	#Metal Gauze	Nominal Packing Sizes(mm)
<b>Raschig Rings</b>	28	20	1	3	2			6 up to 50
<b>Sulzer BX</b>	1						1	n/a
<b>Tellerette®</b>			2	1				25
<b>Pall Rings</b>	12		2	7		1		15 up to 50
<b>I®-13 Rings</b>	1						1	25
<b>Bialecki Rings</b>	2		1			1		12 up to 50
<b>Envipak</b>	2			2				#3;32;60;80
<b>Hiflow® ring</b>	5	1	2	2				20; 50; 90-6; 90-6
<b>Top-Pack®</b>	2		2					#2 and 50
<b>Berl Rings</b>	5	2		1				6 up to 38
<b>Spheres</b>	4	1			2			13 up to 38
<b>Rods</b>	1							14
<b>Intalox® saddles</b>	4		2	2				25 up to 38
<b>Norton Intalox® saddles</b>	1		1					25 up to 50

### 4.3. TRANSLATING THE LIQUID MASS TRANSFER COEFFICIENT INTO PACKED COLUMN EFFICIENCY

Transfer units (NTU) are employed in relating mass transfer coefficients to industrial column design [8, 47, 22]. This is preferred, since volumetric mass transfer coefficients vary notably with both concentration and pressure, while the NTU remains theoretically constant [51]. This is advantageous for extrapolating trends across wide ranges, as the reference values for the liquid mass transfer coefficient are often limited to low concentrations and atmospheric systems.

#### 4.3.1. TRANSFER UNIT APPROACH (NTU)

The NTU(number of transfer units) approach was developed in 1935 by Chilton and Colburn [51] in an attempt to fundamentally approximate packed column heights. The ensuing model was based on differentially evaluating a packed column, under the assumption of perfect plug flow. The numerical value for the NTU is used as a depiction of the extent to which the system is removed from equilibrium. Figure 4.1 is provided as a graphical representation of the implications of the NTU model on desorption.



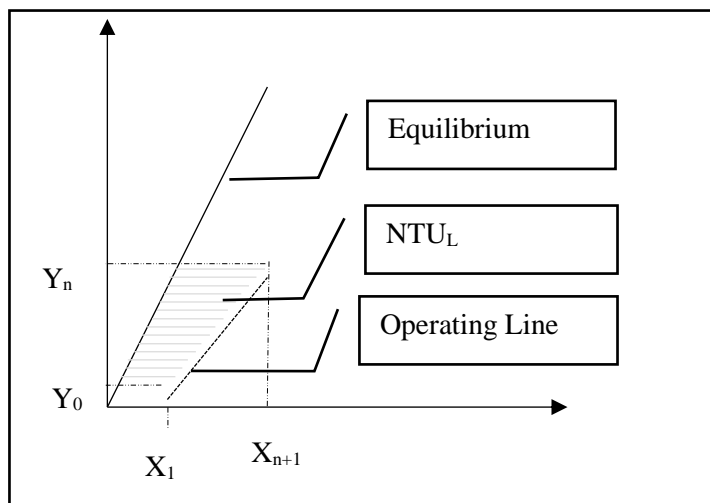


**FIGURE 4.1: GRAPHICAL ILLUSTRATION OF THE NUMBER OF TRANSFER UNITS**

The NTU method is based on evaluating a column as a series of differential transfer areas. A representation of such a differential analysis, for a packed stripping tower is presented in Figure 4.2 (Redrawn from Cussler [22]).

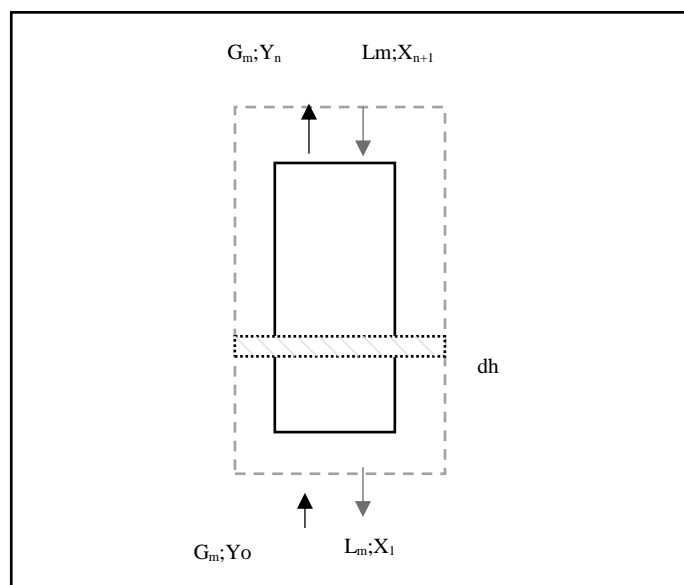


**FIGURE 4.2: DIFFERENTIAL PACKED COLUMN ANALYSIS (REDRAWN FROM CUSSLER [24]).**

A steady state material balance was derived from the presented differential analysis:

$$-d(L' \cdot X) = N_A \cdot a_e \cdot dh = L' \cdot dX + X \cdot d(L') \tag{4.22}$$

With the simplification of binary systems, the rate of mass transfer is approximated as the change in liquid flow rate. Subsequently substituting and solving for the height of packing.

$$H = \int_{x_{n+1}}^{x_1} \frac{L'}{k_L a \cdot \rho_{mol,L} \cdot (X - X^*) (1 - X)} dX. \quad 4.23$$

When considering dilute systems, as in the case of industrial desorbers,  $(1 - X)$  may be assumed to approach unity, simplifying the equation to:

$$H = \int_{x_{n+1}}^{x_1} \frac{L'}{k_L a \cdot \rho_{mol,L} \cdot (X - X^*)} dX. \quad 4.24$$

The basis for the number of transfer unit model is thereby derived through splitting the abovementioned equation into two parts, with HTU representing the Height of the Theoretical Transfer Unit. This analogy is fully illustrated in Equations 4.25 to 4.27.

$$H = HTU_{OL} \cdot NTU_{OL} \quad 4.25$$

Where:

$$HTU_{OL} = \frac{L'}{k_L a \cdot \rho_{mol,L}} = \frac{\dot{L}}{K_{OL} a}; \quad 4.26$$

$$NTU_{OL} = \int_{x_{n+1}}^{x_1} \frac{1}{(X - X^*)} dX. \quad 4.27$$

For cases where both the equilibrium curve and operating line are considered straight, an analytical solution to the integral for NTU may be obtained. The solution (Equation 4.30), through substituting Equations 4.28 and 4.29 into Equation 4.27, was presented by Colburn [51] in a follow-up article in 1939.

$$Y = m \cdot X^* \quad 4.28$$

$$Y = (X_{n+1} - X_1) \cdot \frac{L_m}{G_m} + Y_0 \quad 4.29$$

$$NTU_{OL} = \frac{1}{(1-A)} \ln \left( (1-A) \cdot \left( \frac{X_{n+1} - \frac{Y_n}{m}}{X_1 - \frac{Y_n}{m}} \right) + A \right) \quad 4.30$$

Where the Absorption factor is defined as:

$$A = \frac{L_m}{m \cdot G_m} = \frac{1}{\lambda} \quad 4.31$$

An alternative approximation was presented by Kavanaugh and Trussel [52], for the number of liquid phase mass transfer units. The correlation, Equation 4.32, assumes isothermal plug flow conditions and near linear equilibrium relations.

$$NTU_{OL} = \left(1 - \frac{m_i V_L}{V_G}\right)^{-1} \cdot \ln\left(\frac{m_i V_L}{V_G} \left(1 - \frac{c_{i,1}}{c_{i,2}}\right) + \frac{c_{i,1}}{c_{i,2}}\right) \quad 4.32$$

Equation 4.32 was chosen for use in the experimental evaluation in this thesis, as ample sample data were found upon which to validate the calculation and translation to  $K_{OLA}$ . The calculation procedure for the packed column section of this project, was validated against the works of Linek [18].

#### 4.3.2. COLUMN EFFICIENCY

Although empirical, efficiencies are readily employed in designing new columns. Approximations into column performance are accordingly utilized in estimating either the required packed height, or the number of required trays.

Distillation applications are often considered predominantly gas phase mass transfer limited. As such, it is considered convention to represent efficiencies in terms of the number of overall gas transfer units. The overall number of vapour mass transfer units are therefore related to the single-phase values, in a manner analogous to the mass transfer coefficient approach (presented in Equation 3.12 of Section 3.1). This relationship may be represented as:

$$\frac{1}{NTU_{OG}} = \frac{1}{NTU_G} + \frac{\lambda}{NTU_L} \quad 4.33$$

The NTU-HTU efficiency is often expressed in terms of an empirical height equivalent to a theoretical trays (HETP). This is preferential, since most conventional computational design software are based on tray column calculations, which evaluate the number of theoretical trays required (McCabe Thiele or Ponchon–Savarit). As such, through simple multiplication, the height of the required packed column is calculated. The mathematical transposition of the  $HTU_{OG}$  to HETP is provided in Equation 4.34.

$$HETP = \lambda \cdot HTU_{OL} \cdot \frac{\ln(\lambda)}{\lambda - 1} = HTU_{OG} \cdot \frac{\ln(\lambda)}{\lambda - 1} \quad 4.34$$

The efficiency of a packed column can subsequently be presented through HETP, where a large value depicts low efficiencies, and vice versa.

#### 4.4. CONCLUDING REMARKS ON LIQUID PHASE VOLUMETRIC MASS TRANSFER MEASUREMENTS

On the foundation of the literature systems evaluation (Table 4.4), it was concluded that authors historically favoured the absorption and desorption of either oxygen or carbon dioxide from water, when measuring volumetric liquid phase mass transfer coefficients.

Although proven to be liquid phase limiting, these systems are hampered by two large drawbacks, namely:

- [1] Sizable costs are related to evaluating mass transfer coefficients with this method. This is the case since fresh oxygen and nitrogen are continuously required at flow rates varying from 500 to 2500kg/hr. This estimation is based on the minimum industrially applicable column size of an internal diameter (ID) of 400mm.
- [2] The once-through experimental setup adopted by all authors, requires large plant footprint while extending experimental times. An example of testing times in excess of hour was found quoted by Linek [18].

From the limitations listed above, an alternative method is proposed, stripping volatile organics from an aqueous phase with air (ADIBAA). This method is expected to produce comparable results, as the interfacial transport mechanism remains constant irrespective of component and direction [22, 18, 25]. Validation for this assumption is presented in the volatilization of organics from wastewater by Linek [18]. Similar results follow from recent work by the SRP (Separation Research Program at the University of Texas) on toluene stripping with air [53].

It was, however, opted not to adopt the exact systems published by Linek [18, 29, 26] and Wang [25], with motivation provided as follows:

- [1] In the published works of Linek [18, 29, 26], a column diameter of 290mm was used. This is smaller than the industrially applicable minimum of 400mm. On this parameter, most of the author's work is considered industrially inapplicable, resulting from excess wall effects. It should, however, be noted that with the progression of science, this recommended minimum diameter has changed from 200mm to the now approximated 400mm. The works in question were completed prior to this shift in industrial perceptions.
- [2] Both Linek [18] and Wang [25] neglected the effect of solvent (water) vaporization. The subsequent humidification of the inlet air is expected to skew the results. This is amplified by the parts per million levels of the solute.

- [3] Both authors used once-through experimental setups. This involved continuously using fresh liquid and vapour and expelling the products to either a liquid storage tank or the atmosphere. The systems were allowed one hour to stabilize before quantification of the mass transfer coefficients. Upon completion, the liquid inventory in the storage tank was re-analysed and make-up solute was added. In the case of the industrially preferred oxygen desorption system, the liquid was either re-saturated with oxygen or aerated to return the solution to the initial conditions. After the solution was returned to the required composition, it was reused in consecutive tests.

The aforementioned procedure notably contributes to the overall experimental times. In addition, the experimental setups required sizable holdup tanks which added to overall plant footprint. In considering a 400mm ID (internal diameter) column, this is expected to translate into at least two, 15 m<sup>3</sup> tanks for use up- and downstream of the column.

- [4] Both authors used desorption of cyclic hydrocarbons (toluene [25] and benzene [18]) into air for measuring the volumetric liquid phase mass transfer coefficient. These solutes are known carcinogens and entail notable risks to both human and animal life. They are thus considered unfit for use.

Based on the shortcomings of both desorption of oxygen and cyclic hydrocarbons, this thesis proceeded with the development of an alternative method for measuring liquid phase mass transfer. The resulting ADIBAA-method is presented in Section 6.1. This method focuses on using simple and cost-effective liquid phase mass transfer coefficients to evaluate complex packing interactions



# CHAPTER 5: TRAY COLUMN LITERATURE

## 5.1. LIQUID VERSUS VAPOUR MASS TRANSFER LIMITING

Both liquid and vapour phase measurements were conceptually considered for evaluating and comparing mass transfer in tray columns. The inclusion of the liquid phase analysis was warranted as Lockett [16] suggested that liquid phase limitations are incorrectly discounted in tray columns. Motivation for this statement is presented in Figure 5.1. The figure is presented on the basis of a model comparison by Lockett [16] in his 1986 publication of tray column fundamentals. The capacity and flow factors used for the duration of this thesis, are defined in the glossary under *Column flow definitions* (page xxvi).

According to Lockett, the Zuiderweg [8] slope method provided a sufficiently accurate approximation of relative resistances [16]. In contrast, the AIChE [54], Chan & Fair [55] and Stichlmair [47] approximations have been proven to underestimate the effect of liquid resistance [16], due to the use of Equation 5.23 (Section 5.5.1) in correlating both vapour and liquid phase efficiencies. This is further discussed in Section 5.5.

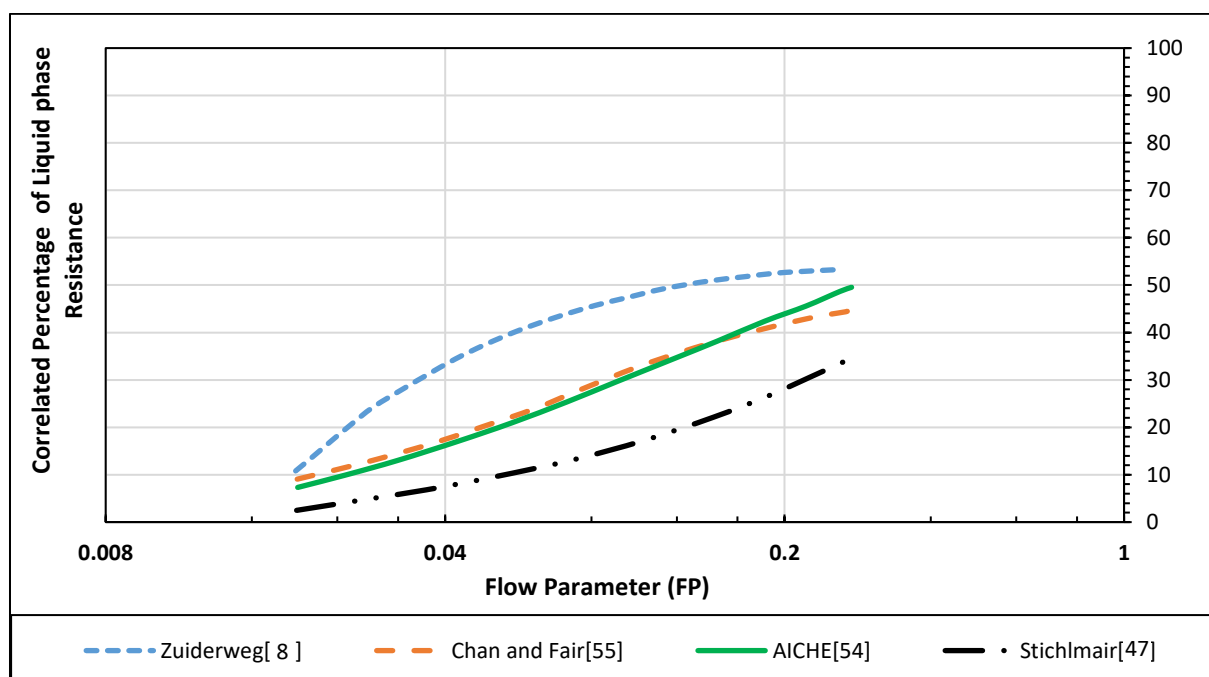


FIGURE 5.1: PERCENTAGE LIQUID PHASE RESISTANCE IN TRAY COLUMNS REDRAWN FROM LOCKETT [16].

Figure 5.1 presents the notion of notable liquid phase resistance at medium to high flow parameters. This notable significance of the liquid phase resistance suggested the possibility of using liquid phase resistance in quantifying tray column performance.

This is beneficial as it traditionally involves simplified and cost-effective sampling techniques. Warranting further evaluation, a review was conducted on liquid phase mass transfer in tray columns.

This review illustrated that tray systems focused on liquid phase mass transfer, presented very low vapour point efficiencies (Section 5.5.2) as a result of the high volatility of the solutes (large equilibrium values) [16]. Efficiencies as low as 1% (quoted by Lockett [16]) were found as a case in point.

Stemming from the low efficiencies, little differentiation between column internals is expected in using liquid phase mass transfer to approximate tray column efficiency. This eliminated the use of this method. It was consequently decided to focus the tray column section on vapour phase mass transfer, as efficiencies between 60% and 80% were common for most sieve trays [16].

In a similar strategy to that employed in the packed column section, a full literature review was conducted with the idea of highlighting possible alternatives as well as presenting comparative models with which to validate the HA-method.

## 5.2. VAPOUR PHASE PREDICTIVE CORRELATIONS

Mass transfer efficiencies are predominantly related to tray column applications by way of the NTU model proposed by Chilton and Colburn [51] in 1935. This preference, compared to mass transfer coefficients in the packed column section, resulted from the dependence of mass transfer coefficients on froth or spray heights atop the trays.

### 5.2.1. VAPOUR NTU MODELS

Based on a variety of literature experimental data, the provided correlations (Table 5.1) illustrated relatively poor predictive capabilities [16]. According to Lockett [16], this is as a result of the simplified basis upon which all the authors related the measured Murphree vapour phase point efficiencies to the NTU model (Equation 5.23). The use of Equation 5.23 therefore provides an underestimation of the  $NTU_G$  by a factor that ranges between 4 and 20 times [16]. This translates into bias of the relevant correlations (Table 5.1) toward overpredicting point efficiencies. These correlations are consequently not expected to illustrate applicable predictive capabilities on systems with largely varying physical properties.



TABLE 5.1: CORRELATIONS FOR THE PREDICTION VAPOUR PHASE TRANSFER UNITS (NTU).

Source	Date	Equations	Equation ID	Systems evaluated
AIChE [16, 54]	1958	<b>Bubble caps and Sieve Trays</b> $NTU_G = \left( 0.776 + 4.57 \cdot h_w - 0.238 \cdot F_s + 104.8 \cdot \frac{Q_L}{W} \right) \cdot Sc_G^{-0.5}$ $NTU'_L = 1.97 \times 10^4 \cdot D_{iL}^{0.5} \cdot (0.4 \cdot F + 0.17) \cdot t_L$ where $t_L = h_{cl} \cdot Z \cdot \frac{W}{Q_f}$ $NTU_{OG} = \left( \frac{1}{NTU_G} + \frac{\lambda}{NTU'_L} \right)^{-1}$ $h_{cl} = (0.29' \cdot h_w - 0.0135 \cdot F_s + 2.45 \cdot \frac{Q_L}{W} + 0.04$ $) + \frac{u_s \cdot \rho_g (u_h - u_s)}{\rho_l \cdot g}$	5.1	Absorption of NH <sub>3</sub> from air in water; Distillation or acetone/benzene
		<b>For Sieve trays</b> $NTU_G = (0.3 + 15 \cdot t_G) \cdot Sc_G^{-0.5}$ $t_G = \frac{\beta}{u_{s'}}$ $\beta = (h'_f - h_{cl}') / 12$ $hf = 0.25 + F_{s'} + 0.75 \cdot \frac{h_w'}{0.0254} + 0.1 \cdot Q_{w1}'$ $h_{cl} = 0.25 + 0.58 \cdot h_w' + 0.03 \cdot Q_{w1}' - 0.28 \cdot h_w' \cdot F'_s$ $NTU'_L = \left( 5 + 10 \cdot t_L (1 + 0.17(0.82 \cdot F_s - 1)(39.2 \cdot h_w + 2)) \right) \cdot Sc_L^{-0.5}$	5.2	Humidification of air
Asano & Fujita [16]	1966	<b>Sieve Trays</b> $NTU_G = 5.85 \cdot Sc_G^{-0.5} \cdot \left( u_h \cdot d_h \cdot \frac{\rho_G}{\mu_G} \right)^{-0.25} \cdot P$ $NTU'_L = 460 \left( n_r \cdot \frac{d_h}{\text{Diameter of Column}} \right) \cdot Sc_L^{-0.5} \cdot \left( \frac{h_{CL}}{d_h} \right)^{-0.5} \cdot P$ where $P = \left( u_h^2 \cdot \frac{\rho_G}{d_h \rho_L} \right)^{0.17} \left( \frac{h_{CL}}{d_h} \right)^{0.15} \cdot \left( \frac{d_h^2 \cdot g \cdot \rho_L}{\sigma} \right)^{0.1}$	5.3	Desorption
Jeromin et al [57, 16]	1969	<b>Sieve Trays</b> $NTU_G = Sc_G^{-0.5} \left( 1.2 + 4.57 \cdot h_w - 0.238 \cdot F_s + 106 \cdot \frac{Q_L}{W} \right) + \Gamma$ <i>Where <math>\Gamma = \text{Foaming Factor}</math></i> $NTU'_L = 2.03 \times 10^4 \cdot D_{iL}^{0.5} \cdot (0.175 \cdot F + 0.15) \cdot (1 - \lambda^2)$	5.4	Desorption
Chan and Fair [55, 16]	1984	$NTU_G = \frac{1000 \cdot (D_G)^{0.5} \cdot (10.3 \cdot (FF) - 8.67 \cdot (FF)^2) \cdot t_G}{h_{cl}^{0.5}}$ <i>where</i> FF= Fractional approach to flooding Offering best fit when coupled with Bennet (1983) $t_G = (1 - \alpha_e) \cdot \frac{h_{CL}}{\alpha_e \cdot u_s}$ $h_{CL} = \alpha_e \cdot (h_w + C \cdot \left( \frac{Q_L}{W \cdot \alpha_e} \right)^{0.67})$ $\alpha_e = \exp(-12.55 \cdot \left( u_s \cdot \left( \frac{\rho_G}{\rho_L - \rho_G} \right)^{0.5} \right)^{0.91})$ $C = 0.5 + 0.438 \cdot \exp(-137.8 \cdot h_w)$ With the number of liquid transfer units evaluated by way of the AIChE model	5.5	Distillation
Chen and Chuang [58]	1993	$NTU_G = C_1 \cdot \frac{1}{\mu_L^{0.1} \cdot \phi^{0.14}} \cdot \left( \rho_L \cdot \frac{F_s^2}{\sigma_L} \right)^{\frac{1}{3}} \cdot \left( D_G \cdot \frac{h_L}{u_s} \right)^{0.5}$ Where $\phi = \text{Fraction tray open area}$ $C_1$ is a fitted constant	5.6	Distillation from Yanagi and Sakata [59]

## 5.2.2. VAPOUR SIDE MASS TRANSFER AND EFFECTIVE INTERFACIAL AREA CORRELATIONS

Present knowledge of the interfacial area in tray columns is still considered poor, as published data were found to differ by a factor of 10, due to the implementation of contradicting techniques [47]. Taking this into account, very few predictive correlations were found applicable within this section. The predictive correlations are presented in Table 5.2.

With the exception of the presented models, the separate evaluation of the interfacial area and vapour phase mass transfer coefficients, were industrially received with very little acceptance [16]. This is based on their lack of theoretical foundation [16]. Both the Stichlmair [47, 16] and Zuiderweg [8] correlations (Equations 5.7 and 5.8) were developed through reverse engineering distillation column efficiency data (thus constant reflux). In using distillation data (from the Fractionation Research Institute (FRI)), no isolation could be made regarding the effect of individual physical properties. This is as physical properties change in unison in distillation evaluations. As is the case, the predictive accuracy of the provided correlations is questionable in cases of changing physical properties [16].

Although Stichlmair [47, 16] claimed good fit to experimental data, the contrary was proven by Lockett [16] in comparing the model to a variety of other literature sources. Justification for this lack of fit was attributed to difficulties in predicting flooding velocities, as well as the uniform bubble formation simplification used. Additionally, the model made no attempt to quantify bubble coalescence, which in itself can notably affect bubble sizes and the interfacial area.

Opting to address the problem from a different angle, the Neuburg [60] correlation (Equation 5.9) evaluated the comparison between counter current mass transfer and the Girdler-Sulphide process of producing heavy water [16]. This method translates well with the bubble diameters fitted to pilot plant data.

**TABLE 5.2: PREDICTIVE CORRELATIONS FOR BOTH VAPOUR MASS TRANSFER COEFFICIENT AND EFFECTIVE INTERFACIAL AREA WITHIN TRAY COLUMNS.**

Source	Vapour Phase Mass Transfer Coefficient	Source	Effective Interfacial Area	Equation ID
	<b><u>Extrapolation of distillation data</u></b>		$h_f = \frac{h_{cl}}{(1 - \varepsilon)}$ $\alpha = 1 - \left( \frac{F_s}{F_{s,max}} \right)^{0.28}$ $F_{s,max} = 2.5 \cdot (\phi^2 \cdot \sigma_L \cdot (\rho_L - \rho_G) \cdot g)^{0.25}$ Where $F/F_{max} < 0.7$ $a = a_b - \left( \frac{F_s}{F_{s,max} \cdot 0.7} \right)^2 \cdot (a_B^* - a_T^*)$ $a_B = \left( \frac{F}{F_{max} \cdot 0.7} \right)^2 \cdot (a_B^* - a_T^*)$ Where $a_B = 6 \cdot \left( \frac{(\rho_L - \rho_G) \cdot g}{6 \cdot \sigma} \right)^{0.5} \cdot \left( \frac{F}{F_{max}} \right)^{0.28}$ $a_B^* = 6 \cdot \left( \frac{(\rho_L - \rho_G) \cdot g}{6 \cdot \sigma} \right)^{0.5} \cdot (0.7)^{0.28}$ $a_T^* = \frac{(0.7 \cdot F_{max})^2}{2 \cdot \sigma \cdot \phi^2} \cdot (1 - 0.7^{0.28})$	
Stichlmair (1978) [47, 16]	$k_G = 2 \cdot \left( \frac{D_{1,G} \cdot u_{s,G}}{\pi \cdot h_f \cdot \varepsilon} \right)^{0.5}$ $k_L = 2 \cdot \left( \frac{D_{1,L} \cdot u_{s,G}}{\pi \cdot h_f \cdot \varepsilon} \right)^{0.5}$ $\varepsilon = 1 - \alpha$ $h_{cl} = (1 - \varepsilon) \cdot \left( h_w + \frac{0.49}{C_d^{0.67}} \cdot \left( \frac{Q_L}{(1 - \varepsilon) \cdot W} \right)^{0.67} + \frac{125 \cdot (u_s - u_b)^2 \cdot \rho_G}{g \cdot (\rho_L - \rho_G) \cdot \varepsilon^2} \right)$ $u_b = 1.55 \cdot \left( \sigma_L \cdot (\rho_L - \rho_G) \cdot \frac{g}{\rho_L^2} \right)^{0.25} \cdot \left( \frac{\rho_G}{\rho_L} \right)^{\frac{1}{24}}$ Cd=0.61 According to Lockett	Stichlmair (1978) [47, 16]	Where $F/F_{max} > 0.7$ $a = \frac{F^2}{2 \cdot \sigma \cdot \phi^2} \cdot (1 - (F/F_{max})^{0.28})$	5.7
	$k_G = \frac{0.13}{\rho_G} - \frac{0.065}{\rho_G^2}$ $k_L = 0.024 \cdot D_{1,L}^{0.25}$		<b>Spray Regime</b> $a \cdot h_f = \frac{40}{\phi^{0.3}} \cdot \left( \frac{u_{s,G} \cdot \rho_G \cdot FP \cdot h_{cl}}{\sigma_L} \right)^{0.37}$ <b>Mixed Froth and Emulsion Regime</b> $h_{cl} = 0.6 \cdot (\psi \cdot p)^{0.25} \cdot h_w^{0.5}$ $\psi = \frac{Q_L}{W \cdot u_s} \cdot \left( \frac{\rho_L}{\rho_G} \right)^{0.5}$ where $0.007m < d_h < 0.01m$	
Zuiderweg (1982) [8, 16]	Where densities range between 1 and 80 kg.m <sup>-3</sup>	Zuiderweg [8]		5.8
Neuburg and Chuang [16, 60]	$K_{OG} a = 12 \cdot \left( D_L \cdot u_s \cdot \frac{\varepsilon}{\pi \cdot d_b^3} \right)^{0.5} \cdot \left[ \left( \frac{D_L}{D_G} \right)^{0.5} + \frac{m \cdot \rho'_G}{E' \cdot \rho'_L} \right]^{-1}$ Where E' =Enhancement factor for chemical reactions. Distillation E'=1			5.9

CONTINUATION OF TABLE 5.2.

Source	Vapour Phase Mass Transfer Coefficient	Source	Effective Interfacial Area	Equation ID
	$E_{OG} = (1 - f_i)E_B + f_i \cdot E_j$ $E_b = (1 - \pm F_{SB}) + E_{LB} \cdot E_{SB}$ $NTU_G = a_G \cdot k_G \cdot t_G$ $NTU_G = a_L \cdot k_L \cdot t_L$ $a_L \cdot t_L = \frac{\rho_L \cdot \dot{M}_G}{\rho_G \cdot \dot{M}_L} \cdot a_G \cdot t_G$ $NTU_{OG} = \frac{1}{NTU_G} + \frac{\lambda}{NTU_L}$ $E_{OG} = 1 - \exp(-NTU_{OG})$ $a_G = \frac{6}{d_{32L}}$ $t_{GLB} = \frac{h_F}{u_{LB}}$ $d_{32L} = 0.887 \cdot d_h^{0.846} \cdot u_h^{0.21}$ $u_{LB} = 2.5 \cdot V_{LB}^{\frac{1}{6}} + u_s$ $k_{LLB} = 1.13 \cdot \left( \frac{D_G}{t_{GLB}} \right)^{0.5}$ <p>If <math>40 &lt; Pe &lt; 200</math>  <math>Sh = -11.878 + 25.879 \cdot (\log(Pe_G)) - 5.64 \cdot (\log(Pe_G))^2</math>                      If <math>Pe &gt; 200</math> the <math>Sh = 17.9</math></p> <p>Offering best fit when coupled with Bennet (1983)</p> $t_G = (1 - \alpha_e) \cdot \frac{h_{CL}}{\alpha_e \cdot u_s}$ $h_{CL} = \alpha_e \cdot (h_w + C \cdot \left( \frac{Q_L}{W \cdot \alpha_e} \right)^{0.67})$ $\alpha_e = \exp(-12.55 \cdot \left( u_s \cdot \left( \frac{\rho_G}{\rho_L - \rho_G} \right)^{0.5} \right)^{0.91})$ $C = 0.5 + 0.438 \cdot \exp(-137.8 \cdot h_w)$ $h_f = \frac{h_{cl}}{a_e}$ $\overline{N_f} = N_{iB} \cdot \exp(-k\Delta t)$ $\overline{N_s} = 2 \cdot (N_{iB} - \overline{N_f})$ $F_{SB} = \overline{N_s} \cdot \frac{V_s}{(\overline{N_s} \cdot V_s + \overline{N_f} \cdot V_L)}$ $k\Delta t = C'' \cdot \frac{h_w^{0.5} \cdot \rho_L^{0.1} \cdot \rho_G^{0.3}}{\sigma^{0.4}} \cdot (u_s \cdot g)^{0.6}$ $C'' = 0.16$		<p><b>Spray Regime</b></p> $ah_f = \frac{40}{\phi^{0.3}} \cdot \left( \frac{u_{s,G} \cdot \rho_G \cdot FP \cdot h_{CL}}{\sigma_L} \right)^{0.37}$ $k_G = \frac{0.13}{\rho_G} - \frac{0.065}{\rho_G^2}$ $k_L = 0.024 \cdot D_{i,L}^{0.25}$ $E_j = 1 - \exp(-K_{OG} \cdot a \cdot \frac{h_f}{u_s})$ $h_{CL} = 0.6 \cdot \frac{h_w^{0.5}}{W/A_b} \cdot FP^{0.25}$ $f_i = -0.1786 + 0.9857 \cdot (1 - \exp(-1.43 \cdot F_s, \text{ bubbling}))$ $V_s/V_s=5$	
Syeda (2007) [61]				5.10

The final and most computationally intensive model (Equation 5.10) by Syeda [61] proceeded to evaluate the froth regime as a series of separate bubbles and jets. This model made use of various correlations in predicting mass transfer coefficients, interfacial area as well as the fraction of vapour bypassing in the jets. The contribution provided by this model, was the bubble breakage theory, solved for the critical Webber number. Although novel in their approach, various discrepancies were found. These discrepancies warrant display in the main body of this report, as this model is the latest publication that attempts to quantify the interfacial area in a tray column.

- [1] The equations highlighted **Red** and blocked (Table 5.2) were found to be either doubtful or incorrect. In the case of the liquid height, the equation was misquoted from the original Zuiderweg [8] paper. Evaluation of the bubble breakage model also found that when comparing the equation with the original training data published by Yanagi [59] (1982), the small bubble fraction ( $F_{SB}$ ) remained equal to one for all flow rates. It was thus deduced the “3.8” was effectively lumped in  $C''$  factor and accidentally misquoted in the Syeda [61] paper.
- [2] The evaluation of the data used to train the Syeda model provoked further scepticism. The Yanagi paper quoted the maximum attainable flow factor (at flooding under total reflux ;14% open area Sieve tray) to be:
  - i.  $F_S = 2.5$  at Pressure 34 kPa;
  - ii.  $F_S = 2.3$  at Pressure 165 kPa;
  - iii.  $F_S = 1.6$  at Pressure 1138 kPa.

This was found to be in contradiction with the recreated values in the Syeda graphs. The Syeda [61] graphs quoted:

- i.  $F_S = 3.2$  at Pressure 34 kPa;
- ii.  $F_S = 3.8$  at Pressure 165 kPa;
- iii.  $F_S = 2.3$  at Pressure 1138 kPa.

The Syeda [61] evaluation of efficiencies above the flooding point seemed highly unlikely (quoting flooding efficiencies in excess of 80%).

- [3] Additionally, the Syeda published work quoted Murphree point efficiencies in the Yanagi [59] paper. This, however, seemed unlikely as the original author only evaluated an overall Murphree tray efficiency, which averaged over nine trays. The original data only presented compositional measurements in the reboiler and reflux pot. This suggests that Syeda [61] used the Lewis case models (see Section 5.5.2), in translating point to tray efficiencies. The proposed technique requires an accurate estimation of flow distribution and hydrodynamic variables. This creates a further notion of doubt regarding the model, as only entrainment was evaluated in the Yanagi [59] work.

- [4] The final motivation of the reported cynicism was found to be resulting from a mathematical inconstancy, intrinsic to the model. The author quoted binary bubble breakage, with the insinuation that one bubble divides into two.

This approximation in itself is not mathematically inconstant. The author [61], however, approximated the number of small bubbles as twice the that of the difference between large and the small bubbles (Equations 5.11 and 5.12). This suggests that a single large bubble breaks into two smaller bubbles and therefore fails to conserve mass (See Equation 5.13).

$$\bar{N}_f = N_i \cdot \exp(-k \cdot \Delta t) \quad 5.11$$

$$\bar{N}_s = 2 \cdot (N_i - \bar{N}_f) \quad 5.12$$

$$\text{Mass Ratio} = \frac{\frac{4}{3} \cdot \pi \cdot \left(\frac{d_{LB}}{2}\right)^3 \cdot \rho_G}{\frac{4}{3} \cdot \pi \cdot \left(\frac{d_{SB}}{2}\right)^3 \cdot \rho_G} = \left(\frac{d_{LB}}{d_{SB}}\right)^3 = 125 \quad 5.13$$

The balance presented in Equation 5.13, is based on the assumption of constant vapour density and a quoted ratio of the large to small bubble diameter, of five [61]. The mass of a single small bubble is thus considered to be 1/125<sup>th</sup> that of the large bubble. The mathematical depiction in Equation 5.12 thus fails to conserve mass as one bubble of mass “x” breaks into two of equal mass “1/125.x”. More than 98% of the vapour mass is therefore lost through this correlation.

Considering the motivations presented above, little predictive accuracy is expected for any of these correlations.

### 5.2.3. CONCLUDING REMARKS ON THE PREDICTIVE CORRELATIONS

The correlation presented in Section 5.2 were evaluated for additional validation of the HA-method. The following are proposed for comparison in Chapter 7:

- [1] AIChE [54] - Equation 5.1
- [2] Harris [56] - Equation 5.2
- [3] Chan & Fair [55] - Equation 5.5
- [4] Stichlmair [47] - Equation 5.7
- [5] Syeda [61] - Equation 5.10
- [6] Zuiderweg [8] - Equation 5.8

The use of the presented correlations was justified at hand the of the author’s experimental setups and available parameters. The AIChE [54] and Harris [56] models were included as both were derived from desorption data, being ammonia and water respectively. The Chan & Fair [55] correlation used a combination of distillation and absorption data, while Zuiderweg [8], Syeda [61] and Stichlmair [47]

focussed on constant reflux. The spread of the experimental setups was therefore included to provide an adequate representation of tray column systems.

### 5.3. HISTORIC EXPERIMENTAL EVALUATION OF MASS TRANSFER IN TRAY COLUMNS

Most of the industrially applicable experimental data on tray column mass transfer, were produced in conjunction with the Fractionation Research Institute (FRI, Stillwater USA). This inhibited the movement of the data into the public domain. As such, very few sources presented data and opted to rather publish models. Table 5.3 is presented, summarizing the relevant findings.

TABLE 5.3: HISTORIC TRAY COLUMNS EXPERIMENTAL EVALUATIONS.

Source	Date	System	Bubbling Area	Number of trays	Tray Types
Ashley [62]	1955	Air/water; Helium/water; Freon/water; Helium/isobutyl alcohol; Nitrogen/isobutyl alcohol and Helium/ isobutyl ketone	Illegible from scanned document	5	bubble cap
Zuiderweg [8]	1982	cyclohexane/n-heptane	FRI data not disclosed	FRI data	Sieve Trays
Zuiderweg [8]	1982	i-butane/n-butane.	FRI data not disclosed	FRI data	Sieve Trays
Yanagi et al [59]	1982	i-butane /n-butane	0.859 m <sup>2</sup>	FRI data	Sieve 14% open Area
Yanagi et al [59]	1982	cyclohexane/n-heptane	0.859 m <sup>2</sup>	FRI data	Sieve 14% open Area
Scheffe & Weiland [63]	1987	Chemical Absorption of SO <sub>2</sub> into aqueous buffer solutions.	0.372 m <sup>2</sup>	1	Glitch V1 Stainless Steel
Peytavy <i>et al.</i> [64]	1990	Chemical Absorption of SO <sub>2</sub> into aqueous buffer solutions.	0.527 m <sup>2</sup>	3	Sieve + Bubble cap + Valve

Both Scheffe & Weiland [63] and Peytavy et al. [64] evaluated the vapour phase volumetric mass transfer coefficient using chemical absorption. The relevant systems were considered outside the scope of this project, due to the added electrolytes interfering with bubble coalesce [16]. As a result, the experimental data varied widely between the authors. In addition, these methods entail sizable waste production, as the lye solution is to be treated before disposal. This is in disagreement with initial aims outlined in Section 1.4.

From the literature models (Table 5.2) and experimental data (Table 5.3), it was deduced that tray column efficiencies were preferentially evaluated under conditions of constant reflux, using the Fenske-Underwood equations. The literature experimental evaluations used composition measurements in quantifying the extent of the achieved separation. Section 5.4 and 5.5 and subsequently provided in





$$NTU_{OG} = \int_0^{h_f} K_{OG} \cdot \rho_{mol,V} \cdot a \cdot \frac{dh}{G'} = \frac{K_{OG} a \cdot h_f \cdot \rho_{mol,V}}{G'} \quad 5.16$$

Equation 5.16 is simplified using the twin resistance model proposed in Equation 3.12 of Section 3.1 [16]. In cases where the resistance in either the vapour or liquid phase approaches zero, the following refinements are considered [16]:

Gas phase resistance limiting ( $K_{OG}=k_g$ ):

$$NTU_G = \frac{k_G a \cdot h_f \cdot \rho_{mol,V}}{G'} \quad 5.17$$

Liquid phase resistance limiting ( $K_{OG}=k_L/m$ ):

$$NTU_L = \frac{k_L a \cdot h_f \cdot \rho_{mol,L}}{G' \cdot K} \quad 5.18$$

## 5.5. TRAY COLUMN EFFICIENCY

Analogous to packed columns, tray column efficiencies are evaluated in terms of the number of vapour transfer units. However, as a result of different derivations illustrated in Section 4.3.2, separate expressions are employed. Subsequently, through combination of Equations 5.17 and 5.18, the number of overall vapour transfer units for tray columns is expressed as:

$$\frac{1}{NTU_{OG}} = \frac{1}{NTU_G} + \frac{1}{NTU_L} \quad 5.19$$

In relating experimental efficiencies to the NTU model, a combination of Murphree point, tray and overall section efficiencies are employed. Elaboration on the differences is presented in Figure 5.3 (Adapted from Lockett [16]).

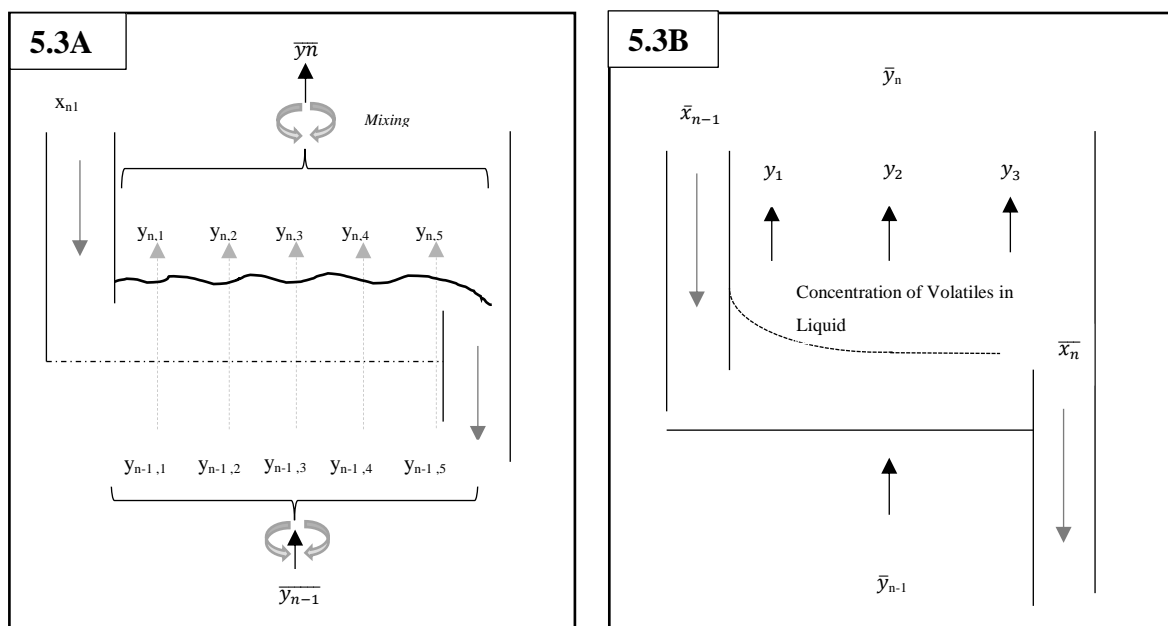


FIGURE 5.3: SCHEMATIC OF DIFFERENT EFFICIENCIES. 5.3A DEPICTS THE MURPHREE TRAY EFFICIENCIES. 5.3B PRESENTS MURPHREE POINT EFFICIENCIES. ADAPTED FROM LOCKETT [18]

Based on the assumption of plug flow in the vapour phase, Murphree point efficiencies are defined on the streamline of vapour at the outlet weir of a tray (See Figure 5.3 B). This is mathematically defined as:

$$E_{OG} = \frac{y_3 - \bar{y}_{n-1}}{y_N^* - y_{n-1}} \quad 5.20$$

where

$$y_N^* = m \cdot \bar{x}_N^* + b \quad 5.21$$

As the liquid travels along the tray, the concentration of the volatile components in the liquid phase decreases. This decreases the driving force for mass transfer and creates profiles similar to those presented in Figure 5.3B. Murphree tray efficiencies (Equation 5.22) are therefore used in translating the efficiencies recorded at the outlet weir (point efficiency), to an average efficiency (See Figure 5.6A):

$$E_{MV} = \frac{\bar{y}_N - \bar{y}_{n-1}}{y_N^* - \bar{y}_{n-1}} \quad 5.22$$

Tray efficiencies are predominantly expected to be larger than point efficiencies, resulting from changing liquid composition across the flowpath. A variety of literature sources have extensively studied this behaviour and approximated it to multiple well-mixed pools in a plug flow. [16, 65, 66]. As evident from their studies, favourable cases have been noted to evaluate efficiencies in excess of 100% [16]. This phenomenon is known as crossflow enhancement, where notably higher tray efficiencies are evaluated compared to point efficiencies.

Many authors have opted to evaluate and model points efficiencies rather than the average composition counterpart, due to the fundamental superiority. This led to the creation of various models, aiming to predict the relationship between Murphree point and tray efficiencies, as well as the translation of these models into the NTU approach.

### 5.5.1. RELATING MURPHREE POINT EFFICIENCIES TO NTU APPROACH

Two historical approaches are widely found in early literature, depending on the assumption of plug-flow or a well-mixed (vertical) vapour phase. These approximations are known to oversimplify complex phenomena [16]. Amongst others, these models propose an equal vapour residence time, regardless of bubble size. This adversely affected the literature models that used these relationships [55, 58, 8, 57].

***Presented for vapour plug flow:***

$$E_{OG} = 1 - \exp(-NTU_{OG}) \quad 5.23$$

**Presented for a well-mixed (Vertical) vapour phase:**

$$E_{OG} = \frac{NTU_{OG}}{NTU_{OG}+1} \quad 5.24$$

Although more computationally intensive models have been proposed in recent years, they have found very little industrial traction. This results from their empirical approximation of key parameters that have been unquantifiable to date. One such model, proposed by Ashley and Haselden [67], attempted to individually evaluate separate bubble size fractions, their mass transfer coefficients and bubble rise velocities. This model is based on the plug flow approximation of Equation 5.23 and divided the evaluation to two size factions.

Methodically stated:

$$E_{OG} = 1 - f_1 \cdot \exp\left(\frac{-6 \cdot NTU_{OG} \cdot u_S}{a \cdot d_{b1} \cdot u_{b1}}\right) - (1 - f_1) \cdot \exp\left(\frac{-6 \cdot NTU_{OG} \cdot u_S}{a \cdot d_{b2} \cdot u_{b2}}\right) \quad 5.25$$

$$u_{b2} = \frac{u_S(1-\varepsilon'_1)}{\varepsilon-\varepsilon'_1} - \frac{u_{b1} \cdot \varepsilon'_1 \cdot (1-\varepsilon)}{\varepsilon-\varepsilon'_1} \quad 5.26$$

$$f_1 = \frac{u_{b1} \cdot \varepsilon'_1 \cdot (1-\varepsilon)}{u_S(1-\varepsilon'_1)} \quad 5.27$$

$$a = 6 \cdot u_S \sum_{i=1}^n \frac{f_i}{d_{b,i} \cdot u_{b,i}} \quad 5.28$$

where the parameters in Equations 5.25 to 5.28 are defined as

$f$  is the fraction of bubbles within the specified fractions;

$d_b$  is the bubble diameter;

$u_b$  is the bubble rise velocity;

$\varepsilon'$  is the volume fraction of small bubbles;

$\varepsilon$  is the volume fraction of vapour holdup.

This approximation requires various simplifications in order to be solvable. This limits the applicability of this model, as most of the variables were found unquantified in literature. However, it still provided added insight on the simplifications made by Equations 5.23 and 5.24. A comparison of these models, based on varying interfacial area, is presented in Figure 5.4. This comparison was initially presented by Lockett [16]. Parameter assumptions, similar to those presented by Lockett [16], were used in solving Equations 5.25 to 5.28 .

The simplifications made in Equations 5.23 and 5.24 are seen to over-predict point efficiencies (in Figure 5.4), when evaluating NTU greater than 0.1. The greater driving force behind larger NTU values, cause the smaller bubbles to approach equilibrium, slowing down the kinetics of mass transfer and

decreasing the effective interfacial area [16]. This suggests the dominating effect of larger bubbles in systems where  $NTU > 0.1$ , as the numerous smaller bubbles contribute little to the greater molecular bulk vapour. This size dependence (Figure 5.4) presents the count intuitive notion of the irrelevance of total interfacial area, on the mass transfer in tray columns (under high NTU). This is explicitly evaluated in Figure 5.5, through the use of a small bubble vapour fraction of 0.5 (calculated though Equations 5.25 to 5.28).

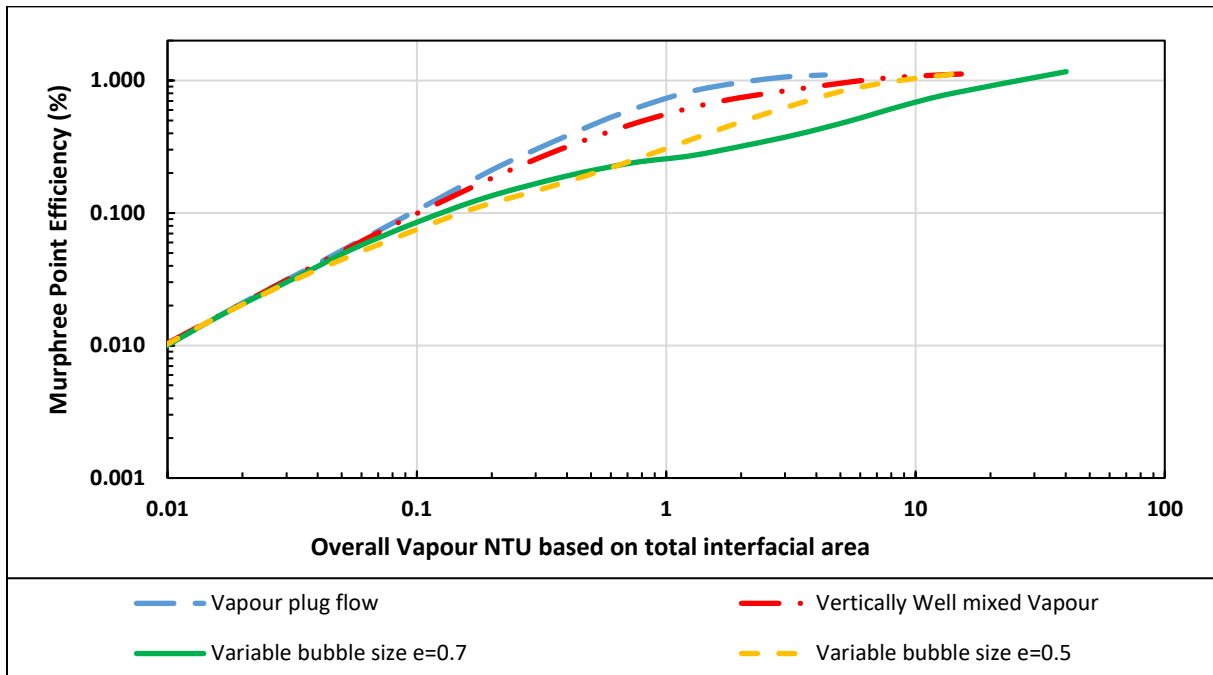


FIGURE 5.4: MODELS RELATING POINT EFFICIENCIES TO NTU.

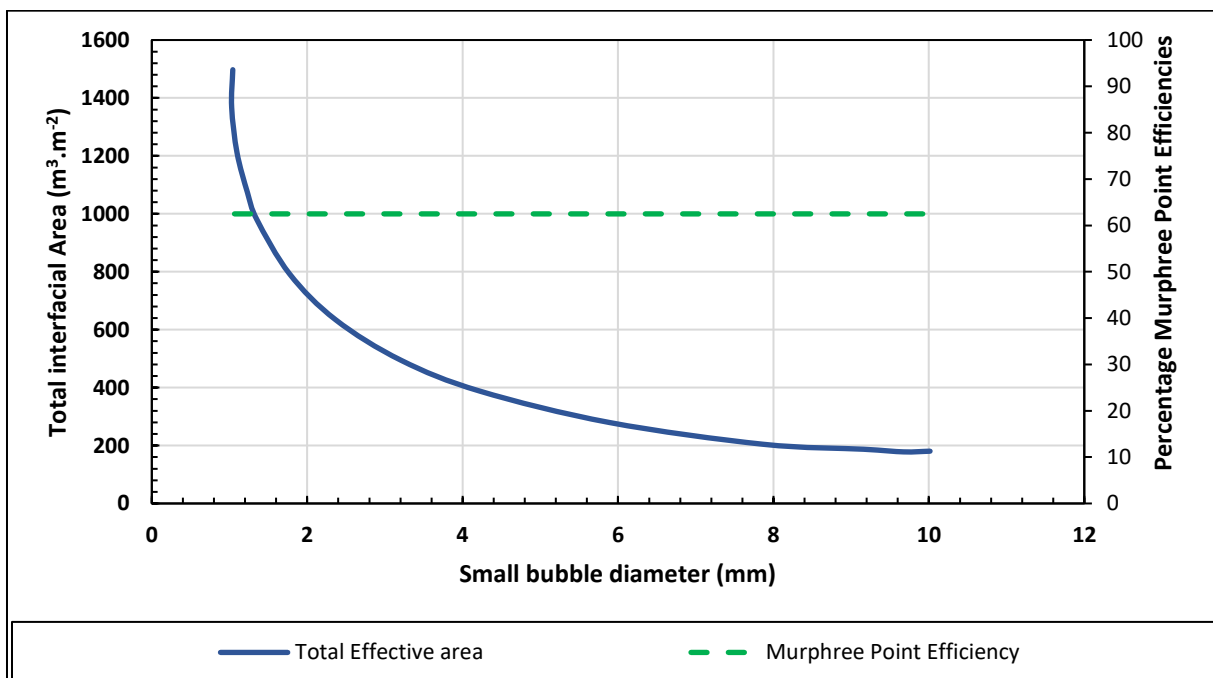


FIGURE 5.5: EFFECT OF INTERFACIAL AREA ON POINT EFFICIENCIES.

Although it offers limited practical implications, the model presented in Equations 5.25 to 5.28 illustrates the inapplicability when using Equations 5.23 and 5.24, for efficiencies above 10%. This suggests accurate prediction of liquid phase limiting systems as the efficiencies range from 0 to 10%.

### 5.5.2. RELATING POINT EFFICIENCIES TO COLUMN DESIGN

Quantitative relationships between tray and point efficiencies were first developed by Lewis [66] in 1936. The proposed relationships attempted to evaluate counter current flow in terms of three situations. These situations are presented in order:

- [1] Complete vapour mixing between trays with no influence attributed to the liquid flow direction.
- [2] Plug flow vapour approximations, evaluating unidirectional liquid flow.
- [3] Plug flow vapour evaluations within conventional alternating flow direction.

The implications of adopting the relevant approximations on volatile component concentration are presented in Figure 5.6, in order of favourability from left to right.

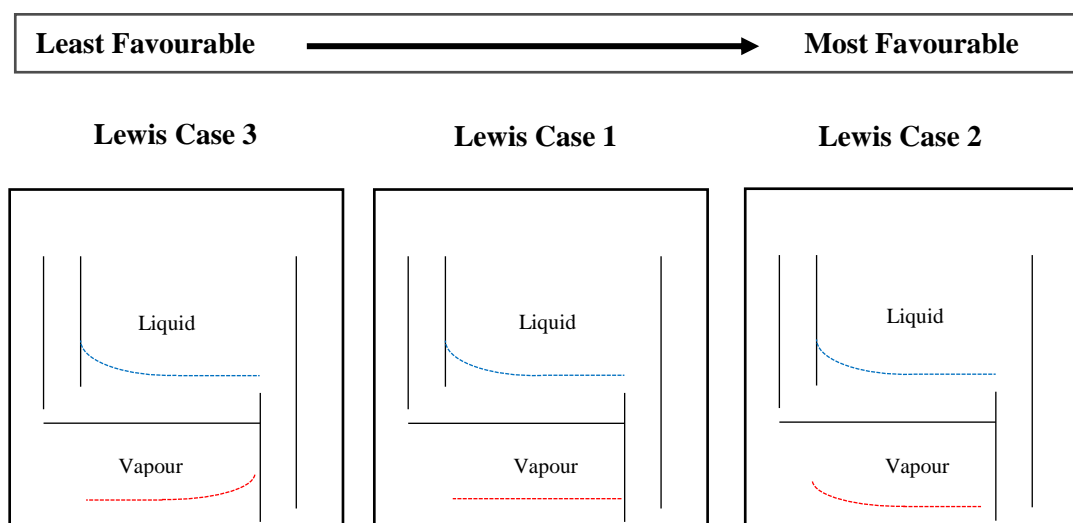


FIGURE 5.6: LEWIS CASE REPRESENTATION, ILLUSTRATING THE CONCENTRATION PROFILES ABOVE AND BELOW THE EVALUATED TRAYS

The reasoning behind the differences in favourability, is related to the average driving force across a tray. The mathematical representations of all three cases are presented as follows:

**Lewis case 1:**

$$E_{MV} = \frac{1}{\lambda} \exp((\lambda E_{OG}) - 1) \quad 5.29$$

**Lewis case 2:**

$$E_{OG} = \frac{\alpha-1}{\lambda-1} \quad 5.30$$

**where**

$$\lambda = \left( \frac{1}{E_{OG}} + \frac{1}{\alpha-1} \right) \cdot \ln(\alpha) \quad 5.31$$

**Lewis case 3:**

$$E_{OG} = \frac{\alpha-1}{\lambda-1} \quad 5.32$$

**where**

$$\alpha < 1$$

$$\lambda = \left[ \frac{\alpha^2 - (1-E_{OG})^2}{E_{OG}^2(\alpha^2-1)} \right]^{0.5} \cos^{-1} \left[ 1 - \frac{(1-\alpha) \cdot (\alpha-1+E_{OG})}{\alpha(2-E_{OG})} \right] \quad 5.33$$

$$\alpha > 1$$

$$\lambda = \left[ \frac{\alpha^2 - (E_{OG}-1)^2}{E_{OG}^2(\alpha^2-1)} \right]^{0.5} \cosh^{-1} \left[ 1 - \frac{(\alpha-1) \cdot (\alpha-1+E_{OG})}{\alpha(2-E_{OG})} \right] \quad 5.34$$

The resulting Lewis case models present an approximate relationship between tray and point efficiencies. These models, however, fail in their estimation that both the liquid and vapour approach plug flow behaviour. Various models utilizing Peclet numbers have since been developed in bridging the gap, between the real columns and perfect plug flow approximations [16].

Models using Peclet numbers were not considered for this project, as the experimental setup was designed to show negligible back-mixing or eddies. The experimental validation for this statement can, however, not be released as it is the intellectual property of the industrial facility. Qualitative justification is presented in the heuristics of rectangular column sections, being well document in illustrating approximate liquid plug flow behaviour [16].

Most efficiencies recorded in distillation setups, represent Murphree tray, or overall efficiencies. This is as the vapour samples are taken directly from the reflux liquid, representing an average composition. The Lewis models are consequently used in solving the point efficiency.

Finally, for design purposes, the resulting tray efficiencies are transposed to represent the efficiency of a whole section. This is done to simplify design procedures, as the actual columns size may be computed through dividing the theoretical height with the efficiency.

A mathematical representation of the transposition, is included in Equation 5.35 [16].

$$E_O = \frac{\ln(1+E_{MV}(\lambda-1))}{\ln(\lambda)} \quad 5.35$$

## 5.6. CONCLUDING REMARKS ON TRAY COLUMN LITERATURE

From the abovementioned models and literature data, it was deduced that tray column efficiencies were preferentially evaluated under conditions of constant reflux, using the Fenske-Underwood equations. Although providing sufficient accuracy, these systems were found to be time-consuming in their approach of steady state, taking up to 8 hours (in the case the column diameter requirements for dual pass trays). This, in combination with the hazardous compounds used, was considered to delay and limit the process of tray column design and prototyping.

In evaluating literature (Table 5.3), the most advantageous alternative was found to be vaporization of water in air (HA-method). This system was proven to be vapour phase mass transfer limiting in various packed column evaluations from the 1940's to 1970's [31, 19]. Additionally, this alternative proposes little to no environmental impact, decreased costs as well as improved safety. Two literature cases were found presenting the adaptation of this method into tray columns.

Ashley [62] was the first to attempt to use humidity in tray column vapour phase mass transfer approximations. This approach entailed using anhydrous sodium sulphate drying tubes to evaluate the humidity above and below a single bubble-cap testing tray, sporting nine bubble caps. Testing was carried out under adiabatic conditions. The author proposed using a second dry tray to eliminate any possible entraining liquid from affecting results.

A second attempt was by made by Harris [56], evaluating sieve trays under adiabatic conditions at 93.5°C (200°F). The system made use of a single tray and used wet and dry bulb thermometers in evaluating the respective humidities.

A thorough evaluation of both their experimental setups and methods presented various discrepancies in their logic. These discrepancies are highlighted as follows:

- [1] In both cases, a single tray was used. This suggests that the effects of entrainment and weeping were left unaccounted for, producing artificially large efficiencies. This argument is substantiated in a comparison of the Ashley data with the AIChE [16, 54] model. The resulting graph (Figure 5.7) presents a comparison for 20 m<sup>3</sup>.m<sup>-2</sup>.h<sup>-1</sup> liquid loading across a 181mm weir width and outlet weir height of 38 mm. The NTU model was transposed to point efficiencies using Equation 5.23. The use of this equation is widely considered to provide an over prediction of point efficiency (See Figure 5.4). In contrast to the expected trend, it provided an under estimation of 20% to the Ashley data [16].

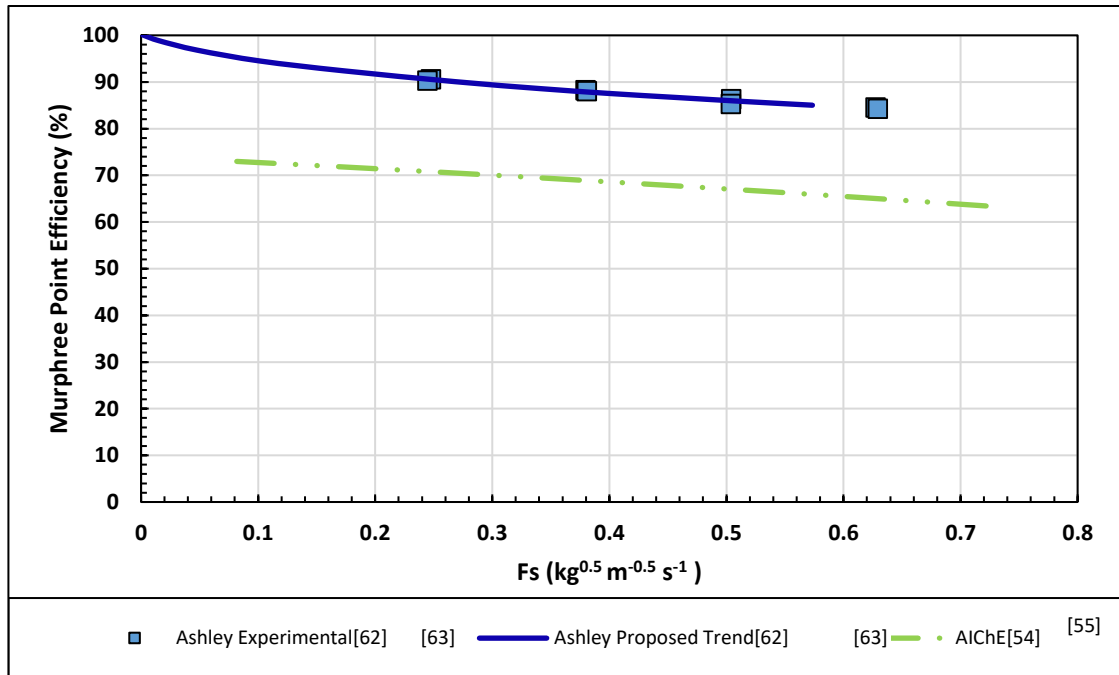
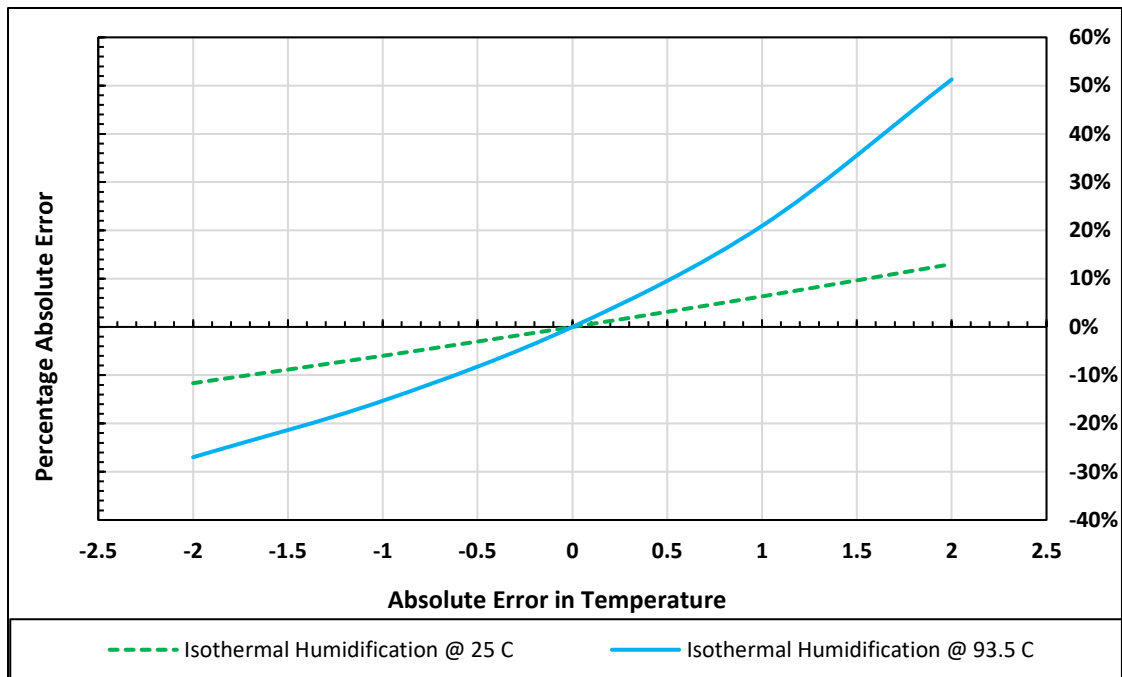


FIGURE 5.7: COMPARISON BETWEEN AICHE MODEL AND ASHLEY DATA.

- [2] Both Ashley [62] and Harris [56] noted considerable problems in measuring humidity, to the point where Ashley employed additional tray as de-entrainer. This introduced additional effective contact area for vapour liquid contact, skewing the results.
- [3] Harris attempted to increase the driving force in the vapour phase, through raising the operating temperature to 93.5°C (or 200°F). This is introduced additional uncertainty, due to the exponential nature of the humidity curve. At a temperature uncertainty of  $\pm 1^\circ\text{C}$ , a relative error spanning -15% to +21% was noted at conditions of 200°F. This was found to be excessive, compared to the  $\pm 6\%$  Relative Humidity (RH) at 25°C (77°F). A graphical representation of the uncertainty is provided in Figure 5.8.





**FIGURE 5.8: SENSITIVITY ANALYSIS OF OPERATING TEMPERATURE.**

- [4] As a final consideration, both authors opted for both short and narrow flowpaths. This is known to misinterpret flow distribution across the tray, as well as generate artificial contact area on the column walls [16].

All things considered, the above-mentioned methods were found to be lacking as alternatives on which to base column efficiency measurements for this project. It was subsequently opted to change selected parameters, while still using humidification of water in air (HA-method).

The chosen parameters were set as follows:

- [1] Operating temperature of 25 °C.
- [2] Increasing and stabilizing the vapour driving force through cooling rather than heating of the air.
- [3] Evaluating an 864mm flowpath with a 762mm flow width.
- [4] Most importantly, using a multi-tray system to attenuate the influence of weeping on efficiency.



---

# CHAPTER 6: MATERIALS AND METHODS

## 6.1. LIQUID PHASE MASS TRANSFER: METHOD DEVELOPMENT

The literature study presented in Chapter 4, highlighted the need for alternative systems for the measurement of the liquid phase mass transfer coefficient in packed columns. This is as the industrially preferred desorption of oxygen from water is expensive, time-consuming (rarely operated continuously) and requires a large plant footprint.

From the listed limitations, it was opted to evaluate the desorption of an organic solute from water. This method was expected to produce comparable results to the oxygen-water system, as the interfacial transport mechanism remains constant irrespective of component or direction. This was previously validated by Linek [18], as presented in Chapter 4. Having motivated the need for alternative, different solutes were evaluated at the hand of economic, environmental and physical reasoning.

### 6.1.1. SOLUTE CONSIDERATIONS

As a rule of thumb, systems exhibiting high Henry's constants, are considered liquid phase mass transfer limiting [4, 18]. However, little numerical quantification exists in terms of defining the exact point at which the resistance in the liquid phase becomes dominating. As such, it was opted to base the solute selection process on a regression model of known liquid phase mass transfer limiting systems.

The approach was developed using the Onda [19] correlations (Equations 4.12 and 4.13) for the prediction of the ratio between liquid and vapour phase mass transfer coefficients (in packed columns). Hydrodynamic data was chosen at both the upper and lower limits of operability ( $6-120 \text{ m}^3 \cdot \text{m}^{-2} \cdot \text{h}^{-1}$ ,  $F_s > 0.5$ ). The diffusion coefficients were collected either from their relevant literature sources or the group contribution models found in Perry [68], with the relevant parameters approximated using the DIPPR [69] database.

In regressing, the model attempted to quantify the minimum Henry's volatility coefficient at which a solute is considered liquid phase mass transfer limiting. A mathematical relationship, derived from the resistance analogy of mass transfer, was employed in relating the separate mass transfer coefficient to a fraction of liquid resistance. This mathematical relationship is provided in Equation 6.1 .

$$\frac{R_{\text{Liquid}}}{R_{\text{Total}}} = \frac{100}{1 + \frac{1}{(k_G/k_L)_{H_c}}} \quad 6.1$$

Solving the relationship for a 95% confidence interval ( $R_{\text{Liquid}} / R_{\text{Total}} = 0.95$ ), provided the limiting Henry's volatility constant at which desorption operations remained liquid phase mass transfer limiting. In using the regression, organic solutes were listed and ordered with respects to both aqueous solubilities and Henry's volatility constants. The subsequent ordered data are provided in Appendix A,

Section 9.1.4. The applicable solutes were further arranged with regard to their environmental impact and ease of quantification. As a final measure, a cost study was conducted on the chemicals to aid in selecting a viable alternative. Upon adhering to all the set requirements, isobutyl acetate was chosen as the solute to be stripped from water with air. This is referred to as the ADIBAA-method. The flow diagram of the algorithm is supplied in Figure 6.1 with the full regression model presented in Appendix A.

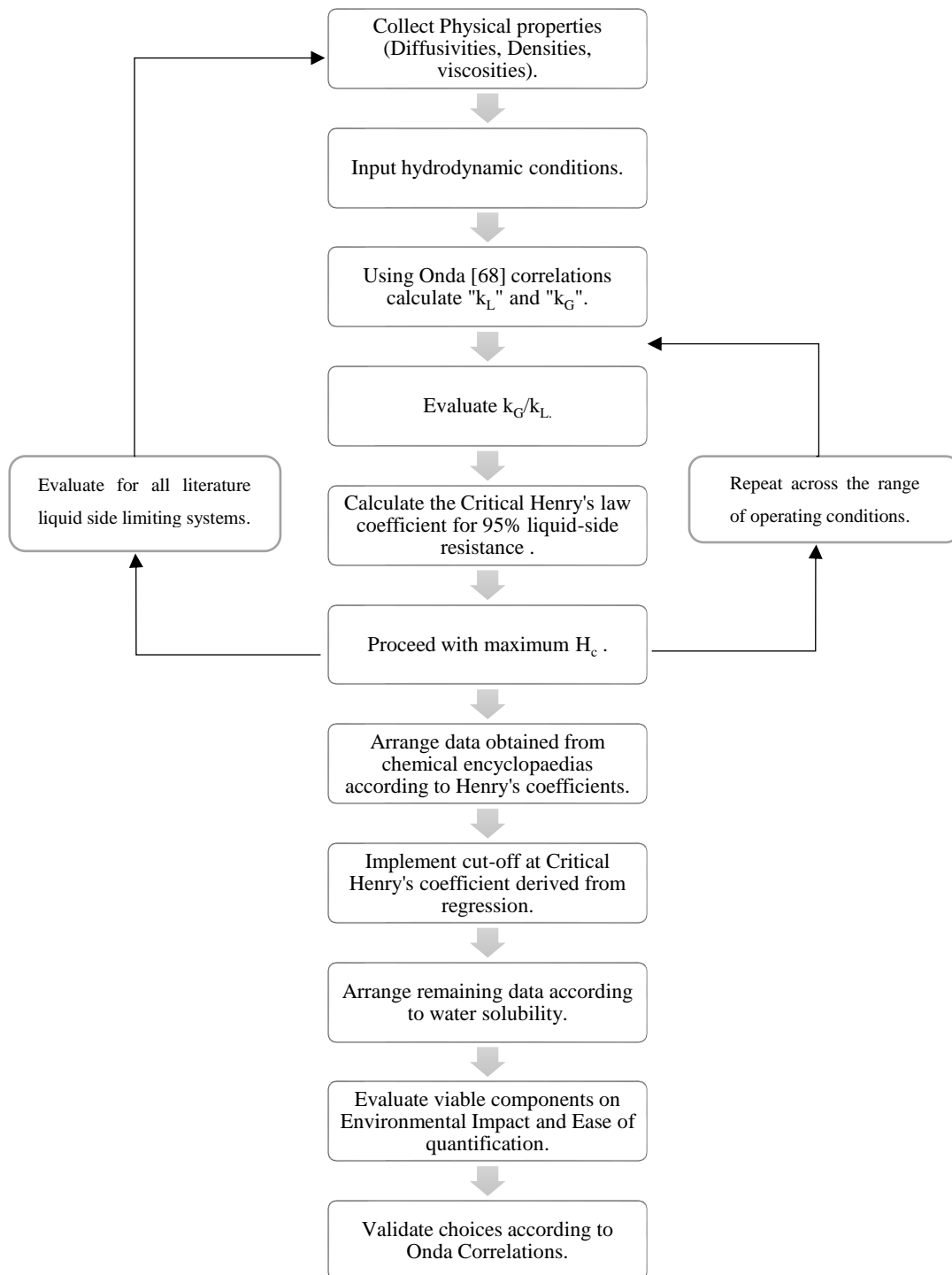


FIGURE 6.1: REGRESSION FLOW DIAGRAM.

## 6.1.2. LIQUID PHASE QUANTIFICATION

Although presented separately, the quantification methods were considered throughout the solute selection process. Due to the large economic motivation of the project, it was opted to evaluate cost-effective solute and quantification combinations. Apart from accurate and reliable quantification, the following requirements were set:

- [1] The quantification method was required to be cost-effective and available in most industrial laboratories.
- [2] The chosen method was required to be simplistic and straight forward to limit operator training requirements.

In adhering to the requirements, UV-VIS spectrophotometry was chosen. This quantification method is easily incorporable and requires a smaller capital investment than conventional gas chromatography. In opting for UV absorption quantification, the solutes were limited to components with free electrons (double bonds, oxygens etc.). This played a large part in the selection of an ester (double bond with oxygen). For ease of use, the organic chemical was also required to be in the liquid phase at room temperature.

In optimizing the system for rapid evaluation, the UV-spectrophotometer was customized with an aftermarket celling changer and in a flow cell configuration. This meant that with two flow cells, one for the inlet and one for the outlet, the spectrophotometer could quantify the composition of both streams sequentially. The continuous UV quantification was prominent in continuously quantify and control the inlet composition. Consequently, a liquid recycle loop was designed, in which the solute (the organic component) was continuously dosed and the solvent reused. The aforementioned notably decreased the plant footprint as large holdup tanks were avoided.

## 6.2. VAPOUR MASS TRANSFER: METHOD DEVELOPMENT

In contrast to the liquid phase evaluation, solutes exhibiting a low Henry's volatility constant are conventionally considered to be vapour phase mass transfer limiting. This is as they are rarely far removed from the equilibrium in the vapour phase. In the situations where the solute itself is water, the Henry's volatility constant effectively approaches zero. This is reasoned through the definition of the dimensionless Henry's volatility constant (Equation 3.13). For water, the liquid phase is effectively pure solute. This suggests that very little resistance remains in the liquid phase. The subsequent HA-method, was proven to be vapour phase mass transfer limiting in various packed column evaluations from the 1940's to 1970's [31, 19].

Additionally, the proposed humidification of air involves little environmental impact. Consequently, very few additional safety measures are required on the plant. This marks an improvement of the convention constant reflux operations. The measurement of humidity is also both cost-effective and requires little operator training.

The outlined improvements of the ADIBAA- and HA-methods, justified the project in designing and constructing the relevant pilot plants for the experimental evaluation.

### 6.3. METHOD PROCEDURES

The experimental and calculation procedures of the respective methods are provided in flow diagram format in Figures 6.2 and 6.3. These diagrams summarise the process of translating the simplistic measurements into comparable efficiencies.

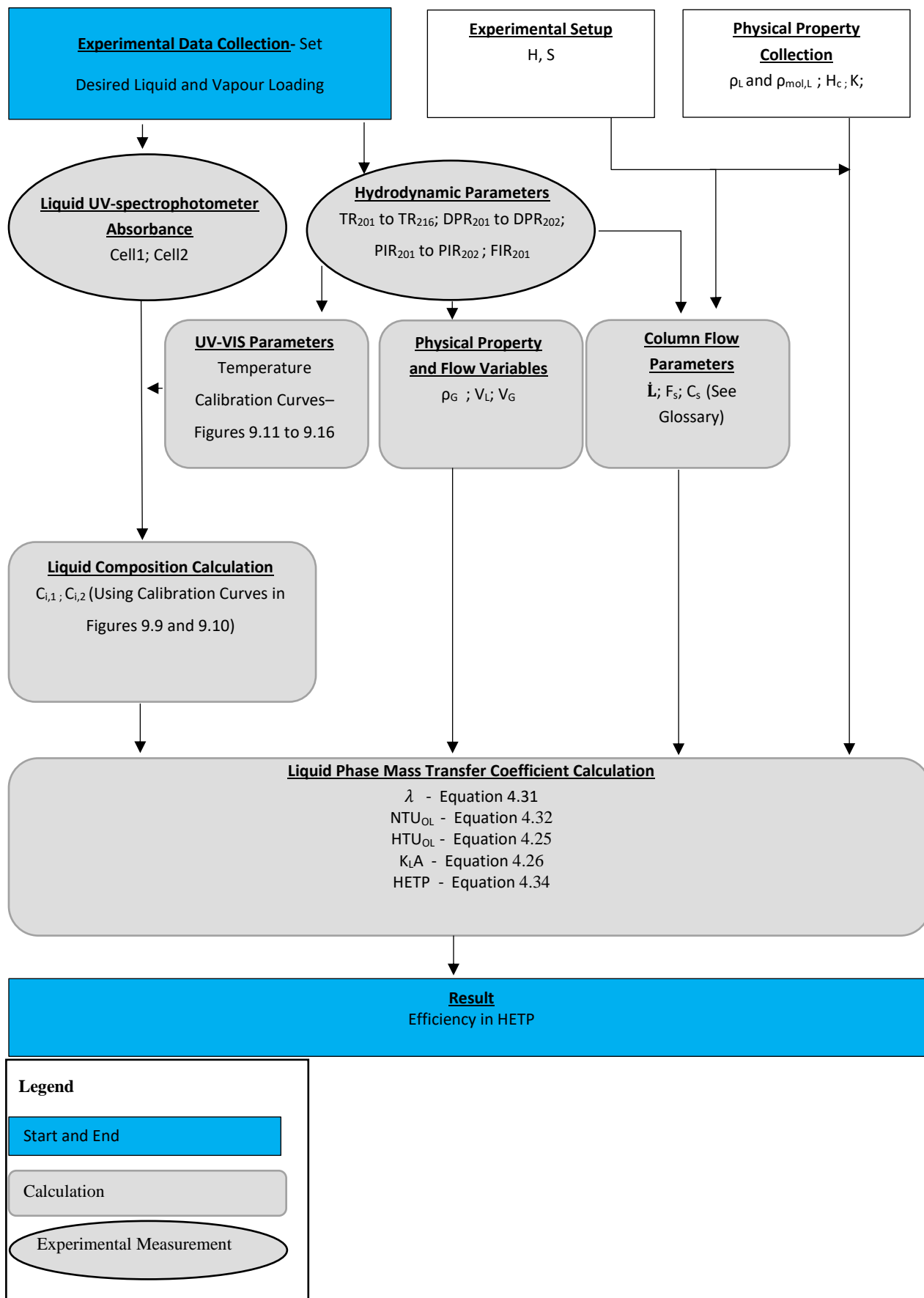


FIGURE 6.2: ADIBAA - METHOD FLOW DIAGRAM AND CALCULATION PROCEDURE

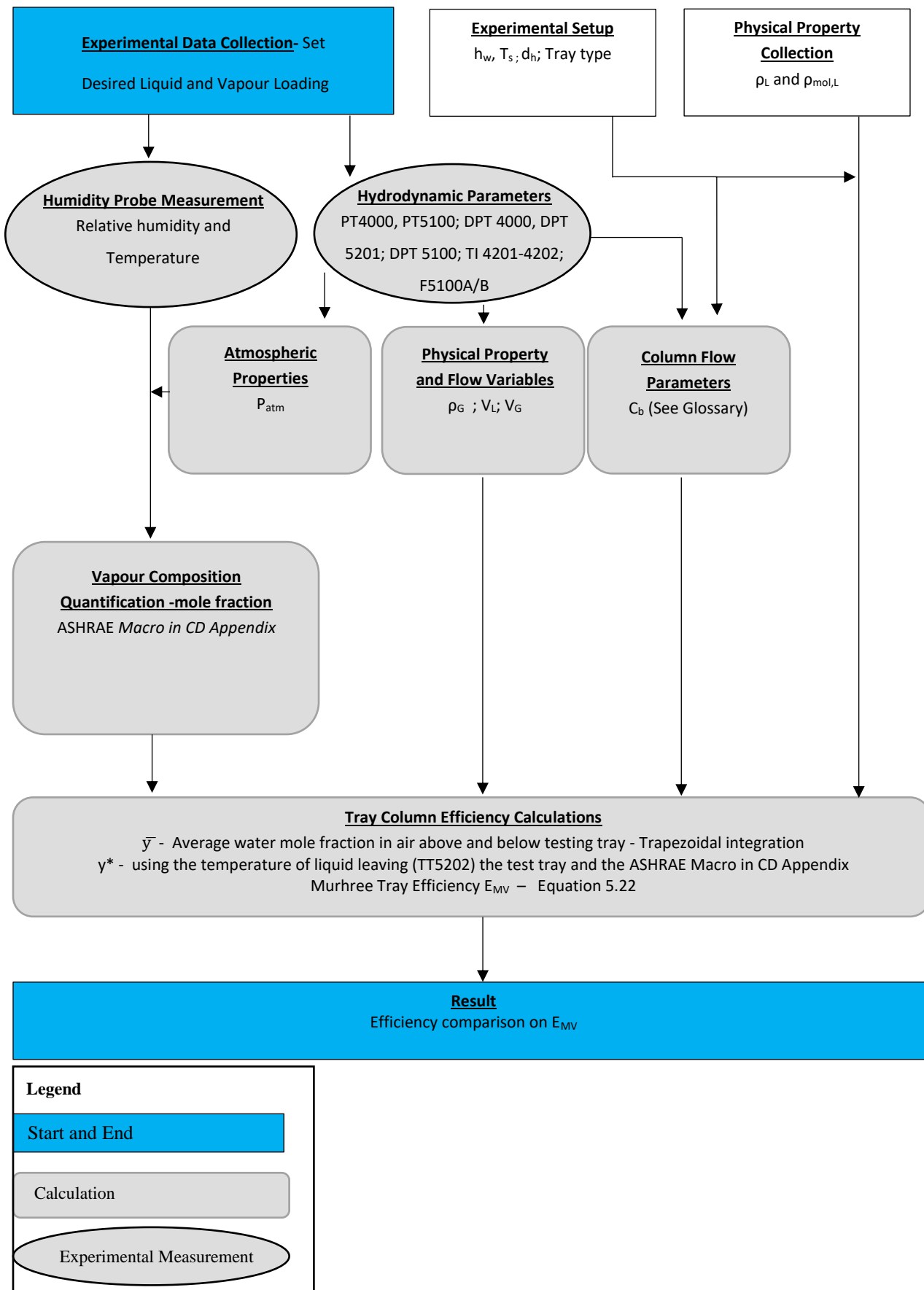


FIGURE 6.3: HA – METHOD FLOW DIAGRAM AND CALCULATION PROCEDURE



## 6.4. DESIGN CONSIDERATIONS

### 6.4.1. PACKED COLUMN

The experimental section of this report is based on the use of multiple setups, located respectively at Stellenbosch University and at an industrial research facility, specializing in column internal design. The proceeding experimental procedures are presented in two sections.

As neither location offered applicable facilities at the time, varying grades of redesign and construction were required. In the case of the packed column, the available facilities lacked industrially relevant size as well as a viable quantification system. It was consequently opted to retrofit the carbon monoxide capture system built by Kritzinger [20] (200mm ID, structured packed column), in favour of a 400mm stainless column. The redesign included:

- [1] A humidification column section with transition to the required column size,
- [2] A Chimney vapour distributor,
- [3] Liquid sampling system with a trap for air bubbles,
- [4] Solute dosing and mixing system,
- [5] Continuous Quantification System: UV-spectrophotometry,
- [6] A holdup grid for minimized pressure drop,
- [7] Liquid and Vapour pipe layout,
- [8] Full electrical rework, with PLC redesign,

For the sake of brevity, the relevant designs find are presented in Appendix A (Section 9.1.6) with mechanical drawings on the provided disc. An illustration of the designed column and plant surroundings is provided Figure 6.4.

### 6.4.2. TRAY COLUMN

To protect the interests of the industrial facility, an in-depth discussion is not provided regarding the design of the column. It is, however, worth noting that notable construction and redesign were required since no such system was available. A broad summary of the design included:

- [1] Various mass balances and energy balances for use in design of the cooling and pump networks,
- [2] Spray Nozzle Liquid Distributor design,
- [3] Vapour, liquid piping layout,
- [4] Design of various column internals,
- [5] Colling and heating network design,
- [6] Tray design.

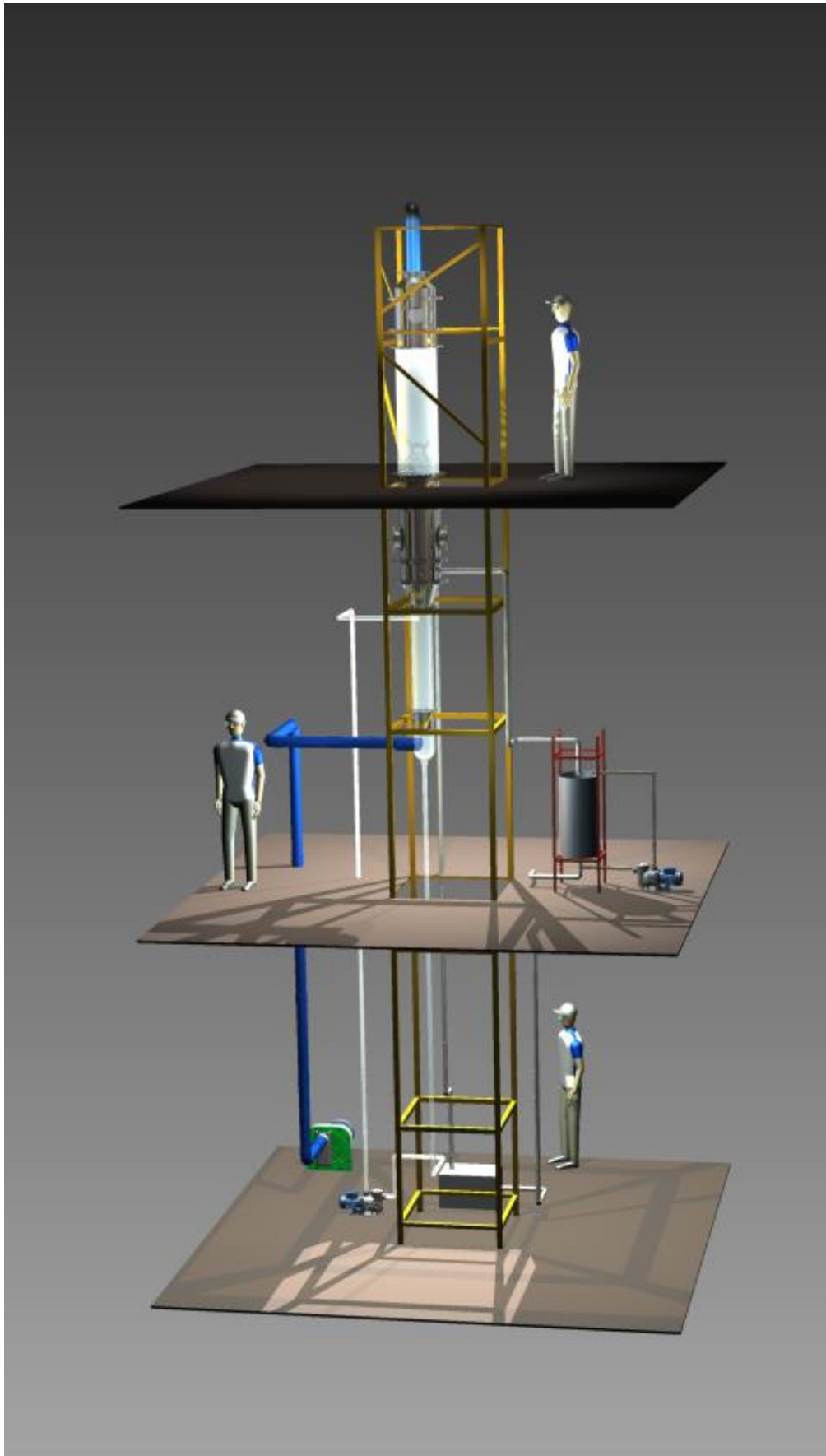


**FIGURE 6.4: PACKED COLUMN DESIGN: INVENTOR MODEL.**

## 6.5. EXPERIMENTAL SETUP

### 6.5.1. PACKED COLUMN

Packed column liquid phase mass transfer evaluations were performed at Stellenbosch University, through the stripping of isobutyl acetate from water with air. The experimental setup, made use of both a humidification as well as a stripping section. A representation of the setup is presented in Figure 6.5.

#### 6.5.1.1. PROCESS FLOW

Colour was used in Figure 6.5, in differentiating between process flow streams. This theme is carried across to the tray column section (Figure 6.8). The subsequent legend can be used in navigating the process flow:

- [1] Vapour -Red
- [2] Potable Water-Green
- [3] Solvent/Solute solution- Blue
- [4] Recirculate mixing or utilities – Black

##### 6.5.1.1.1. FLOW DESCRIPTION

Air is taken from the atmosphere, humidified (V202) and transported to the stripping section. Within this column section (V201), isobutyl acetate is stripped from water with the incoming air. The vapour is expelled to the atmosphere via a duct. The water / isobutyl acetate solution is kept at a constant composition through continual dosing in the sump (V218). The dosing mixture is introduced into a mixing venturi while the contents of the vessel is mixed by a centrifugal pump (E211). The stock solution is subsequently pumped into the stripping section via centrifugal pump (E301)

In the humidification section (V202), potable water is recirculated via a centrifugal pump (E207). Some of the water is evaporated during the consequent phase contact with the entering vapour.

#### 6.5.1.2. SETUP DESCRIPTION AND PROCESS FLOW

Vapour was introduced into the column through centrifugal blowers (E201A/E201B) via PVC pipe, and quantified by way of user-calibrated venturi. The venturi was designed according to ISO 5167-1:1991 specifications and calibrated in accordance with the specified compressible fluid model. The venturi was placed in a straight run pipe-section, 10 diameter lengths from the nearest flow obstruction. Both atmospheric pressure and temperature readings were taken upstream of the venturi, for the purpose of calculating vapour densities. The ideal gas law was used in calculating the density of the vapour. This was applicable as the blower operated at low pressure, never exceeding 120kPa (absolute). The pitot tube calibration procedure is outlined in Appendix A (Section 9.1.6). Further confirming the accuracy of the mass flow rate, the calculation process was validated against sample calculations presented in Fox *et al.* [70].

The vapour stream perpendicularly transitioned into a 200mm ID, Schott bellbottom, section via a 90mm inlet port. A static mixer, designed by Erasmus [3], was used to distribute the vapour. A single 900mm column section filled with 2.5' FlexiRings® was used for humidification purposes. The humidification (green line in Figure 6.5), was included as a pre-treatment step, to the limit the evaporation of the solvent (water) within the stripping section. This was put in place, since any evaporation within the main section(V201) would skew the results. Ambient humidity readings were taken throughout the experimental process with a Raspberry Pi DHT22 sensor, accurate to within 5% RH (Relative humidity). This was used to track the influence of ambient conditions on experimental data. The relative humidity across the whole of the testing cycle, remained above 40% RH.

As an additional measure, simultaneous mass and energy balances were solved over the stripping section. This was done using data collected from plant operations, modelling for 40% relative humidity. As limited heat of vaporization data was available on isobutyl acetate, the evaluation was conducted for the available isomer *n*-Butyl Acetate. A maximum error of 1.5 % was recorded over a range of flow rates. The relevant excel spreadsheet is presented in the attached CD Appendix under “*Validation of Humidification*”.

Siemens differential pressure sensors were used on the venturi, claiming manufacturer accuracies to within 0.15% across a range of 0.04 to 4 bar. A variable speed drive was employed in controlling the blower feed rate between 50 and 1000 kg/h. No temperature control was implemented on the vapour line leading to the column. This simplification was based on the consideration that:

- [1] The diffusion coefficients for isobutyl acetate in air show a 3% absolute deviation within a band of  $\pm 5^{\circ}\text{C}$  from the vapour set-point of  $25^{\circ}\text{C}$ . This approximation was made on the basis of a group contribution model, for the evaluation of the rate of diffusion of hydrocarbons in air. According to the reference found in Perry, the average deviations for this specific model is known not to exceed 9% [68]. (The exact equation can be found in the Perry's Chemical Engineering Handbook, 7<sup>th</sup> Edition, in Section 2-370 Equation 2-152)
- [2] The ratio of specific heat capacities of the vapour to the liquid was sufficiently small to suggest that the vapour would heat up with limited impact on the liquid temperatures. This in turn would lead to little or no effect on the diffusion coefficient of isobutyl acetate in the water solution.
- [3] The physical properties of the liquid and vapour are expected to exhibit little to no variation across a  $\pm 5^{\circ}\text{C}$  band
- [4] Within this framework, it was decided against installing additional vapour heating or cooling as the vapour temperatures during testing, cycled between  $20^{\circ}\text{C}$  and  $25^{\circ}\text{C}$ .

The stripping (Blue line in Figure 6.5) section comprised of a single 1.1m, 400mm diameter, stainless column section. A liquid distributor previously validated by Lamprecht [9] was used. This distributor used 19 pipes and a drip point density of  $157\text{m}^{-2}$ . A holdup grid, similar to one used by Lamprecht [9]

was fabricated from Stainless wire-mesh. Wire mesh, as opposed to hexagonally perforated sheet (used by Lamprecht), was chosen based on economic considerations. Validation of the wire mesh alternative is presented through open area modelling available in Appendix A (Table 9.7). The subsequent design was fabricated for 1/8<sup>th</sup> of the cost of the hexagonal equivalent, whilst sacrificing only 0.7% of the open area.

The temperature of liquid entering the stripping section was regulated by way of a 2kW electrical heater, which was controlled, through utilizing a platinum resistance thermometer (PT-100) with an accuracy of 0.5° C (within 0-100°C).

A chimney vapour distributor design, similar to Lamprecht [9] was used in segregating the exiting liquid with the entering vapour. The distributor was designed with an open area of 85%, to limit pressure drop, while still inhibiting channelling. The chimney design was successfully incorporated in creating two separate liquid loops.

Differential pressure readings were taken across the bed, using a similar Siemens pressure transmitter to the one used for the vapour venturi. The bed pressure drop data, however, offers limited applicability. This is as a direct result of the exaggeration of end effects over a very short bed height. The pressure drop data was subsequently only used in determining steady state.

Liquid composition measurements were taken in the pipe leading to the distributor and directly below the packing, to limit the quantification of mass transfer outside the testing bed. A sampling port was designed and fabricated to sample liquid 50 mm below the packing. This sampling pipe allowed for continuous liquid refreshment at the inlet of the sampling pump. A 1/2' (12mm) halfpipe, angled and fitted with a recirculation loop, feeding to a settling cup and back into the sump. The aforementioned settling cup, of similar design to a water trap, was used to deaerate the sampled liquid. This was critical, as spectral absorption of air bubbles introduced unwanted variability in the data. The volume of the deaerating instrument was limited to 150ml to ensure that residence time was shorter than 2 minutes. Thus, if the compositional measurements were constant for more than 2 minutes, the system could be assumed at steady state.

A simulated stock solvent was prepared, using demineralised water from the departmental utilities, dosed with 99.9% Sodium Chloride to produce a solution of  $\pm 30\text{mS}$  conductivity. This was done as the magnetic flowmeter on the stripping line was found to drift under conditions below 10mS. The artificial dosing of sodium chloride was mitigated drift, while eliminating possible impacts related to varying water quality.

The solute concentration of liquid stripping feedstock (Liquid in vessel V218) was kept constant at 400 ppm throughout, through continually dosing fresh isobutyl acetate, using a Grundfos DDC diagraph

pump. The pump was retrofitted with custom PTFE non-return valves, as the stock EDPM was susceptible to chemical deterioration.

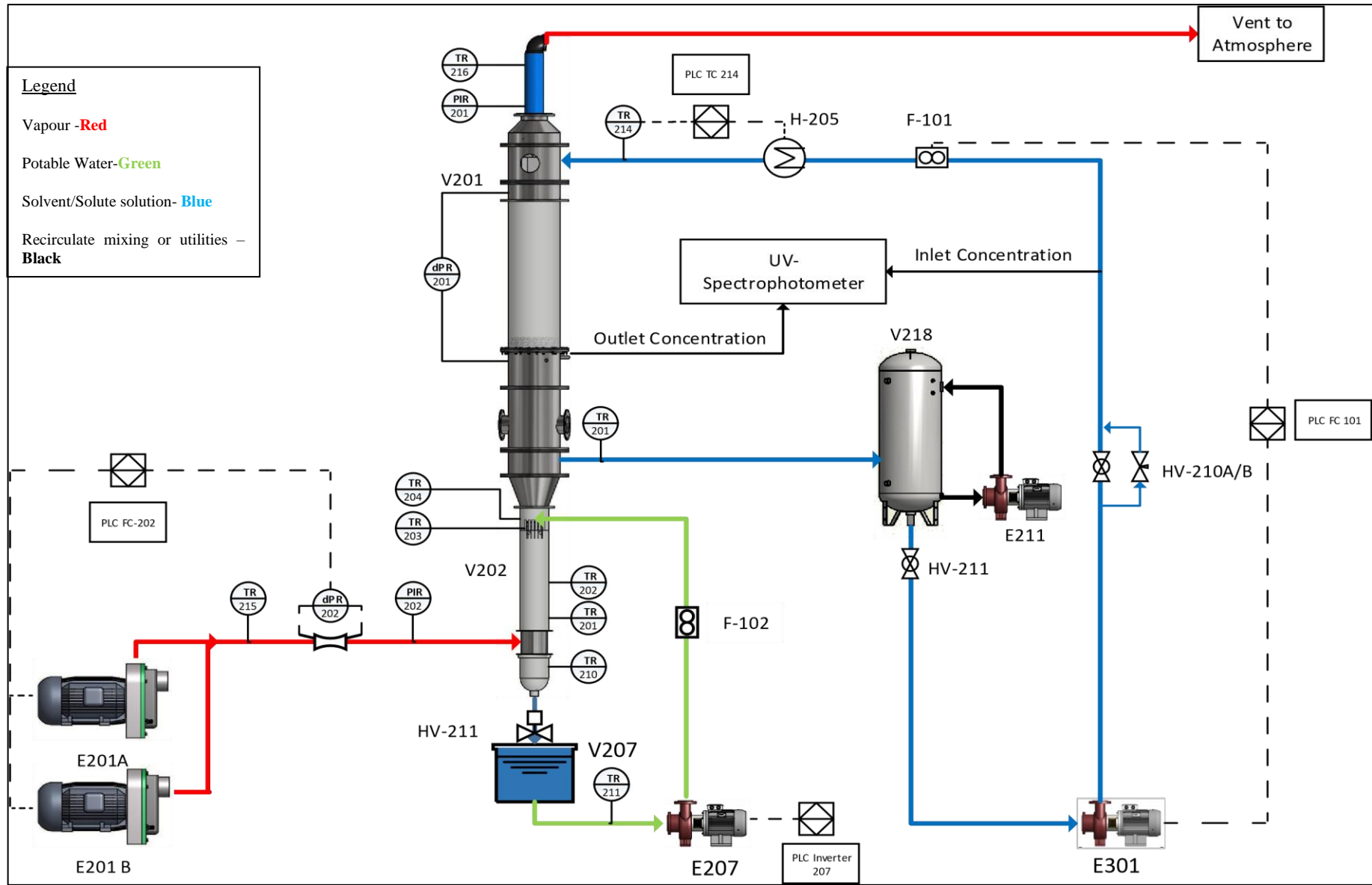


FIGURE 6.5: RANDOM PACKING EXPERIMENTAL SETUP.

### 6.5.1.3. QUANTIFICATION

A UV-VIS spectrophotometer from Pharma Test was used to quantify the composition of the liquid phase at the inlet and outlet the stripping section. The instrument offered variable spectral bandwidth with a wavelength accuracy of  $\pm 0.3\text{nm}$  and reproducibility of  $0.2\text{nm}$ . The spectrophotometer was fitted with an aftermarket 8 cell changer and dual Hanna quartz flow cells for continuous measurement. The cells offered a 10mm pathlength and 550 microliter sampling volume. All computational measurements were taken at 203nm. This was chosen as it coincided with the peak absorbance of isobutyl acetate in water (See Figure 6.6).

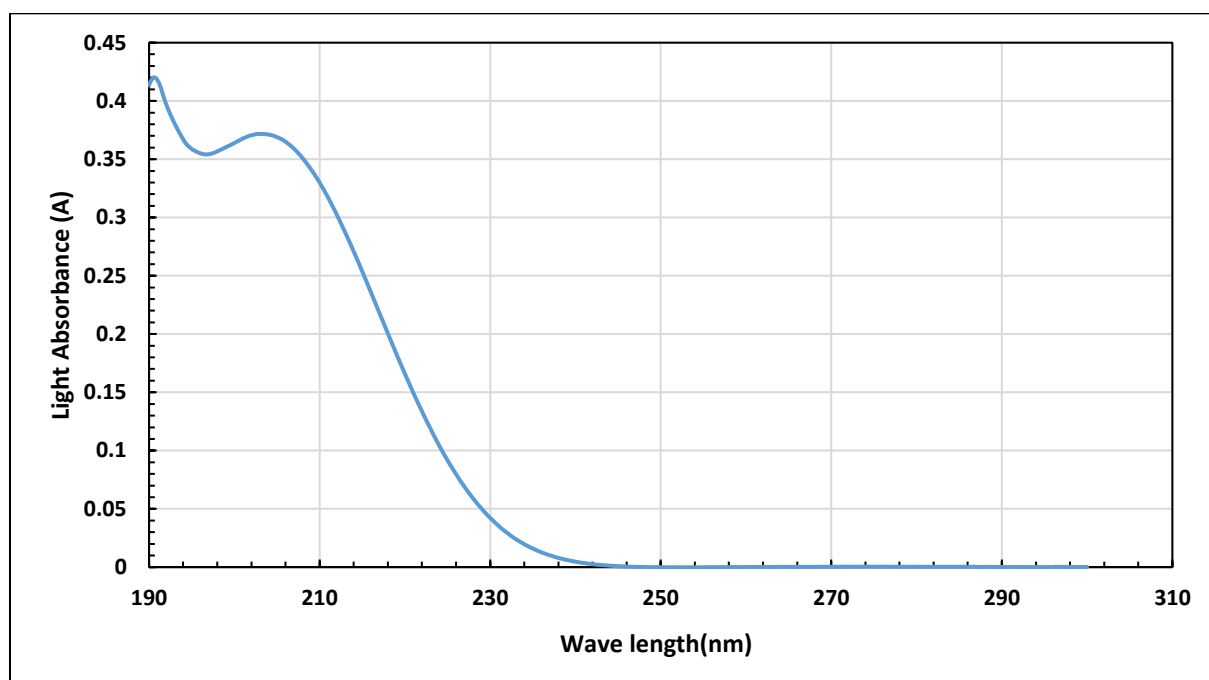


FIGURE 6.6: ISOBUTYL ACETATE SPECTRUM SCAN USING UV-VIS SPECTROPHOTOMETER.

A dual dosing pump system operating at 100ml/min, controlled through a Raspberry Pi, was used to continually refresh the liquid sampled in the flow cells. This translated to a refreshment time of 0.33 seconds, inhibiting contaminant accumulation in the Quartz flow cells. The retrofitted UV-VIS spectrophotometer was verified to introduce no additional stray light, as water initialized in the stock system remained at null absorbance with the fabricated flow panel (within experimental variance). The peristaltic pump system was found to operate under near plug flow conditions with a 3 mm ID tube, eliminating lag times in measurements.

The aftermarket cell changer was set to intermittently change between the two cells, quantifying each sample in succession and limiting the need for a separate analytical instrument. Samples were analysed every five seconds, based on user quantified calibration curves. Calibration curves were generated every two weeks to mitigate any instrumental drift. An example of the calibration curves generated for the final experimental evaluation is presented in Appendix A (Section 9.1.8.1)



The instrument was initialized before each set of experimental evaluations on a synthetic stock solution at 25°C. Obtaining the null absorbance value with the solvent in the sump, attenuated for any impurities(oxidation) presented at the start of the evaluation. The temperature dependence of the flow cells, being the sole function of the absorbance of water, was attenuated through separate temperature calibration functions. These functions were derived through a series (ten hours) synthetic solvent evaluations, in which the temperature on the column was incrementally varied to cover a wide spectrum of temperatures. This was done inline, limiting the probe calibration error. The graphical representation of each ten-hour run is presented in Appendix A (Section 9.1.8.2, Figures 9.11 to 9.16).

To ensure complete wetting of the packing, high and low liquid loadings were intermittently evaluated. This limited the need for an additional wetting cycle prior to testing.

Although compositional measurements were taken continuously, only the applicable steady state data points were considered of worth, for use in mass transfer coefficient quantification. As such, ten minutes of temperature, pressure and compositional flat-lining was required before the measurements were taken. After ten minutes of steady behaviour, the measurements were taken over a five-minute average time interval. This limited sudden impurities from passing over the sampling beam and affecting the readings. Data point was collected on average once every twenty-five to thirty minutes.

## 6.5.2. TRAY COLUMN

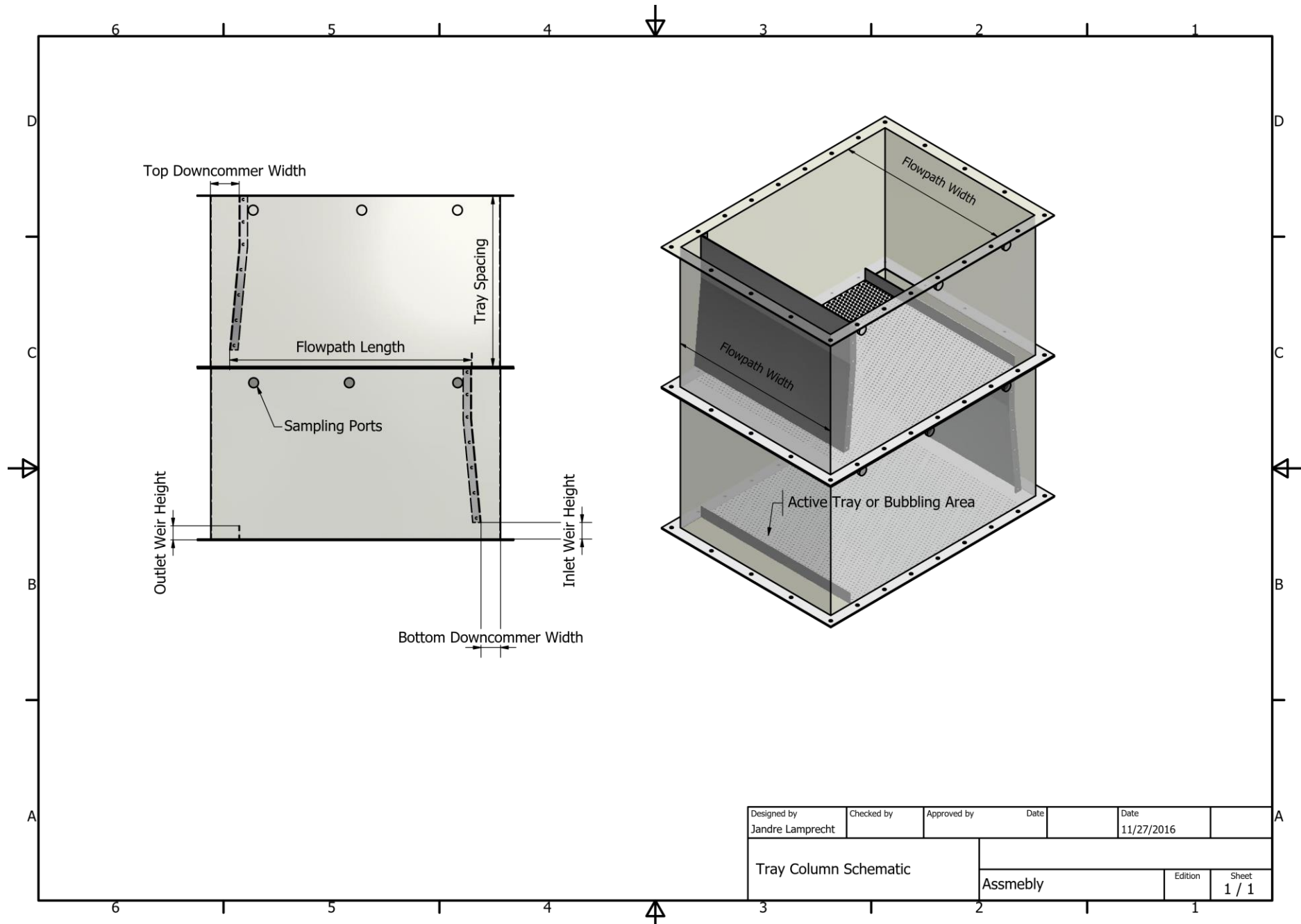
In a bid to limit the capital expenditure of building an additional industrially sized tray column, it was opted to evaluate the alternative methods for vapour phase mass transfer coefficients at an industrial facility. Working around existing equipment as well as environmental restrictions, it was decided to evaluate humidification as an alternative method for vapour phase mass transfer coefficients. An illustration of the setup is presented in Figure 6.8. The provided P&ID opposes convention in the flow of material (normally from left to right).

### 6.5.2.1. COLUMN DESIGN DETAIL

A rectangular, single pass, column was used in the experimental evaluation of the HA method. The design allowed for the downcomer height to be changed depending on the liquid loading. Acrylic side windows were used to visually measure froth heights. Clarification of the relevant parameter's is provided in Figure 6.7 .

TABLE 6.1: TRAY COLUMN DESIGN DETAIL.

<b>Tray Column Parameters</b>	
Tower dimensions (nom.) (mm x mm)	762 x 1040
Number of Flowpaths	1
Tray Spacing (mm)	610
Deck Thickness (mm)	2
Flowpath Width (mm)	762
Flowpath Length (mm)	870
Downcomer Clearance (mm)	20
Outlet Weir Height (mm)	50
Inlet Weir Height (mm) at $<61 \text{ m}^3 \cdot \text{m}^{-2} \cdot \text{h}^{-1}$	11
Inlet Weir Height (mm) at $>61 \text{ m}^3 \cdot \text{m}^{-2} \cdot \text{h}^{-1}$	62
Effective Inlet weir length (FPW)	762
Top Downcomer width (mm)	102
Bottom Downcomer width (mm)	67.4
Tower Length (mm)	1040
Tower Area ( $\text{m}^2$ )	0.79
Active Area ( $\text{m}^2$ )	0.66
Free Area ( $\text{m}^2$ )	0.71



Designed by Jandre Lamprecht	Checked by	Approved by	Date	Date 11/27/2016	
Tray Column Schematic			Assmebly		
			Edition	Sheet 1 / 1	

FIGURE 6.7: SCHEMATIC OF TRAY COLUMN PARAMETERS

### 6.5.2.2. *PHYSICAL SETUP*

A broad description of the tray column experimental setup will be provided, to protect the interests of the industry. The complete P&ID is provided in Figure 6.8.

The experimental setup for tray testing comprised of a two-stage design, similar the packed column setup presented in Section 6.5.1. The initial pre-treatment stage, entailed dehumidifying the inlet vapour stream, through cooling the inlet air to below the dew point. This was done in two consecutive cooling stages, with the first being an aluminium-finned vapour heat exchanger. The second stage of cooling, involved direct contact heat exchange within a 914mm diameter packed column, with a five-meter packed height. The packed column acted as a de-entrainer, removing any spray from the vapour feed. In both cooling stages, a 30% Propylene Glycol and water solution was used as cooling brine. Through the dual cooling stages the temperature of the vapour leaving the packed column, was controlled to between 4-7°C, depending on ambient temperatures and humidity.

Vapour mass flow measurements were taken using a pre-calibrated averaging pitot-tube. The vapour leaving the packed column was reheated, using steam in a finned heat exchanger and controlled to 25°C. The dehumidified air entered the tray testing column through a V-baffle designed for optimal vapour distribution. The specialized column used a segregated sump to limit re-humidification from the draining liquid, leaving the testing tray. A chimney-design vapour distributor was used to segregate the wept liquid from entering vapour.

The testing section was equipped with two identical trays, with the top tray conditioning the liquid flow. This tray allowed liquid to weep onto the testing tray (bottom tray), simulating real application conditions. The liquid leaving the test tray was collected and allowed to flow through to the segregated sump, without further contact with the vapour. In contrast, the liquid that wept from the testing tray was collected on the chimney vapour distributor and drained through a paddle flowmeter to the sump. This measured the weeping flow rate.

Compensating for the latent heat of vaporization, heat was added to the testing column through a steam heat exchanger. This was used in controlling the liquid temperature at the inlet to the test tray at 25°C. Liquid flow measurements on both columns were taken with magnetic flowmeters through a parallel system of two and 4' lines (FT5100A/B and FT4200A/B in Figure 6.8).

### 6.5.2.3. *HUMIDITY QUANTIFICATION*

Relative humidity and temperature measurements were taken using a single Dwyer 485B, handheld probe. The probe quoted a manufacturer accuracy of  $\pm 2\%$  RH within  $\pm 0.5^\circ\text{C}$ . The aforementioned was sent for manufacturer recalibration, less than 3 months prior to testing.

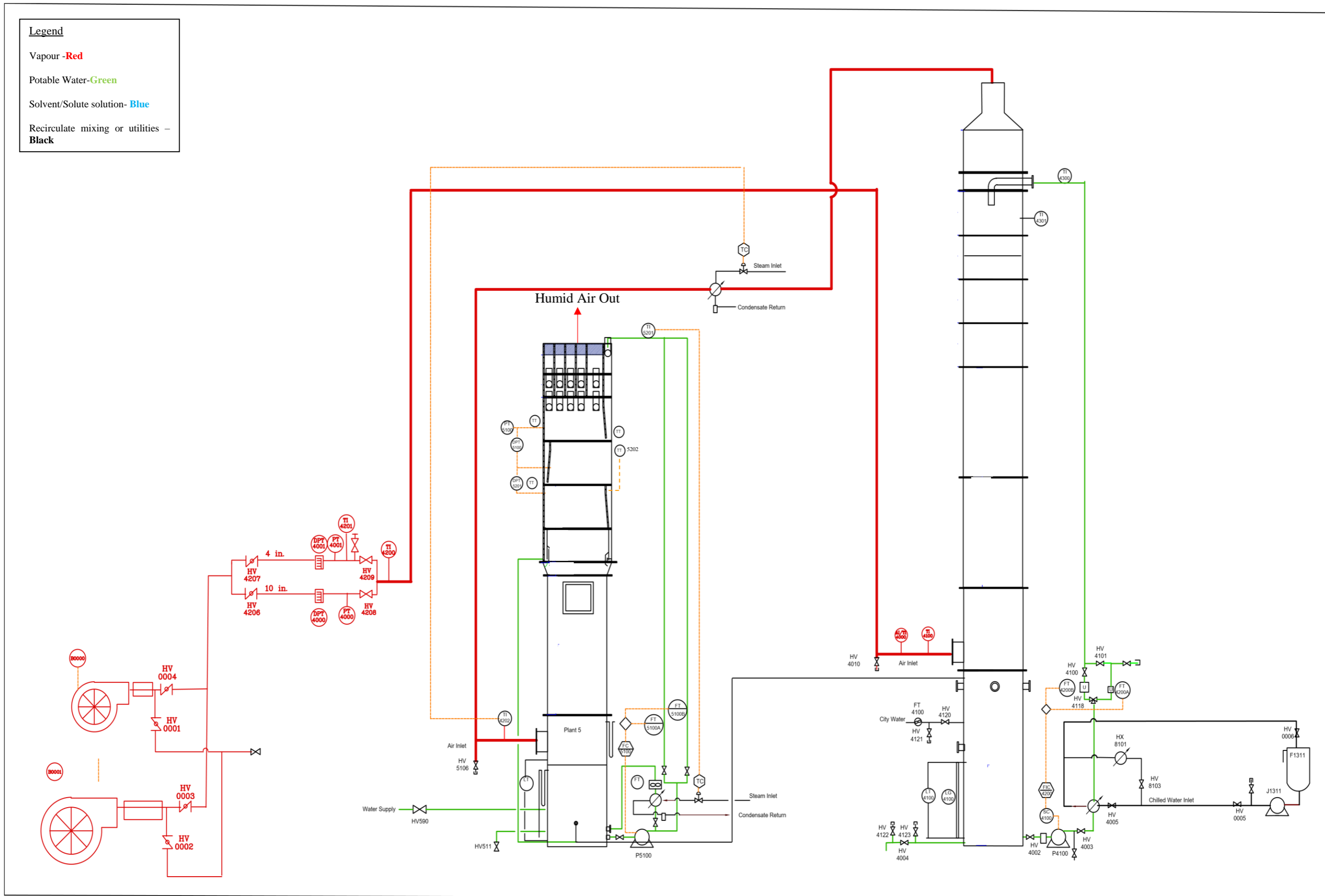


FIGURE 6.8: EXPERIMENTAL SETUP FOR TRAY COLUMN.

The same probe was used for measurements, both above and below the testing tray, to limit compound errors. The probe sensor was covered with a specially designed cap, to inhibiting direct contact with both weeping and entraining liquid. It was dried over a dehumidifier between experimental runs, to remove any excess droplets.

Testing involved humidity measurements at three discrete sample ports, both above and below the tray. This provided the benefit of being able to evaluate both point and tray efficiencies. The sampling points were respectively positioned as follows:

- [1] 50mm along the flowpath, following the inlet weir.
- [2] Halfway down the flowpath, 432mm from the inlet weir.
- [3] Within 25mm of the outlet weir.

Upon achieving steady state for 10 minutes, three sequential measurements were taken both below and above the testing tray. Measurements regarding the vapour and exiting liquid temperature were also taken with four PT-100 transmitters, and averaged over the testing interval.

Tabulated data, found in ASHRAE (American Society of Heating, Refrigerating and Air-conditioning Engineers) Fundamentals Handbook [71], was used in translating the measured relative humidity into mass fractions. The aforementioned data (from original authors Hyland and Wexler [72, 73]) was regressed and implemented in the form of various VBA (Visual Basic for Applications) functions. The functions were based the modified Rault theorem, while assuming ideal vapour phase behaviour. This was assumed applicable, as low pressures were evaluated. The exact VBA functions are presented in the included CD.

## 6.6. EXPERIMENTAL DESIGN

### 6.6.1. RANDOM PACKED COLUMN

The experimental evaluation of the packed column was considered within the context of industrial absorption processes. These processes are often reliant on large blowers, optimized for flow volume and not pressure. As a result, they are rarely operated in the loading regime, favouring operations at 40% to 50% of the manufacturer's stated flooding velocity [74, 75, 76]. This led the packed column section of this project to focus on the preloading range.

#### 6.6.1.1. LIQUID LOADINGS

The liquid loadings for the experimental evaluation were chosen to cover a range of flow rates, equally distributed between 6 and 100  $\text{m}^3 \cdot \text{m}^{-2} \cdot \text{h}^{-1}$ . This is considered within the range of random packing applicability (6-120  $\text{m}^3 \cdot \text{m}^{-2} \cdot \text{h}^{-1}$ ). The exact flowrates were adjusted for minimum deviation within the two-stage liquid distributor.

The distributor required liquid to fill to a set level on the draining pipes (with vertically spaced holes), before draining into testing column section. This ensured even distribution across the bed. At higher liquid loadings, the pressure drop over the submerged holes limited drainage, increasing the level within the first distributor stage. This level increased with increased loading until the level of the next drainage hole was reached.

The liquid loadings were therefore adjusted to limit operations at liquid levels close to the draining holes. This mitigated discrepancies in the friction coefficients of the holes, as well as variations in the levelling of the distributor.

#### 6.6.1.2. VAPOUR LOADINGS

The vapour loadings were incrementally increased for the minimum of an  $F=0.8 \text{ kg}^{0.5} \text{ m}^{-0.5} \text{ s}^{-1}$  to the blower's maximum capacity. This minimum loading was dictated by the regression parameter specifying an  $F \geq 0.8 \text{ kg}^{0.5} \text{ m}^{-0.5} \text{ s}^{-1}$ .

### 6.6.2. TRAY COLUMN

#### 6.6.2.1. LIQUID AND VAPOUR LOADING

The tray column liquid and vapour loadings were chosen to operate within the mixed froth regime, with the exception being the first prototype. This was justified, since conventional industrial columns preferentially operate within this regime. As an additional consideration, it was opted to avoid areas of excessive weeping or entrainment, as these phenomena could interfere with the humidity measurements.

## 6.7. ERROR ANALYSIS

An error analysis was conducted on both experimental setups in order to provide quantification of the uncertainty related to the data. The ensuing analysis is presented with respect to both composition and hydrodynamic quantification.

As a result of the exceedingly low compositions evaluated, it was decided to normalize all errors in terms of their average effect. This provided an adequate representation of the variability in the data, instead of representing the small standard deviation values. Mathematically, this is related as:

$$\text{Normalized Deviation} = \frac{\left[ \sum_{i=0}^n \frac{\text{STDEVA}}{\text{Average}} \right]}{n} \quad 6.2$$

### 6.7.1. VARIABILITY IN COMPOSITION QUANTIFICATION: PACKED COLUMN

The absolute instrument error of the UV-VIS spectrophotometer was quoted by the manufacturer to be within 0.3nm and 0.002A (absorbance). This was considered to be negligible, since the same measurement unit was used for both inlet and outlet quantification, cancelling any compound error. Consequently, the largest contributing factor was the reproducibility of the instrument itself. The manufacturer wavelength reproducibility was quoted at 0.2nm with photometric reproducibility amounting to 0.001A.

The error related to the use of the UV-VIS spectrophotometer was thus negligibly small when evaluated within the larger scope. This statement is justified through the use of Figure 6.9. The illustrated spectrum (enlarged from ) suggests that the influence of the wavelength variability (around 203nm) is limited to maximum error of  $2 \times 10^{-4}$ A due to the irregular fluctuations ( $\pm 1 \times 10^{-4}$ A). Through summation, this relates to  $1.2 \cdot 10^{-3}$  A.

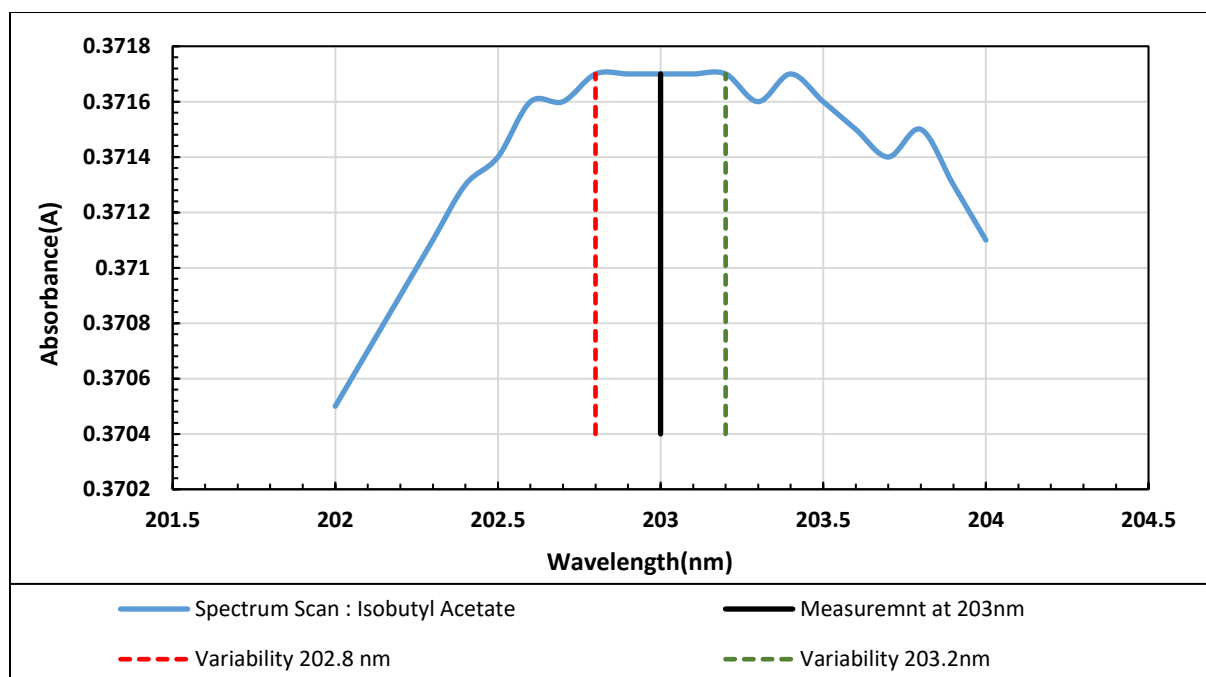


FIGURE 6.9: ISOBUTYL ACETATE ERROR SCAN USING THE UV-VIS SPECTROPHOTOMETER.

Combining this with the linear calibration curves of the isobutyl acetate cells (Figures 9.9 to 9.10), a maximum error of 7 ppm for both inlet and outlet streams, was occluded. At 3.5% for the outlet composition, this is considered acceptably small.

Table 6.2 is presented in comparing the theoretical error analysis with the experimental data. In evaluating averages ranging from 100 to 400 parts per million, the theoretical analysis was found to be valid, with the slight variations resulting from possible errors in the calibration curves.



**TABLE 6.2: PACKED COLUMN LIQUID COMPOSITION MEASUREMENT VARIABILITY (UV-VIS-SPECTROPHOTOMETER).**

<b>Normalized Deviation</b>	
Inlet composition deviation (%)	2%
Outlet composition deviation (%)	3%

### 6.7.2. VARIABILITY IN COMPOSITION QUANTIFICATION: TRAY COLUMN

Through similar considerations to those presented for the packed column, a single humidity probe was used to eliminate absolute errors, leaving only reproducibility variations. As no manufacturer data was found on the reproducibility of the Dwyer probe (485B), duplicate measurements were taken at steady state. The results being a variability of  $1.7 \cdot 10^{-4}$  in water mass fraction of the vapour. Given the nature of the sampling technique, this was considered negligible at below 2% variance in the Murphree tray efficiency.

### 6.7.3. HYDRODYNAMIC AND ATMOSPHERIC VARIABILITY: PACKED COLUMN

The variability in the measurements, aside from the composition of the solute, is presented in Table 6.3. At less than 5%, the error was considered negligibly small within the project scope and was attributed to experimental variation.

**TABLE 6.3: PACKED COLUMN NORMALIZED ERRORS FOR HYDRODYNAMIC MEASUREMENTS.**

<b>Normalized Error</b>	
Vapour Density	0%
Vapour F factor	1%
Liquid Loading	1%
Pressure Drop	4%

### 6.7.4. HYDRODYNAMIC AND ATMOSPHERIC VARIABILITY: TRAY COLUMN

The succeeding table (Table 6.4) is provided as summary of the normalized variability in the tray column setup. The large normalized errors reported in the weepage rate, resulted from measurements outside the range of the sensor. In such case, the reported weepage was below 11.3 litres per hour within a 2' line. The relative effect of the weepage is thus insignificant in these cases.

**TABLE 6.4: TRAY COLUMN NORMALIZED STANDARD DEVIATIONS FOR HYDRODYNAMIC MEASUREMENTS.**

	<b>Tray C<sub>b</sub></b>	<b>Weir Load</b>	<b>Pitot DP</b>	<b>Test Tray DP</b>	<b>Top Tray DP</b>	<b>Liquid Outlet Weir Temp</b>	<b>Weepage Rate</b>	<b>Testing Tray Liquid Temp</b>	<b>Cooled Vapour Temp</b>	<b>Vapour Temperature at column Inlet</b>
Sieve Tray 183 m <sup>3</sup> .m <sup>-2</sup> .h <sup>-1</sup> .	0.392%	0.575%	9.611%	0.283%	0.538%	0.084%	2.313%	0.077%	0.204%	0.277%
Sieve Tray 122 m <sup>3</sup> .m <sup>-2</sup> .h <sup>-1</sup> .	0.429%	0.777%	10.756%	0.255%	0.405%	0.109%	3.996%	0.106%	0.190%	0.192%
Sieve Tray 61 m <sup>3</sup> .m <sup>-2</sup> .h <sup>-1</sup> .	0.404%	1.249%	10.035%	0.272%	0.389%	0.245%	3.989%	0.267%	0.229%	0.221%
Sieve Tray 12 m <sup>3</sup> .m <sup>-2</sup> .h <sup>-1</sup> .	0.463%	4.903%	12.255%	0.309%	0.528%	0.272%	5.721%	0.284%	0.167%	0.540%
Prototype B 122 m <sup>3</sup> .m <sup>-2</sup> .h <sup>-1</sup> .	2.196%	2.456%	12.675%	1.416%	2.083%	0.278%	97.401%	1.323%	2.073%	2.632%
Prototype B 61 m <sup>3</sup> .m <sup>-2</sup> .h <sup>-1</sup> .	0.403%	1.206%	9.195%	0.192%	0.264%	0.138%	63.238%	0.139%	0.292%	0.800%
Prototype B 183 m <sup>3</sup> .m <sup>-2</sup> .h <sup>-1</sup> .	0.510%	0.506%	12.952%	0.217%	0.502%	0.075%	78.532%	0.079%	0.212%	0.505%



# CHAPTER 7: RESULTS AND DISCUSSION

## 7.1. PACKED COLUMN LIQUID PHASE EVALUATION

### 7.1.1. METHOD VALIDATION

The proposed ADIBAA-method was validated through a combination of four independent literature models. The experimental validation was limited to the preloading range, as Rejl [27] suggested a consensus between literature sources within this band. Due to limited data on 4<sup>th</sup> generation packing, verification was done on 2' FlexiRings® (Provided by Koch Glitsch L.P). The results of the verification experiments are presented in Figures 7.1 to 7.2.

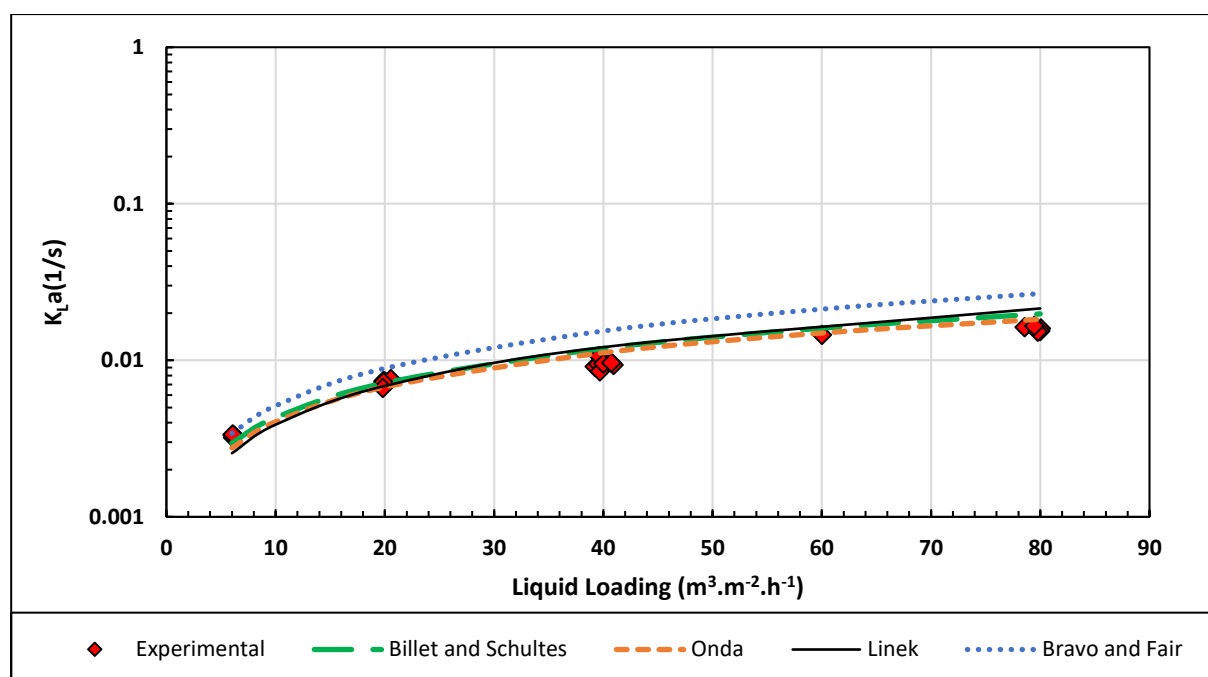


FIGURE 7.1: PACKED COLUMN EXPERIMENTAL VERIFICATION: LITERATURE MODEL COMPARISON WITH OWN DATA.

A variety of authors were found either misquoting or misusing the liquid phase volumetric mass transfer correlations (from the literature evaluation in Chapter 4). An example of the related confusion is presented in the Senol [77] publication. The author mistakenly quoted and used the Bravo and Fair [45] model with SI (International System of Units) units, while original equation was based on the English unit system [77].

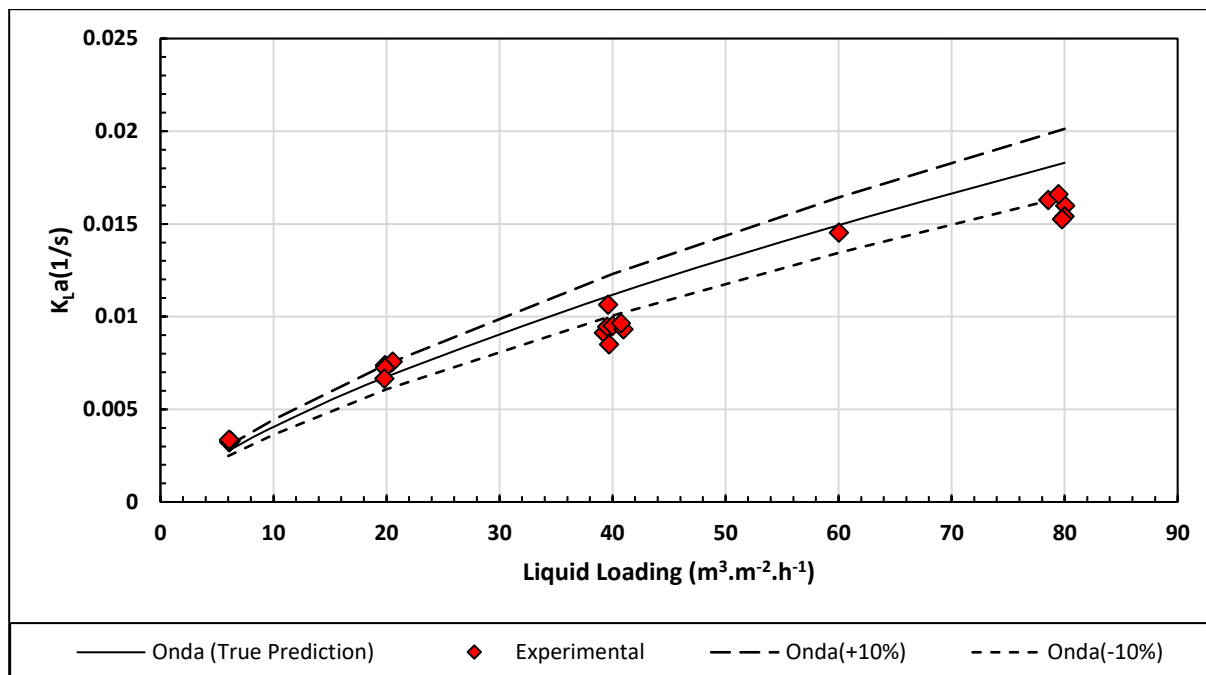


FIGURE 7.2: VERIFICATION OF EXPERIMENTAL DATA WITH THE ONDA [19] MODEL.

The models used in this project, were consequently validated on the calculations presented in Stichlmair and Fair's, *Distillation Principles and Practises* [47]. The deviations recorded were insignificant and attributed to rounding in the textbook. This validation is presented in the CD Appendix.

The experimental setup provided satisfactory replication of literature models, as presented in Figures 7.1 to 7.2. Quantitatively, the experimental data was found to remain within 10% of the Onda [19] correlation (Equations 4.12 and 4.13). This provided the needed justification to continue with the experimental evaluation, while satisfying the project deliverable of producing a viable alternative-hence forth named the ADIBAA-method.

The non-normal error distribution evident in Figure 7.2, was considered due to the use of the penetration theory in relating the mass transfer of oxygen to that of isobutyl acetate. This simplification introduced by Higbie [78], was derived on a stagnant system of a pure liquid and vapour. Although extrapolated and widely used in literature, this model introduces an intrinsic error. This error is exaggerated in instances of higher interfacial turbulence (and subsequently higher liquid loadings in the preloading regime), which explains the non-normally distributed errors across the range of liquid loadings. (See discussion of the Penetration Theory in Table 9.9)

### 7.1.2. REPEATABILITY

The repeatability of the experimental setup was evaluated over three independent runs. The results presented (Figure 7.3), suggested an average standard deviation in liquid phase volumetric mass transfer coefficients of  $4.1 \cdot 10^{-4} \text{ (s}^{-1}\text{)}$  or 2.7% at a liquid loading of  $80 \text{ m}^3 \cdot \text{m}^{-2} \cdot \text{h}^{-1}$ . This was within the experimental band of accuracy of the UV-VIS spectrophotometer.

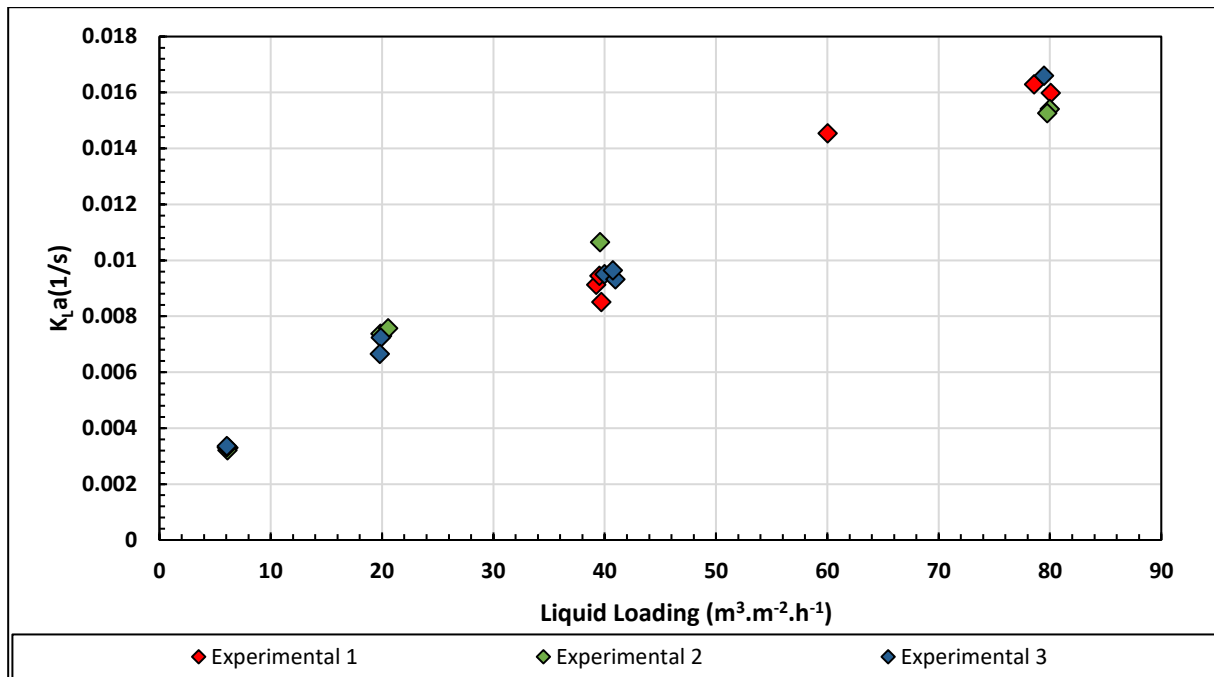


FIGURE 7.3: EXPERIMENTAL REPEATABILITY OF THE PACKED COLUMN DATA ACROSS VARYING LIQUID FLOW RATES.

Having established the repeatability and validity of the ADIBAA-method (and the experimental setup) in measuring liquid phase volumetric transfer coefficients, the project continued in evaluating the method as a design tool. Consequently, the ADIBAA-method was evaluated on its capability of differentiating of column internals based on efficiency (HETP).

### 7.1.3. COMPARING COLUMN INTERNALS ON LIQUID PHASE MASS TRANSFER

The evaluated mass transfer coefficients are presented in terms of a HETP (Height equivalent to a theoretical tray). This was done to condense the high quantities of experimental data into comparable graphs. In the resulting graphs, a high value of HETP depicts low efficiencies and vice versa.

In reviewing the capabilities of the proposed method in differentiating column internals, stainless FlexiRings® (1.5') were compared to the latest generation Intalox® Ultra™ (Size A or 1.5'). The results of the comparison are presented in Figures 7.4 to 7.6.

The presented graphs are divided into ranges of liquid loadings. The loadings are given in terms of the hourly volumetric flow rate per cross-sectional area (m<sup>3</sup>.m<sup>-2</sup>.h<sup>-1</sup>). This removes the area from the evaluations and promotes easier extrapolation to different columns. The capacity factor used in the representation of the data are defined as:

$$C_s = u_s \sqrt{\frac{\rho_G}{\rho_L - \rho_G}} \quad 7.1$$

The data are represented in this form as it compensates for the relative liquid / vapour densities. This capacity factor subsequently provides a quantitative measure of the vapour flow rate and buoyancy forces. A more conventional representation, in terms of vapour flow factors, is provided in Figure 9.17 to 9.25.

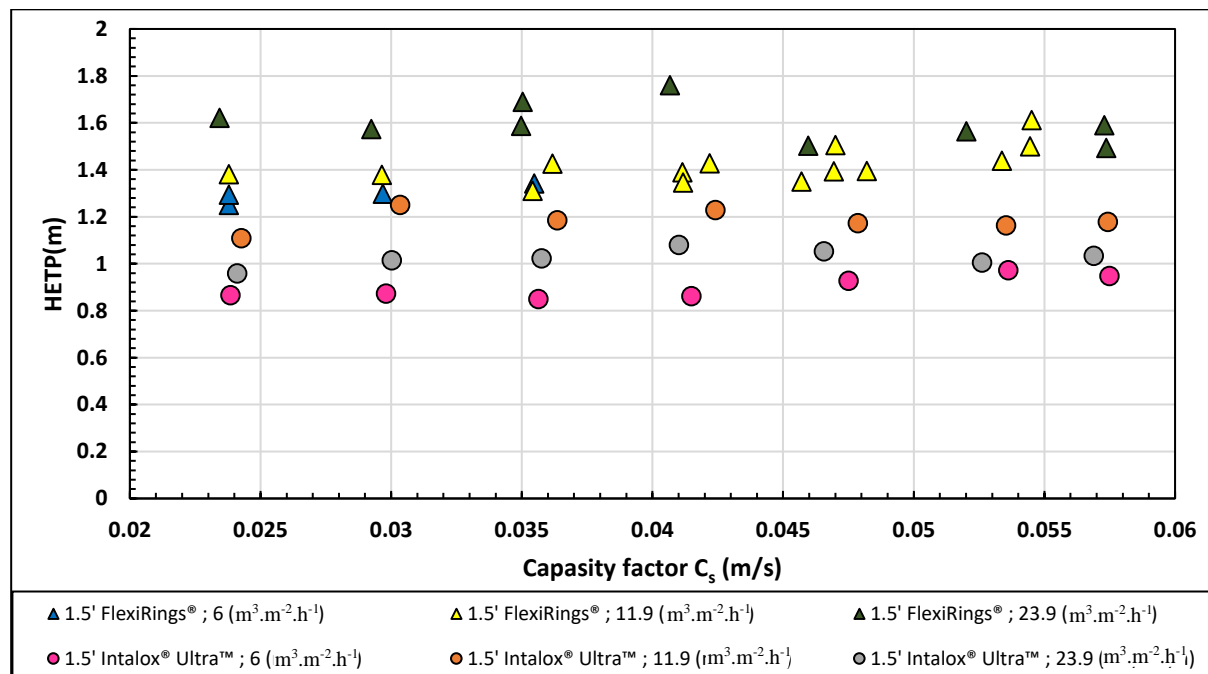


FIGURE 7.4: HETP COMPARISON OF 1.5' FLEXIRINGS® AND INTALOX® ULTRA™ (6 TO 23.9  $\text{m}^3\cdot\text{m}^2\cdot\text{h}^{-1}$ ).

The data presented in Figures 7.4 and 7.5, illustrate clear differentiation between column internal performance. An average performance increase of 15% was calculated for the Intalox® Ultra™, in the liquid range of 6 to 47  $\text{m}^3\cdot\text{m}^2\cdot\text{h}^{-1}$ . The experimental data were found to agree with various literature [79, 74, 18, 29, 26] sources, in that the HETP remained effectively constant throughout the pre-loading regime.

Reasoning for the Intalox® Ultra™ performance increase in Figures 7.4 and 7.5, is given in terms of interfacial turbulence, as this parameter notably effects the liquid phase mass transfer coefficient ( $k_L$ ). The resulting higher interfacial turbulence promotes surface renewal, increasing the effective concentration driving force. This leads to higher values of  $k_L$  and thus  $K_La$  and HETP.

It is therefore deduced that the greater open area Intalox® Ultra™ constantly disrupts the flowpath of the liquid, creating randomized streams. Each time the liquid is forced to change direction, interfacial turbulence is created while renewing the effective surface. In contrast the enclosed design of the FlexiRings® mostly use the specific outer area of the packing, coating each rivulet to create phase contact. The directional changes are therefore much less pronounced and the liquid is envisioned flowing

across the packing in a film rather than in randomized streams. This decreases the interfacial turbulence and thus the driving force for mass transfer.

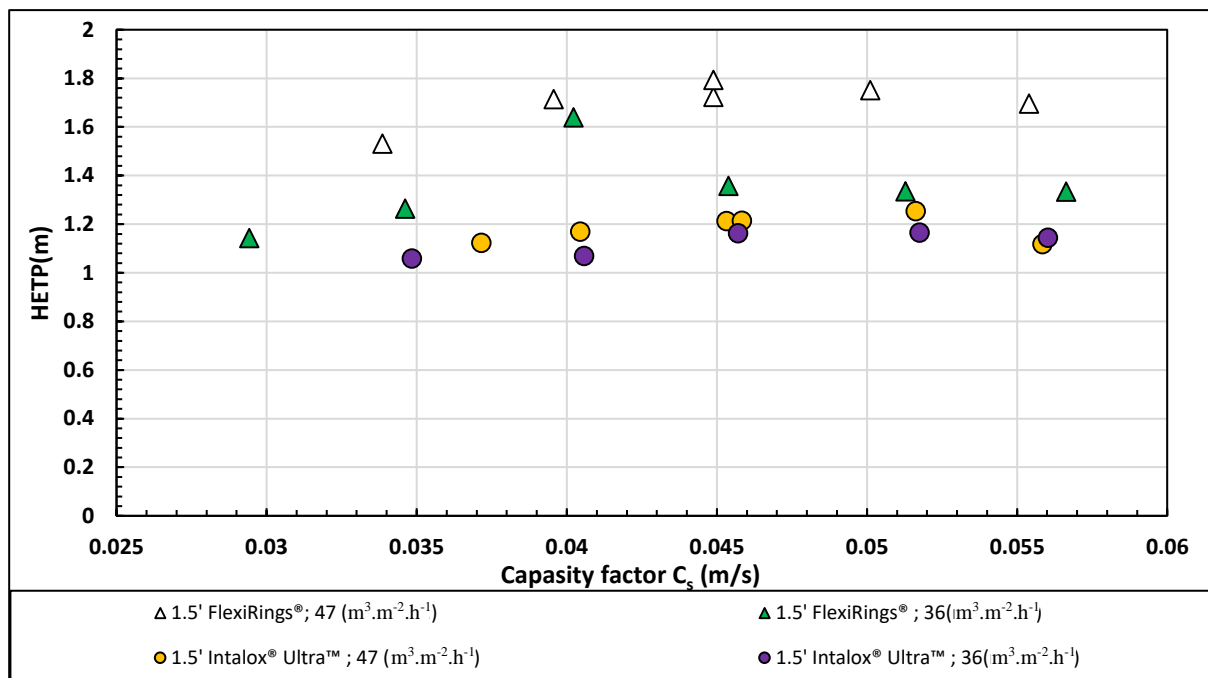


FIGURE 7.5: HETP COMPARISON OF 1.5' FLEXIRINGS® AND INTALOX® ULTRA™ (36 TO 47  $\text{m}^3\cdot\text{m}^{-2}\cdot\text{h}^{-1}$ ).

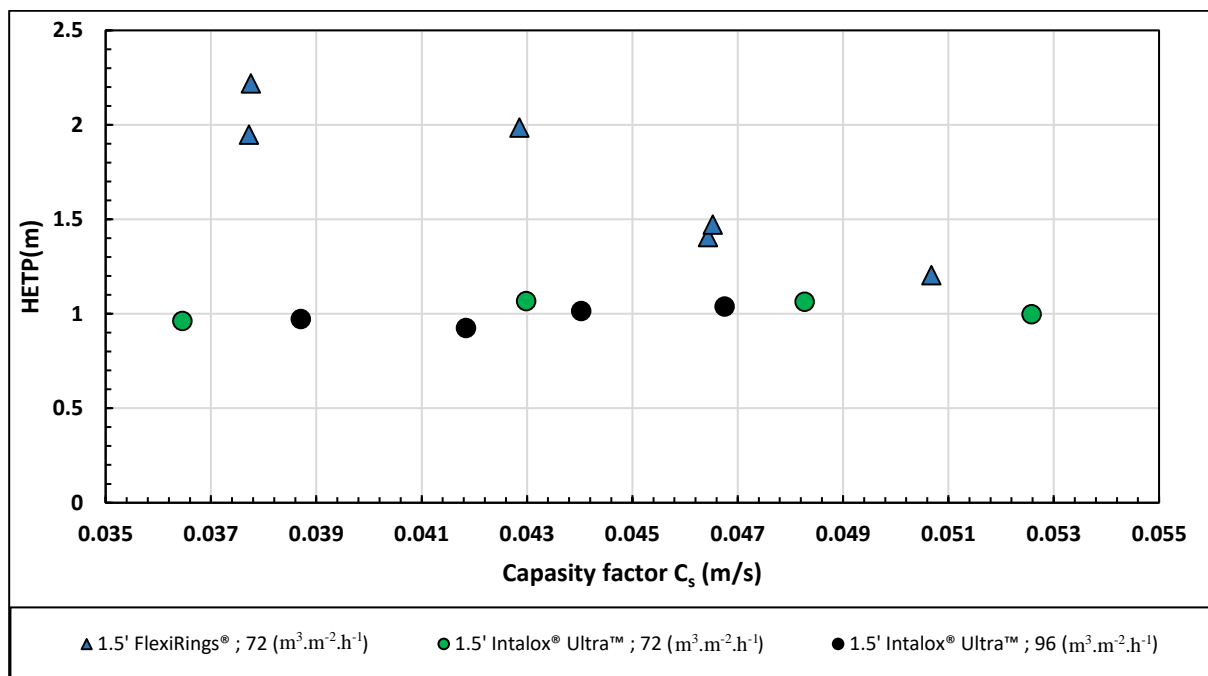


FIGURE 7.6: HETP COMPARISON BETWEEN 1.5' FLEXIRINGS® AND INTALOX® ULTRA™ (72 TO 96  $\text{m}^3\cdot\text{m}^{-2}\cdot\text{h}^{-1}$ ).

A declining trend in HETP (increasing efficiency) is presented for the 1.5' FlexiRings® at 72  $\text{m}^3\cdot\text{m}^{-2}\cdot\text{h}^{-1}$  in Figure 7.6. This is indicative of the system entering the loading range, with increased liquid holdup



and effective interfacial area. Although outside the preloading scope, the trend indicates the applicability of the ADIBAA-method within the loading range.

In a bid to further evaluate the robustness of the ADIBAA-method in quantifying variations in efficiency, this report chose to investigate the relationship between efficiency and packing size in the Intalox® Ultra™ range. The presented experimental results are arranged by liquid (Figures 7.7 to 7.11).

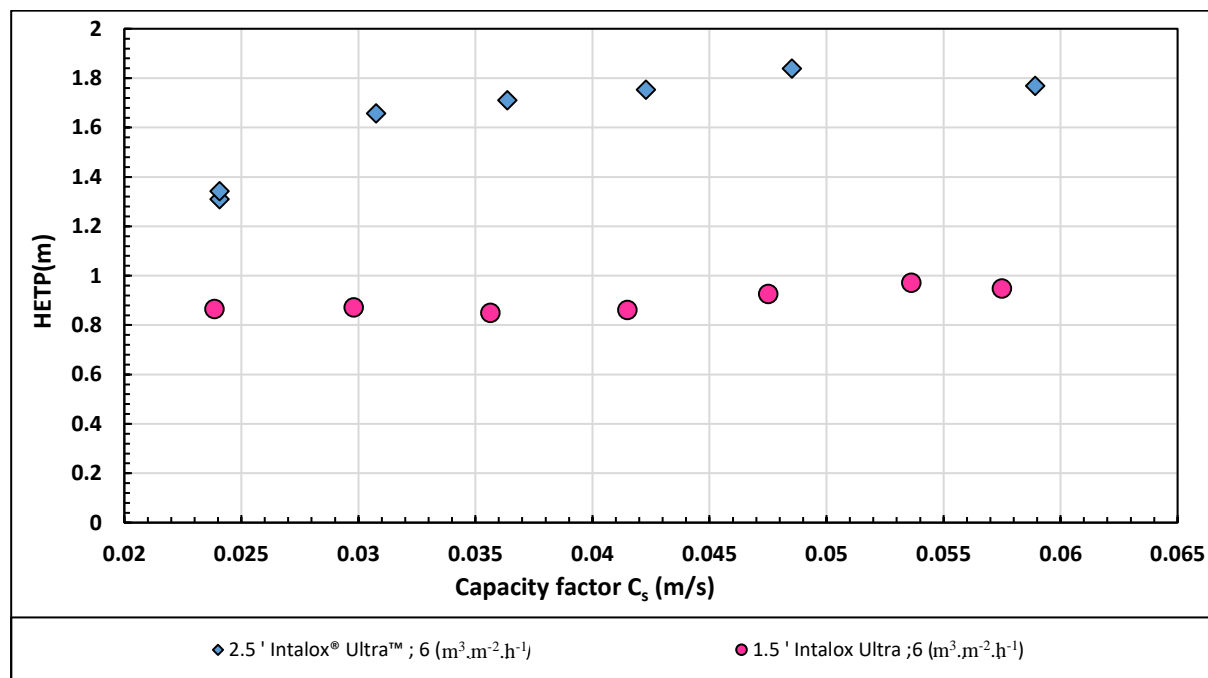


FIGURE 7.7: HETP COMPARISON OF 1.5' AND 2.5' INTALOX® ULTRA™ ( $6 \text{ m}^3 \cdot \text{m}^{-2} \cdot \text{h}^{-1}$ ).

The results of the performance evaluation (Figures 7.7 and 7.8) at low liquid rates ( $6 \text{ m}^3 \cdot \text{m}^{-2} \cdot \text{h}^{-1}$ ), were considered indicative of inadequate exploitation of the packing area on the part of the 2.5' variant. This occurred since most of the liquid passed through the large open area in the 2.5' bed, with minimized interaction with the packing.

Little interfacial turbulence was therefore created by the packing during the descent, ultimately minimizing the liquid phase mass transfer coefficient ( $k_L$ ). As the liquid rate increased, the difference in performance of the 1.5' and 2.5' decreased (Figure 7.8). From this reasoning, the higher liquid Reynolds numbers increased both the renewal of the effective surface and the interactions with the packing itself.

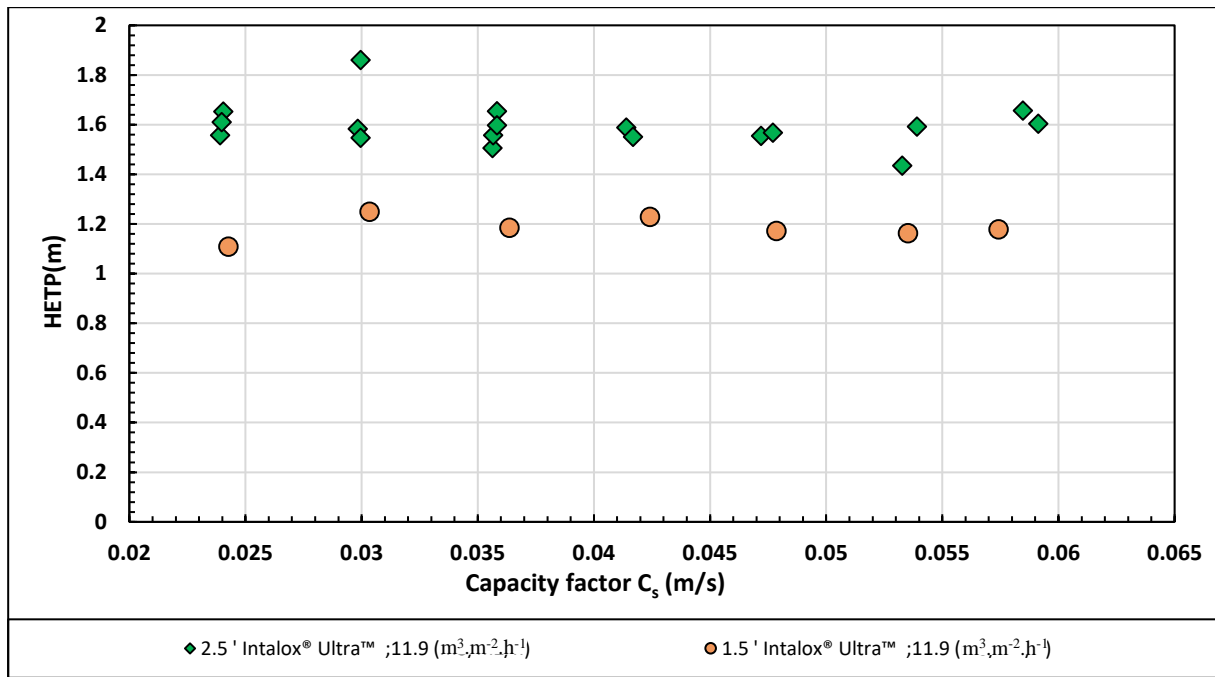


FIGURE 7.8: HETP COMPARISON OF 1.5' AND 2.5' INTALOX® ULTRA™ (11.9 m³.m⁻².h⁻¹).

Further increase in the vapour loadings is conventionally thought to yield a constant efficiency across the pre-loading range [50]. This is as the vapour momentum is not yet sufficient to exert a perceivable force on the liquid. The experimental data, however, yielded an unconventional relationship between vapour flow rates and the efficiency in the preloading range. This phenomenon is presented Figures 7.10 to 7.11.

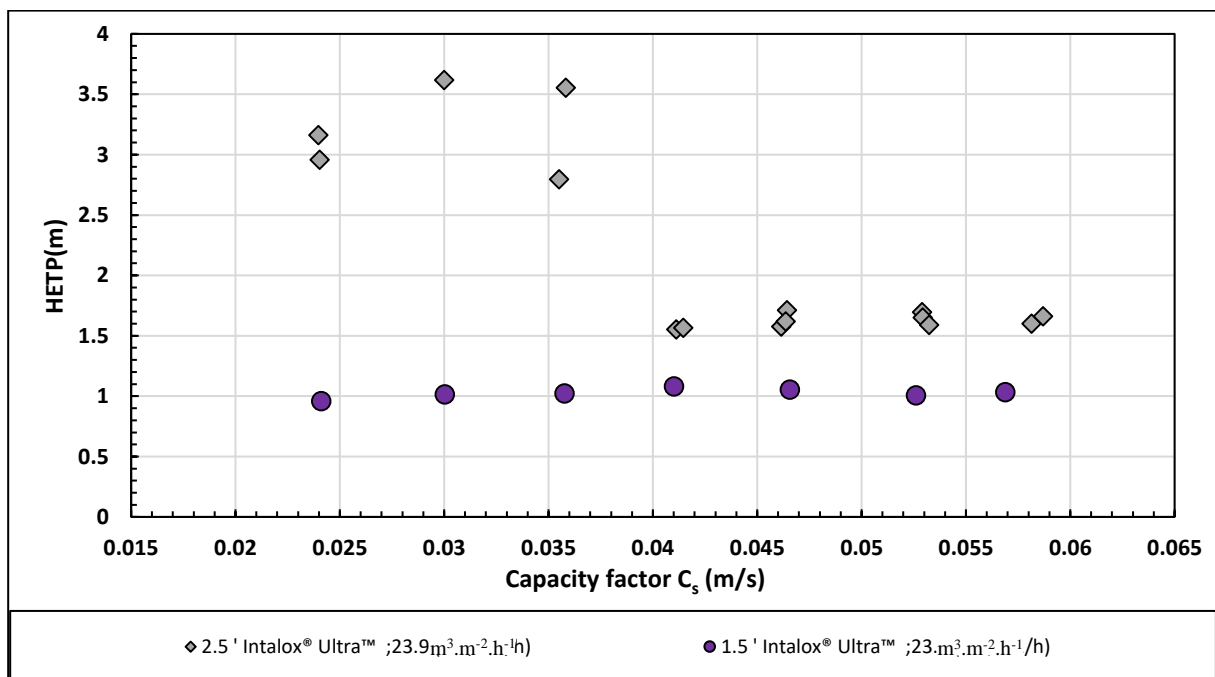


FIGURE 7.9: HETP COMPARISON OF 1.5' AND 2.5' INTALOX® ULTRA™ (23.9 m³.m⁻².h⁻¹).

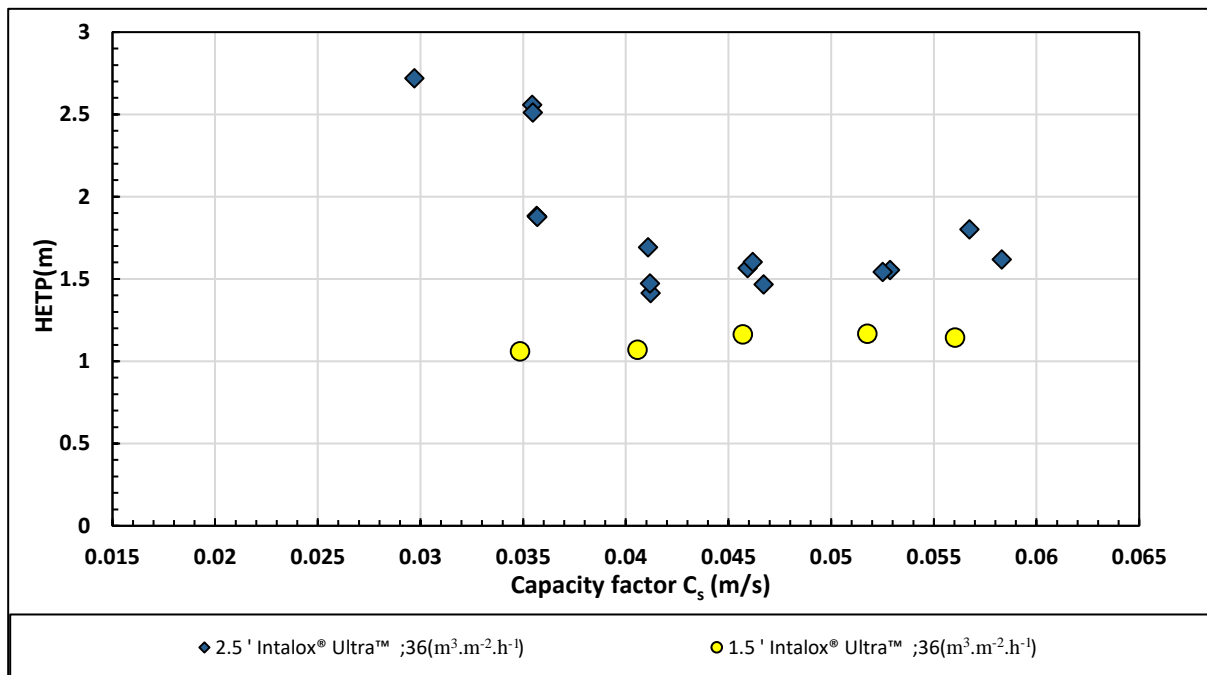


FIGURE 7.10: HETP COMPARISON OF 1.5' AND 2.5' INTALOX® ULTRA™ (36 m³.m⁻².h⁻¹).

Sudden and substantial disturbances in efficiency were consequently reported in the medium to high liquid rates (Figures 7.10 to 7.11). This transcended the errors attributed to both the system variations and quantification repeatability. The sudden changes in efficiency were accompanied by oscillatory behaviour close to the point of transition, based on vapour loading. The behaviour in question was found to continue for stretches greater than 30 minutes, without stabilizing. As a result, the data points close to the transition point were considered immeasurable, as steady state could not be attained.

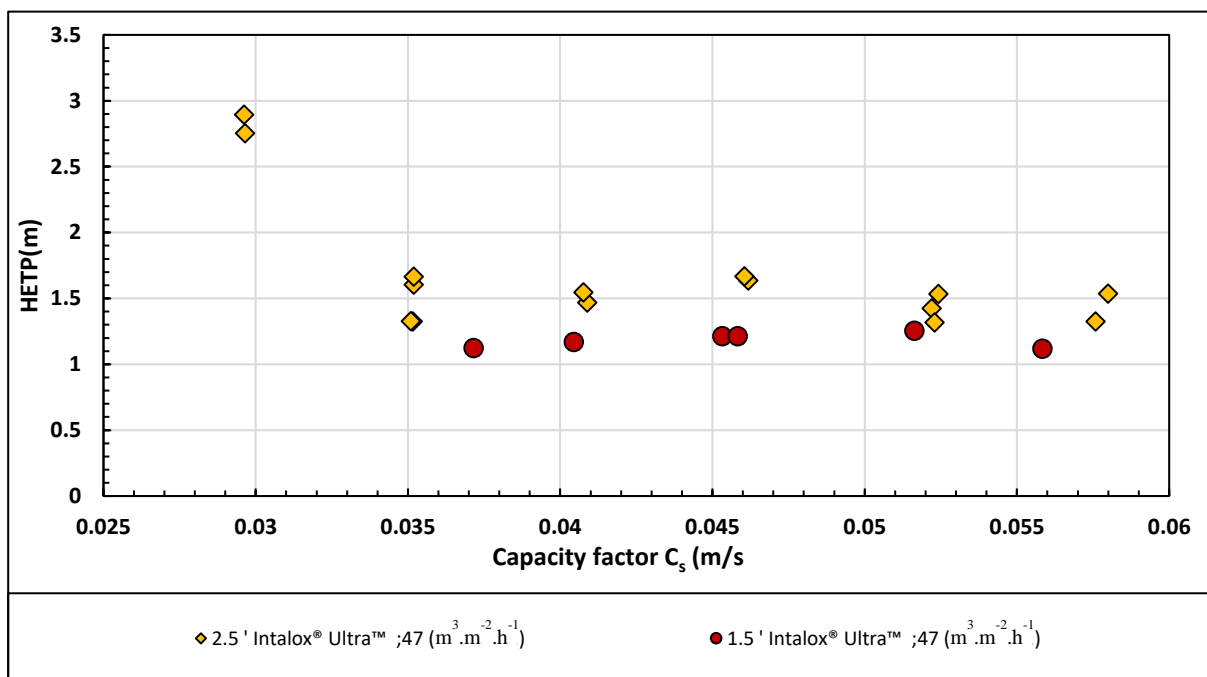


FIGURE 7.11: HETP COMPARISON OF 1.5' AND 2.5' INTALOX® ULTRA™ (47 m³.m⁻².h⁻¹).

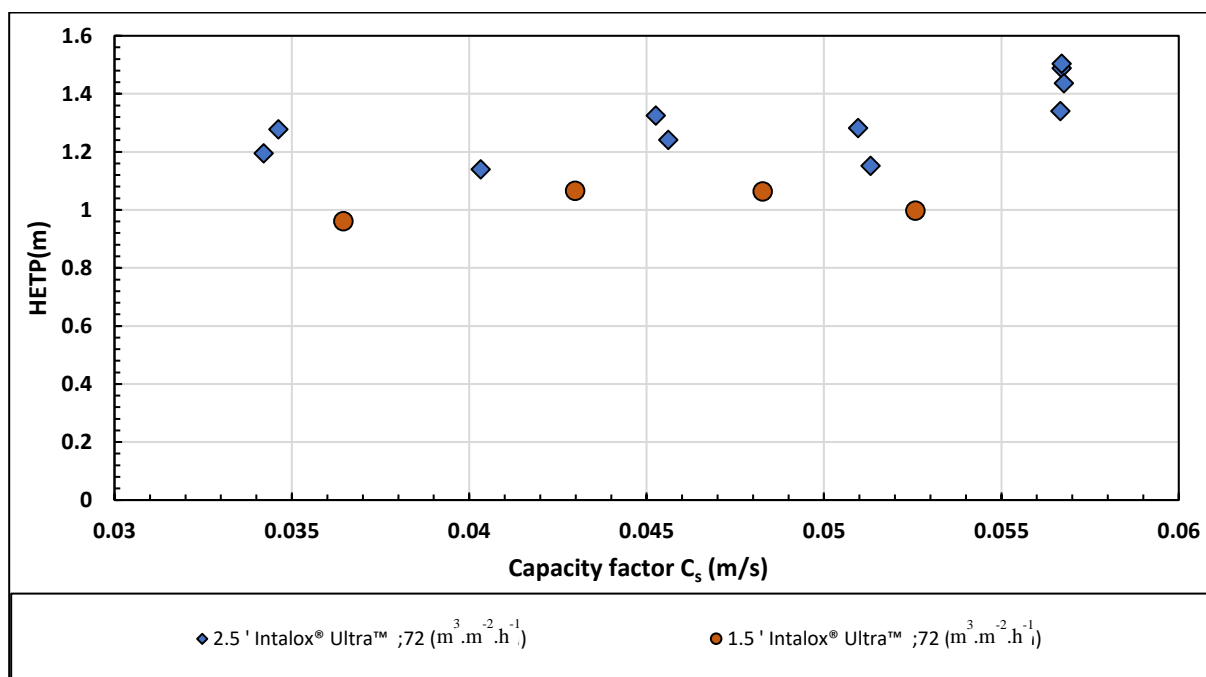


FIGURE 7.12: HETP COMPARISON OF 1.5' AND 2.5' INTALOX® ULTRA™ ( $72 \text{ m}^3 \cdot \text{m}^{-2} \cdot \text{h}^{-1}$ ).

To confirm the existence of both the oscillatory behaviour and the accompanied changes in efficiency, three independent experiments were conducted with the column repacked for each. The evaluations provided comparative results, confirming the existence of this behaviour at similar flow rates. The experimental setup was further screened, using pure water, in an attempt to quantify any instrumental drift in the relevant range. This notion was disproved, as the water produced a constant baseline at a value of zero absorbance. This justified this thesis in hypothesizing that the behaviour was a characteristic of the packing and related the hydrodynamics.

An example of the oscillatory behaviour (Figure 7.14) is presented in terms of UV-absorption. In contrast, a dataset from the previous 1.5' FlexiRings® evaluation is presented as reference (Figure 7.13). The aforementioned oscillatory behaviour was found to have a notable impact on the effective quantification, further compounded by the low component concentrations.

Having repeated the experimental evaluations three times with the same oscillatory result (at the same vapour/ liquid flow rates), the trends (Figure 7.14) suggested that variations in hydrodynamic conditions were to blame for both the sudden changes in efficiency and the oscillatory behaviour.

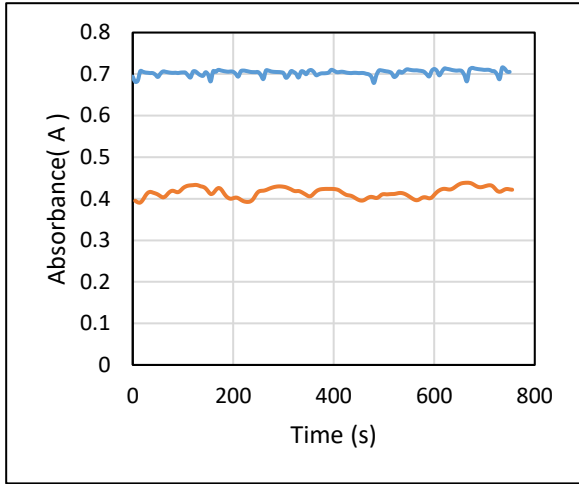


FIGURE 7.14: OSCILLATORY BEHAVIOUR.

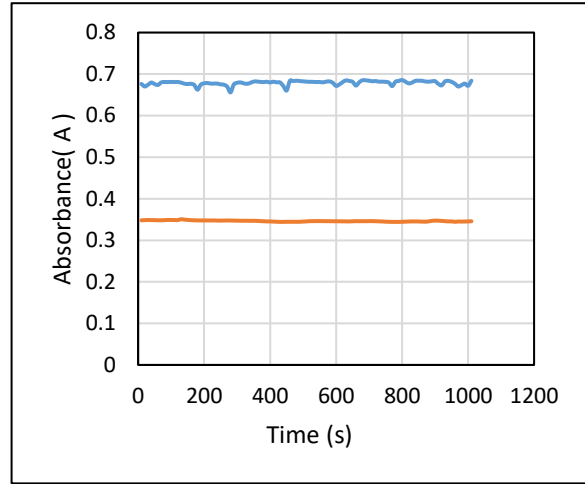


FIGURE 7.13: NON-OSCILLATORY BEHAVIOUR

KG-Tower® approximations for the relative flooding velocities were employed in attempting to explain the sudden variations in efficiency. The subsequent evaluation (Figures 7.15 to 7.17) presented an interesting observation regarding the onset of the substantial and sudden changes in efficiency. In all cases, the sudden increase in efficiency was evaluated on and around 35% to 40% of the proposed flooding velocity. The repeating trend further added to the hypothesis that the phenomenon was hydrodynamically related to the packing. As an added logic test, the 2' Intalox® Ultra™ was evaluated at  $20 \text{ m}^3 \cdot \text{m}^{-2} \cdot \text{h}^{-1}$  and presented a similar, yet diminished effect at 35-40% flooding.

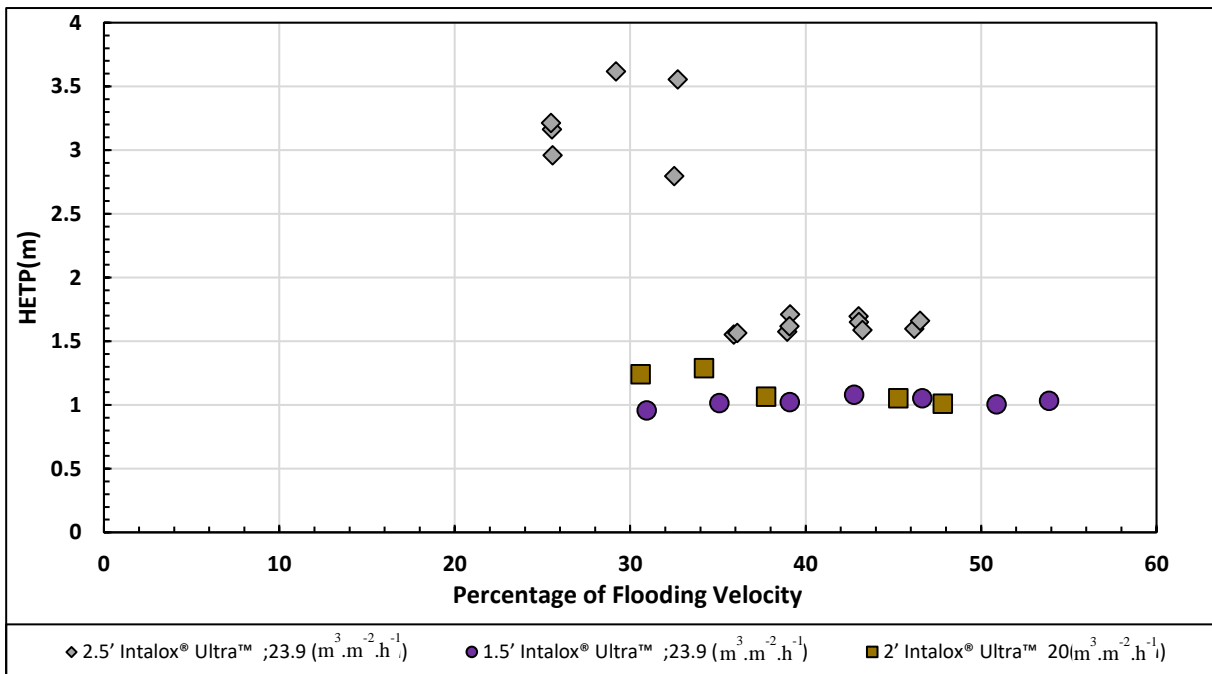


FIGURE 7.15: HETP COMPARISON OF 1.5', 2' AND 2.5' INTALOX® ULTRA™ ( $23.9 \text{ m}^3 \cdot \text{m}^{-2} \cdot \text{h}^{-1}$ ), WITH REFERENCE TO FLOODING VELOCITY.

The aforementioned behaviour presented a fundamental conundrum. As the packing was evaluated in the preloading range, conventional knowledge suggested the negligible effect of vapour velocity. This is as a result of the exerted force not yet being sufficient to increase the liquid holdup, hereby implying a constant interfacial area. In accordance, liquid maldistribution is also not expected to be a function of vapour velocity within this range, as the friction forces are insufficient to overcome the liquid momentum [74].

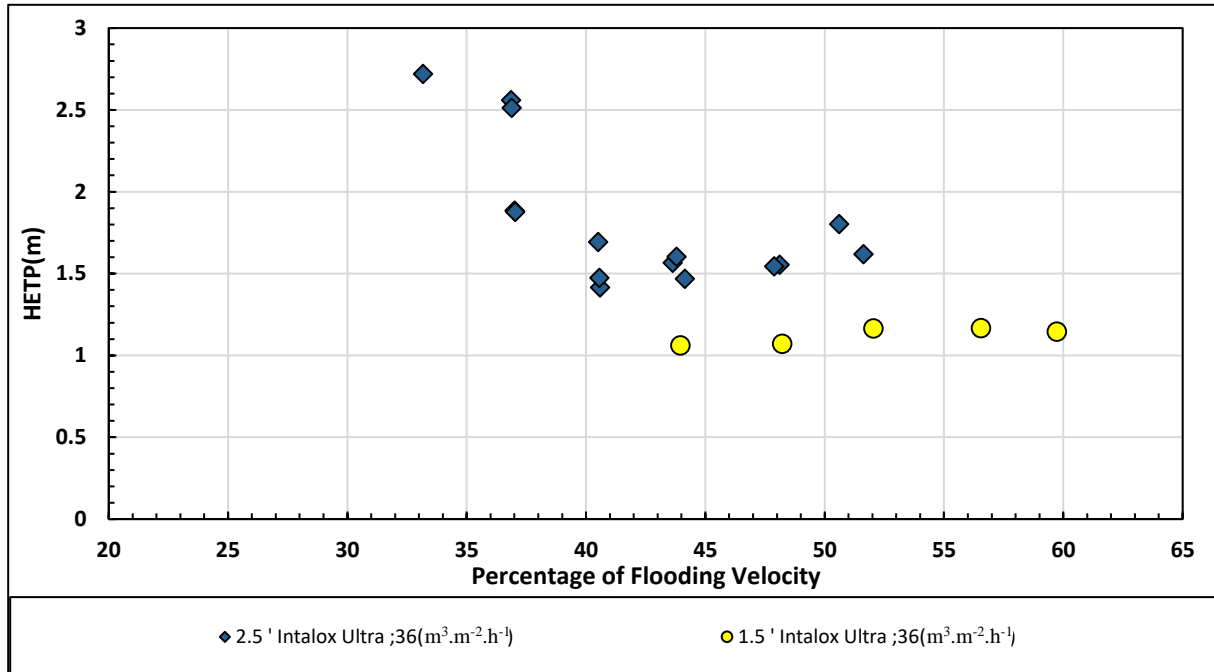


FIGURE 7.17: HETP COMPARISON OF 1.5' AND 2.5' INTALOX® ULTRA™ (36 m<sup>3</sup>.m<sup>-2</sup>.h<sup>-1</sup>), WITH REFERENCE TO FLOODING VELOCITY.

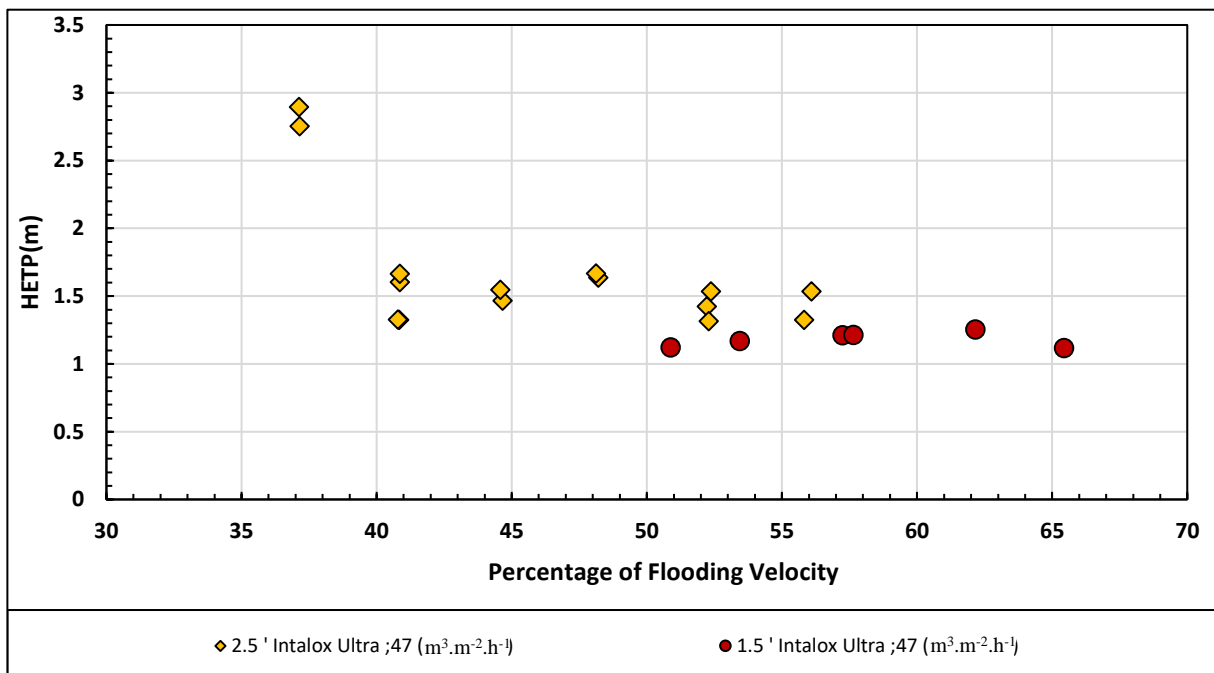


FIGURE 7.16: HETP COMPARISON OF 1.5' AND 2.5' INTALOX® ULTRA™ (47 m<sup>3</sup>.m<sup>-2</sup>.h<sup>-1</sup>), WITH REFERENCE TO FLOODING VELOCITY.

The apparent contradiction with current convention, is justified in the succeeding, hypothesis. The hypothesis is based on the consideration that:

- [1] The relative efficiency increases were directly proportional to the packing size and thus the effective voidage. This was evident as the onset of the sudden changes intensified with the increased packing size.
- [2] Little influence was seen on the 1.5' FlexiRings® evaluation. It was therefore deduced that the sudden efficiency changes were not related to the onset of the loading regime. This was as the 1.5' FlexiRings® entered the loading regime during most of the experimental matrix (According to KG Tower), yet no sudden increases in efficiency was seen in Figures 7.4 to 7.6.

Stemming from proportionality between open area and the packing size, the behaviour was thought to be indicative of liquid maldistribution or short circuiting in the packed bed. In the case of the restrictive Pall-Ring design, the enclosed rivulets provided sufficient interaction to inhibit the liquid from jetting through the column in continuous streams. In contrast, the larger open area Intalox® Ultra™, offered little restriction to the downward flowing liquid. This inefficiently wetted and underexploited the packing rivulets, as the liquid was visualised passing through much of the bed in the original channels created by the distributor. This effect was further exaggerated by the increased packing sizes (accompanied by increased voidage) and the short column section. The liquid was thus conceptualized flowing down the column, in a series of continuous liquid streams.

In deepening the thought process to the physics of descending liquid, droplet formation was conceptualized through visualizing a single stream descending in freefall. The conceptual liquid elongates before breaking off in droplets. In the elongated section the inertial forces dominate surface tension effects, keeping the liquid in a continuous stream. At the onset of droplet creation, the forces strike a balance, creating individual liquid droplets.

As a result of their smaller size, the individual droplets experience a notably decreased drag force. This is due to the inversely proportional relationship that exists between the size of the liquid droplet and the terminal velocity - mathematically depicted in Equation 7.2 [70]. Consequent, larger liquid streams exhibit lower terminal velocities and therefore higher effective friction forces.

$$V_T = \sqrt{2 \cdot \frac{M_L \cdot g}{\rho_L \cdot S \cdot C_d}} \propto \frac{1}{\text{Friction force}} \quad 7.2$$

A similar force balance is hypothesized for the streams of the descending liquid in the high open area Intalox® Ultra™ packed bed. At vapour rates below 30% of the flooding velocity, the inertial and momentum forces are thought to dominate and create continuous liquid streams alternating down the packing. As the vapour rate is increased, the descending liquid streams elongate and alternate from the liquid jets. Due to the continuous liquid streams in higher open area packings, the hypothesized

behaviour originates as the large streams experience greater friction forces. The increased friction subsequently promotes variability in the packed bed. This increases effective interfacial area and consequently efficiency.

Although sound in theory, the abovementioned conceptualization directly contradicts current knowledge. Literature convention suggests the limited effect of vapour velocity on liquid maldistribution in the preloading range. This may in part be as a result of the largely restrictive designs of the previous generation packings, focussing on coating a specific area of packing rather than facilitating droplets (producing an effective interfacial area larger than the specific area).

The presented justification is therefore speculative, as it is founded on the experimentally unverified assumption that the liquid holdup of high open area packings is a function of vapour velocity within the preloading range. At the date of publication, this was still unsubstantiated as no experimental data was currently available.

#### 7.1.4. EVALUATION OF MASS TRANSFER COEFFICIENTS

The mass transfer coefficients used in calculating the relevant efficiencies for the FlexiRing® evaluation, was found in agreement with literature sources [18, 79, 80] on the comparative influence of the liquid load, reflecting an independence on packing size. This is at one with various authors noting the constant influence of liquid loadings (power relationship 0.7-0.8) on Pall Rings, both 1' and 2'. The numerical value of the relevant exponent, however, is the subject of debate, as Rejl [27] (with Linek [27] as co-author) himself noted the effects of axial dispersion related to his use of a substandard 290 mm ID column.

The underestimation related to the use of the column size ranged from 30% at low liquid loads to negligible above  $40 \text{ m}^3\text{m}^{-2}\text{h}^{-1}$  [27]. This suggests decreased curvature as well a decrease in the numerical value related to the power function. An illustration of the comparative effect of liquid loading on liquid phase mass transfer is presented in Figure 7.18, for both evaluated sizes of Pall Rings.

In contrast to the comparative values of the FlexiRing® assessment, size dependent behaviour was reported on the Intalox® Ultra™ packing. The steeper power function on the 2.5' variant was thought to be related to be inadequate wetting under lower liquid loadings. Graphical representation of the difference between 1.5' and 2.5' Intalox® Ultra™ packing, is provided in Figures 7.19 and 7.20.



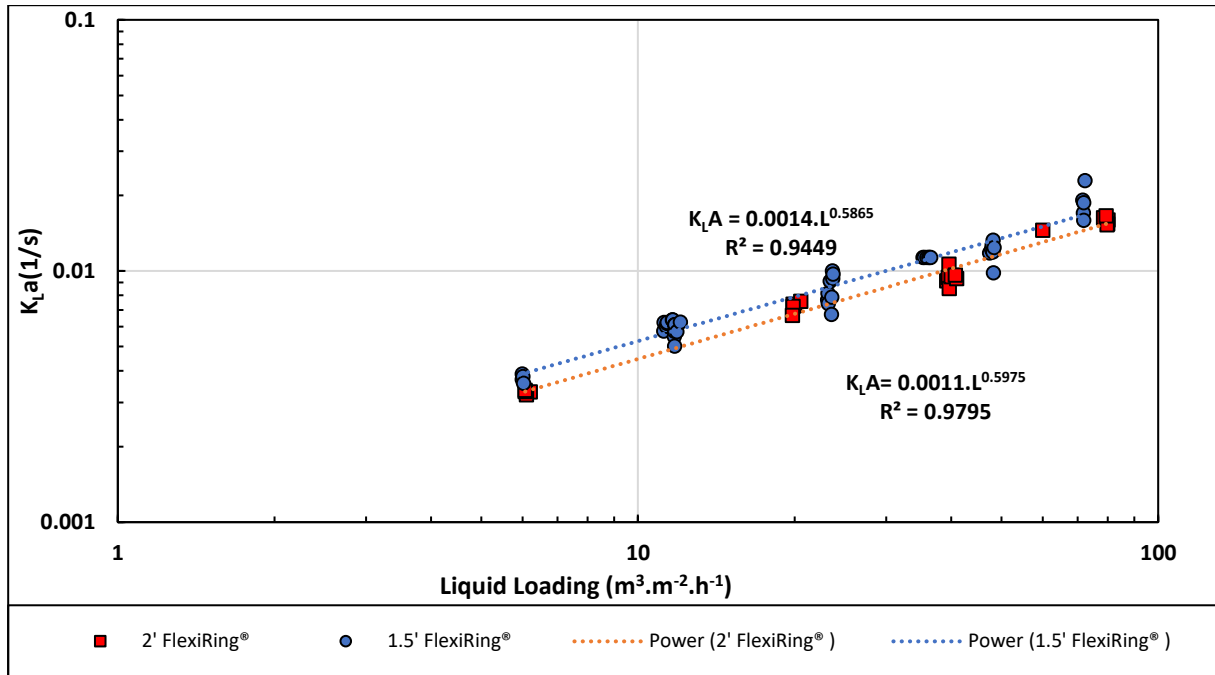


FIGURE 7.18: VOLUMETRIC LIQUID PHASE MASS TRANSFER COEFFICIENTS FOR FLEXIRING®; 1.5' VS. 2'

The unrestrictive design of the Intalox® Ultra™ packing relies notably on droplet formation at the local tips, for interfacial turbulence. However, at low rates, vapour effectively short-circuits through high open area of the packing, with little interaction with the liquid. This promoted lower liquid holdup and effective interfacial area. As a result, a changing power function dependency was noted for the 1.5' and 2.5' Intalox® Ultra™.

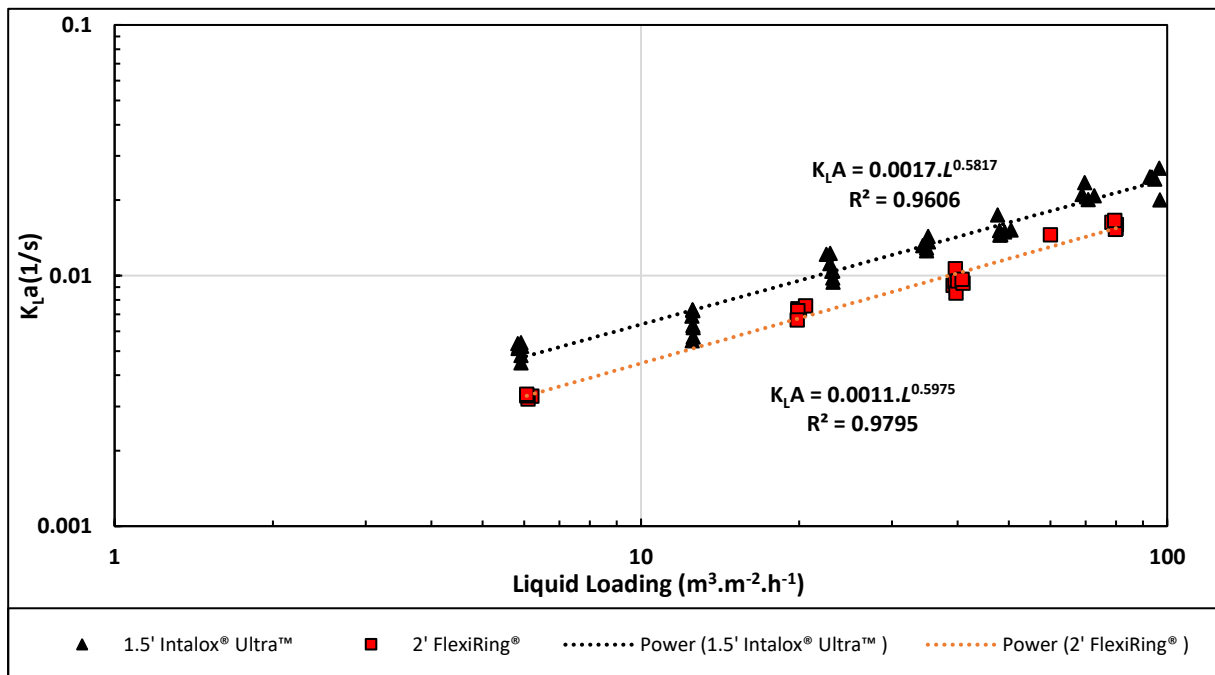


FIGURE 7.19: VOLUMETRIC LIQUID PHASE MASS TRANSFER COEFFICIENTS FOR 1.5' INTALOX® ULTRA™ PACKING VS 2' FLEXIRING®

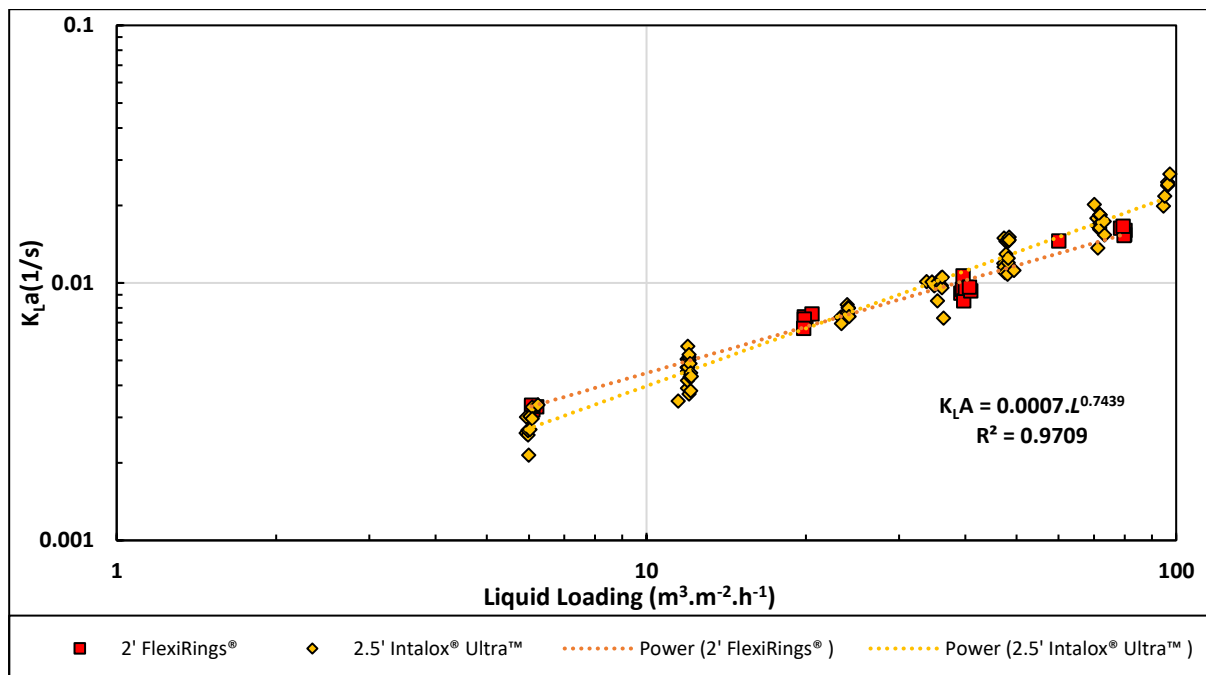


FIGURE 7.20: VOLUMETRIC LIQUID PHASE MASS TRANSFER COEFFICIENTS FOR 2.5' INTALOX® ULTRA™ PACKING VS. 2' FLEXIRING®

### 7.1.5. CONCLUDING REMARKS ON THE ADIBAA-METHOD

The ADIBAA-method was found to illustrate sufficient capabilities, as a simplistic and cost-effective alternative to conventional efficiency quantification. This was justified through the efficiency comparison of 1.5' FlexiRings® and Intalox® Ultra™ packing. A statistically significant and quantifiable performance increase of 15% was consequently measured in favour of the Intalox® Ultra™ packing, across the pre-loading range. This illustrated that the ADIBAA-method was able to differentiate between column internals based on performance. This suggests that the ADIBAA-method could be used in quickly and cost effectively evaluating new internal designs.

Additional robustness of the method was evaluated through a sized based efficiency analysis on Intalox® Ultra™ packing. This illustrated unconventional, hydrodynamically related behaviour. The unconventional behaviour further illustrated that the ADIBAA-method was able to quantify statistically significant hydrodynamically disturbances.

The proceeding Section 7.2, presents the results of the HA-method (Humidification of air). This method focussed on simplifying tray column efficiency quantification, in evaluating a vapour phase limited system.

## 7.2. TRAY COLUMN VAPOUR PHASE EVALUATION

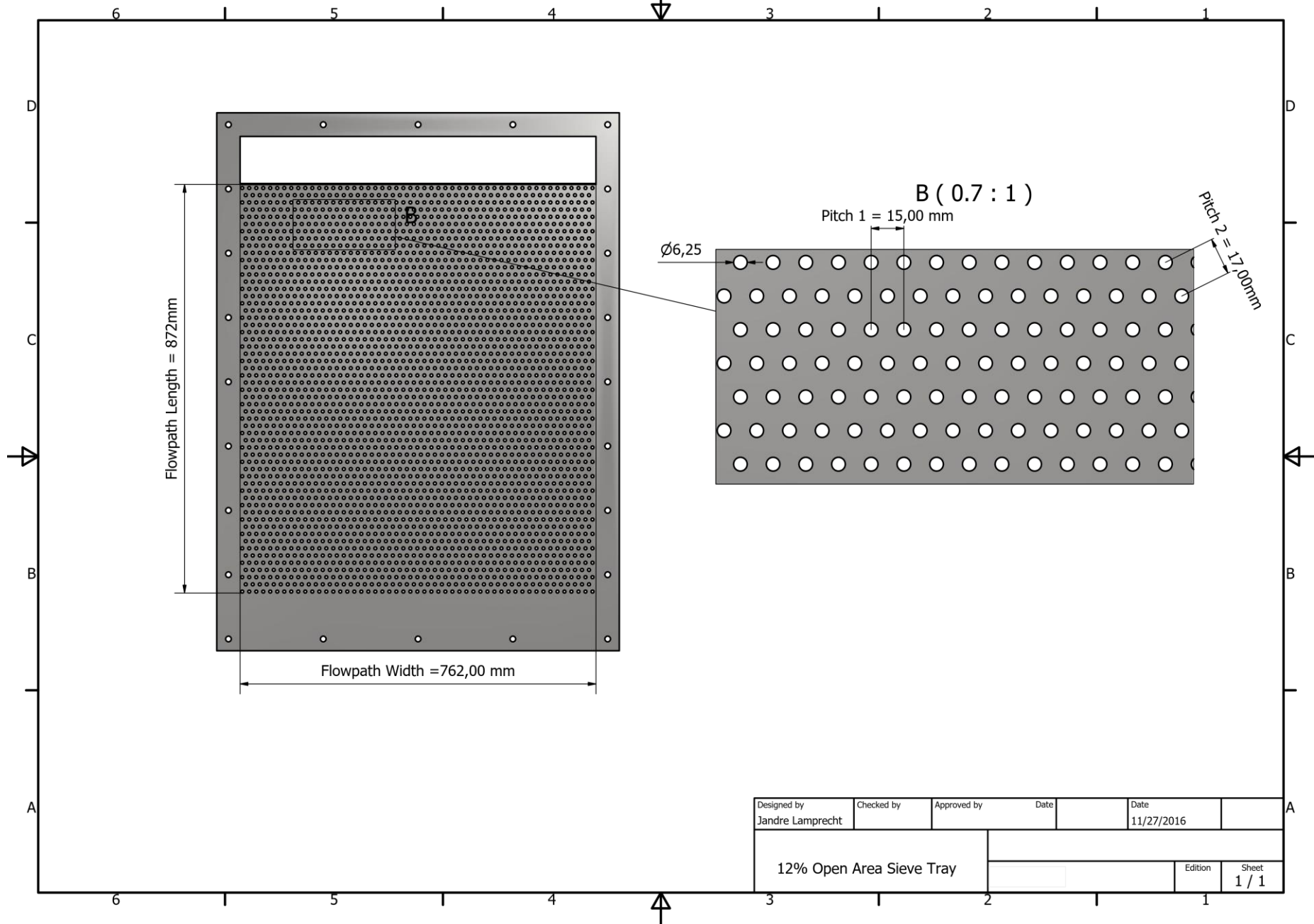
The vapour phase mass transfer data was collected at an industrial research facility. To protect their interests, this report will refrain from going into detail on the confidential tray designs. As such, the non-descript caption of Prototype ‘A’ and ‘B’ will be used for the throughout this section.

### 7.2.1. VALIDATION OF HA-METHOD

A twelve percent open area sieve tray was used in validating the HA (Humidification of air) - method as an efficiency alternative. Table 7.1 is provided as summary of the relevant tray parameters. Clarification towards the presented parameters is given in Figure 7.21.

**TABLE 7.1: SIEVE TRAY PARAMETERS.**

<b>Sieve Tray description</b>	
Primary Contacting Device	6.25mm sieve holes
Tertiary Contacting Device	Mini-Bubble promotors
# of Regular holes	2511
Number of Flowpaths	1
Tray Spacing (m)	0.61
Flowpath Width (m)	0.76
Flowpath Length (m)	0.87
Effective Inlet weir length (FPW)	0.76
Tower Area (m <sup>2</sup> )	0.79
Active Area (m <sup>2</sup> )	0.66
Free Area (m <sup>2</sup> )	0.71
Pitch 1 (mm.)	15
Pitch 2 (mm.)	17
Percent Escape Area (%)	12.00
Escape Area (m <sup>2</sup> )	0.0795



Designed by	Checked by	Approved by	Date	Date	
Jandre Lamprecht				11/27/2016	
12% Open Area Sieve Tray			Edition		Sheet
					1 / 1

FIGURE 7.21: SIEVE TRAY PARAMETER CLARIFICATION

### 7.2.1.1. REPEATABILITY

A repeatability study was conducted at a weir loading of  $50 \text{ m}^3 \cdot \text{h}^{-1} / (\text{m}^2 \text{ of weir})$ . This specific loading was chosen as a representation of the froth regime. It was expected to produce adequate weeping and entrainment at the respective low and high capacity factors, so as to sufficiently represent the main factors that may produce deviations in the humidity readings. A visual representation of the results is provided in Figure 7.22. The presented efficiencies were calculated using Murphree tray efficiency, as discussed in Section 5.5. A similar capacity factor, to that used in the packed column evaluation, is employed in relating vapour flow rates and buoyancy forces. The relevant tray column capacity factors, however, are presented on the active area of the tray (see Figure 7.21).

Experimental repeatability of Murphree tray efficiencies were found within 2%, with exception of a capacity factor of 0.67 m/s presenting an absolute error of 4%. This was considered to be within a viable range, considering probe accuracies.

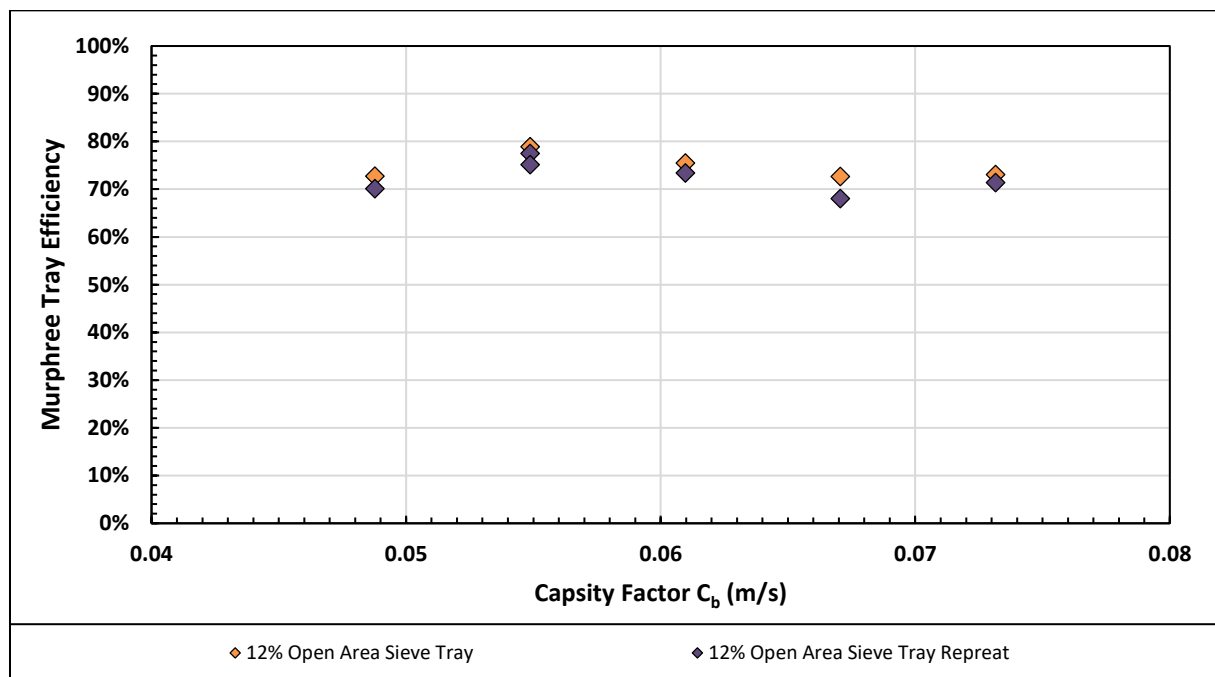


FIGURE 7.22: TRAY COLUMN REPEATABILITY, EVALUATED OVER 2 INDEPENDENT SIEVE TRAY RUNS AT  $122 \text{ m}^3 \cdot \text{m}^{-2} \cdot \text{h}^{-1}$ .

### 7.2.1.2. COMPARISON WITH LITERATURE DATA

In evaluating the applicability of the proposed alternative method, experimental efficiencies were compared to data from the FRI, published by Yanagi in 1982 [59]. To the knowledge of this project, this source was the only to be found in open literature that quoted and supplied applicable data. However, the data could not be considered directly comparative, with reasoning to follow:

- [1] Differing sizes of percentage open area and sieve hole diameter.
- [2] The data collected by the FRI, was done under constant reflux, using the Fenske-Underwood method of efficiency calculation. This limited the system to operate under equal liquid and vapour mass flow rates.
- [3] The presented FRI evaluation was done on the distillation of cyclohexane and n-heptane at 165 kPa and 34 kPa, while the experimental evaluation of this project was done at atmospheric conditions [59].

From the reasoning presented above, the validity of a direct comparison proved nonsensical. The validation was hence done on logic and fundamental knowledge, focusing on pressure, open area and the curvature of the efficiency graph.

**Pressure:** Tray efficiencies are expected to increase with column pressure [16, 59] as a result of the increased interactions. This increase in efficiency can be seen in Figures 7.23 to 7.25, between the 34kPa to 165kpa data. The atmospheric experimental data collected in this report, is therefore expected to lay between the 165kPa and 34kPa efficiency curves.

**Open Area:** An inversely proportional relationship exists between efficiency and tray open area. The ensuing higher pressure drop, corresponds with increased liquid/vapour interactions, creating a finer phase dispersion. This behaviour is also presented in the attached figures (Figures 7.23 to 7.25), where considerably higher efficiency values are reported for the 8% open area trays [59].

**Curvature:** The exact shape of the efficiency curve is both system and condition specific. Therefore, the addition of a bubble promotor in the experimental humidification setup, limited the direct comparison of the data. However, the trends of increasing efficiency up to a local maximum, whereafter steadily decreasing, was seen in both experimental and literature data. This behaviour corresponds to weeping and jetting under higher capacity factors.

Resulting from the presented discussion, the HA-method was considered to be a valid alternative to the conventional constant reflux method of quantifying efficiency. Nonetheless, the comparison presented in Figures 7.23 to 7.25, highlighted that the evaluation of constant vapour density, limited the method to a range of capacity factors from 0.04 to 0.07(m/s). In contrast, the alternative method provides the benefit of being able to evaluate the independent effect of liquid and vapour rates.

It should be noted that although error bars were included, they are not visible due their relative size compared to the markers used.

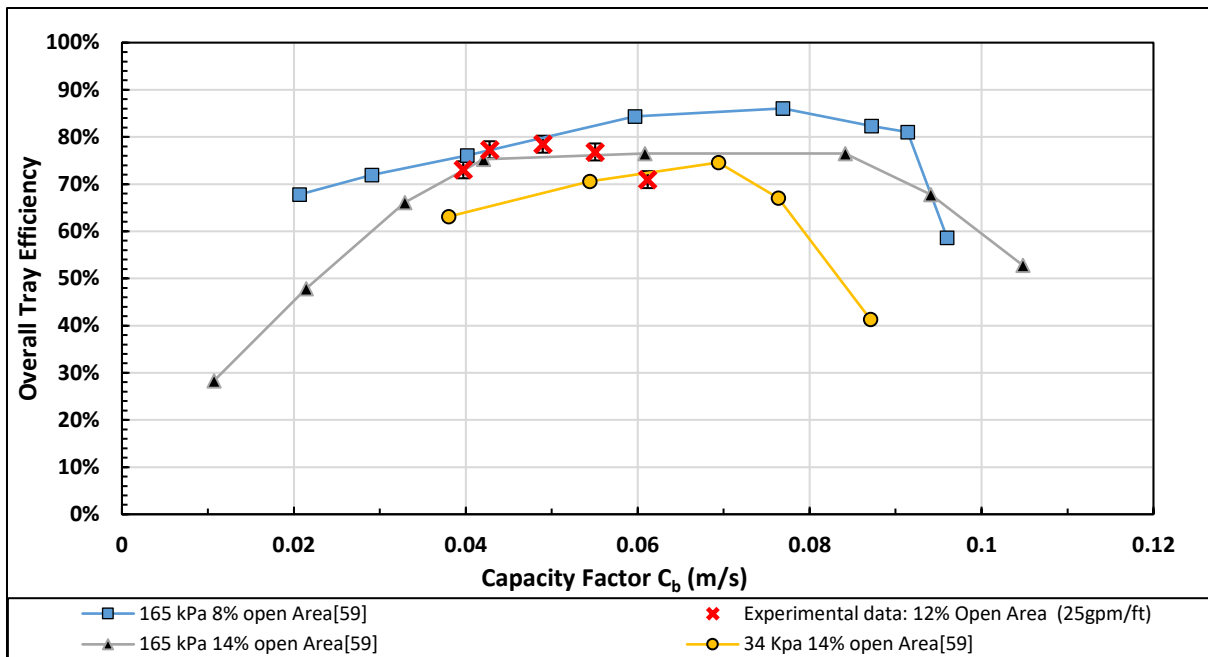


FIGURE 7.23: COMPARISON OF FRI DATA WITH SIEVE TRAY EXPERIMENTAL DATA -61  $m^3.m^{-2}.h^{-1}$  OVER VARYING CAPACITY FACTORS

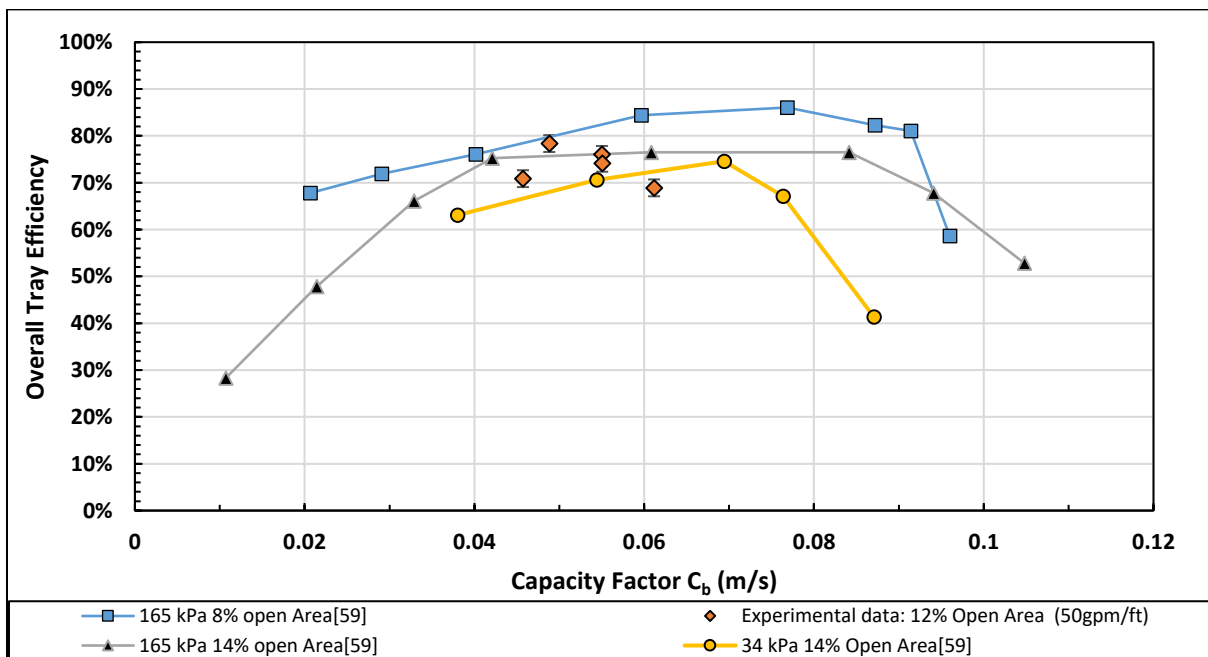


FIGURE 7.24: COMPARISON OF FRI DATA WITH SIEVE TRAY EXPERIMENTAL DATA -122  $m^3.m^{-2}.h^{-1}$  OVER VARYING CAPACITY FACTORS.

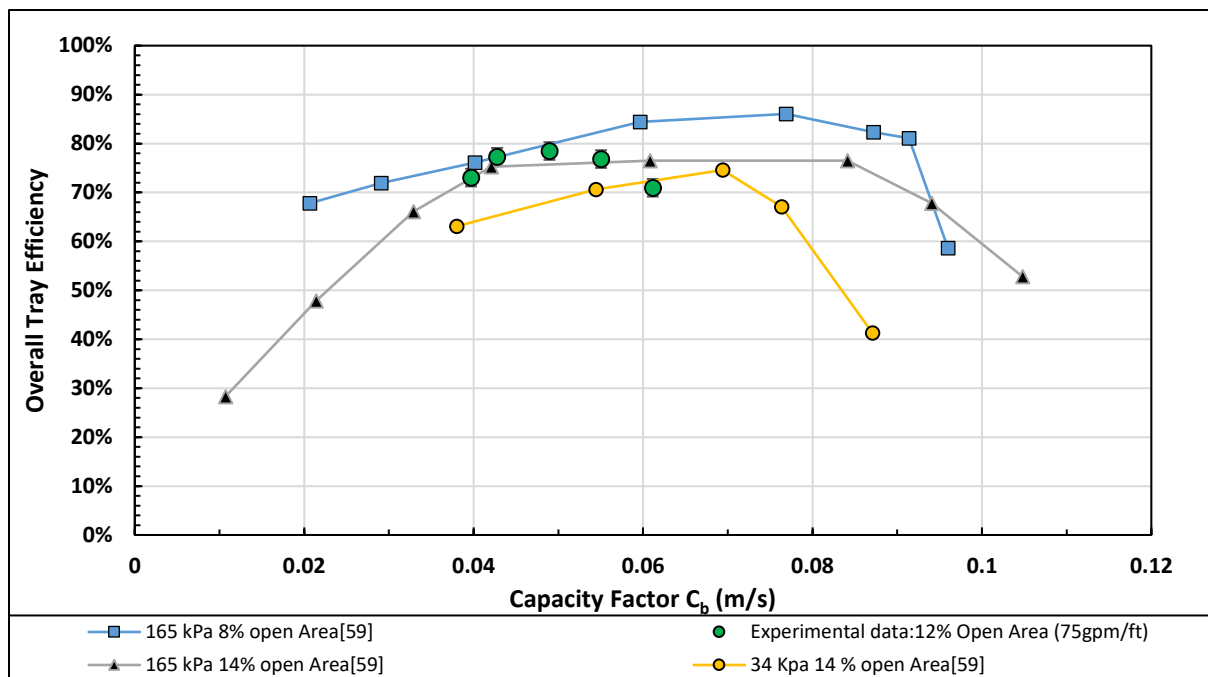


FIGURE 7.25: COMPARISON OF FRI DATA WITH SIEVE TRAY EXPERIMENTAL DATA -  $183 \text{ m}^3 \cdot \text{m}^{-2} \cdot \text{h}^{-1}$  OVER VARYING CAPACITY FACTORS

### 7.2.2. PREDICTIVE CORRELATIONS: POINT EFFICIENCY

As a further measure of validation, the HA-method was compared to various Murphree point efficiency models. Although the experimental setup was constructed with the intent of measuring average composition and thus Murphree tray efficiency, the positioning of the sample ports offered the added option of experimentally evaluating the Murphree point alternative. This was done through using the composition measurement of the sampling port furthest from the inlet weir, above and below the test tray.

The comparative results are presented in Figures 7.26 to 7.28. The graphs are presented over an exceedingly wide range of capacity factors, to better indicate the correlation trends as well as the inability of HA-method in evaluating the full spectrum of capacity factors. As is evident from Figures 7.26 to 7.28, varying degrees of fit was found with regard to the experimental evaluation of the 12% open area sieve tray. Explanation for the deviations between experimental data and the predicted trends, are provided based on model groupings:

Both the AIChE [54] (American Institute of Chemical Engineers) and Harris [56] models were developed through means of desorption, and subsequently provided comparative fit (AIChE combined desorption with distillation data). However, they fail to sufficiently predict the turndown effect at low capacity factors that result from liquid short-circuiting. This comes as no surprise, since at least in the case of Harris [56], a single tray was evaluated. In contrast, limited information was found regarding the experimental setup of the AIChE [54] model.



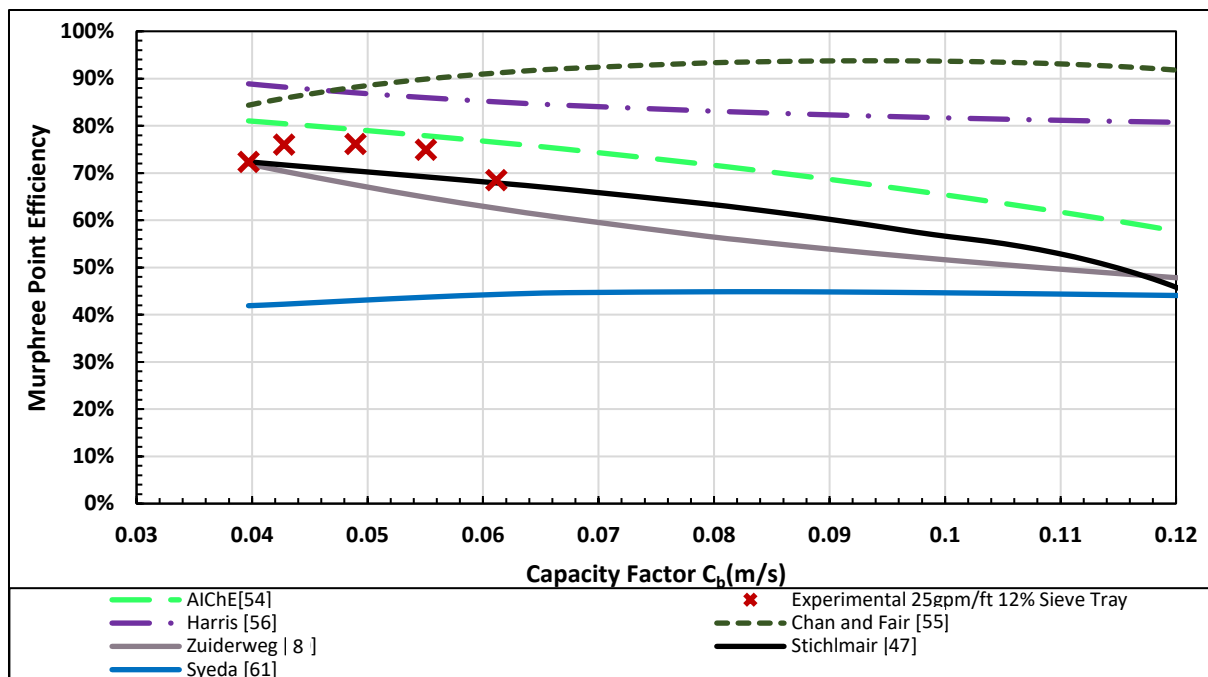


FIGURE 7.26: LITERATURE POINT EFFICIENCY MODELS COMPARED WITH OWN DATA ( $61 \text{ m}^3 \cdot \text{m}^{-2} \cdot \text{h}^{-1}$ ) OVER VARYING CAPACITY FACTORS.

In Harris' single tray [56] evaluation, the wept liquid influenced only the effective liquid loading which decreased the froth height and interfacial area atop the tray. The effect of liquid short-circuiting for the trays above, was consequently not evaluated. This downplayed the turndown effect at low vapour rates, as evident from the lack of curvature in the low capacity factor range.

In addition, the published work of Harris [56] was limited to relatively low liquid and vapour loads (liquid loading  $< 49 \text{ m}^3 \cdot \text{m}^{-2} \cdot \text{h}^{-1}$  [56]). This rationalises the considerably better fit in the  $61 \text{ m}^3 \cdot \text{m}^{-2} \cdot \text{h}^{-1}$  case. The lack of fit under higher loads, with the experimental data of this thesis, is therefore due to inadequate training data. As for the predictive trend under these loadings, the relative influence of the vapour was incorrectly quantified in the correlation [56] due to the use of a single tray. In the author's setup [56], the effective liquid loadings approached the set point as the vapour rate was increased. This is due to decreased weeping at high capacity factors. The consequent increase in froth height and effective area at higher capacity factors, therefore skewed the relative effect of increasing the vapour rates. This is due counter acting mechanisms of increased froth height and vapour bypass (elaborated in Section 7.2.3.4).

Both Zuiderweg [8] and Chan & Fair [55] attempted to evaluate vapour phase efficiencies with distillation data, although through differing methods. Zuiderweg [8] proposed a graphical slope method, dependent on the slope of the equilibrium line. As previously discussed in the literature study (Section 5.5.1), this method is thought to inadequately account for physical properties, as the parameters were regressed from distillation data. The extrapolation onto varying physical properties is reasoned to provided inadequate fit.

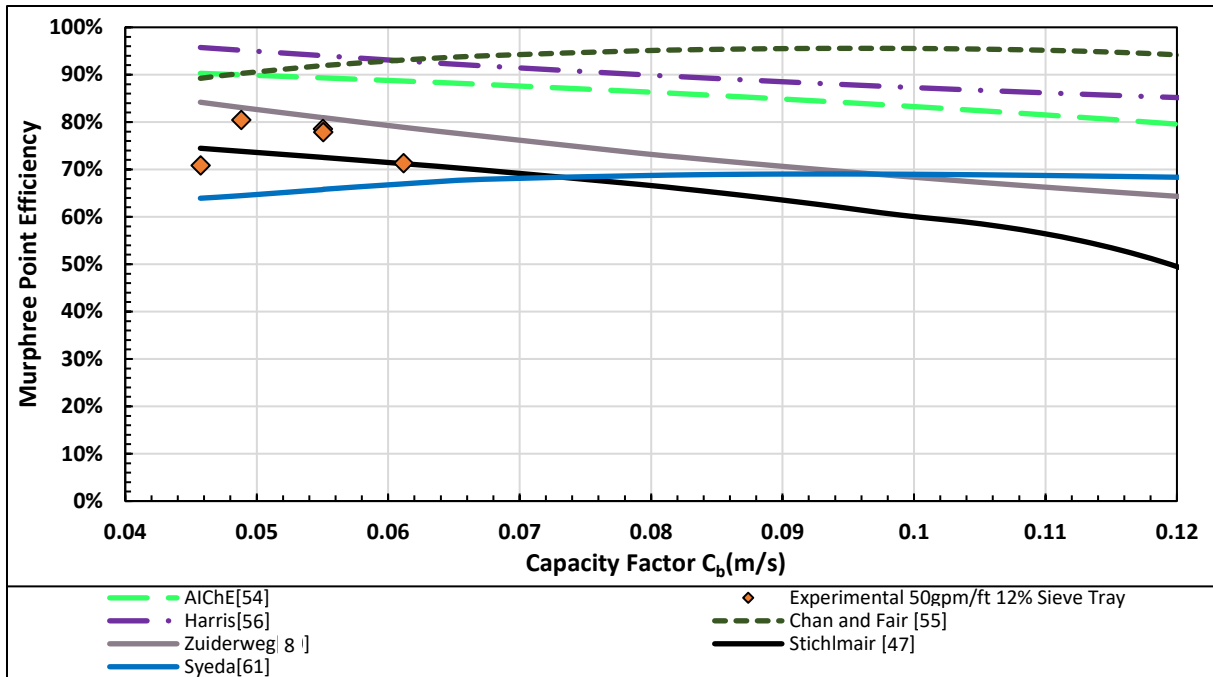


FIGURE 7.27: LITERATURE POINT EFFICIENCY MODELS COMPARED WITH OWN DATA ( $122 \text{ m}^3 \cdot \text{m}^{-2} \cdot \text{h}^{-1}$ ) OVER VARYING CAPACITY FACTORS.

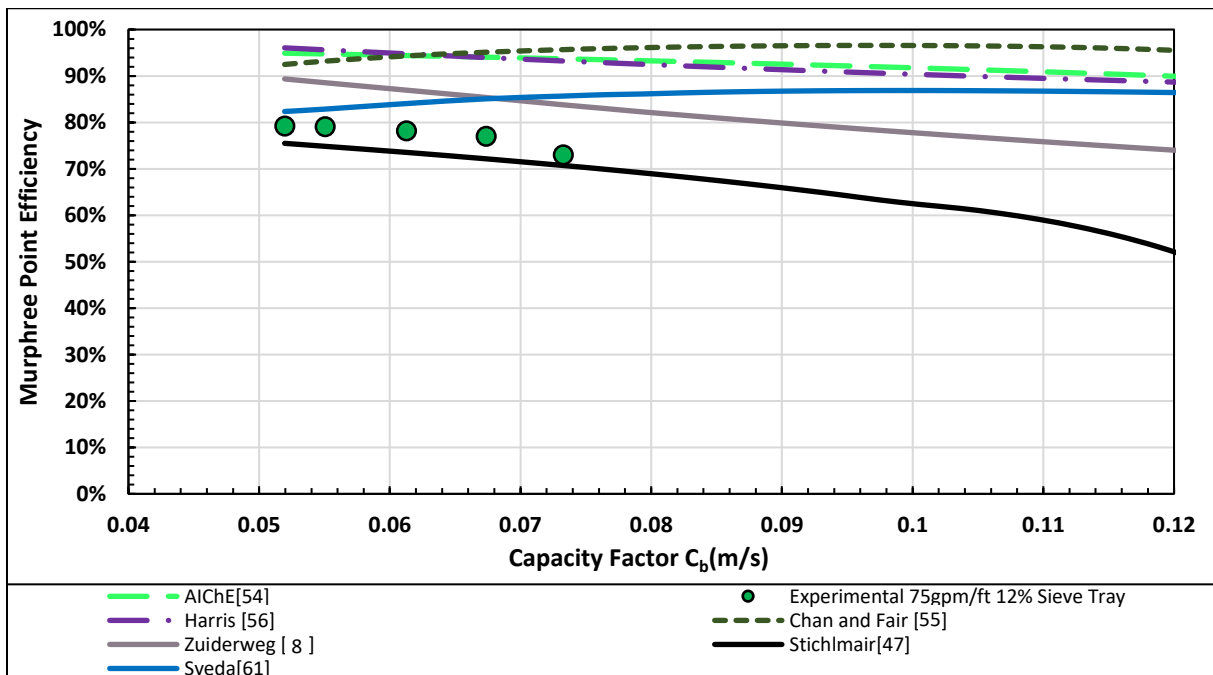


FIGURE 7.28: LITERATURE POINT EFFICIENCY MODELS COMPARED WITH OWN DATA ( $183 \text{ m}^3 \cdot \text{m}^{-2} \cdot \text{h}^{-1}$ ) OVER VARYING CAPACITY FACTORS.

The Chan & Fair [55] correlation opted to relate fractional flooding to point efficiency. The empirical equation provided for its prediction, however, introduces additional errors in assuming a generic tray spacing. As a result, this model arguably provides the worst fit to the experimental data. In addition to the discussion presented above, Lockett [16] equated over predictions from the above-mentioned models, to their use of Equation 5.23 in relating point efficiencies to number of transfer units. This limits

the use of these correlations for physical properties far removed from that of the training data. As such, the best fit should arguable have been achieved by the Harris [56] correlation. This is, however, not the case. The justification thereof is provided in the literature review (Section 5.6).

In an attempt to provide a more fundamentally based model, the Stichlmair [47] equations (5.7) attributed a great deal of influence towards the effect of surface tension in the creation of bubbles in the froth. This analogy was based on singular bubble rise characteristics and excluded the effect of bubble coalescence [16]. Although questioned by the likes of Lockett [16] on the importance of surface tension and hole diameter, this model provided a degree of fit to the sieve tray experimental data of this thesis, with the exception of the turndown at low vapour rates. The calculation process (Equation 5.7) therefore cancels the overestimation of the interfacial area with underestimation of the mass transfer coefficient. The inability of this relationship in providing accurate volumetric coefficients, is given as the reasoning behind the varying degree of fit.

In the latest, and arguably the most computationally intensive model (Equation 5.10), Syeda [61] proposed evaluating point efficiency by way of approximating the fraction of vapour in both the froth and jet bypassing. This model used a solved parameter in predicting the fraction of bubble breaking and the influence of the Webber number (see glossary for definition and equation). As explained in the literature review (Section 5.5), this model is not expected to provide good fit. With questionable equations and training data, this thesis referend from providing further arguments towards the lack of fit.

#### *7.2.2.1. CONCLUDING REMARKS ON THE POINT EFFICIENCY VALIDATION*

The Murphree point efficiency comparison, between literature models and the experimental sieve tray data, present further validation of the HA-method. The experimental data from the aforementioned method illustrated agreeable fit to both the Zuideweg [8] and Stichlmair [47] point efficiency approximations. This justified the further evaluation of column internals with the HA-method.

#### *7.2.3. USING THE HA-METHOD IN TRAY PROTOTYPING*

Two prototypes were tested to evaluate the robustness of the HA-method, as an alternative to hydrocarbon distillation efficiency measurements. The prototypes were assessed on the basis of Murphree tray efficiency (see Section 5.5). In doing so, the concentration readings atop the testing tray were integrated (by way of the trapezium method) to provide an average vapour composition for Equation 5.22. This rudimentary integration technique was valid, as three data points were integrated, eliminating possible curvature. Design parameters including tray spacing, weight height and active area were kept at the values stipulated for the 12% open area sieve tray (Table 7.1).

As per earlier discussion, the prototypes were designed and constructed by an industrial research institution. Due to proprietary conditions, no further detail is provided regarding their design and

material of construction. The specific prototypes illustrate the applicability of the HA-method, in quantifying hydrodynamically induced deviations through efficiency. The succeeding sections present the discussion of the hydrodynamically related efficiency trends, followed by their implication on the HA-method.

### 7.2.3.1. PROTOTYPE A: EFFICIENCY AND HYDRODYNAMIC DISCUSSION

Prototype A was designed to alter the froth dynamics on a low liquid loading sieve tray. Under the normal operating conditions of 5 gallons per minute, the tray exhibited spray like behaviour. The prototype attempted to artificially generate additional froth height. Hydrodynamic evaluations prior to testing illustrated favourable froth generation, justifying further efficiency testing. The results of the experimental evaluation of Prototype A and the 12% sieve tray, are presented Figure 7.29. Per definition, the weeping term in the graph refers to the percentage of the liquid loading that wept onto the successive tray.

As illustrated, Prototype A provided decreased efficiency at low vapour rates, compared to the sieve tray. This is due to the large fraction of liquid bypassing the testing tray through weeping. In changing the froth dynamics, the constricted prototype design introduced artificial areas of high froth density at low and high capacity factors (Figure 7.29). These areas of high density acted as weeping loci, shifting the weeping across the tray as the capacity factor was increased. This decreased the efficiency of the prototype at low capacity factors.

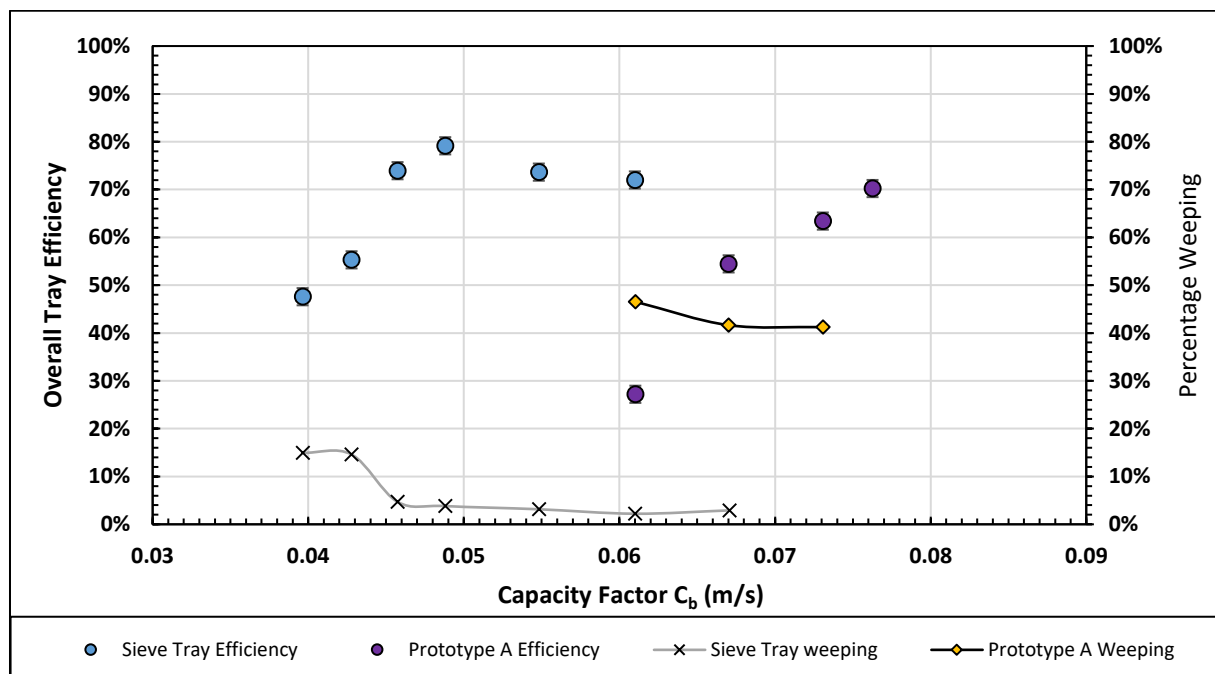


FIGURE 7.29: EFFICIENCY AND WEEPING COMPARISON OF PROTOTYPE 'A' WITH A 12% OPEN SIEVE TRAY; AT  $12 \text{ m}^3 \cdot \text{m}^{-2} \cdot \text{h}^{-1}$ . OVER VARYING CAPACITY FACTORS.

Disregarding the clear adverse effects, the prototype managed to artificially increase the froth/spray height from 152 to 222mm, creating well mixed pools through the physical design. The unexpectedly high efficiencies at high weeping rates (Figure 7.29), were justified as the locus of weeping shifted down the flowpath at high capacity factors. An illustration of the observation of shifting loci is provided in Figure 7.30. In this graph the locus of weeping shifts from the inlet of the tray, at low capacity factors, to the outlet at high capacity factors.

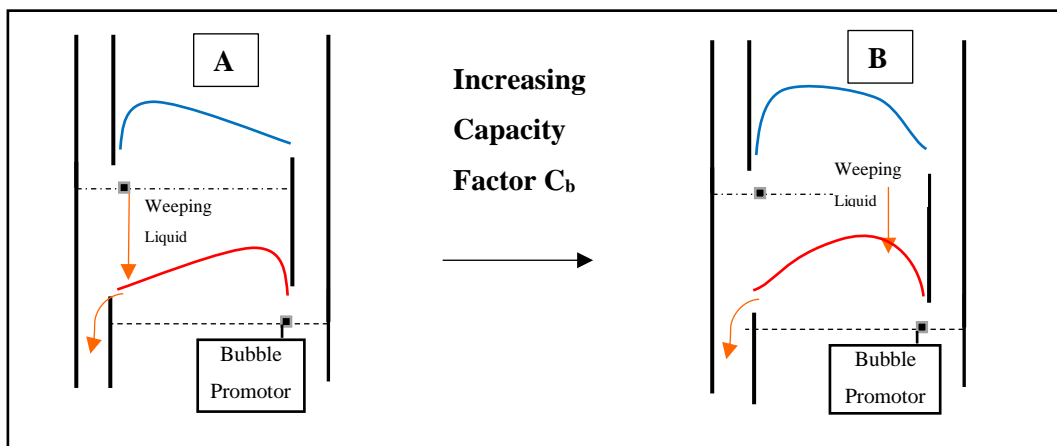


FIGURE 7.30: POSITIONAL WEEPING WITH INCREASE VAPOUR LOADING ON A CONVENTIONAL SIEVE TRAY WITH A BUBBLE PROMOTOR.

In the case where locus follows directly after the inlet weir (Figure 7.30A), the wept liquid effectively short-circuits both trays. As the locus shifted down the flowpath with increased capacity factors (Figure 7.30A), the fraction short-circuiting effectively approached zero. This shifting of the weeping locus was visually observed and is considered justification towards the high efficiencies under high capacity factors, measured in the case of Prototype A.

#### 7.2.3.2. CONCLUDING REMARKS ON PROTOTYPE A

Prototype A offers much promise in artificially manipulating froth densities, although currently unviable for industrial application due to the high rate of weepage. The proceeding step in prototyping is to decrease the open area of the design, therefore increasing dry bed-pressure drop and decreasing weeping tendencies. This is expected to shift the prototype efficiency curve to the left, providing a robust solution to increased froth height.

#### 7.2.3.3. REMARKS ON THE HA-METHOD IN THE EVALUATION OF PROTOTYPE A

The HA-method illustrated advantageous behaviour in translating the rate of weeping into a quantifiable influence on efficiency. This suggests that this method is viable to evaluate efficiencies at the lower end of the operating conditions and capacity factors. In addition, the method was found to be robust in differentiating the liquid composition of the wept liquid, and its effect on efficiency. This could prove useful for future studies, relating the point of weeping to the efficiency.

#### 7.2.3.4. PROTOTYPE B: EFFICIENCY AND HYDRODYNAMIC DISCUSSION

In the case of the second prototype, Prototype B, a 15% open area valve tray was evaluated. The presented evaluation is limited to the froth regime. Efficiency comparisons, with the evaluated 12% open area sieve tray, are presented in Figures 7.31 to 7.33.

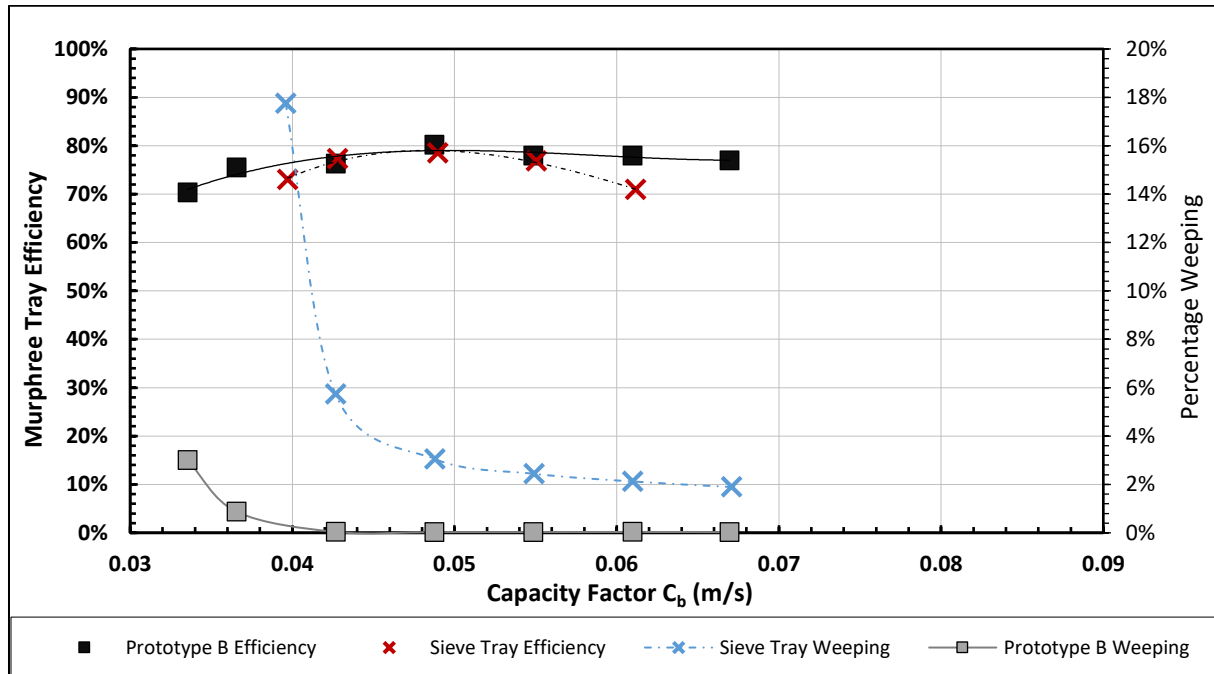


FIGURE 7.31: EFFICIENCY AND WEEPING COMPARISON OF PROTOTYPE 'B' WITH A 12% OPEN SIEVE TRAY- AT  $61 \text{ m}^3 \cdot \text{m}^{-2} \cdot \text{h}^{-1}$  OVER VARYING CAPACITY FACTORS.

Resulting from the specific design parameters of the prototype, quantifiably better weeping characteristics were noted when compared with the sieve tray. Regrettably, this cannot be explained without divulging the physical design of the valves.

Decreased weeping in valve trays is generally due to the design (Figure 7.34), disrupting the downward acting force exerted by the froth. This project abstained from an in-depth hydrodynamic evaluation, due to intellectual property restricting the arguments. Consequently, the evaluation of Prototype B is presented solely on tray efficiency.

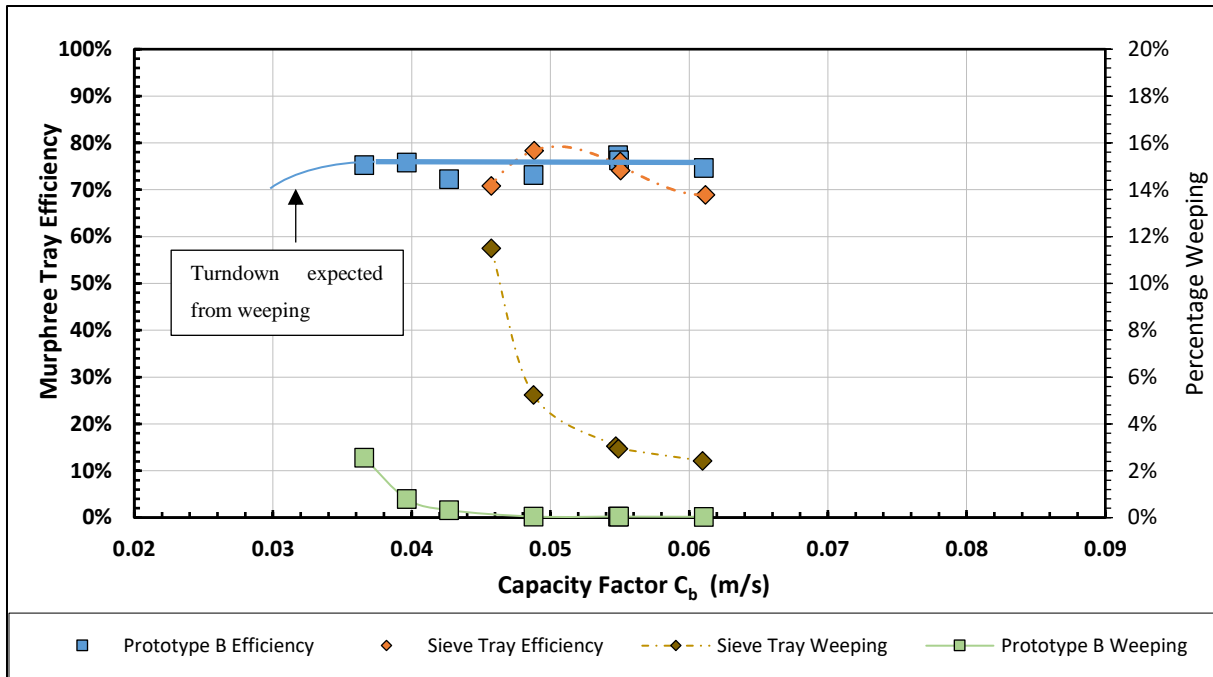


FIGURE 7.32: EFFICIENCY AND WEEPING COMPARISON OF PROTOTYPE 'B' WITH A 12% OPEN SIEVE TRAY- AT 122 m<sup>3</sup>.m<sup>-2</sup>.h<sup>-1</sup> OVER VARYING CAPACITY FACTORS.

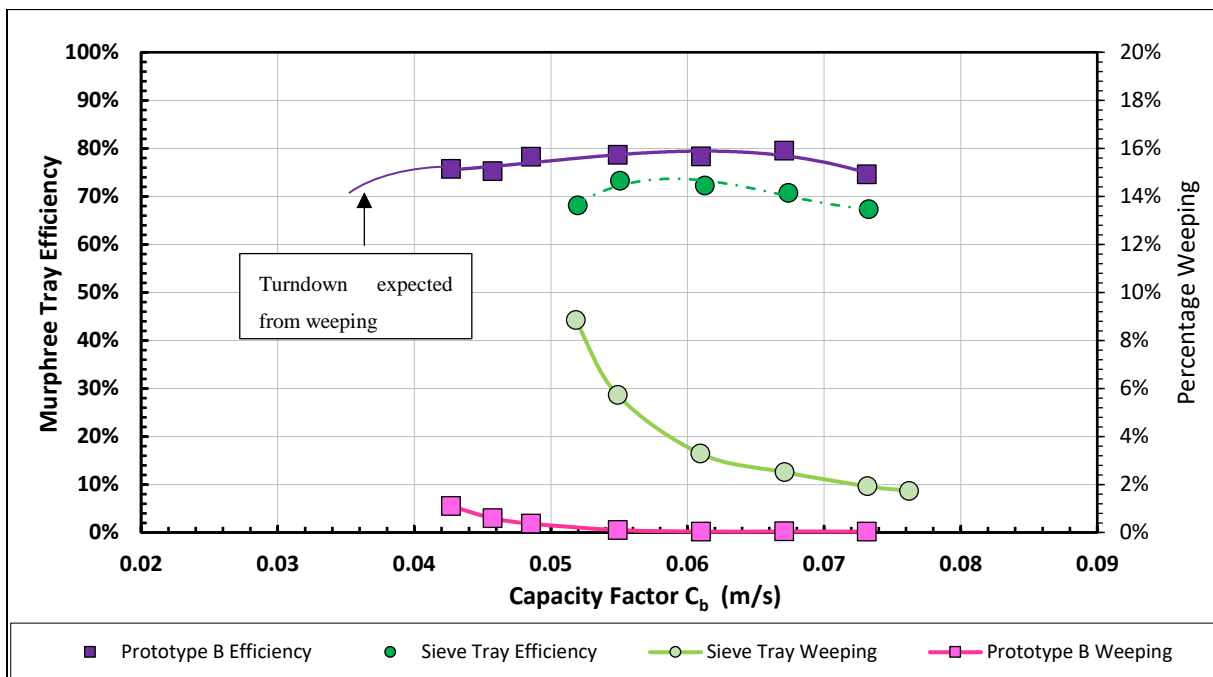
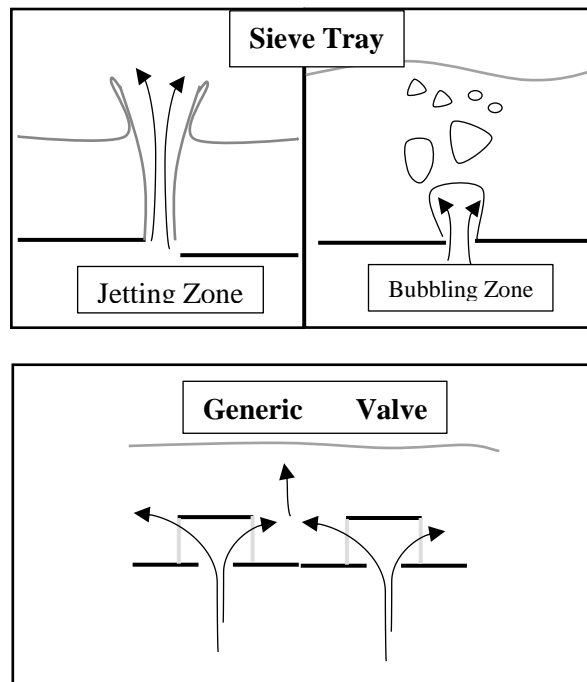


FIGURE 7.33: EFFICIENCY AND WEEPING COMPARISON OF PROTOTYPE 'B' WITH A 12% OPEN SIEVE TRAY- AT 183 m<sup>3</sup>.m<sup>-2</sup>.h<sup>-1</sup> OVER VARYING CAPACITY FACTORS.

From the results presented in Figures 7.31 to 7.33, beneficial prototype behaviour was noted when compared to the sieve tray. The improved performance under low capacity factors was attributed to the better weeping characteristics on the part of the prototype. This increased the effective liquid loading on the valve tray.

In contrast, the weeping liquid in the sieve tray evaluation short-circuited a section of conditioning tray (Figure 7.30). This changed the local liquid concentration on the test tray (graphically seen in Figure 7.30), impeding crossflow enhancement. The aforementioned change in the liquid composition, influences the equilibrium of the tray (Equation 5.22), adversely affecting efficiency. This results in a shift in the local maxima of tray efficiency, towards the right to a higher capacity factor range.



**FIGURE 7.34: SIEVE TRAYS VS VALVE TRAYS UNDER HIGH VAPOUR LOADS.**

Valve tray designs introduced an additional horizontal component to the vapour momentum. This prevents instantaneous vapour bypass and promotes interfacial contact. The improved efficiencies of the prototype under high liquid loads (Figure 7.33) were attributed to a combination of a flow straightening design as well as visibly better phase dispersion (as no vapour bypassed the froth). This design therefore promotes plug flow behaviour across the tray, with its effect proving quantifiable under high liquid Reynolds numbers (See glossary for calculation and definition).

#### 7.2.3.4.1. PRESSURE DROP EVALUATIONS

As an added benefit, the HA-method uses an air-water system, similar to most industrial hydrodynamic evaluations. This highlights to possibility of concurrent hydrodynamic and efficiency evaluations. An example of possible evaluations to follow, is presented in Figures 7.35 to 7.37. The presented graphs indicate the relationship between efficiency and pressure drop for Prototype B and the previously evaluated 12% sieve tray. This relationship plays a large part in tray design as it provides a measure of the trade-off between efficiency and capacity.



Motivated by Figures 7.35 to 7.37, the prototype valve design sacrifices pressure drop for capacity. This is as current convention suggests that the dry bed pressure drop is inversely related to weeping [16]. Therefore, having a restrictive design, increases the dry bed pressure drop and decreases weeping.

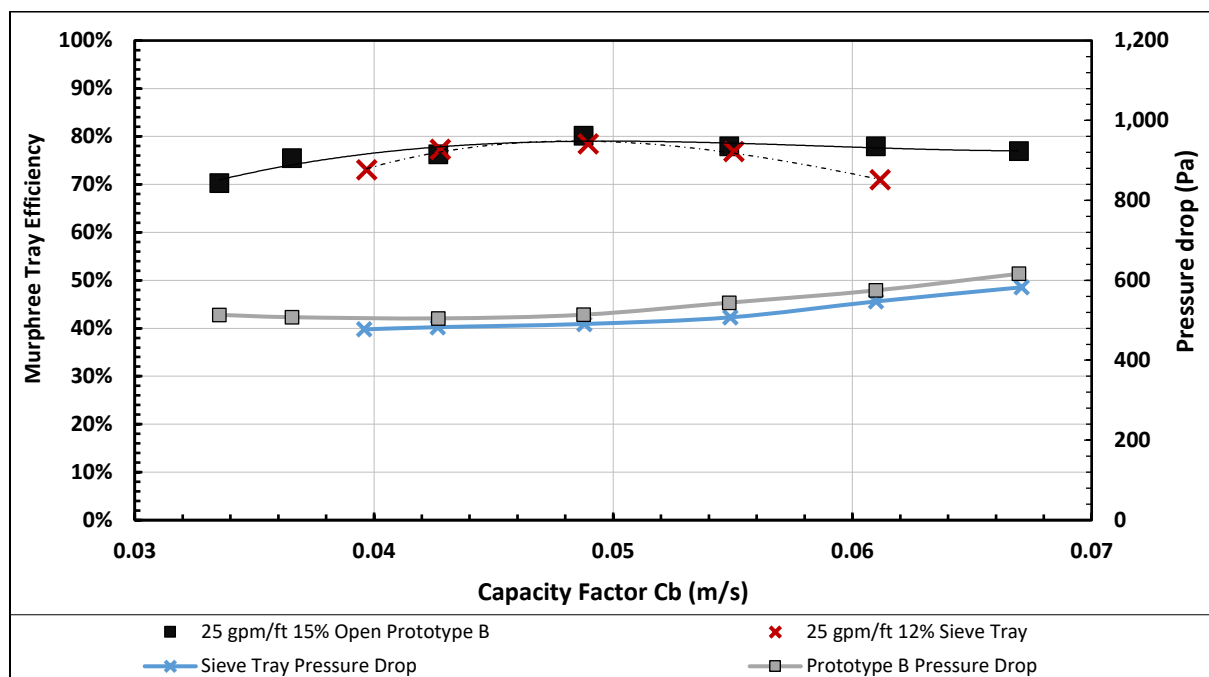


FIGURE 7.35: EFFICIENCY COMPARISON OF PROTOTYPE B AND SIEVE TRAY  $61 \text{ m}^3.\text{m}^{-2}.\text{h}^{-1}$  VS. PRESSURE DROP.

Additional justification towards the lesser pressure drop of the sieve tray is provided in non-uniform froth height on top of a typical sieve tray. At the bubble promotor, near the inlet weir, the froth rapidly expands creating a maximum in the recorded froth height. Continually counteracted by gravity, the expanded froth contracts increasing froth density and decreasing froth height. A schematic of the behaviour is presented in Figure 7.30. The differential froth height self-regulates the head-loss across the tray in distributing the flow of vapour such that higher vapour rates are recorded near the bubble promotors. This effectively short-circuits some of the vapour and decreases pressure drop. In contrast, the absence of a bubble promotor in the prototype design translated into a uniform froth height. The lack of short-circuiting further justifies the increased pressure drop.

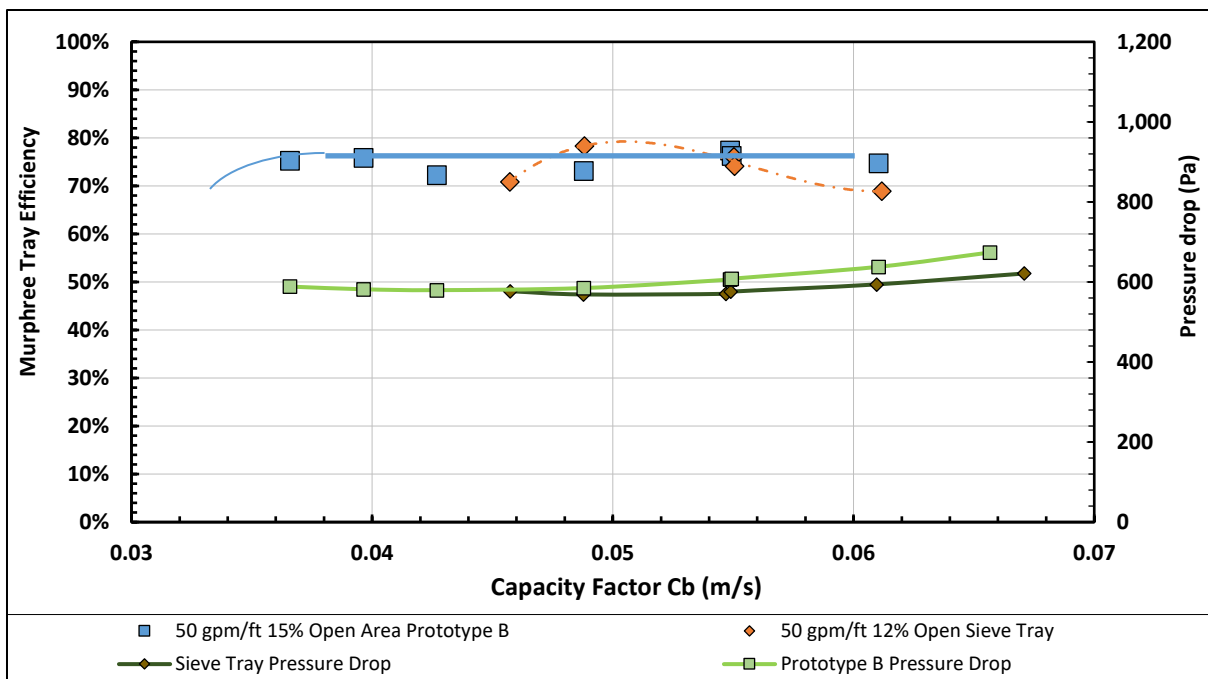


FIGURE 7.36: EFFICIENCY COMPARISON OF PROTOTYPE B AND SIEVE TRAY AT 122 m<sup>3</sup>.m<sup>-2</sup>.h<sup>-1</sup> VS. PRESSURE DROP.

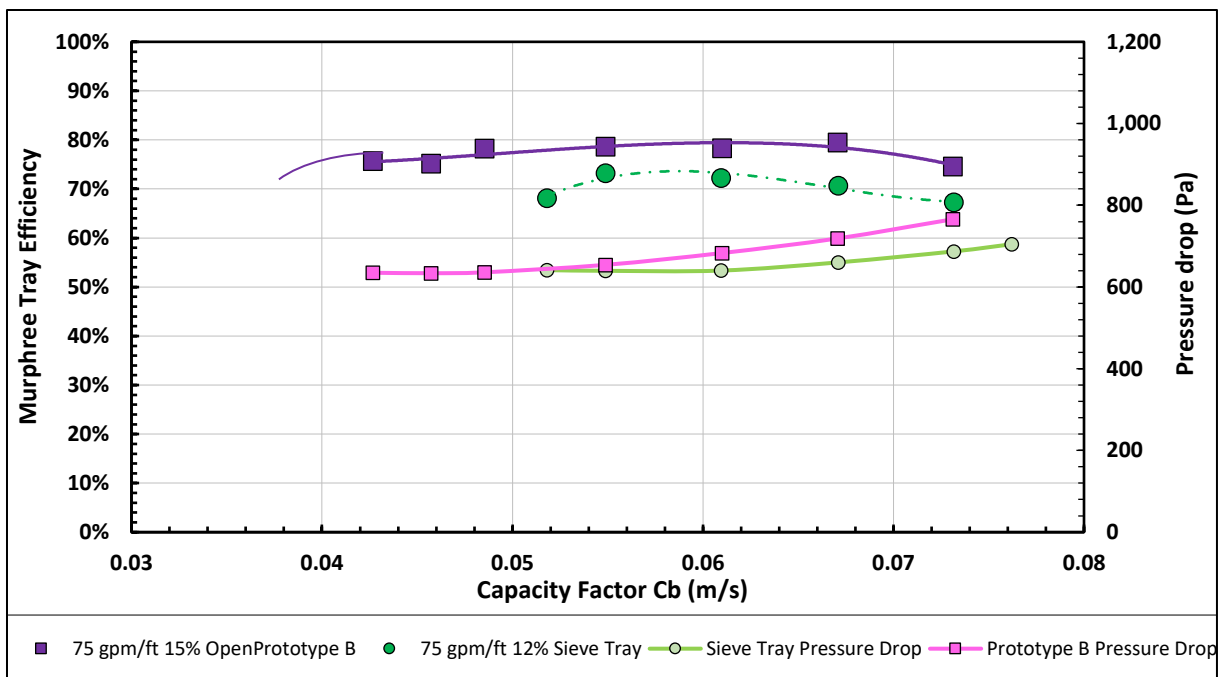


FIGURE 7.37: EFFICIENCY COMPARISON OF PROTOTYPE B AND SIEVE TRAY 183 m<sup>3</sup>.m<sup>-2</sup>.h<sup>-1</sup> VS. PRESSURE DROP.

#### 7.2.3.4.2. CONCLUDING REMARKS ON PROTOTYPE B

From the results presented in Figures 7.31 to 7.37, beneficial prototype behaviour was noted when compared to the conventional sieve tray. The evaluated prototype was found to either outperform or match the sieve tray across the whole experimental range of liquid loadings and capacity factors. This was considered especially impressive as Prototype B had a 15% open area, compared to the 12% of the sieve tray (See discussion on open area in Section 7.2.1.2).

Additionally, comparable pressure drops were recorded for the sieve tray and Prototype B. This justifies the expenditure related to the design of Prototype B, as increased efficiency and capacity is exhibited for comparable pressure drops.

#### 7.2.3.4.3. REMARKS ON THE HA-METHOD IN THE EVALUATION OF PROTOTYPE B

In evaluating Prototype B, the HA-method illustrated applicability in quantifying the complex phenomenon of vapour bypass through quantitative efficiencies. This is highly beneficial as it offers the ability of evaluating the influence of effective contact times on efficiency.

The weeping evaluation of Prototype B and the sieve tray, further justified the previous notion that the HA-method exhibits acceptable efficiency quantification under low capacity factors.

### 7.2.4. EXTENDING THE HA-METHOD TO COLUMN DESIGN

Both Murphree tray and point efficiencies were evaluated in this thesis. The translation of the aforementioned efficiencies is included to present the notion that the HA-method can be used in simplified evaluations of conventional knowledge. The following sections therefore focus on the Lewis [66] models.

#### 7.2.4.1. RELATING POINT TO TRAY EFFICIENCIES VIA THE LEWIS MODELS.

Murphree point efficiencies represent tray performance in terms of the vapour and liquid exiting a tray. In such case, changes in the liquid composition across the tray are not taken into account (crossflow enhancement), as only the exiting streams the tray are evaluated. Appropriately, translation is required into an average tray and subsequently column efficiency (section 5.5.2). This is done either through the Lewis correlations or of the original definition of Murphree Tray efficiency (Equation 5.22). This project opted for the latter, integrating three independent humidity readings to provide average vapour composition. The comparative performance of the two approaches are evaluated in the succeeding section.

The first Lewis case (p 45-47) was considered applicable to the experimental data of this thesis, since the inlet vapour passed through more than 30 meters of 12' piping before being introduced into the column. This suggests that the vapour is well mixed upon entering the column and therefore also below the test tray (see Figure 5.6). Quantitative vindication is provided in the vapour Reynolds number (See

glossary for definition and equation). The resulting values were found to range between 220 000 and 400 000 across the experimental matrix. This suggested highly turbulent, and per definition well mixed, vapour below the test tray [70]. Further proof was presented in evaluating the humidity trends across the three bottom sampling ports. As this graph provided little additional knowledge, it was omitted from the body of the report, in favour of Appendix B (Figure 9.26).

In the Lewis [66] paper of 1936, the concentration profile atop a testing tray is approximated (case one) by the mathematical function of Equation 7.3:

$$y_n = e^{\lambda \cdot E_{OG} \cdot \frac{z_i}{z_{total}}} (y_{n,0} - y_{n-1}) + y_{n-1} \quad 7.3$$

Equation 7.3 is based on the assumption of perfect plug flow in both the vapour and liquid. This results in an exponential concentration profile similar to Figure 5.6 (p 43). The aforementioned implies that the vapour enters and leaves along vertical streamlines and that no vapour is transported across the tray while trapped in the froth. This is doubtful, considering the terminal rise velocities of the microbubbles. To the knowledge of the author, no literature references have attempted to validate this assumption. The conducted research focussed on liquid maldistribution, entrainment and/or weeping and their effects on the Lewis [66] models

An opposing hypothesis for real column operations is presented through Figure 7.38. This figure hypothesises that as the crossflowing liquid exerts a horizontal force on the rising vapour, bubbles are transported along the flowpath before leaving the froth. The resulting vapour entrainment alters the composition profile on top of the tray and therefore limits the applicability of the Lewis [66] models.

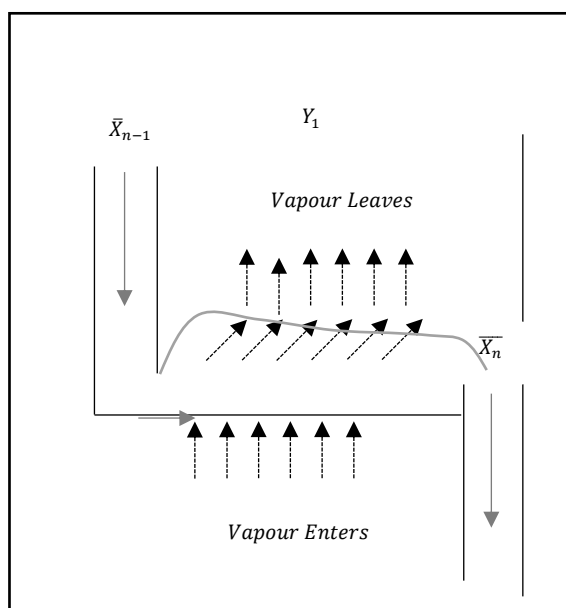


**FIGURE 7.38: EFFECT OF LIQUID FLOW ON VAPOUR ENTRAPMENT IN A TRAY COLUMN**

As a result of the lack of data on this matter, this thesis investigated the effects of vapour entrapment in the froth, through a hypothetical evaluation. In generating this investigation, concentration profiles were measured on the testing tray using three sample ports across the flowpath. The same rectangular experimental setup was used in eliminating liquid phase distribution interference (as described Section 6.5.2). During the investigation, the vapour between the trays was considered in near perfect plug flow, with vapour phase Peclet numbers (see glossary for definition and equation) ranging from 190 to 350. Confirming this assumption, Katayama and Imoto [81] proved that vapour Peclet numbers above 50 approximate plug flow.

To avoid compound errors, a single probe was used in measuring all data points. Duplicate measurements were taken of the system at steady state, evaluating the reproducibility of the probe. The maximum absolute deviation was  $1.73 \times 10^{-4}$  (mass fraction water in the vapour). This value is presented in the error bars of the ensuing graphs (Figures 7.39 to 7.41). The figures, represent the experimentally evaluated concentration profiles over three increasing liquid loadings. The fractional flowpath length used in the graphs is measured from the start of the active tray (0) to the outlet weir (1).

The author of this thesis explicitly states that the curves between the experimental data, used in Figures 7.39 to 7.41, illustrate a **possible** trend. Although it is fundamentally incorrect to fit a curve on three data points, the dashed lines were included in illustrating such a **possibility**. It is, however, recommended in the results section to decrease the distance between samples and increase the confidence regarding the actual trend.

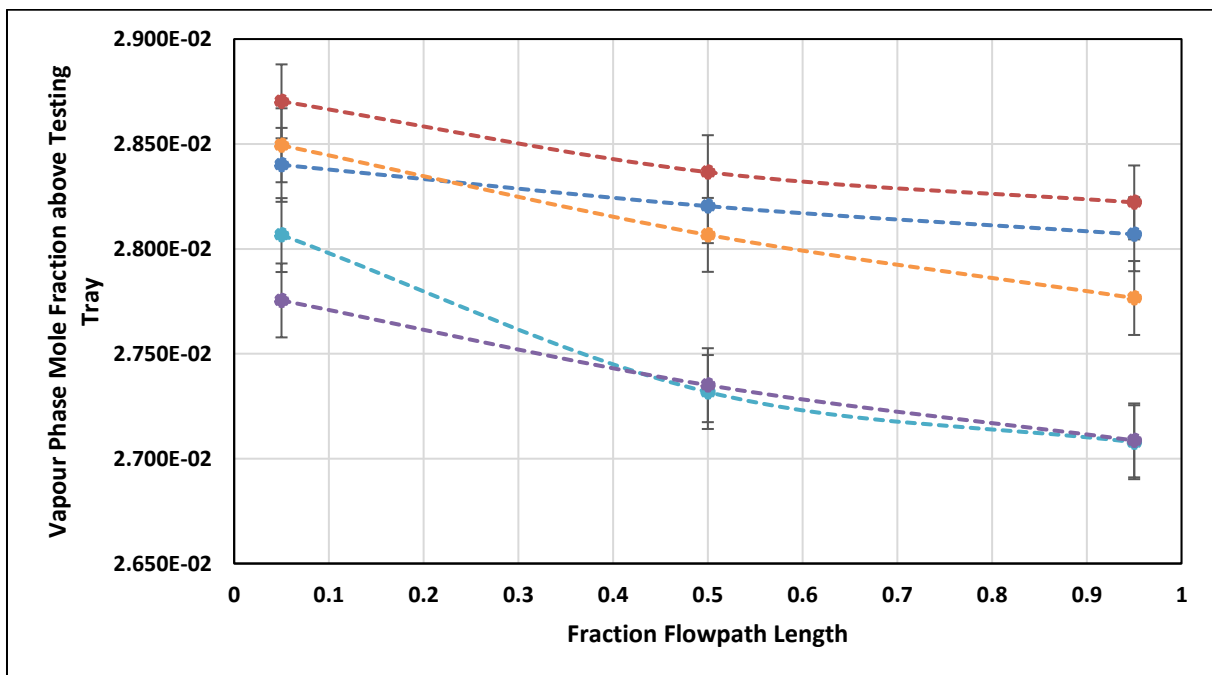


FIGURE 7.39: CONCENTRATION PROFILES ABOVE THE TESTING TRAY FOR A LIQUID LOADING OF  $61 \text{ m}^3 \cdot \text{m}^{-2} \cdot \text{h}^{-1}$ .

Evident from Figures 7.39 to 7.41, the concentration profiles varied in shape, depending on the liquid flow rate. This suggests an unquantified influence regarding the liquid loading. As the liquid rate is increased, the effective concentration profiles are seen to change from the expected trend (presented Figure 5.6) to where the maximum composition either reports to middle or towards the end of the tray. This is highly counter intuitive as the trend is perceived to change from a plug flow to a well-mixed system and back.

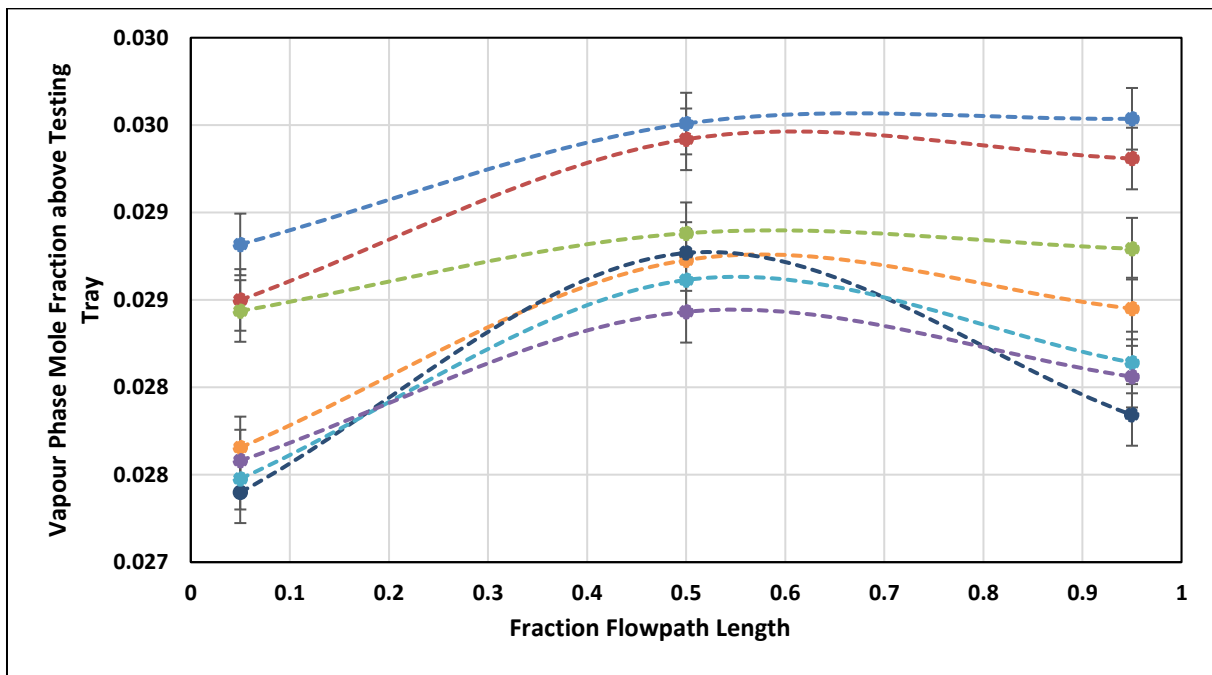


FIGURE 7.40: CONCENTRATION PROFILES ABOVE THE TESTING TRAY FOR A LIQUID LOADING OF  $122 \text{ m}^3 \cdot \text{m}^{-2} \cdot \text{h}^{-1}$ .

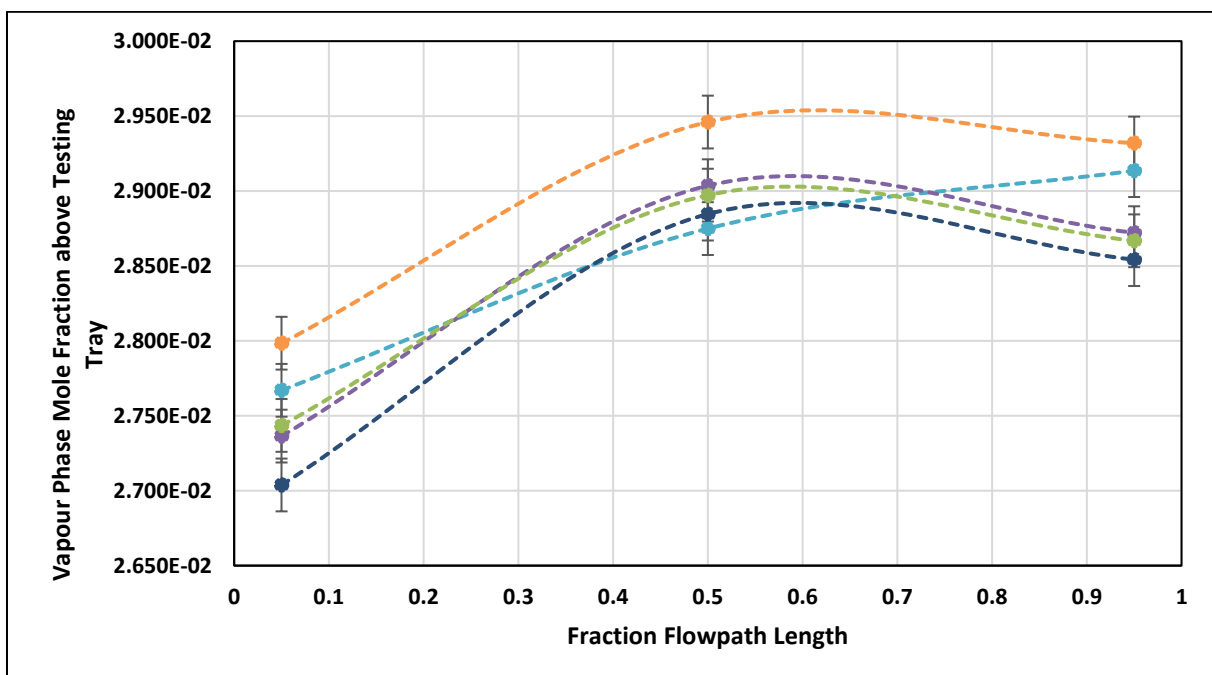


FIGURE 7.41: CONCENTRATION PROFILES ABOVE THE TESTING TRAY FOR A LIQUID LOADING OF  $183 \text{ m}^3 \cdot \text{m}^{-2} \cdot \text{h}^{-1}$ .

In attempting to validate the trends presented in Figures 7.39 to 7.41, a hypothetical evaluation was generated. This evaluation considered the changes in the concentration profile and the limitations incremental sampling. A subsequent graphical representation of hypothesised vapour entrapment in the froth is presented Figures 7.42 to 7.44.

The graphs (Figures 7.42 to 7.44), are presented for a constant average composition (area under the curve) and therefore an identical Murphree tray efficiency. The vapour above the tray, outside of the froth, is considered in perfect plug flow as previously proved in Section 7.2.4.2. Red dots are used indicate fixed sampling points, while the dashed-lines represent the perceived trend of using only three samples. The solid line is provided as an illustration of the actual trend, as if infinite samples were taken. The cases are presented in order of increasing liquid loading with the hypothesis of increased vapour entrapment froth.

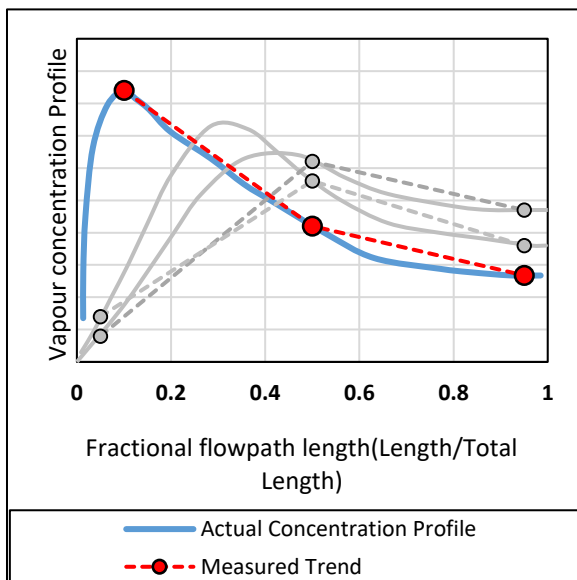


FIGURE 7.42: HYPOTHETICAL CASE 1; LOW LIQUID LOADING.

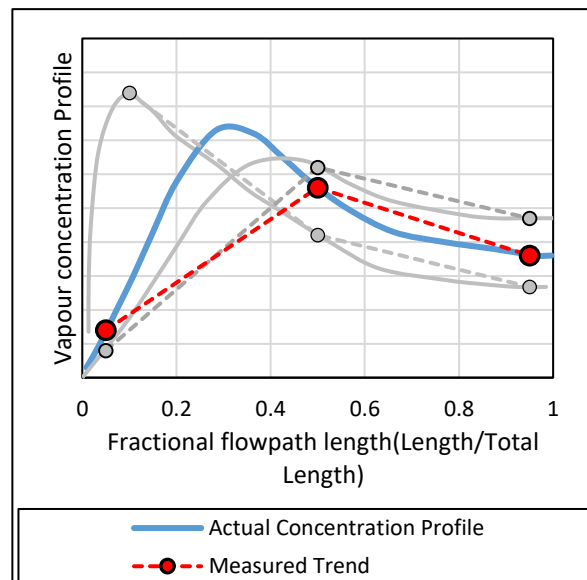


FIGURE 7.43: HYPOTHETICAL CASE 2; MEDIUM LIQUID LOADING.

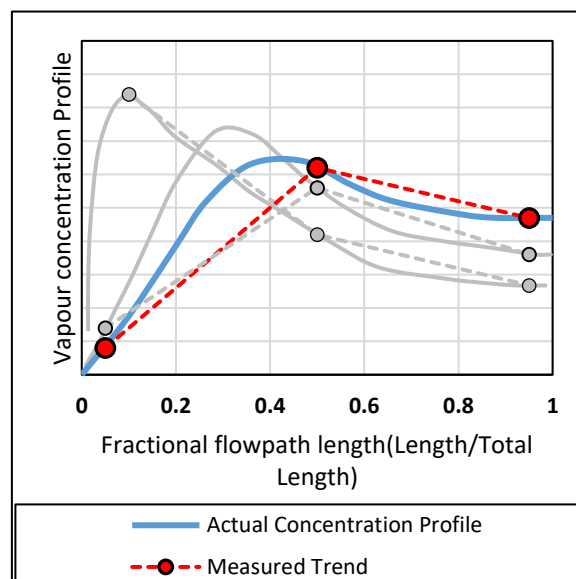


FIGURE 7.44: HYPOTHETICAL CASE 3; HIGH LIQUID LOADING.

Comparing the experimental vapour trends with the hypothetical evaluation, (in Figures 7.42 to 7.44) was found to validate the counter intuitive experimental curves. As the liquid loading is increased, it is hypothesized that the relative forces increase the extent of vapour entrapped in the froth. This alters the vapour concentration profile, therefore creating the trends exhibited in Figures 7.42 to 7.44.

#### *IMPLICATION OF THE HYPOTHETICAL VAPOUR TRAPPING ON THE LEWIS MODELS*

In each of the above-mentioned hypothetical evaluations (Figures 7.42 to 7.44), the vapour composition readings are taken at the large red dots. The red dots at the outlet weir (Fractional length  $\approx 1$ ) illustrate differing vapour concentrations for the different hypothetical cases. Therefore, three widely differing point efficiencies are calculated (Equation 5.22) based on varying grades of the hypothesized vapour entrapment.

Using the Lewis case models in transposing the point efficiencies to the tray counterpart, thus wrongfully presents differing values of Murphree tray efficiency – although the hypothetical cases were based on a constant average composition. This suggests that Lewis approximation of the concentration profile above the tray, fails to attenuate for vapour being carried in the froth.

This effect on the concentration profiles intensify with increased liquid loading, as the momentum of the liquid forces more of the vapour in a lateral direction. This is accompanied by added shear forces that create finer bubbles with slower rise velocities, further extending the vapour-trapping effect.

In evaluating the effect of the liquid loading on the predictive performance of the Lewis model, the experimentally evaluated tray efficiencies were transposed via the first Lewis case approximation. The comparative results are presented in Figures 7.45 to 7.46.

The Lewis models illustrate tendencies of under predicting the point efficiency, with increased liquid loading. This is considered in agreement with hypothesis that vapour entrapment increases with liquid loading. Whilst arguments can be made, regarding the validity of an accurate compositional average over only three sampling points, the absolute error is expected to be reduced as a result of the low volatility of water.

In addition, although unsubstantiated, this project proposes an increased effect in higher pressure systems as the buoyancy of the vapour is expected to decrease. This decrease, reduces the driving force for the vapour to leave the froth, increasing the possibility of vapour trapping.



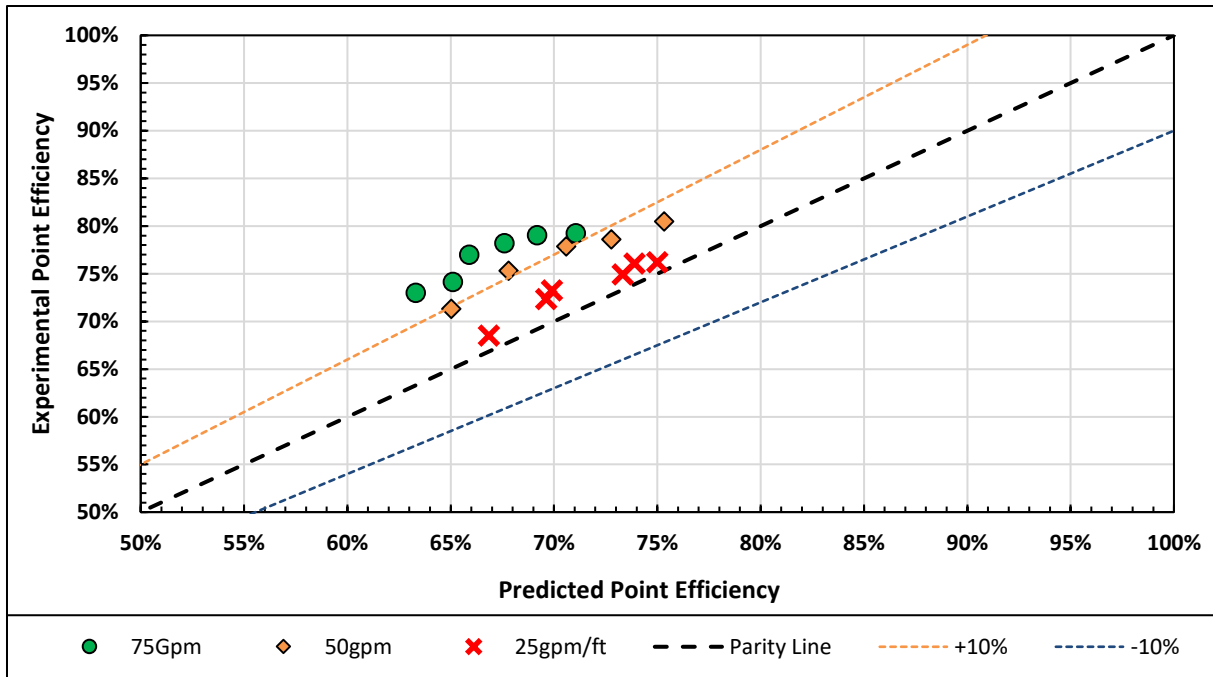


FIGURE 7.45: PARITY EVALUATION OF THE LEWIS APPROXIMATION OF POINT EFFICIENT AND THE EXPERIMENTAL SIEVE TRAY DATA.

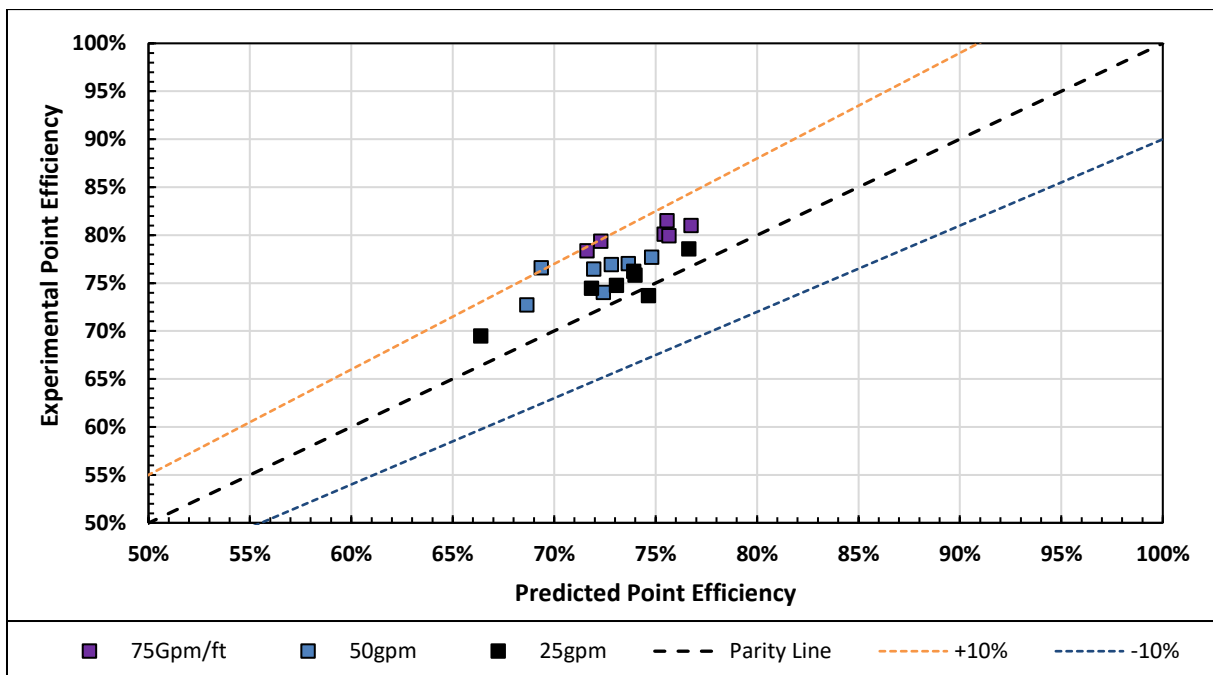


FIGURE 7.46: PARITY EVALUATION OF THE LEWIS APPROXIMATION OF POINT EFFICIENT AND THE EXPERIMENTAL PROTOTYPE B DATA

#### 7.2.4.2. IMPLICATIONS OF VAPOUR TRAPPING ON DESIGN

In correlating efficiency results, distillation data are transposed to point efficiencies and consequently NTU models (via the Lewis cases). Resulting from the physical design of the systems, the data intrinsically reflects either tray or section efficiencies. This is as the sample of the vapour stream is taken directly from the condenser, effectively averaging the concentration profile.

The error of approximating limited vapour entrapment is thus contained in the average concentration. As the data are transposed from tray efficiencies to NTU and back (for predictions) using the same Lewis approximation, the effective error is thought to cancel out.

The extent of the error is, however, most pronounced in absorption and stripping applications. This is as most the authors in literature opted to measure point efficiencies, translating the results to usable tray efficiencies via the Lewis case approximations. As evident from the hypothesis, differing point efficiencies were recorded based on liquid loading. The error in using the Lewis models may thus be, in part responsible for the variations in predictions between distillation and absorption data.

The implication, however, is not suspected to outweigh the relative effect of using Equation 5.23 in correlating the models. Although not necessarily paradigm shifting in itself, this knowledge provides a more fundamental perspective to the century old Lewis approximation. It is the hope of this author that in collecting more data on this phenomenon, the gap between absorption and distillation efficiencies can be bridged.



---

# CHAPTER 8: CONCLUSION AND RECOMMENDATIONS

In evaluating the parameters limiting the progression of column internal design, this project identified ample room for improvement in the field of simplistic and cost-effective efficiency quantification. As conventional testing methods are time-consuming and expensive, it was opted to evaluate alternative, rapid manufacturing orientated methods. This motivated the **development** of the **ADIBAA (aqueous desorption of isobutyl acetate in air)** and **HA (Humidification of air)-methods** for respective evaluation in packed and tray columns.

Two independent **pilot plants** (industrially sized) were **successfully designed and constructed or partially retrofitted** for use in experimentally verifying both the ADIBAA- and HA-methods. The **plants were validated** against existing and available literature data. This was seen as sufficient fulfilment of the second project objective which required the construction of two independent pilot plants.

## 8.1. PACKED COLUMN EFFICIENCY ALTERNATIVE: ADIBAA-METHOD

The desorption of aqueous isobutyl acetate into air was chosen as an alternative for measuring liquid phase mass transfer coefficients. This system was chosen through a regression model, suggesting liquid phase dominance within a 95% confidence interval (based on Onda [19] correlations). The experimental setup was designed with near real-time quantification, using a flow customized UV-spectrophotometer. This used a closed liquid loop, while continually dosing isobutyl acetate. As far as could be ascertained from distillation literature, such closed-loop system with continuous measurement has not been used before to determine liquid phase volumetric mass transfer coefficients. The use of the closed liquid loop notably decreased the plant footprint and provided continual reagent cost savings.

The experimental setup and ADIBAA-method was validated through comparison with relevant literature models. In doing so, little variation was found between the desorption of isobutyl acetate and the oxygen systems presented by Linek [29, 18, 26]. Additionally, the ADIBAA-method illustrated **advantageous behaviour in differentiating between column internals designs**, exhibiting a 15% increase in efficiency (HETP) when comparing the 1.5' Intalox® Ultra™ with its FlexiRing® variant. This was seen as fulfilment of the requirement that the ADIBAA-method be applicable as a tool for simplistic and cost-effective efficiency quantification during the initial design phases.

Further evaluations regarding the robustness of ADIBAA-method, illustrated an interesting phenomenon as exhibited on the larger Intalox® Ultra™ packing pieces. These packings illustrated

notable increases in efficiencies on and around 35 to 40% of the proposed flooding velocity. This is in direct contradiction with current assumption of a stable mass transfer coefficient in the preloading range. The phenomenon observed in this work is argued to be the result of varying liquid flowpaths and distribution behaviour at *ca* 37% of flooding velocity. However, this behaviour may also partly be linked to imperfect liquid distribution and may thus subside with improved initial liquid distribution.

In conclusion, the proposed ADIBAA-method for the liquid phase evaluation sufficiently adhered to the requirements set at the start of the project. The advantages of this method, over conventional efficiency quantification, is provided as follows:

- [1] **Time:** The process of collecting experimental data, took on average between 25 and 30 minutes per data point. In terms of prototyping, that translates into a 600% improvement over the traditional constant reflux method, which takes an approximately two to three hours [3].
- [2] **Quantification:** The UV absorbance quantification technique was found to be cost-effective and reliable in offering near real-time measurements. This provided notable decreases in the plant footprint, which limited the sump to 250 litres instead of the 40m<sup>3</sup> of other equivalent desorption systems.
- [3] **Environmental Considerations:** According to the CDC (Centre for Disease Control and Prevention), isobutyl acetate is considered highly unlikely to accumulate in either animal or plant tissue. Additionally, an atmospheric photochemical degradation half-life of 1.98 days is presented in literature [82]. This suggest fast degrading and subsequently limited environmental impact. This is highly favourable when compared to the carcinogenic solvents conventionally used in constant reflux columns.
- [4] **Safety:** As the system operated well below the lower limit of flammability (2.4% v/v in air), no additional safety measures or interlocks were required.  
Restrictions (150ppm) on the use of isobutyl acetate, as enforced by OSHA (Occupational Safety and Health Administration), act primarily for the prevention of eye irritation [83]. This is reasoned as the US Department of Health and Human Services claim no acute or chronic effects from prolonged overexposure - with the exception of skin irritation [83]. The desorption system subsequently requires little to no exposure control when implemented in a well-ventilated plant.
- [5] **Cost:** The ADIBAA-method was found to sizably decrease the reagent cost, when compared to both oxygen desorption and C<sub>6</sub>/C<sub>7</sub> isomers. This is as only the desorbed component was continually dosed, instead of large amounts of oxygen or hydrocarbons. Additionally, the desorption required much less heating and cooling utilities when compared to constant reflux distillation. This notably decreased overall operating costs.

- [6] **Column internal materials:** Isobutyl acetate, in ppm quantities, illustrated negligible corrosive properties. This suggest compatibility with column internals ranging from stainless steel to HDPE (High-density polyethylene) and PVC (Polyvinyl Chloride).

## 8.2. TRAY COLUMN EFFICIENCY ALTERNATIVE: HA-METHOD

The humidification of water in air is presented as an alternative method for measuring vapour phase mass transfer in tray columns. This system was proven to be vapour phase mass transfer limiting in various packed column evaluations from the 1940's to the 1970's [31, 19]. The subsequent desorption was chosen at the hand of environmental reasoning. Inefficient practises in historical tray desorption, led this thesis to re-evaluate this method in terms of quantification and the design of the experimental setup. Direct validation using literature humidification data was therefore considered nonsensical. The method and experimental setup was thus validated through a combination of Murphree point efficiency models and fundamental reasoning.

In similar fashion to the packed column evaluation, the humidification of water in air, presented **sufficient differentiation between column internals in terms of Murphree tray efficiencies**. This was seen in quantification of both weeping and vapour bypass in the two evaluated prototypes. The advantages of the HA-method, viewed from the perspective of prototyping, is presented as follows:

- [1] **Time:** On average, the experimental evaluations took between 30 and 45 minutes. This was a notable reduction from the 8 hours of an industrially sized tray column under constant reflux. In terms of prototyping, this translated to a order of magnitude difference.
- [2] **Quantification:** Humidity evaluation provided a more cost-effective alternative to the conventional Gas chromatography, in terms of both capital and operating costs. In addition, it involved little operator training, compared to the conventional GC (Gas Chromatography) analysis used for constant reflux systems.
- [3] **Environmental Considerations:** As the system utilizes only air and water, it requires no hazardous classification or additional environmental clearance.
- [4] **Safety:** The safety risks of using the proposed method was considered to be negligible. This is as no reactive or flammable chemicals were used.
- [5] **Cost:** Conventional efficiency evaluations are done at various pressures (up to 10 atmospheres) to provide a full range of liquid and vapour flow rates. This, in combination with the reagent costs, translate to a much higher operating cost.
- [6] **Material Concerns:** The use of room temperature water at low pressures presents negligible restrictions of the materials used in the fabrication of column internals.

Both Murphree tray and point efficiencies were experimentally evaluated for either validation or as an efficiency quantification tool. Having the experimental data, the predictive capacity of the Lewis models

was evaluated. In doing so, the concentration profiles measured on top of the testing tray, were found to contradict the perfect plug flow trends implied by the Lewis models. The behaviour was hypothesized to be the result of vapour entrapment in the froth.

This hypothesis, however, requires additional experimental work in terms of a higher sampling density, to confirm this trend. This is hereby suggested as future work

### 8.3. FINAL CONCLUSIONS

In conclusion, both the HA- and ADIBAA-methods displayed advantageous attributes in being able to effectively save notable time and money when quantifying column internal efficiencies during the prototyping stage. The methods are, however, not proposed as a replacement for the current norm of constant reflux distillation, since both cases evaluate a relatively constant vapour density with limited variation in the physical properties of both liquid and vapour. The methods are suggested to be used in a complementary fashion, generating a shorthand comparative estimate between a prototype and existing designs. This is expected to quickly highlight better performing designs, while limiting unnecessary expenditure on underperforming variations.

The use of the preceding methods is expected to relieve the bottleneck in the efficiency evaluation of new internal designs. The ADIBAA- and HA-methods remove the conventional constraints enforced by constant reflux evaluations. Future combinations with rapid prototyping techniques could thus notably decrease prototyping timelines and capital expenditure.

### 8.4. RECOMMENDATIONS FOR FUTURE WORK

#### 8.4.1. PACKED COLUMNS

- [1] To decrease variability, it is recommended to introduce temperature control on the UV-VIS quantification system. This will limit the need for post quantification temperature correction algorithms.
- [2] Future studies should include additional evaluation of the loading zone, extending the efficiency quantifications over the full hydrodynamic range. This will offer additional applicability outside the range of absorption.
- [3] Evaluating the effect of liquid holdup on the larger packing sizes will either validate or disprove the proposed reasoning behind the sudden jumps in efficiency.
- [4] As the proposed method illustrated sufficient capacity in differentiating column internals on efficiency, it is recommended to evaluate a wide variety of packings (to generate a baseline efficiency). From there, small alterations can be made to the respective designs, and the influence monitored. This can lead to better fundamental understanding regarding the effect of a variety of variables, such as the specific packing geometry.

- [5] Additional continued work is recommended in introducing low-volatility components into the aqueous as a tracer. This would provide joint quantification of both mass transfer coefficients and Peclet numbers.

#### 8.4.2. TRAY COLUMNS

- [1] Building on the weeping behaviour illustrated by Prototype B, further experiments are advised in quantifying the efficiency in terms of the weeping distributing across the tray. This involves stage-wise draining distributor tray.
- [2] As the experimentally measured composition profiles were found contradicting the Lewis models, it is recommended to decrease the sampling length interval across the tray. This is expected to confirm the inapplicability of the Lewis cases in assuming that all vapour enters and leaves in the same streamline.
- [3] In building on the proven applicability, it is recommended that various tray designs be evaluated in order to generate a database for comparative use. This database is to be used for comparative analysis of new prototypes, similar to those evaluated in the tray section.





---

## REFERENCES

- [1] S. Shetty and R. Cerro, "Flow of a Thin Film Over a Periodic Surface," *International journal of multiphase flow*, vol. 19, pp. 1013-1027, 1993.
- [2] "US Energy information administration," 01 01 2015. [Online]. Available: [http://www.eia.gov/dnav/pet/hist/LeafHandler.ashx?n=PET&s=8\\_NA\\_8D0\\_NUS\\_4&f=A](http://www.eia.gov/dnav/pet/hist/LeafHandler.ashx?n=PET&s=8_NA_8D0_NUS_4&f=A). [Accessed 11 04 2015].
- [3] A. Erasmus, "Doctoral Dissertation :Mass transfer in structured packing," Stellenbosch University Department Chemical Engineering, Stellenbosch, 2004.
- [4] Henly, Seader and Roper, Separation Process Principles, T. Edition, Ed., John Wiley and Son's Inc., 2011.
- [5] Intel, "50 Years of Moore's Law," Intel, [Online]. Available: <http://www.intel.com/content/www/us/en/silicon-innovations/moores-law-technology.html>. [Accessed 19 12 2016].
- [6] P. Hofhuis and F. Zuiderweg, "Distillation," *Institute of chemical engineering Symposium 56*, vol. 2.1, no. 1, 1979.
- [7] H. Z. Kister, Distillation Design, New York: McGraw Hill, 1992.
- [8] F. Zuiderweg, "Sieve Trays: A view on state of the art," *Chemical Engineering Science*, vol. 37, no. 10, pp. 1441-1464, 1982.
- [9] S. Lamprecht, "Establishing a Facility to Measure Packed Column Hydrodynamics," Stellenbosch: MSc Dissertation:, University Stellenbosch, 2010.
- [10] K. J. ., Du Preez LJ, "Reactive Absorption Kinetics of CO<sub>2</sub> in Alcoholic Solutions of MEA: Fundamental Knowledge for Determining Effective Interfacial Mass Transfer Area," Stellenbosch University South Africa, Stellenbosch, 2014.
- [11] T. Moucha, V. Linek and E. Prokopova, "Effect of Packing Geometrical Details :Influence of Free Tips on Volumetric Mass Transfer," *Transactions of the Institution of Chemical Engineers*, vol. 83, no. A, pp. 88-92, 2005.

- [12] M. Schultes, "Research on Mass Transfer Columns: Old Hat or Still Relevant," in *Presentation at D&A Conference*, Eindhoven, 2010.
- [13] Z. Olujic', A. Kamerbeek and J. d. Graauw, "A corrugation geometry based model for efficiency of structured distillation packing," *Chemical Engineering and Processing: Process Intensification*, vol. 38, pp. 683-695, 1999.
- [14] H. Z. Kister and J. R. Haas, "Entrainment from Sieve Trays in the Froth Regime," *Industrial and Engineering Chemistry Research*, vol. 27, no. 12, pp. 2331-2341, 1988.
- [15] H. Z. Kister, W. V. Plnctewsk and J. F. Chrstopher, "Entrainment from Sieve Trays Operating in the Spray Regime," *Industrial & Engineering Chemistry Process Design and Development*, vol. 20, no. 3, pp. 528-532, 1981.
- [16] M. J. Lockett, *Distillation Tray Fundamentals*, Cambridge University Press, 1986.
- [17] K. Krummrich, *Quoted in Chemcial Week*, no. 24, p. 18, 1984.
- [18] V. Linek, J. Sinkule and V. Janda, "Design of Packed Aeration Towers to strip Volatile Organic Contaminants from water," *Water Research*, vol. 32, no. 4, pp. 1264-1270, 1998.
- [19] K. Onda, H. Takeuchi and Y. Okumoto, "Mass transfer coefficients between gas and liquid phases in packed columns," *Chemcial Engineering Journal of Japan*, vol. 1, pp. 56-62, 1968.
- [20] L. Kritzinger, "Establishing a Pilot Plant Facility for Post Combustion Carbon Dioxide Capture Studies," MSc Dissertation: University Stellenbosch., Stellenbosch, 2013.
- [21] M. Pilling and B. Holden, "Chhosing Trays and Packing for distillation," *American Institute of Chemical Engineers CEP*, no. September, pp. 44-50, 2009.
- [22] E. Cussler, *Diffusion Mass tranfer in fluid systems*, Cambridge: University of Cambridge Press, 1984.
- [23] T. K. Sherwood , R. L. Pigford and C. R. Wilke, *Chemical Engineering Series: Mass Transfer*, New York: Mcgraw Hill, 1975.
- [24] M. H. De Brito, "Gas absorption experiments in a pliot plant column with the sulzer structured packing Mellapak," Lausanne EPFL: PHD Thesis, Lausanne, 1992.

- [25] C. Wang, G. T. Rochelle and F. Seibert, "Packing Characterization : MAss Transfer Properties," *Energy Procedia*, vol. 12, pp. 23-32, 2012.
- [26] V. Linek, P. Petricek, P. Benes and P. Braun, "Effective interfacial area and liquid side mass transfer coeffieints in absorbtion columns packed with hydrophilised and untreated plastic packings," *Chemical Engineering Research and Design*, vol. 62, no. 1, pp. 13-21, 1984.
- [27] J. Rejl, V. Linek, T. Moucha and L. Valenz, "Methods standardization in the measurement of mass-transfer characteristics in packed absorption columns," *Chemical Engineering research and Design*, vol. 87, pp. 695-704, 2009.
- [28] A. Hoffmann, J. Mackowiak, A. Gorak, M. Haas, J. Loning, T. Runowski and K. Hallenberger, "Standardization of mass transfer measurements: A basis for description of Absorption Processes," *Chemical Engineering Research and Design*, vol. 85, no. A1, pp. 40-49, 2007.
- [29] V. Linek, V. Ttoy, V. Machon and Z. Krivsky, "Increasing the effective interfacial area in plastic packed absorbtion columns," *Chemcial Engineering Science*, vol. 29, pp. 1955-1960, 1974.
- [30] V. Linek and V. Vacek, "Cehmical engineerings use if catalyzed sulfite oxidation kinetics for the determination of mass transfer characteristics of gas-liquid contactors," *Chemcial Engineerings Science*, vol. 36, no. 11, pp. 1747-1768, 1981.
- [31] T. Sherwood and F. Holloway, "Performance of packed tower-Liquid film data for several packings," *Transaction of the American Institute of Chemcial Engineering*, vol. 36, pp. 181-182, 1940.
- [32] W. Norman , *Absorption , Distillation and Cooling towers*, New York: John Wiley and Son's, 1961.
- [33] D. Mohunta, A. Vaidyanathan and G. Laddha, "Effective interfacial areas in packed columns," *Indian Chemcial Engineer*, no. April, pp. 39-42, 1969 a).
- [34] D. Mohunta, A. Vaidyanathan and G. Laddha, "Prediction of liquid phase mass transfer coefficients in columns packed with raschig rings," *Indian Chemcial Engineers*, no. July, pp. 73-79, 1969 b).
- [35] R. Mangers and A. Ponter, "Effect of viscosity on liquid film resistance to mass transfer in a packed column," *Indsutrial Engineering Chemical Process Design and Development*, vol. 19, no. 4, pp. 530-537, 1980.

- [36] R. Billet, "Fluiddynamisches Verhalten und Wirksamkeit von Gegenstromapparaten für Gas-Flüssig Systemen bei flüssigkeitsseitigem Stoffübergangswiderstand," Ruhr-Universität Bochum, Bochum, 1983.
- [37] R. Billet and J. Mackowiak, "Neuartige Fullkörper aus Kunststoffen für thermische Stofftrennverfahren," *Chemie Technik*, vol. 9, no. 5, pp. 219-226, 1980.
- [38] M. Lockett, *Distillation tray Fundamentals*, New York: Cambridge University Press, 1986.
- [39] D. Van Krevelen and P. Hofstijer, "Kinetics of gas liquid reactions Part I- General theory," *Recueil: Journal of the Royal Netherlands Chemical Society*, vol. 67, pp. 563-586, 1947 a.
- [40] D. Van Krevelen and P. Hofstijer, "Studies of gas absorption-I Liquid film resistance to gas in scrubbers," *Recueil: Journal of the Royal Netherlands Chemical Society*, vol. 47, pp. 49-66, 1947 b.
- [41] R. Semmelbauer, "Die Berechnung der Schutthöhe bei Absorptionvorgängen in Fullkörperkolonnen," *Chemical Engineering Science*, vol. 22, pp. 1237-1255, 1967.
- [42] J. Zech and A. Mersmann, "Liquid flow and liquid phase mass transfer in irrigated packed columns," *International Chemical Engineering Symposium Series*, vol. 56, pp. 39-47, 1979.
- [43] K. Onda, E. Sada and Y. Murase, "Liquid-side mass transfer coefficients in packed towers," *American Institute of Chemical Engineers Journal*, vol. 5, no. 2, pp. 235-239, 1959.
- [44] K. Onda, H. Takeuchi and Y. Koyama, "Effect of packing material on the wetted surface area," *Chemical Engineering Journal of Japan*, vol. 31, pp. 126-134, 1967.
- [45] J. Bravo and J. R. Fair, "Generalized correlation for mass transfer in packed distillation columns," *Industrial Engineering Chemical Process Design and Development*, vol. 21, pp. 162-170, 1982.
- [46] J. Fair and J. Bravo, "Distillation columns containing structured packing," *Chemical Engineering Progress*, vol. January, pp. 19-29, 1990.
- [47] J. R. Fair and J. G. Stichlmair, *Distillation: Principles and Practice*, New York: Wiley-VCH, 1998.
- [48] N. Kolev, "Wirksame Austauschfläche von Fullkörperschüttungen," *Verfahrenstechnik*, vol. 7, no. 3, pp. 71-75, 1973.

- [49] N. Kolev, "Wirkungsweise von Fullprperschuttengen," *Chemical Engineering Technology*, vol. 48, no. 12, pp. 1105-1112, 1976.
- [50] R. Billet and M. Schultes, "Prediction of mass transfer columns with dumped and arranged Packings," *Transactions of the Institution of Chemical Engineers*, vol. 77, no. A, pp. 498-504, 1999.
- [51] T. H. Chilton and A. P. Colburn, "Distillation and Absorption in packed columns - A convenient design and correlation method," *Industrial Engineering Chemistry*, vol. 37, no. 3, pp. 255-260, 1935.
- [52] K. M. C. and T. R.R., "Design of aeration towers to strip volatile contaminants from drinking water," *Journal of the American Water Works Association*, no. 72, pp. 684-692, 1980.
- [53] C. Wang, M. Perry, G. T. Rochelle and A. F. Seibert, "Packing Characterization: Mass Transfer Properties," *Energy Procedia*, vol. 12, pp. 23-32, 2012.
- [54] Distillation Subcommittee of the Research Committee, "Bubble Tray Design Manual," *American Institute of Chemical Engineers*, 1958.
- [55] H. Chan and J. Fair, "Prediction of Point Efficiencies on Sieve Trays," *Industrial & engineering chemistry process design and development*, vol. 23, pp. 814-820, 1984.
- [56] I. Harris and G. Hooper, "Performance Characteristics of a 12 in. Diameter Sieve Plate," *The Canadian Journal of Chemical Engineering*, vol. December, pp. 245-249, 1962.
- [57] L. Jeromin, H. Holik and H. Knapp, "Efficiency calculation method for sieve-plate columns of air separation plants," *ICHEME Symposium Series*, vol. 32, pp. 45-57, 1969.
- [58] K. T. Chuang and G. X. Chen, "Prediction of Point Efficiency for Sieve Trays in Distillation," *Industrial & Engineering Chemistry Research*, vol. 32, pp. 701-712, 1993.
- [59] T. Yanagi and M. Sakata, "Performance of a Commercial Scale 14% Hole Area Sieve Tray," *Industrial & engineering chemistry process design and development*, vol. 21, pp. 712-717, 1982.
- [60] H. Neuberg and K. Chuang, "Mass Transfer Modeling for GS Heavy Water Plants," *Canadian Journal of Chemical Engineering*, no. 60, pp. 504-510, 1982.

- [61] S. Syeda, A. Afacan and K. Chuang, "A fundamental model Prediction of sieve tray efficiency," *Chemical Engineering Research and Design*, vol. 85, no. A2, pp. 269-277, 2007.
- [62] B. B. Ashley, "Gas phase resistance to mass transfer in bubble cap column," University of Michigan, Michigan, 1955.
- [63] R. Scheffe and R. Weiland, "Mass-Transfer Characteristics of Valve Trays," *Industrial Engineering Chemical Research*, vol. 26, pp. 228-236, 1987.
- [64] J. L. Peytavy, M. H. Huor, R. Bugarel and A. Laurent, "Interfacial Area and Gas-Side Mass Transfer Coefficient of a Gas-Liquid Absorption Column: Pilot-Scale Comparison of Various Tray Types," *Chemical Engineering Processes*, vol. 27, pp. 155-163, 1990.
- [65] R. Krishna, H. Martinez, R. Shreedhar and G. Standart, "Murphree Point efficiencies in multi-component systems," *Transactions of the Institution of Chemical Engineers*, vol. 55, p. 177, 1977.
- [66] W. Lewis, "Rectification of Binary Mixtures," *Industrial Engineering Chemistry*, vol. 28, no. 1, p. 399, 1936.
- [67] M. Ashley and G. Haselden, "Effectiveness of vapour liquid contacting on Sieve Trays," *Transactions of the Institution of Chemical Engineers*, vol. 50, p. 119, 1972.
- [68] D. W. Green and R. H. Perry, *Perry's Chemical Engineers Handbook*, 8th Edition ed., McGraw Hill, 2007.
- [69] Design Institute for Physical Properties, "DIPPR Project 801," American Institute of Chemical Engineers, 2005.
- [70] R. W. Fox, P. J. Pritchard and A. T. McDonald, *Introduction to Fluid Mechanics*, vol. 7th edition, John Wiley & Sons, 2009.
- [71] American Engineers Society of Heating Refrigerating and Air-conditioning, *ASHRAE Handbook Fundamentals*, Amer Soc of Heating, Refrigerating & A-C Engineers, 2001.
- [72] R. Hyland and A. Wexler, "Formulations for the thermodynamic properties of the saturated phases of H<sub>2</sub>O from 173.15 K to 473.15 K.," *ASHRAE Transactions*, vol. 89, no. 2A, pp. 500-519.

- [73] R. Hyland and A. Wexler, "Formulations for the thermodynamic properties of dry air from 173.15 K to 473.15 K, and of saturated moist air from 173.15 K to 372.15 K, at pressures to 5 MPa," *ASHRAE Transactions*, vol. 2A, no. 89, pp. 520-535.
- [74] E. Sørensen, *Absorption and Distillation*, IChemE, Technology and Engineering, 2006.
- [75] P. Danckwerts and A. Guillham, "The design of gas absorbers I-Method for predicting rates of absorption with chemical reaction in packed columns, and tests with 1 1/2 in raschig rings," *Transactions of the institute of chemical engineers*, vol. 44, pp. 42-54, 1966.
- [76] D. Deed, P. Schutz and T. Drew, "Comparison of rectification and desorption in packed columns," *Industrial Engineering Chemistry*, vol. 39, no. 6, pp. 766-774, 1947.
- [77] A. Senol, "Predicting the effective area in a randomly packed column: Design Considerations," *Journal of Scientific and Industrial Research*, vol. 62, no. November, pp. 777-789, 2003.
- [78] R. Higbie, "The rate of absorption of a pure gas into a still liquid during short periods of exposure," *Transactions of the American Institute of Chemical Engineers*, vol. 31, pp. 365-389, 1935.
- [79] R. Billet and M. Schultes, "Prediction of mass transfer columns with dumped and arranged packing," *Institute of Chemical Engineers*, vol. 77, no. A, pp. 498-504, 1999.
- [80] M. Sharma and P. Danckwerts, "Chemical methods of measuring interfacial area and mass transfer coefficients in two-fluid systems," *British Chemical Engineering*, vol. 15, no. 4, pp. 522-528, 1967.
- [81] H. Katayama and T. Imoto, "Effect of vapour mixing on tray efficiency of Distillation Columns," *The Chemical Society of Japan*, no. 9, p. 1745, 1972.
- [82] P. H. Howard, *Handbook of Environmental Fate and Exposure Data for Organic Chemicals*, CRC Press, 1993.
- [83] "Centre for disease control and prevention," 07 04 2015. [Online]. Available: <http://www.cdc.gov/niosh/ipcsneng/neng0912.html>.
- [84] P. Au-Yeung and A. Ponter, "Estimation of liquid film mass transfer coefficients for randomly packed absorption columns," *The Canadian journal of Chemical Engineering*, vol. 61, no. 4, pp. 481-493, 1983.



- [85] F. Yoshida and T. Koyanagi, "Liquid phase mass transfer rates and effective interfacial area in packed absorption columns," *Industrial Engineering Chemistry*, vol. 50, no. 3, pp. 365-374, 1958.
- [86] J. Echarte, H. Campana and E. Brignole, "Effective areas and liquid film mass transfer coefficients in packed columns," *Industrial Engineering chemical Process Design and Development*, vol. 23, no. 2, pp. 349-354, 1984.
- [87] K. Huttinger and F. Bauer, "Benetzung und Stoffaustausch in Filmkolonnen," *Chemical Engineering Technology*, vol. 54, no. 5, pp. 449-460, 1982.
- [88] J. Fair and J. Bravo, "Prediction of mass transfer efficiencies and pressure drop for structured tower packings in vapour/liquid service," *International Chemical Engineerings Symposium Series*, vol. 104, pp. A183-A203, 1987.
- [89] A. Ponter and P. Au-Yeung, "Estimation of the liquid mass transfer coefficients for columns randomly packed with partially wetted rings," *The Canadian journal of chemical Engineering*, vol. 60, pp. 94-99, 1982.
- [90] C. M. Cooper, R. J. Christl and L. C. Peery, "Packed tower performance at high liquid rates," *Transactions of the American Institute for chemical Engineers*, vol. 37, pp. 979-996, 1941.
- [91] F. Rixon, "The absorption of carbon dioxide in and the desorption from water using packed towers," *Transaction of the institute for Chemical Engineering*, vol. 26, pp. 119-130, 1948.
- [92] H. Koch, L. Stutman, H. Blum and L. Hutchings, "Gas absorption :Liquid transfer coefficients for the carbon dioxide air-water system," *Chemical Engineering Progress*, vol. 45, no. 11, pp. 677-682, 1949.
- [93] E. Knoedler and C. Bonilla, "Vacuum degasification in a packed column," *Chemical Engineering Progress*, vol. 50, no. 3, pp. 125-133, 1954.
- [94] J. Vivian and C. King, "The mechanism of liquid -phase resistance to gas absorption in packed columns," *American Institute for Chemical Engineering*, vol. 10, no. 2, pp. 221-227, 1964.
- [95] J. Vivian, P. Brain and V. Krukoni, "Gas absorption in packed columns: liquid phase resistance in loading region," *American Institute of Chemical Engineering*, vol. 13, no. 1, pp. 174-175, 1967.

- [96] R. Coughlin, "Effect of Liquid-Packing surface interactions on gas absorption and flooding in a packed column," *American Institute of Chemical Engineers*, vol. 15, no. 5, pp. 654-659, 1969.
- [97] B. Sahay and M. Sharma, "Effective interfacial area and liquid and gas side mass transfer coefficients in a packed column," *Chemical Engineering Science*, vol. 28, pp. 41-47, 1973.
- [98] W. Bereiter, "Druckverlust und Flüssigkeitsseitiger Stoffaustausch in Sulzer Gewebepackungen," ETH Zurich, Zurich, 1975.
- [99] R. Billet and J. Mackowiak, "Flüssigkeitsseitiger Stoffübergang bei der Absorption in Fullkörperkolonnen und ihr verfahrenstechnischer Vergleich," *Chemie Technik*, vol. 6, no. 11, pp. 455-461, 1977.
- [100] K. J. Arwikaar and O. C. Sandall, "Liquid phase mass transfer resistance in a small scale packed distillation column," *Chemical Engineering Science*, vol. 35, no. 11, pp. 2337-2343, 1980.
- [101] J. Merchuk, "Mass transfer characteristics of a column with small plastic rings," *Chemical Engineering Science*, vol. 35, pp. 743-745, 1980.
- [102] P. Krotzsch, "Measurements of liquid-phase mass transfer in packed columns," *German Chemical Engineering*, vol. 5, pp. 131-139, 1982.
- [103] S. W. Dharwadkar and S. B. Sawant, "Mass transfer and hydrodynamic characteristics of tower packings larger than 0.025m nominal size," *The Chemical Engineering Journal*, vol. 31, pp. 15-21, 1985.
- [104] K. Bornhutter and A. Mersmann, "Stoffübergang mit modernen Fullkörpern grosser Abmessungen," *Chemical Engineering Technology*, vol. 63, no. 2, pp. 132-133, 1991.
- [105] M. Delaloye, U. Von Stockar and X. Lu, "The influence of the viscosity on the liquid-phase mass transfer resistance in packed columns," *The Chemical Engineering Journal*, vol. 47, pp. 51-61, 1991.
- [106] A. S. Kertes, Solubility Data Series, International Union of Pure and Applied Chemistry, vol. 38, Oxford: Pergamon Press, 1988.
- [107] A. L. Horvath, Molecular Design: Chemical Structure Generation from the Properties of Pure Organic Compounds, Amsterdam: Elsevier, 1992.

- [108] A. S. Kertes, Solubility Data Series, International Union of Pure and Applied Chemistry, vol. 37, Oxford: Pergamon Press, 1988.
- [109] Semichem, *AMPAC 5.0*, Shawnee, KS: Semichem, 1994.
- [110] N. R. Draper and H. Smith, *Applied Regression Analysis*, New York: Wiley, 1996.
- [111] J. Riddick, W. Bunger and T. and Sakano, *Organic Solvents*, New York: John Wiley & Sons, 1986.
- [112] L. Gevantman, *CRC Handbook of Chemistry and Physics*, Boca Raton FL.: CRC Pres, 1996.
- [113] D. Mackay and W. Shiu, "A Critical review of Henry's Law constants for chemicals of Environmental interest," *Journal of Physical Chemistry Reference Data*, no. 10, p. 1175, 1981.
- [114] E. Wilhelm, R. Battino and R. Wilcock, "Low-pressure solubility of gases in liquid water," *Chemical Reviews*, no. 77, pp. 219-262, 1977.
- [115] Aldrich, *Aldrich Catalog Handbook of Fine Chemicals*, Milwaukee, WI: Aldrich Chemical Company, 1996.
- [116] R. Stephenson, "Mutual solubilities: water-ketones, water-ethers, and water-gasoline-alcohols," *Journal of Chemical Engineering Data*, no. 37, p. 80, 1992.
- [117] W. Shiu and D. Mackay, "A Critical Review of Aqueous Solubilities, Vapour Pressure, Henry's Law Constants, and Octanol-water Partition Coefficients of the Polychlorinated Biphenyls," *Journal of Physical Chemistry Reference Data*, no. 15, p. 911, 1986.
- [118] T. D. Le and J. G. Weers, "QSPR and GCA Models for Predicting the Normal Boiling Points of Fluorocarbons," *Journal of Physical Chemistry*, no. 34, p. 581, 1994.
- [119] A. S. Kertes, Solubility Data Series, International Union of Pure and Applied Chemistry, vol. 20, Oxford: Pergamon Press, 1985.
- [120] A. Horvath, *Halogenated Hydrocarbon*, New York: Marcel Dekker, 1982.
- [121] Serena Software, "PC Model," Serena Software, Bloomington, IN, 1992.
- [122] A. S. Kertes, Solubility Data Series, International Union of Pure and Applied Chemistry, vol. 15, Oxford: Pergamon Press, 1982.

- [123] R. Pearlman and S. Yalkowsky, "Water Solubilities of Polynuclear Aromatic and Heteroaromatic Compounds," *Journal of Physical Chemistry Reference Data*, no. 13, p. 975, 1984.
- [124] S. Banerjee, S. Yalkowsky and S. Valvani, "Water solubility and octanol/water partition coefficients of organics. Limitations of the solubility-partition coefficient correlation," *Environ. Sci. Technol.*, no. 14, p. 1227, 1980.
- [125] "Benzoates CAS N<sup>o</sup>:65-85-0, 532-32-1, 582-25-2, 100-51-6," UNEP PUBLICATIONS.
- [126] "Benzyl alcohol Material Safety Data Sheet," Science Lab.
- [127] "LINALOOL CAS N<sup>o</sup>: 78-70-6," UNEP PUBLICATIONS:OECD SIDS, 2004.
- [128] "OECD Screening Information DataSet (SIDS) High Production Volume Chemicals," 07 04 2015. [Online]. Available: <http://www.inchem.org/pages/sids.html>.
- [129] "Occupational Safety & Health Administration," 07 04 2015. [Online]. Available: <https://www.osha.gov/dsg/annotated-pels/>.
- [130] "NDT Resource Centre," [Online]. Available: <http://www.ndt-ed.org/EducationResources/CommunityCollege/Materials/Structure/alloying.htm>. [Accessed 24 02 2014].
- [131] "VANILIN CAS N<sup>o</sup>: 121-33-5," UNEP Publications:OECD SIDS.
- [132] "Test plan for phenethyl alcohol," The Flavor and Fragrance High Production Volume Chemical Consortia, 2002.
- [133] D. L. Bennett, A. S. Kao and L. W. Wong, "A mechanistic analysis of sieve tray froth," *American Institute of Chemical Engineers*, vol. 41, no. 9, pp. 2067-2082, 1995.
- [134] A. Koziol and J. Mackowiak, "Liquid entrainment in tray columns with downcomers," *Chemical Engineering Process*, vol. 27, pp. 145-153, 1990.
- [135] W. Licht and G. S. Narasimhamurthy, "Rate of Fall of Single Liquid Droplets," *American Institute of Chemical Engineers*, no. 3, pp. 366-373, 1955.
- [136] F. B. Petlyuk, *Distillation Theory and its application to optimal Design of separation Units*, Cambridge University Press, 2004.

- [137] K. E. Porter and J. D. Jenkins, "The interrelationship between industrial practice and academic research in distillation and adsorption," *Institution of Chemical Engineers Symposium Series No. 56*, pp. 5.1/1-5-5.1/47, 179.
- [138] R. Turton, R. C. Bailie, W. B. Whiting, J. A. Shaeiwitz and D. Bhattacharyya, *Analysis, Synthesis and Design of Chemical Processes*, Pearson, 2013.
- [139] E. C. Uys, C. E. Schwarz, A. J. Burger and J. H. Knoetze, "New froth behaviour observations and comparison of experimental sieve tray entrainment with existing correlations," *Chemical Engineering Research and Design*, no. 90, pp. 2072-2085, 2012.
- [140] E. Uys, "Entrainment in a sieve tray column, Masters Thesis," Stellenbosch University, South-Africa, 2010.
- [141] A. H. Van Sinderen, E. F. Wijn and R. W. Zanting, "Entrainment and Maximum Vapour Flow Rate of Trays," *Chemical Engineering Research and Design*, vol. 81, no. 1, pp. 94-107, 2003.
- [142] R. Taylor and R. Krishna, *Multicomponent Mass transfer*, New York: John Wiley and Son's Inc., 1993.
- [143] F. Petlyuk, *Distillation Theory and its Application of Optimal Design of Separation Units*, Cambridge University Press, 2004.
- [144] C. D. Holland, *Multicomponent Distillation*, New Jersey: Prentice Hall, 1963.
- [145] U. Allenbach, H. P. Wirges and W. D. Deckwer, "Ermittlung von Stoffaustauschparameteren in Gas-Flussig-Reaktoren mit Hilfe der saurekatalysierten," *Verfahrenstechnik*, vol. 12, no. 12, pp. 751-754, 1977.
- [146] J. Andrieu and B. Lespinasse, "Mesure directe de l'aire mouillée d'un garnissage d'anneaux de raschig en verre pyrex dans une colonne arrosée à contre-courant," *Chimie et Industrie: Génie chimique*, vol. 106, no. 11, pp. 825-833, 1973.
- [147] G. Baldi and S. Sicardi, "Effective mass transfer areas in packed column during chemical absorption," *Chemical Engineering Science*, vol. 30, no. 7, pp. 769-770, 1975.
- [148] A. Bennet and F. Goodridge, "Hydrodynamic and mass transfer studies in packed bed absorption columns Part II : Measurement of total interfacial area," *Transactions of the Institution of Chemical Engineers*, vol. 48, pp. T241-T244, 1970.

- [149] R. Bergauer, B. Horner and K. Dialer, "Zur interpretation effektiver Austauschflächen in Systemen Gas/Flüssigkeit," *Chemical Engineering Technology*, vol. 51, no. 1, pp. 38-39, 1979.
- [150] W. L. Bolles and J. R. Fair, "Improved mass transfer model enhances packed-column design," *Chemical Engineering*, vol. 89, no. July 12, pp. 109-116, 1982.
- [151] P. Bomio, "Stoffaustauschmessungen an der Sulzer-Packungen aus Kunststoff," *Chemical Engineering Technology*, vol. 49, no. 11, pp. 895-897, 1977.
- [152] J. Bridgewater and A. M. Scott, "Statistical models of packing application to gas absorption and solid mixing," *Transaction of the Institute for chemical Engineers*, vol. 52, pp. 317-324, 1974.
- [153] D. Cornell, W. Knapp and J. R. Fair, "Mass transfer efficiency-Packed Columns Part I," *Chemical Engineering Progress*, vol. 56, no. 7, pp. 68-74, 1960.
- [154] P. Danckwerts and S. Rizvi, "The design of absorbers .Part II : Effective interfacial areas for several types of packing," *Transaction of the Institute of Chemical Engineers*, vol. 44, pp. 124-127, 1971.
- [155] P. Deckwerts and M. Sharma, "The absorption of carbon dioxide in solutions of alkalis amines (with some notes on the hydrogen sulphide and carbonyl sulphide)," *The Chemical Engineers*, vol. 44, pp. 244-280, 1966.
- [156] J. Davidson, "The hold-up and liquid film coefficient of packed towers .Part II: Statistical models of random packing," *Transaction of the Institute of Chemical Engineers*, vol. 37, pp. 131-136, 1959.
- [157] A. Zakeria, A. Einbub, P. O. Wiigb, L. Oic, E. Hallvard and F. Svendsena, "Experimental Investigation of Pressure Drop, Liquid Hold-Up and Mass Transfer Parameters in a 0.5 m Diameter Absorber Column," *Energy Procedia*, no. 4, pp. 606-613, 2011.
- [158] Z. Olujić, A. Seibert and J. Fair, "Influence of corrugation geometry on the performance of structured packings: an experimental study," *Chemical Engineering Processing*, vol. 39, pp. 335-342, 2000.
- [159] M. Delaloye, "Influence de la viscosité de liquide sur le transfert de matière dans une colonne à garnissage à l'échelle pilote," Lausanne: PHD EPFL, 1986.

- [160] M. Duss and P. Bomio, "Rückgewinnung organischer Dämpfe aus Abgasströmen mit Absorptionsverfahren," *Chemical Engineering Technology*, vol. 63, no. 4, pp. 388-389, 1991.
- [161] P. Grassmann and F. Widmer, *Einführung in die thermische verfahrenstechnik*, Berlin: Walter de Gruyter, 1974.
- [162] J. Guillen, M. Pitarch and F. Mateos, "Determinacion del area interfacial y de los coeficientes de materia en sistemas de contacto gas-liquido metodos quimicos," *Ingeniera Quimica*, vol. 14, pp. 179-186, 1982.
- [163] L. Hutchings, L. Stutzman and H. Koch, "Gas absorption : mass transfer coefficients as function of liquid, gas rates , tower packing characteristics," *Chemical Engineering Process*, vol. 45, no. 4, pp. 253-268, 1949.
- [164] G. Jackson and J. Marchello, "Effective and wetted area in a packed columns," *Journal of Chemical Engineering Japan*, vol. 3, no. 2, pp. 263-264, 1970.
- [165] A. Jhaveri and M. Sharma, "Effective interfacial area in a packed column," *Chemical Engineering Science*, vol. 23, pp. 669-676, 1968.
- [166] G. Joosten and P. Danckwerts, "Chemical reaction and effective interfacial areas in gas absorption," *Chemical Engineering Science*, vol. 25, pp. 563-461, 1973.
- [167] F. Samb, M. Dermont, N. Adler and P. Peringer, "Dynamic Liquid Holdup and Oxygen transfer in a cocurrent upflow bioreactor with small packing at low Reynolds numbers," *The Biochemical Engineering Journal*, vol. 62, pp. 237-240, 1996.
- [168] G. Wang, X. Yuan and K. Yu, "A method for calculating effective interfacial area of structured packed distillation columns under elevated pressures," *Chemical Engineering and Processing*, vol. 45, pp. 691-697, 2006.
- [169] P. Krotzsch and H. Kurten, "Druckverlust und Stoffaustauschfläche in Fullkorpschüttungen," *Verfahrenstechnik*, vol. 13, no. 12, pp. 939-944, 1979.
- [170] J. Kunesh, "Recent developments in packed columns," *The Canadian Journal of Chemical Engineering*, vol. 65, pp. 907-913, 1987.

- [171] J. Landau, J. Boyle, H. Gomma and A. Al Taweel, "Comparison of methods for measuring interfacial areas in gas-liquid dispersions," *The Canadian Journal of Chemical Engineering*, vol. 55, pp. 13-18, 1977.
- [172] A. Laurent and J. Charpentier, "Aires interfaciales et coefficients de transfer de matiere dans les divers types d'absorbours et de reacteurs gaz-liquide," *The Chemical Engineering Journal*, vol. 8, pp. 85-101, 1974.
- [173] W. Lee and Y. Kim, "Effective mass transfer area and mass transfer coefficients in a packed gas-absorber," *Journal of the Korean Institute of Chemical Engineering*, vol. 20, no. 2, pp. 123-132, 1982.
- [174] A. Laurent, C. Prost and J. Charpentier, "Determination par methode chimique des aires interfaciales et de coefficients de transfer de matiere dans les divers types d'absorbours et de reacteurs gaz-liquide," *Journal de Chimie physique*, vol. 72, no. 2, pp. 263-244, 1975.
- [175] O. Levenspiel, *Chemical Reaction Engineering*, John Wiley and son's Inc., 1972.
- [176] W. Lewis and W. Whitman, "Principles of gas absorption," *Industrial Engineering Chemistry*, vol. 16, no. 12, pp. 1215-1220, 1924.
- [177] F. Mayo, T. Hunter and A. Nash, "Wtted surface in ring-packed towers," *Journal of the society of Chemical Industry*, vol. 54, pp. 375-385, 1935.
- [178] W. Meier, *Sulzer kolonnen fur rektifikation und absorption*, Technische Rundschau Sulzer, 1979, pp. 49-61.
- [179] W. Meier, R. Hunkeler and W. Stocker, "Sulzer Mellapak-Eine neue , geordnete packung fur stoffaustausch-Apparate," *Chemical Engineering Technology*, vol. 51, no. 2, pp. 119-122, 1979.
- [180] W. Meier, W. Stoecker and B. Weinstein, "Performance of a new ,high efficiency packing," *Chemical Engineering Process*, vol. 73, no. 11, pp. 71-77, 1977.
- [181] M. Murthy and A. Rao, "Interfacial area for packed towers," *Journal of the Indian Institute of Science*, vol. 61, no. 1, pp. 1-19, 1979.
- [182] K. Neelakantan and J. Gehlawat, "New chemical systems for the determination of the liquid-side mass transfer coefficient and effective interfacial area in gas-liquid contactors," *The chemical Engineering Journal*, vol. 24, pp. 1-6, 1982.



- [183] A. Ponter, G. Penningsworth and R. Mangers, "Estimation of the liquid mass transfer coefficients for packed columns using organic and aqueous systems," *Chemical Engineering Technology*, vol. 52, no. 8, pp. 656-657, 1980.
- [184] S. Puranik and A. Vogelpohl, "Effective interfacial area in irrigated packed columns," *Chemical Engineering Science*, vol. 29, pp. 501-507, 1974.
- [185] G. Richards, G. Ratcliff and P. Danckwartz, "Kinetics of CO<sub>2</sub> absorption -III First order packed column," *Chemical Engineering Science*, vol. 12, pp. 325-328, 1964.
- [186] L. Rizzuti and A. Brucato, "Liquid viscosity and flow rate effects on interfacial area in packed columns," *The Chemical Engineering Journal*, vol. 41, pp. 49-52, 1989.
- [187] R. Sedelies, A. Steiff and P. Weinspach, "Mass transfer area in different gas-liquid reactors as a function of liquid properties," *Chemical Engineering Technology*, vol. 10, pp. 1-15, 1987.
- [188] M. Shi and A. Mersmann, "Effective interfacial area in packed columns," *German Chemical Engineering*, vol. 8, pp. 87-96, 1985.
- [189] H. Shulman, C. Ullrich and N. Wells, "Performance of packing columns-I; Total, static and operating holdups," *American Institute for Chemical Engineering*, vol. 1, no. 2, pp. 247-253, 1955.
- [190] H. Shulman, C. Ullrich, A. Proulx and J. Zimmerman, "Performance of packing columns -II Wetted and effective interfacial areas, gas and liquid-phase mass transfer rates," *American Institute of Chemical Engineering*, vol. 1, no. 2, pp. 253-258, 1955 b.
- [191] L. Spiegel and W. Meier, "Correlations of the performance characteristics of the various Mellapak types," *International Chemical Engineering Symposium Series*, vol. 104, pp. 203-215, 1987.
- [192] K. Shridharan and H. Sharma, "New systems and methods for the measurement of effective interfacial area and mass transfer coefficients in gas-liquid contactors," *Chemical Engineering Science*, vol. 31, pp. 767-774, 1976.
- [193] A. Vidwans and M. Sharma, "Gas-side mass transfer coefficient in packed columns," *Chemical Engineering Science*, vol. 22, pp. 673-684, 1967.

- [194] U. Von Stockar and X. Lu, "Simple and accurate short-cut procedure to account for axial dispersion in countercurrent separation columns," *Industrial Engineering Chemical Research*, vol. 30, pp. 1248-1257, 1991.
- [195] U. Von Stockar and C. Wilke, *Absorption*, John Wiley and Sons, 1991.
- [196] F. Yoshida and T. Koyanagi, "Mass transfer and effective interfacial areas in packed columns," *American Institute of Chemical Engineering*, vol. 8, no. 3, pp. 309-316, 1962.
- [197] F. Yoshida and Y. Miura, "Effective interfacial area in packed columns for absorption with chemical reaction," *American Institute for chemical Engineering*, vol. 9, no. 3, pp. 331-337, 1963.
- [198] S. Shetty and R. Cerro, "Fundamental Liquid Flow Correlations for the Computation of Design Parameters for Ordered Packings," *Industrial Engineering Chemistry Research*, vol. 35, pp. 771-783, 1997.
- [199] J. A. Wesselingh, "Non-Equilibrium Modelling of Distillation," *Transactions of the Institute of Chemical Engineering*, vol. 75, p. 529, 1997.
- [200] S. Ellis and J. Hardwick, "Effect of reflux ratio on plate efficiency," *ICHEME Symposium Series*, vol. 32, pp. 29-37, 1969.
- [201] C. Nickson, "Advances in Mobile Phones," 9th October 2016. [Online]. Available: <http://www.atechnologysociety.co.uk/advances-mobile-phones.html>. [Accessed 1st November 2016].
- [202] D. Mackay, W. Shiu and K. Ma, *Illustrated Handbook of Physical-Chemical Properties and Environmental Fate for Organic Chemicals*, Boca Raton: Lewis Publishers/CRC Press, 1992.
- [203] D. Mackay, W. Shiu and K. Ma, *Illustrated Handbook of Physical-Chemical Properties and Environmental Fate for Organic Chemicals*, vol. 2, Boca Raton: Lewis Publishers/CRC Press, 1992.
- [204] D. Mackay, W. Shiu and K. Ma, *Illustrated Handbook of Physical-Chemical Properties and Environmental Fate for Organic Chemicals*, vol. 3, Boca Raton: Lewis Publishers/CRC Press, 1993.

- [205] P. Howard, Handbook of Environmental Fate and Exposure Data for Organic Chemicals, Boca Raton: Lewis Publishers/CRC Press, 1989.
- [206] P. Howard, Handbook of Environmental Fate and Exposure Data for Organic Chemicals, vol. II, Boca Raton: Lewis Publishers/CRC Press, 1990.
- [207] K. Satyanarayana and M. C. Kakati, "Correlation of Flash Points," *Fire Mater.*, no. 15, pp. 97-100, 1991.
- [208] C. E. Rechsteiner, W. J. Lyman, W. F. Reehl and D. H. Rosenblatt, Handbook of Chemical Property Estimation Methods-Chapter 12, New York: McGraw-Hill, 1982.
- [209] R. C. Weast, Handbook of Chemistry and Physics, Cleveland, OH: CRC Press, 1976.
- [210] N. S. Zefirov, M. A. Kirpichenok, F. F. Izmailov and M. I. Trofimov, "Scheme for the Calculation of the Electronegativities of Atoms in a Molecule in the Framework of Sanderson's Principle," *Dokl. Akad. Nauk SSSR (Engl. Transl.)*, no. 296, pp. 440-443., 1987.
- [211] M. Miller, S. Ghodbane, S. P. Wasik, Y. Tewari and D. Martire, "Aqueous Solubilities, Octanol/Water Partition Coefficients, and Entropies of Melting of Chlorinated Benzenes and Biphenyls," *Journal of Chemical Engineering Data*, no. 29, pp. 184-190, 1984.
- [212] R. Stephenson, J. Stuart and M. Tabak, "Mutual Solubility of water and Aliphatic Alcohols," *Journal of Chemical Engineering Data*, no. 29, p. 287, 1984.
- [213] D. Varhanickova, S. Lee, W. Y. Shiu and D. Mackay, "Aqueous Solubilities of chlorocatechols, chlorovanillins, chlorosyringols, and chlorosyringaldehydes at 25-degrees-c," *Journal of Chemical Engineering Data*, no. 40, pp. 620-622, 1995.
- [214] M. O. Hertel and K. Sommer, "Limiting Separation Factors and Limiting Activity Coefficients for 2-Phenylethanol and 2-Phenylethanal in Water at 100 °C," *Journal of Chemical Engineering Data*, pp. 1905-1906, 2005.
- [215] S. Wang, G. W. A. Milne and G. Klopman, "Graphic Theory and Group Contributions in the Estimation of Boiling Points.," *Journal of Physical Chemistry*, no. 99, pp. 6739-6747, 1995.
- [216] F. Scargiali, F. Grisafi and A. Brucato, "Analysis of the differences in kLa values determined by different variants of the dynamic method in stirred tanks," Università di Palermo, Dipartimento di Ingegneria Chimica, Viale delle Scienze ED.6, 90128 Palermo, Italy.

- [217] D. Bennet, R. Agrawal and P. Cook, "New Pressure drop correlations for Sieve tray distillation columns," *American Institute of Chemical Engineers*, vol. 29, no. 3, p. 434, 1983.
- [218] D. Jenkins, D. Mcullum, R. Ruzbacky, S. Saunders and A. Brent, "Air stripping of ammonia and methanol in a bubble-cap column," *American Institute of Chemical Engineers: Environmental Progress*, vol. 26, no. 4, pp. 365-374, 2007.
- [219] M. Karelson, V. S. Lobanov and A. R. Katritzky, "Quantum-Chemical Descriptors in QSAR/QSPR Studies," *Chemical Reviews*, no. 96, pp. 1027-1043, 1996.
- [220] A. R. Katritzky, V. S. Lobanov and M. Karelson, "QSPR: The Correlation and Quantitative Prediction of Chemical and Physical Properties from Structure," *Chemical Society Reviews*, no. 24, pp. 279-287, 1995.
- [221] C. d. Hunt, D. N. Hanson and C. R. Wilke, "Capacisty Factors in the Performance of Perforated plate columns," *Americal Institute for Chemcial Engineers*, vol. 1, no. 4, pp. 441-451, 1955.
- [222] US Department and Human Services, "Occupational health and Safety documentation for Butanone".
- [223] A. Gianetto and S. Sicardi, "Interfacial area in countercurrent absorption columns," *Ingegneria Chimica Italiana*, vol. 8, no. 6, pp. 181-182, 1972.
- [224] C. Fisher, "Boiling Point Gives Critical Temperature," *Chemical Engineering*, no. 96, pp. 157-158, 1989.
- [225] A. T. Balaban, N. Joshi, L. B. Kier and L. H. Hall, "Correlation between Chemical Structure and Normal Boiling Points of Halogenated Alkanes C1-C4.," *Journal of Chemical Information and Computer Sciences*, no. 32, pp. 233-237, 1992.
- [226] A. T. Balaban, S. C. Basak, T. Colburn and G. D. Grunwald, "Correlation between Structure and Normal Boiling Points of Haloalkanes C1-C4 Using Neural Networks," *Journal of Chemical Information and Computer Sciences*, no. 34, pp. 1118-1121, 1994.
- [227] A. T. Balaban, L. B. Kier and N. Joshi, "Correlations between Chemical Structure and Normal Boiling Points of Acyclic Ethers, Peroxides, Acetals, and Their Sulfur Analogues," *Journal of Chemical Information and Computer Sciences*, no. 32, pp. 237-244, 1992.

- [228] L. M. Egolf, M. D. Wessel and P. C. Jurs, "Prediction of Boiling Points and Critical Temperatures of Industrially Important Organic Compounds from Molecular Structure," *Journal of Chemical Information and Computer Sciences*, no. 34, pp. 947-956, 1994.
- [229] L. M. Egolf and P. C. Jurs, "Prediction of Boiling Points of Organic Heterocyclic Compounds Using Regression and Neural Network Techniques," *Journal of Chemical Information and Computer Sciences*, no. 33, pp. 616-625, 1993.
- [230] P. Simamora, A. H. Miller and S. H. Yalkowsky, "Melting Point and Normal Boiling Point Correlations: Applications to Rigid Aromatic Compounds," *Journal of Chemical Information and Computer Sciences*, no. 33, pp. 437-440, 1993.
- [231] D. T. Stanton, P. C. Jurs and M. G. Hicks, "Computer-Assisted Prediction of Normal Boiling Points of Furans, Tetrahydrofurans, and Thiophenes.," *Journal of Chemical Information and Computer Sciences*, no. 31, pp. 301-310, 1991.
- [232] S. E. Stein and R. L. Brown, "Estimation of Normal Boiling Points from Group Contributions," *Journal of Chemical Information and Computer Sciences*, no. 99, pp. 6739-6747, 1995.
- [233] M. D. Wessel and P. C. Jurs, "Prediction of Normal Boiling Points for a Diverse Set of Industrially Important Organic Compounds from Molecular Structure," *Journal of Chemical Information and Computer Sciences*, no. 35, pp. 841-850, 1995.
- [234] M. D. Wessel and P. C. Jurs, "Prediction of Normal Boiling Points of Hydrocarbons from Molecular Structure," *Journal of Chemical Information and Computer Sciences*, no. 35, pp. 68-76, 1995.
- [235] M. Karelson, "Quantum-Chemical Treatment of Molecules in Condensed Disordered Media," *Advances in Quantum Chemistry*, no. 28, pp. 141-157, 1997.
- [236] F. Garica-Ochoa and E. Gomez, "Bioreactor scale-up oxygen transfer rate in microbial processes: An overview," *Biotechnology Advances*, vol. 27, pp. 153-176, 2009.
- [237] M. J. S. Dewar, E. G. Zoebisch, E. F. Healy and J. J. P. A. Stewart, "A New General Purpose Quantum Mechanical Molecular Model," *Journal of the American Chemical Society*, no. 107, pp. 3902-3909, 1985.
- [238] D. E. Needham, I.-C. Wei and P. G. Seybold, "Molecular Modeling of the Physical Properties of the Alkanes," *Journal of the American Chemical Society*, no. 110, pp. 4186-4194, 1988.

- [239] University of Florida,, CODESSA 2.0, Gainesville, FL: University of Florida, 1994.
- [240] A. R. Katritzky, E. S. Ignatchenko, R. A. Barcock, V. S. Lobanov and M. Karelson, "Prediction of Gas Chromatographic Retention Times and Response Factors Using a General Quantitative Structure-Property Relationship Treatment," *Analytical Chemistry*, no. 66, pp. 1799-1807, 1994.
- [241] D. T. Stanton and P. C. Jurs, "Development and Use of Charged Partial Surface Area Structural Descriptors in Computer-Assisted Quantitative Structure-Property Relationship Studies.," *Analytical Chemistry*, no. 62, pp. 2323-2329, 1990.
- [242] V. Athès, P. Paricaud, M. Ellaite, I. Souchon and W. Fürst, "Vapour-liquid equilibria of aroma compounds in hydroalcoholic solutions: Measurements with a recirculation method and modelling with the NRTL and COSMO-SAC approaches," *Fluid Phase Equilibria* 265, p. 139-154, 2008.
- [243] A. R. Katritzky, L. Mu, V. Lobanov and M. Karelson, "Correlation of Boiling Points with Molecular Structure. 1. A Training Set of 298 Diverse Organics and a Test Set of 9 Simple Inorganic," *Journal of Physical Chemistry*, no. 100, pp. 10400-10407, 1996.



---

# CHAPTER 9: APPENDICES

## 9.1. PACKED COLUMNS

### 9.1.1. CORRELATION DISCUSSION: VOLUMETRIC LIQUID MASS TRANSFER

#### COEFFICIENT

Resulting from their pioneering experimental work, Sherwood and Holloway [31] proposed the first correlation for the prediction of the volumetric mass transfer coefficient (Equation 4.1). The ensuing equation is considered to have doubtful predictive ability as it was not dimensionally sound, requiring the dimensional constant  $C_1$  to balance. This led many authors [24] to question the applicability of the model.

In an attempt to provide a generally applicable alternative, a standardised correlation (Equation 4.2) for different sizes of Berl saddles and Raschig Rings was developed by Norman [32] in 1961. Although the corresponding training data was collected from various external sources, mostly aqueous systems were considered. As a result, the correlation downplayed the effect surface tension on wetting. Taking this into account, the acclaimed [32] predictive accuracy of 20 % was considered mostly applicable to aqueous systems [24].

The correlation (Equation 4.3) proposed by Mohunta [33, 34] in 1969, was the product of theoretical reasoning and experimental data as tabulated in Tables 9.1 to 9.4. The correlation was evaluated for respects to Raschig Rings of sizes ranging from 5 to 19 mm. In a review paper published by Au-Yeung and Ponter [84], the correlation was found to fit relevant literature within 20% [24].

An inaugural investigation into the effect of liquid viscosity was presented by Mangers and Ponter [35]. Although the initial correlation illustrated a dependence between the  $k_{LA}$  and liquid contact angle, it was later simplified as illustrated in Equation 4.4. This was done through the assumption that in the case of very viscous fluids, the liquid phase would become continuous instead of the gas. As a result, the viscosity was no longer considered a function of the contact angle [35].

Both Billet [36] and Schultes (1990) attempted to forward the science through adopting packing specific correlations (Equations 4.5 and 4.6), with the Schultes model providing the best fit [24]. The accuracy of the subsequent model is estimated to be within 20% of literature alternatives [24]. Noting the large similarities between the proposed models, the authors later combined forces in producing correlations for the liquid phase mass transfer coefficients and interfacial areas [50].

Linek *et al.* [30, 26, 18] proposed the only a fully empirical approach present in this thesis. The subsequent correlation (Equation 4.7) is largely limited to use within the scope of derivation. This limits the predictive applicability of the correlations for varying physical properties.



### 9.1.2. CORRELATION DISCUSSION: THE LIQUID MASS TRANSFER COEFFICIENT

Although Krevelen and Hoftijzer [39, 40] were credited with the inaugural representation of the liquid phase mass transfer coefficient, presented in Equations 4.8 and 4.9, it was later suggested that the correlation provided an inaccurate depiction of liquid flow dependence [84, 24]. This was as a result of the wrongful assumptions regarding the exponent of the diffusion coefficients. The authors used two film theory in approximating mass transfer (see Table 9.9 in Section 9.3.2).

Semmelbauer [36] proposed a model (Equations 4.10 and 4.11), resulting from a combination of dimensionless modelling and external data. As stated in the original article Semmelbauer [36], the proposed model illustrated large unquantifiable deviations, limiting its applicability. This was attributed to the implementation of indirect methods in measuring interfacial area. The Semmelbauer experimental setup used sublimation as a representation of mass transfer. However, Yoshida and Koyanagi [85] proved that sublimation produces larger estimates of the effective interfacial area. This is as semi stagnant pockets were shown to be effective for vaporization, but not for absorption [85, 24].

With the progression of knowledge and adoption of the penetration theory (see Table 9.9 in Section 9.3.2), Onda *et al.* [19] proposed an alternative correlation for the liquid phase mass transfer coefficient. This approach entailed dividing literature  $k_{LA}$  values with their correlation for effective interfacial area. The subsequent model (Equation 4.12 and 4.13) was found to be more applicable than prior estimates. As pointed out by Echarte *et al.* [86], the Onda [19] correlation, however, fails to adequately represent systems with large deviations in liquid viscosity. Additional questions were raised by Huttinger and Brauer [87] on the ability of the equation to predict the effect of surface tension on wetting. Although questioned, Equations 4.12 and 4.13 are still frequently used with maximum expected deviations of 20 % reported (except for Pall Rings).

In an attempt to remedy the shortcomings of the Onda [19] correlations, Bravo and Fair [88] proposed alternative effective interfacial area correlation, on the backbone of the original experimental data. The subsequent model was aimed at rectifying the correlations inability to distinguish between wetting and non-wetting systems. This model was the first to acknowledge the effect of gas velocity on the height of required packing.

Endeavouring to further improve on the predictive power of liquid mass transfer models, Kolev [48, 49] correlated data from a variety of authors, evaluating both packing and liquid loads [24]. The subsequent equations (4.14, 4.15) are claimed to provide a predictive accuracy of 20% [24].

Contradictory to all other models, Zech and Mersmann [42] proposed an independence between the liquid mass transfer coefficient and viscosity. This assumption was later dismissed by Ponter *et al.* [89] in claiming that it provided no more predictive power the empirical correlations derived by Sherwood [31] in 1940.

The latest addition to the predictive correlations was proposed by Billet and Schultes [79] in 1993 and refined in 1999. The correlation was evaluated in fitting a dimensionless model to more 50 systems with 70 types of packing. As a result, small deviations as small as 12.4 % is expected [79].

Resulting from their experimental methodologies, many authors opted to evaluate alternating liquid rates, with constant gas loadings. As a result, the significance of the loading zone was underestimated. Subsequently the equations presented in

Table 4.2, largely neglect the effect of the loading zone on the effective interfacial area (with the exception of the Billet & Schultes [79] and Bravo and Fair [88]). Defined as the gas flow rate at which friction forces start to influence the liquid hold-up, the loading zone is known to have a profound effect on the effective interfacial area in approximating the effective interfacial area to be independent of the gas velocity, large deviations are expected in utilizing the above-mentioned equations.

### 9.1.3. SUMMARY OF EVALUATED LITERATURE: VOLUMETRIC LIQUID MASS TRANSFER COEFFICIENT

TABLE 9.1: SUMMARY OF EVALUATED LITERATURE.

Source	ID	Method	System evaluated	Date
Sherwood & Halloway [23]	1	Desorption	O <sub>2</sub> ,N <sub>2</sub> ,H <sub>2</sub> and He from water into air	1940
Cooper <i>et al.</i> [90]	2	Desorption	CO <sub>2</sub> from water into Air	1941
Rixon [91]	3	Desorption	CO <sub>2</sub> from water into Air	1948
Rixon [91]	3	Absorption	CO <sub>2</sub> into water	1948
Koch <i>et al.</i> [92]	4	Absorption	CO <sub>2</sub> from air into tap & Distilled water	1949
Knoedler & Bonilla [93]	5	Vacuum Desorption	O <sub>2</sub> from Water	1954
Yoshida & Koyanagi [85]	6	Absorption	CO <sub>2</sub> into tap water and methanol	1958
Onda <i>et al.</i> [43]	7	Absorption	CO <sub>2</sub> and H <sub>2</sub> into water	1959
Vivian & King [94]	8	Desorption	C <sub>3</sub> H <sub>6</sub> , CO <sub>2</sub> , O <sub>2</sub> , H <sub>2</sub> from water into air	1964
Vivian <i>et al.</i> [95]	9	Desorption	CO <sub>2</sub> from water into Air	1967
Onda <i>et al.</i> [44]	10	Absorption	CO <sub>2</sub> into water, CCl <sub>4</sub> and methanol	1968
Couglin [96]	11	Chemical Absorption	O <sub>2</sub> into Na <sub>2</sub> SO <sub>3</sub> solutions	1969
Mohunta <i>et al.</i> [33]	12	Desorption	O <sub>2</sub> from water with air	1969
Mohunta <i>et al.</i> [34]	12	Absorption	CO <sub>2</sub> from aqueous glycerol with air	1969
Sahay & Sharma [97]	13	Absorption	CO <sub>2</sub> into tap water	1973
Bereiter [98]	14	Absorption	CO <sub>2</sub> into Ethanol	1975
Billet and Mackowiak [99]	15	Desorption	CO <sub>2</sub> from water into Air	1977
Arwika And Scandal [100]	16	Absorption	CO <sub>2</sub> into Water	1980
Billet and Mackowiak [37]	17	Absorption	CO <sub>2</sub> into Water	1980
Mangers & Ponter [35]	18	Absorption	CO <sub>2</sub> into Water and Glycerol solutions	1980
Merchuk [101]	19	Absorption	CO <sub>2</sub> into Water	1980
Krotsch [102]	20	Chemical Absorption	CO <sub>2</sub> into sodium carbonate and bicarbonate solutions	1982
Echarte <i>et al.</i> [86]	12	Desorption	CO <sub>2</sub> from water Glycerol	1984
Linek <i>et al.</i> [26]	22	Absorption	Atmospheric O <sub>2</sub> in Degassed water	1984
Linek <i>et al.</i> [26]	22	Desorption	Of O <sub>2</sub> from water with N <sub>2</sub>	1984
Dharwadkar & Sawant [103]	23	Chemical Absorption	CO <sub>2</sub> into sodium carbonate and bicarbonate solutions	1985
Bornhutter & Mersmann [104]	24	Desorption	CO <sub>2</sub> from water into Air	1991

TABLE 9.2: SUMMARY OF EVALUATED LITERATURE CONTINUED.

Source	ID	Method	System evaluated	Date
Delaloye <i>et al.</i> [105]	25	Desorption	O <sub>2</sub> from water, glycerol, sodium alginate and polyethylene	1991
Schultes [50]	26	Desorption	CO <sub>2</sub> from water into air	1991
Linek <i>et al.</i> [18]	27	Desorption	Tetrachloroethylene, trichloroethylene, trichloromethane, chlorobenzene, bromobenzene and benzene from water into air	1996
Benadda <i>et al.</i>	28	Chemical Absorption	CO <sub>2</sub> into sodium carbonate and bicarbonate solutions at elevated pressures (1.3Mpa)	2000
Linek <i>et al.</i> [18, 11]	29	Absorption	O <sub>2</sub> into Water (using Air)	2005
Hoffman [28]	30	Absorption	NH <sub>3</sub> in water	2007
Wang <i>et al.</i> [53]	31	Stripping	Toluene from water	2012

TABLE 9.3: COLUMN INTERNALS RELATED TO THE LITERATURE EVALUATIONS.

ID	Name	Column Diameter(mm)	Column Height(m)	Nominal Packing Size(mm)	Packing Type	Material		
1	Sherwood & Halloway [23]	79	60-550	6	Raschig Rings	Ceramic		
2	Cooper <i>et al.</i> [90]	185	171	Structured packing	Sulzer BX	Metal Gauze		
3	Rixon [91]	150	1400	25	Tellerette®	Plastic		
4	Koch <i>et al.</i> [92]	300	700 and 1200	25	Pall Rings	Plastic		
				50	Raschig Rings	ceramic		
				25	I® Rings	Metal Gauze		
				25;35;50	Bialecki Rings	Inox		
5	Knoedler & Bonilla [93]	1000	No information given	50	Pall Rings	Plastic		
				number3	Envipak	Plastic		
				50,90-0,90-6	Hilflow®ring	Plastic		
				50	Hilflow®ring	Metal		
				number 2	Top-Pack®	Metal		
					Snowflake®	Metal		
6	Yoshida & Koyanagi [85]	Square column 762mm	2184	50	Raschig Rings	Metal		
7	Onda <i>et al.</i> [43]	76	1524	9.5	Raschig Rings	Ceramic		
					Raschig Rings	Plastic		
8	Vivian & King [94]	300	1000	25	Raschig Rings	Glass		
9	Vivian <i>et al.</i> [95]	385	1155	38	Pall Rings	Inox		
				38	Pall Rings	Plastic		
				50	Pall Rings	Steel		
				50	Pall Rings	Plastic		
				38	Intalox® saddles	Plastic		
10	Onda <i>et al.</i> [44]	400	330-900	25	Raschig Rings	Ceramic		
				58	Raschig Rings	Ceramic		
11	Couplin [96]	152	610		Stedman Triangular Packing	No information given		
12	Mohunta <i>et al.</i> [34] [33]	152	1323	9.5	Raschig Rings	Ceramic		
				254	1030	13	Raschig Rings	Ceramic
					1052	19	Raschig Rings	Ceramic
					1137	32	Raschig Rings	Ceramic
13	Sahay & Sharma [97]	300	700 and 1400	1024	32	Raschig Rings	Ceramic	
				25	Tellerettes®	Plastic		
14	Bereiter [98]	290	1000	15,25,35,50	Pall rings	Plastic		
15	Billet and Mackowiak [99] [37]	100	500	25	Raschig Rings	Glass		
16	Arwikar And Scandal [100]	100	600	4,6,9,5	Raschig Rings	Plastic		
				9.5	Raschig Rings	Ceramic		
				6	Berl saddles	Plastic		
					Spirals and flat plastic rings			

TABLE 9.4: TABLE 10.3 CONTINUED.

ID	Name	Column Diameter(mm)	Column Height(mm)	Nominal Packing Size(mm)	Packing Type	Material
26	Schultes [50]	120	406	13,25	Spheres	Ceramic
				15,25	Raschig Rings	Ceramic
				13,14	Berl saddles	Ceramic
27	Linek <i>et al.</i> [26]	62	1000	6.4	Berl saddles	No information given
28	Benadda <i>et al.</i>	290	1050	25	Pall Rings	hydrophilized polypropylene
				25	Pall Rings	nonhydrophilized polypropylene
29	Linek <i>et al.</i> [18, 11]	290	1050	25,40,50	Norton Intalox® saddles	Metal
				25,40,50	Intalox® saddles	Metal
30	Hoffman [28]	300	300	25,50	Pall Rings	Metal
31	Wang <i>et al</i> [53]	420	3050	12.5;25	Pall Rings	Plastic

#### 9.1.4. CHEMICAL REGRESSION

This section is set around evaluating feasible alternatives for oxygen absorption and desorption in an aqueous solution. The solutes were assessed according to their aqueous solubility and Henry's coefficients.

##### 9.1.4.1. REGRESSION APPROACH

A series resistance model was adopted to visualise mass transfer across a phase boundary. The subsequent resistance to mass transfer between the liquid and gas phases is mathematically expressed in Equation 9.1.

$$\frac{1}{K_{OL}} = \frac{1}{k_L} + \frac{H}{k_G} = R_{Total} = R_{gas} + R_{Liquid} \quad 9.1$$

In an attempt to ensure that the system remains liquid-side resistance limiting, the standard overall mass transfer equation was mathematically transposed to evaluate the fraction of liquid phase resistance:

$$\frac{R_{Liquid}}{R_{Total}} = \frac{100}{1 + \frac{1}{(k_G/k_L) \cdot H_c}} \quad 9.2$$

As an estimation of the lumped factor  $k_G/k_L$ , the Onda [19] correlations (Equations 4.12 and 4.13) were employed in modelling nine representing stripping and absorption systems. The systems were specifically chosen, as they were noted literature to be liquid be mass transfer limiting. From the definition of the mass transfer coefficient,  $k_g$  and  $k_l$  are expected to be functions of the hydrodynamic and physical properties of the system.

$$k_g; k_L = f(\rho_l, \rho_g, \sigma, \mu, D_{i,j}, G, L)$$

#### 9.1.4.2. *PHYSICAL PROPERTIES OF SYSTEMS EVALUATED*

In simulating the diffusivity parameters and mass phase transfer ratio, the following systems were used as they presented experimental proof of being liquid side mass transfer limiting [29, 30, 18]:

- Desorption of CO<sub>2</sub> in water with air [27]
- Adsorption of O<sub>2</sub> in water [26]
- Desorption CHCl<sub>3</sub> in water with Air [18]
- Desorption CHCl<sub>2</sub>Br in water with Air [18]
- Desorption CHClBr<sub>2</sub> in water with Air [18]
- Desorption CHBr<sub>3</sub> in water with Air [18]
- Desorption Benzene in water with Air [18]
- Desorption Toluene in water with Air [25]

#### 9.1.4.3. *HYDRODYNAMIC CONDITIONS OF SYSTEMS EVALUATED*

To estimate the hydrodynamic behaviour of packed columns (G/L), literature operating conditions were chosen, at the upper and lower limits of feasibility (6-120m<sup>3</sup>.m<sup>-2</sup>.h<sup>-1</sup>).

#### 9.1.4.4. RESULTS

The results of the lumped parameter modelling ( $k_G/k_L$ ) are presented in Table 9.5.

**TABLE 9.5: REGRESSION OF SYSTEMS EXPERIMENTALLY PROVEN TO EXHIBIT LIQUID PHASE MASS TRANSFER LIMITING BEHAVIOUR.**

Vapour Loading ( $\text{m}^3\cdot\text{m}^{-2}\cdot\text{s}^{-1}$ )	Liquid Loading ( $\text{m}^3\cdot\text{m}^{-2}\cdot\text{s}^{-1}$ )	$k_G/k_L$								
		Desorption: CO <sub>2</sub> / air	Absorption: O <sub>2</sub> /water	Desorption: CHCL <sub>3</sub> /Air	Desorption: CHCL <sub>2</sub> Br / Air	Desorption CHCLBr <sub>2</sub> /Air	Desorption CHBR <sub>3</sub> / Air	Desorption Benzene / Air	Desorption: Toluene/Air	Desorption: aniline /Air
0.91	24.5	5739.14	6732.22	5431.78	5388.50	5326.51	5253.22	5808.44	5785.44	4958.44
0.84	10.4	8180.09	9595.54	7742.01	7680.31	7591.95	7487.50	8278.86	8246.08	7067.34
0.58	15.6	5214.59	6116.90	4935.32	4895.99	4839.67	4773.08	5277.55	5256.65	4505.24
0.27	15.6	3063.38	3593.45	2899.32	2876.22	2843.13	2804.01	3100.37	3088.09	2646.66
2.03	3.1	26046.72	30553.74	24651.79	24455.35	24174.00	23841.40	26361.21	26256.84	22503.55
1.81	2.3	27318.63	32045.73	25855.58	25649.55	25354.46	25005.62	27648.48	27539.01	23602.44
0.54	91.7	2035.39	2387.58	1926.38	1911.03	1889.05	1863.06	2059.96	2051.81	1758.51
3.5	6	28491.28	33421.28	26965.43	26750.54	26442.79	26078.98	28835.28	28721.11	24615.56
0.6	120	1896.33	2224.47	1794.77	1780.47	1759.99	1735.77	1919.23	1911.63	1638.37
0.2	120	1427.74	1674.80	1351.28	1340.51	1325.09	1306.86	1444.98	1439.26	<b><u>1233.53</u></b>

From the data presented above, it was deduced that the vapour phase resistance would likely become relevant at high liquid and low vapour loadings. This transition point was chosen to be at a  $k_G/k_L$  of 1233.



From the analysis, it was deduced, that the operating conditions largely affect the controlling resistance. As industrial columns are rarely expected to operate under a gas flow factors of 0.5, it was decided to limit the evaluation to  $F > 0.5$ . It should be noted that according to Fair & Stichlmair, the Onda (1968) correlations are expected to provide an underestimation of up to 30% of the true mass transfer coefficients. This, in combination with better wetting for decreased surface tension, acts as a built-in safety factor for the regression.

Solving Equation 9.2 with the lumped factor (1200) and a 95% confidence interval, yields a critical Henry's volatility constant (dimensionless concentration) of **0.01583** (Equilibrium constant  $y/x = 19.7$ ). This suggests that all solutes with a Henry's coefficient larger or equal to **0.01583**, will be liquid side mass transfer limiting (under hydrodynamic conditions suited for stripping).

The subsequent regression may be used as an alternative to the inferred rule of thumb often used. It states that desorption columns are operated at stripping factors ( $K.G_m/L_m$ ) above one (preferably 1.4). Under these conditions, liquid-side resistance is expected to be dominant, as the system is expected to operate far from equilibrium. Although this thumb rule may be adequate for designing strippers, it fails to quantify the minimum gas flow rate at which a system transitions for gas to liquid side resistance limiting. This subsequently hampers its ability to predicting whether a system is governed by gas or liquid side resistance.

Using the regression, although imperfect, may provide an alternative approach of choosing a solute. The project objectives require that the system be liquid phase resistance limiting. This may be affirmed through the regression, and selection of any solute above the critical limit. Alternatively, choosing from the projected critical Henry's volatility constant upward, may be useful in selecting the least volatile component, while still meeting the other standards.

## 9.1.4.5. CHEMICALS EVALUATED

A list of the evaluated chemical is depicted in Table 9.6. As a result of special constraints, no environmental data are included.

TABLE 9.6: EVALUATED CHEMICALS.

Name	Solubility in water (ppm)	Ref	Hc	Ref	Boiling temperature (C)	K	K.G <sub>m</sub> /L <sub>m</sub> @ L=120 m <sup>3</sup> /m <sup>2</sup> /h +F=0.5
4-Methyloctane	0.115	[106]	403.621	[107]	Not yet sourced	546756.13	5163.87
Dodecane	0.0037	[106]	302.716	[107]	216.35	410067.10	3872.90
Isopentane	48.5	[108]	193.334	[109]	27.85	261896.19	2473.49
Decane	0.015	[106]	193.334	[109]	174.15	261896.19	2473.49
3-Methylheptane	0.79	[106]	151.761	[107]	Not yet sourced	205580.30	1941.62
2-Methylhexane	2.5	[108]	139.653	[107]	90.05	189177.62	1786.70
Nonane	0.17	[106]	134.406	[109]	150.85	182069.79	1719.57
2,4-Dimethylpentane	4.2	[108]	130.370	[109]	Not yet sourced	176602.23	1667.93
2,2-Dimethylpentane	4.4	[108]	128.351	[107]	Not yet sourced	173868.45	1642.11
Octane	0.71	[106]	125.526	[109]	125.65	170041.16	1605.96
2,2,4-Trimethylpentane	2.2	[106]	123.912	[109]	99.25	167854.13	1585.31
Helium	-	-	105.000	[110]	-269.00	142235.91	1343.36
Chloropentafluoroethane	60	[111]	104.941	[109]	Not yet sourced	142156.59	1342.61
3-Methylhexane	2.6	[108]	100.502	[109]	91.85	136142.28	1285.80
2,2,5-Trimethylhexane	0.8	[106]	99.291	[109]	Not yet sourced	134502.01	1270.31
Neopentane	33.2	[108]	88.797	[109]	9.45	120286.35	1136.05
Heptane	2.4	[108]	84.357	[107]	98.45	114272.03	1079.25
2,3,4-Trimethylpentane	1.8	[106]	83.146	[109]	Not yet sourced	112631.76	1063.76
2,2-Dimethylbutane	21	[108]	80.321	[109]	49.75	108804.47	1027.61
3,3-Dimethylpentane	5.9	[108]	75.073	[107]	Not yet sourced	101696.64	960.48
Pentylcyclopentane	0.115	[106]	74.670	[107]	Not yet sourced	101149.88	955.32
Hexane	11	[108]	73.863	[109]	68.75	100056.37	944.99
2-Methylpentane	13.7	[108]	71.037	[109]	60.25	96229.08	908.84
2,3-Dimethylpentane	5.2	[108]	70.634	[107]	89.75	95682.32	903.68
3-Methylpentane	12.9	[108]	68.616	[109]	Not yet sourced	92948.54	877.86
1,1,3-Trimethylcyclopentane	3.7	[106]	64.176	[107]	Not yet sourced	86934.22	821.06
Nitrogen	1.75	[68]	62.300	[110]	-196.00	84393.30	797.06
2,3-Dimethylbutane	21	[108]	58.121	[109]	57.95	78732.88	743.60
Hydrogen	-	-	52.100	[110]	-253.00	70576.10	666.56
Pentane	41	[108]	51.663	[109]	36.05	69984.78	660.98
1,2-Dichlorotetrafluoroethane	130	[111]	51.260	[109]	Not yet sourced	69438.03	655.81
Isobutane	53.5	[112]	48.435	[107]	-11.75	65610.74	619.66
1,1,3-Trimethylcyclohexane	1.77	[106]	42.380	[109]	Not yet sourced	57409.39	542.21
1-Octene	2.7	[106]	38.869	[109]	121.25	52652.62	497.28
Butane	72.4	[112]	38.707	[107]	-0.55	52433.91	495.22
Propylcyclopentane	2	[106]	36.407	[107]	130.95	49317.40	465.78
trans-1,4-Dimethylcyclohexane	3.84	[106]	35.599	[107]	119.35	48223.89	455.45

TABLE 9.6 CONTINUED.

Name	Solubility in water (ppm)	Ref	Hc	Ref	Boiling temperature (C)	K	K.G <sub>m</sub> /L <sub>m</sub> @ L=120 m <sup>3</sup> /m <sup>2</sup> /h +F=0.5
Oxygen	0.08	[106]	31.900	[68]	-183.00	43212.62	408.12
Propane	66.9	[112]	28.899	[107]	-42.05	39147.74	369.73
Methane	22.7	[112]	27.204	[107]	Not yet sourced	36851.36	348.04
4-Methyl-1-pentene	48	[108]	25.509	[107]	53.85	34554.99	326.36
3-Methyl-1-butene	130	[108]	22.078	[107]	20.05	29907.56	282.46
Ethane	56.8	[112]	20.423	[107]	Not yet sourced	27665.86	261.29
Methylcyclohexane	15.1	[108]	17.477	[109]	100.95	23674.54	223.60
trans-2-Heptene	150	[108]	17.033	[109]	Not yet sourced	23073.11	217.92
1-Hexene	53	[108]	16.871	[107]	63.45	22854.41	215.85
Dichlorodifluoromethane	280	[113]	16.548	[109]	Not yet sourced	22417.00	211.72
1-Pentene	148	[108]	16.266	[107]	29.95	22034.27	208.10
1-Heptene	320;18.2 source variance	[108]	16.266	[109]	93.65	22034.27	208.10
Methylcyclopentane	43	[108]	14.813	[107]	71.85	20065.95	189.51
cis-1,2-Dimethylcyclohexane	6	[106]	14.530	[107]	129.75	19683.22	185.90
1,1,2-Trichlorotrifluoroethane	170	[111]	12.916	[109]	Not yet sourced	17496.20	165.24
2-Methyl-1-pentene	78	[108]	11.342	[107]	61.85	15363.85	145.10
1-Butene	222	[113]	10.333	[109]	-6.25	13996.96	132.20
cis-2-Pentene	203	[108]	9.203	[107]	37.00	12466.04	117.74
Ethylene	133.6	[114]	8.759	[107]	Not yet sourced	11864.61	112.06
Isobutene	263	[113]	8.718	[109]	-6.85	11809.93	111.54
Propene	200	[113]	8.597	[107]	Not yet sourced	11645.91	109.99
1,3-Butadiene	735	[113]	8.355	[109]	-4.45	11317.85	106.89
Cyclohexane	58	[108]	7.830	[109]	80.75	10607.07	100.18
Cyclopentane	157	[108]	7.709	[109]	49.25	10443.04	98.63
1,5-Hexadiene	170	[108]	5.500	0.00	59.45	7450.45	70.37
1,4-Pentadiene	560	[108]	4.843	[107]	26.00	6561.07	61.97
2,3-Dimethyl-1,3-butadiene	128	[113]	4.610	[68]	69		
Cyclooctane	7.9	[106]	4.319	[109]	Not yet sourced	5850.29	55.25
Trichlorofluoromethane	1100	[113]	4.117	[109]	Not yet sourced	5576.91	52.67
Cycloheptane	30	[108]	3.871	[109]	Not yet sourced	5243.39	49.52
1-Octyne	24	[106]	3.176	[109]	Not yet sourced	4302.97	40.64
2-Methyl-1,3-butadiene	610	[108]	3.140	[107]	34.00	4253.76	40.17
Chlorotrifluoromethane	90	[111]	2.785	[109]	Not yet sourced	3772.62	35.63
Cyclopentene	540	[108]	2.648	[109]	44.25	3586.72	33.87
Cycloheptene	66	[108]	1.978	[109]	Not yet sourced	2679.11	25.30
Cyclohexene	160	[108]	1.845	[109]	82.95	2498.68	23.60
1-Heptyne	94	[108]	1.804	[109]	Not yet sourced	2444.00	23.08
1-Hexyne	360	[108]	1.671	[109]	Not yet sourced	2263.57	21.38
1-Bromopropane	2300	[111]	1.534	[109]	70.95	2077.67	19.62
Isobutylbenzene	10	[106]	1.340	[115]	172.75	1815.23	17.14

TABLE 9.6 CONTINUED

Name	Solubility in water (ppm)	Ref	Hc	Ref	Boiling temperature (C)	K	K.G <sub>m</sub> /L <sub>m</sub> @ L=120 m <sup>3</sup> /m <sup>2</sup> /h +F=0.5
Carbon disulfide	2100	[111]	1.240	[68]	46.30	1679.74	15.86
Chlorodifluoromethane	3000	[111]	1.211	[109]	Not yet sourced	1640.27	15.49
trans-Decahydronaphthalene	0.89	[106]	1.211	[109]	Not yet sourced	1640.27	15.49
Tetrachloromethane	650	[116]	1.207	[109]	Not yet sourced	1634.80	15.44
Carbon dioxide	1501	[112]	1.200	[68]	-78.50	1625.55	15.35
Chloroethylene	2700	[113]	1.082	[109]	Not yet sourced	1465.31	13.84
1,1-Dichloroethylene	400	[113]	1.057	[109]	Not yet sourced	1432.50	13.53
1,2,4,5-Tetramethylbenzene	3.48	[106]	1.029	[115]	Not yet sourced	1394.23	13.17
1-Pentyne	1570	[108]	1.009	[107]	40.20	1366.89	12.91
Acetylene	1081	[114]	0.969	[68]	-84.00	1312.63	12.40
1-Chloropentane	200	[111]	0.957	[109]	108.35	1295.81	12.24
1-Butyne	2870	[113]	0.771	[107]	Not yet sourced	1044.30	9.86
sec-Butylbenzene	14	[106]	0.763	[115]	173.65	1033.37	9.76
1-Iodobutane	120	[111]	0.755	[109]	129.95	1022.43	9.66
1,1,1-Trichloroethane	720	[113]	0.710	[109]	74.05	962.29	9.09
Tetrachloroethylene	260	[116]	0.698	[109]	Not yet sourced	945.89	8.93
Pentylbenzene	10.5	[113]	0.682	[115]	Not yet sourced	924.02	8.73
1-Chlorobutane	1100	[111]	0.622	[109]	78.00	842.00	7.95
Isopropylbenzene	56	[106]	0.593	[115]	Not yet sourced	803.73	7.59
1-Chloropropane	2710	[111]	0.569	[109]	Not yet sourced	770.93	7.28
Butylbenzene	15	[106]	0.537	[115]	183.35	727.19	6.87
tert-Butylbenzene	32	[106]	0.517	[115]	Not yet sourced	699.85	6.61
2-Bromopropane	2860	[111]	0.513	[109]	59.45	694.38	6.56
Bromoethane	9100	[111]	0.496	[109]	38.35	672.51	6.35
1-Bromobutane	608	[111]	0.484	[109]	101.65	656.11	6.20
Propyne	3640	[113]	0.448	[107]	Not yet sourced	606.90	5.73
3-Chloropropene	3300	[113]	0.444	[107]	44.95	601.43	5.68
1,3,5-Trichlorobenzene	6.55	[113]	0.444	[115]	Not yet sourced	601.43	5.68
Propylbenzene	55	[106]	0.420	[115]	159.25	568.63	5.37
Trichloroethylene	1100	[113]	0.416	[109]	Not yet sourced	563.16	5.32
1,4-Cyclohexadiene	800	[108]	0.416	[109]	Not yet sourced	563.16	5.32
Chloroethane	5700	[113]	0.412	[109]	Not yet sourced	557.69	5.27
Chloromethane	5350	[113]	0.396	[109]	Not yet sourced	535.82	5.06
trans-1,2-Dichloroethylene	6300	[113]	0.387	[109]	Not yet sourced	524.89	4.96
1-Iodopropane	1040	[111]	0.375	[109]	Not yet sourced	508.48	4.80
Ethylbenzene	169	[106]	0.358	[68]	136.25	484.97	4.58
Hexachloroethane	50	[113]	0.343	[109]	Not yet sourced	464.74	4.39
2,2,4,4,6,6-Hexachlorobiphenyl	0.0007	[117]	0.330	[118]	Not yet sourced	447.25	4.22
p-Cymene	23.4	[106]	0.323	[107]	177.15	437.40	4.13

TABLE 9.6 CONTINUED

Name	Solubility in water (ppm)	Ref	Hc	Ref	Boiling temperature (C)	K	K <sub>m</sub> G <sub>m</sub> /L <sub>m</sub> @ L=120 m <sup>3</sup> /m <sup>2</sup> /h +F=0.5
1,3,5-Trimethylbenzene	48.9	[106]	0.315	[115]	Not yet sourced	427.02	4.03
m-Xylene	160	[106]	0.295	0.00	139.15	399.13	3.77
Fluorobenzene	1540	[119]	0.283	[115]	84.95	382.73	3.61
Toluene	530	[108]	0.274	0.00	110.65	371.79	3.51
Bromomethane	18000	[113]	0.254	[109]	Not yet sourced	344.46	3.25
1,1-Dichloroethane	5100	[113]	0.254	[109]	57.25	344.46	3.25
1,2,3,5-Tetrachlorobenzene	3.46	[119]	0.238	[115]	Not yet sourced	322.59	3.05
p-Xylene	180	[106]	0.233	[68]	138.35	316.03	2.98
1,2,4-Trimethylbenzene	56	[106]	0.230	[115]	169.35	311.10	2.94
o-Xylene	173	[106]	0.228	[109]	144.45	308.92	2.92
Benzene	1770	[108]	0.225	[115]	80.05	304.54	2.88
Iodomethane	14000	[111]	0.218	[109]	Not yet sourced	295.25	2.79
Furan	10000	[111]	0.218	[109]	Not yet sourced	295.25	2.79
o-Ethyltoluene	93	[113]	0.214	[109]	165.15	289.23	2.73
Iodoethane	38800	[111]	0.210	[109]	Not yet sourced	284.31	2.69
p-Ethyltoluene	94	[113]	0.202	[109]	162.05	273.38	2.58
Dibutyl ether	300	[111]	0.194	[109]	Not yet sourced	262.44	2.48
1,3,5-Cycloheptatriene	640	[108]	0.190	[109]	Not yet sourced	256.98	2.43
cis-1,2-Dichloroethylene	3500	[113]	0.186	[109]	Not yet sourced	251.51	2.38
1-Butanethiol	597	[111]	0.185	[68]	Not yet sourced	250.61	2.37
Trichloromethane	8000	[116]	0.174	[109]	Not yet sourced	235.11	2.22
Chlorobenzene	495	[119]	0.153	[115]	131.75	207.77	1.96
m-Dichlorobenzene	106	[119]	0.152	[115]	173.05	205.58	1.94
2,3-Dichloropropene	2150	[113]	0.145	[107]	Not yet sourced	196.83	1.86
1,2,3-Trimethylbenzene	69	[106]	0.138	[115]	176.15	187.54	1.77
Dichloromethane	17300	[116]	0.121	[109]	39.75	164.03	1.55
Styrene	250	[106]	0.121	[109]	145.15	164.03	1.55
1,2-Dichloropropane	2470	[111]	0.117	[109]	96.35	158.56	1.50
1,2,4-Trichlorobenzene	37.9	[119]	0.112	[115]	213.05	151.45	1.43
Dipropyl ether	4900	[111]	0.105	[109]	Not yet sourced	142.16	1.34
Diisopropyl ether	12000	[111]	0.105	[109]	68.25	142.16	1.34
Pentachloroethane	480	[113]	0.101	[109]	159.85	136.69	1.29
o-Dichlorobenzene	147	[119]	0.098	[115]	180.45	133.41	1.26
1,2,3-Trichlorobenzene	30.9	[119]	0.098	[115]	Not yet sourced	132.31	1.25
1,1,1,2-Tetrachloroethane	1100	[113]	0.097	[109]	130.55	131.22	1.24
cis-1,3-Dichloropropene	2700	[113]	0.097	[107]	Not yet sourced	131.22	1.24
Bromobenzene	445	[119]	0.085	[107]	156.05	114.82	1.08
Bromochloromethane	17000	[111]	0.073	[109]	Not yet sourced	98.42	0.93
trans-1,3-Dichloropropene	2800	[113]	0.073	[107]	Not yet sourced	98.42	0.93
p-Dichlorobenzene	82.9	[119]	0.065	[115]	174.05	87.48	0.83

Cut-off  
from  
rule of  
thumb

TABLE 9.6 CONTINUED

Name	Solubility in water (ppm)	Ref	Hc	Ref	Boiling temperature (C)	K	K.G <sub>m</sub> /L <sub>m</sub> @ L=120 m <sup>3</sup> /m <sup>2</sup> /h +F=0.5
1,2,3,4-Tetrachlorobenzene	0.433	[119]	0.058	[115]	Not yet sourced	78.73	0.74
1,2-Dichloroethane	7500	[116]	0.057	[109]	83.45	76.55	0.72
Hexachlorobenzene	0.005	[119]	0.053	[115]	309.45	71.63	0.68
1,2,4,5-Tetrachlorobenzene	0.606	[119]	0.049	[115]	Not yet sourced	66.70	0.63
1-Chloro-2-methylpropene	9160	[113]	0.048	[107]	Not yet sourced	65.61	0.62
1,1,2-Trichloroethane	4420	[113]	0.037	[109]	113.85	50.30	0.48
Diethyl ether	60400	[111]	0.036	[109]	35.45	48.11	0.45
Dibromomethane	11400	[120]	0.035	[109]	96.95	47.02	0.44
Pentachlorobenzene	0.55	[119]	0.034	[115]	Not yet sourced	46.47	0.44
Iodobenzene	226	[119]	0.031	[115]	187.95	42.65	0.40
2-Ethynaphthalene	8	[106]	0.031	[121]	Not yet sourced	42.65	0.40
Dimethyl ether	353000	[111]	0.031	[109]	-24.85	42.10	0.40
Ethyl hexanoate	629	[113]	0.030	[68]	Not yet sourced	40.10	0.38
2-Chlorobiphenyl	5.5	[117]	0.028	[118]	Not yet sourced	38.33	0.36
Methyl tert-butyl ether	36200	[116]	0.028	[109]	55.25	38.27	0.36
1,2-Dibromoethane	1700	[113]	0.027	[109]	131.35	36.09	0.34
Vinyl acetate	20000	[111]	0.024	[68]	Not yet sourced	32.38	0.31
Isobutyl formate	10000	[111]	0.024	[68]	98.05	32.38	0.31
Hexyl acetate	200	[111]	0.021	[68]	Not yet sourced	28.99	0.27
2-Methylnaphthalene	25	[106]	0.021	[121]	Not yet sourced	27.88	0.26
2,4,6-Trichlorobiphenyl	0.2	[117]	0.020	[118]	Not yet sourced	27.06	0.26
Tribromomethane	3000	[113]	0.019	[109]	Not yet sourced	25.70	0.24
Isobutyl acetate	6300	[111]	0.019	[68]	116.65	25.06	0.24
1-Decanol	37	[122]	0.018	[68]	230.25	24.60	0.23
1-Methylnaphthalene	28	[106]	0.018	[121]	Not yet sourced	24.60	0.23
Naphthalene	31	[106]	0.017	[68]	Not yet sourced	23.51	0.22
trans-Stilbene	0.29	[106]	0.016	[121]	Not yet sourced	21.87	0.21
1-Ethynaphthalene	10.1	[106]	0.016	[121]	Not yet sourced	21.32	0.20
2,2,3,3,5,5,6,6-Octachlorobiphenyl	0.003	[117]	0.015	[118]	Not yet sourced	20.83	0.20
1,2,3-Trichloropropane	1900	[111]	0.015	[109]	156.85	20.78	0.20
Propyl formate	20500	[111]	0.015	[68]	Not yet sourced	20.45	0.19
2,2,4,5,5-Pentachlorobiphenyl	0.01	[117]	0.014	[118]	Not yet sourced	19.41	0.18
Diiodomethane	1240	[111]	0.013	[109]	Not yet sourced	17.50	0.17
Ethyl formate	118000	[111]	0.011	[68]	54.35	15.31	0.14
Isopropyl acetate	29000	[111]	0.011	[68]	88.45	15.31	0.14
Diphenyl ether	18	[123]	0.011	[109]	258.35	14.76	0.14
1,1,2,2-Tetrachloroethane	3000	[113]	0.010	[109]	145.15	14.22	0.13
Anisole	1900	[116]	0.010	[109]	153.70	13.67	0.13
2,4,5-Trichlorobiphenyl	0.14	[117]	0.010	[118]	Not yet sourced	13.29	0.13
Methyl formate	230000	[111]	0.009	[68]	31.75	12.25	0.12

Cut-off  
from  
regression

TABLE 9.6 CONTINUED

Name	Solubility in water (ppm)	Ref	Hc	Ref	Boiling temperature (C)	K	$K_m G_m / L_m @$ $L=120 \text{ m}^3/\text{m}^2/\text{h}$ $+F=0.5$
Ethyl propanoate	19200	[111]	0.009	[68]	Not yet sourced	11.99	0.11
Decachlorobiphenyl	0.0000012	[117]	0.008	[118]	Not yet sourced	11.37	0.11
2,5-Dichlorobiphenyl	2	[117]	0.008	[118]	Not yet sourced	10.99	0.10
1,2-Diphenylethane	4.4	[123]	0.007	[121]	Not yet sourced	9.29	0.09
2,2,3,3,4,4-Hexachlorobiphenyl	0.0006	[117]	0.005	[118]	Not yet sourced	6.51	0.06
Dibenzofuran	6.56	[123]	0.004	[121]	Not yet sourced	6.01	0.06
Butanal	71000	[111]	0.004	[68]	Not yet sourced	5.74	0.05
1,1-Diethoxyethane	50000	[111]	0.004	[68]	Not yet sourced	5.51	0.05
2-Methyltetrahydrofuran	139000	[111]	0.004	[68]	Not yet sourced	5.04	0.05
Methyl acetate	245000	[111]	0.004	[68]	56.95	5.01	0.05
Methyloxirane	405000	[111]	0.004	[109]	Not yet sourced	4.76	0.04
Propanal	306000	[111]	0.003	[68]	Not yet sourced	4.24	0.04
Chrysene	0.0019	[106]	0.002	[121]	Not yet sourced	3.28	0.03
2-Methylpropanoic acid	228000	[111]	0.002	[68]	Not yet sourced	3.06	0.03
2,2,3,3,4,4,6-Heptachlorobiphenyl	0.002	[117]	0.002	[118]	Not yet sourced	2.95	0.03
Phenanthrene	0.5	[106]	0.001	[68]	Not yet sourced	1.75	0.02
Epichlorohydrin	65800	[111]	0.001	[109]	Not yet sourced	1.64	0.02
Bis(2-chloroethyl) ether	10300	[116]	0.001	[109]	Not yet sourced	1.64	0.02
Nitrobenzene	2100	[124]	0.001	[68]	210.90	1.33	0.01
trans-2-Butenal	156000	[111]	0.001	[68]	Not yet sourced	1.06	0.01
9H-Fluorene	1.41	[106]	0.000	[68]	Not yet sourced	0.55	0.01
Diphenylmethane	1.41	[106]	0.000	[121]	264.25	0.55	0.01
Fluoranthene	0.24	[106]	0.000	[121]	Not yet sourced	0.55	0.01
Pyrene	0.132	[106]	0.000	[121]	Not yet sourced	0.50	0.00
2,4,6-Trichlorophenol	400	[119]	0.000	[68]	Not yet sourced	0.43	0.00
Benz[a]anthracene	0.011	[106]	0.000	[121]	Not yet sourced	0.32	0.00
N-Nitrosodiphenylamine	35	[124]	0.000	[68]	Not yet sourced	0.28	0.00
2,4,5-Trichlorophenol	1000	[119]	0.000	[68]	Not yet sourced	0.24	0.00
2,4-Dichlorophenol	4500	[119]	0.000	[68]	Not yet sourced	0.18	0.00
Aniline	33800	[111]	0.000	[68]	184.45	0.11	0.00
Benzo[ghi]perylene	0.00026	[106]	0.000	[121]	Not yet sourced	0.04	0.00
Benzo[a]pyrene	0.0038	[106]	0.000	[121]	Not yet sourced	0.03	0.00
Phenol	86600	[111]	0.000	[68]	181.85	0.02	0.00
Methacrylic acid	89000	[111]	0.000	[68]	161.05	0.02	0.00
Benzo[e]pyrene	0.0046	[106]	0.000	[121]	Not yet sourced	0.01	0.00
Triphenylene	0.041	[106]	0.000	[121]	Not yet sourced	0.01	0.00
Naphthacene	0.0006	[106]	0.000	[121]	Not yet sourced	0.00	0.00

TABLE 9.6 CONTINUED

Name	Solubility in water (ppm)	Ref	Hc	Ref	Boiling temperature (C)	K	$K.G_m/L_m @$ $L=120 \text{ m}^3/\text{m}^2/\text{h}$ $+F=0.5$
Perylene	0.0004	[106]	0.000	[121]	Not yet sourced	0.00	0.00
Pentachlorophenol	10	[119]	0.000	[68]	Not yet sourced	0.00	0.00
Carbazole	1.2	[123]	0.000	[68]	Not yet sourced	0.00	0.00
Bromotrifluoromethane	320	[120]	0.000	[68]	Not yet sourced	0.00	0.00
Tribromofluoromethane	400	[120]	0.000	[68]	Not yet sourced	0.00	0.00
Tetrabromomethane	240	[120]	0.000	[68]	Not yet sourced	0.00	0.00
Tetrafluoromethane	18.7	[114]	0.000	[68]	Not yet sourced	0.00	0.00
Dichlorofluoromethane	9500	[111]	0.000	[68]	Not yet sourced	0.00	0.00
Trifluoromethane	900	[120]	0.000	[68]	Not yet sourced	0.00	0.00
Triiodomethane	120	[120]	0.000	[68]	Not yet sourced	0.00	0.00
Chlorofluoromethane	10500	[120]	0.000	[68]	Not yet sourced	0.00	0.00
Fluoromethane	1770	[113]	0.000	[68]	Not yet sourced	0.00	0.00
Nitromethane	111000	[111]	0.000	[68]	101.25	0.00	0.00
Carbon monoxide	27.6	[112]	0.000	[68]	Not yet sourced	0.00	0.00
1,1,2,2-Tetrachloro-1,2-difluoroethane	120	[111]	0.000	[68]	Not yet sourced	0.00	0.00
Tetrafluoroethylene	158	[114]	0.000	[68]	Not yet sourced	0.00	0.00
1,1,2,2-Tetrabromoethane	651	[111]	0.000	[68]	243.55	0.00	0.00
1-Bromo-2-chloroethane	6830	[111]	0.000	[68]	Not yet sourced	0.00	0.00
Fluoroethane	2160	[120]	0.000	[68]	Not yet sourced	0.00	0.00
Acetamide	408000	[111]	0.000	[68]	Not yet sourced	0.00	0.00
Nitroethane	46800	[111]	0.000	[68]	114.05	0.00	0.00
Dimethyl sulfide	20000	[111]	0.000	[68]	37.35	0.00	0.00
Hexachloropropene	17	[120]	0.000	[68]	Not yet sourced	0.00	0.00
Perfluoropropene	194	[120]	0.000	[68]	Not yet sourced	0.00	0.00
Perfluoropropane	15	[120]	0.000	[68]	Not yet sourced	0.00	0.00
2-Propenenitrile	73500	[111]	0.000	[68]	Not yet sourced	0.00	0.00
Acrolein	208000	[111]	0.000	[68]	Not yet sourced	0.00	0.00
Propanenitrile	103000	[111]	0.000	[68]	Not yet sourced	0.00	0.00
Cyclopropane	484	[114]	0.000	[68]	Not yet sourced	0.00	0.00
1,2-Dibromopropane	1430	[111]	0.000	[68]	Not yet sourced	0.00	0.00
Hexahydro-1,3,5-trinitro-1,3,5-triazine	60	[124]	0.000	[68]	Not yet sourced	0.00	0.00
2-Chloropropane	3420	[111]	0.000	[68]	Not yet sourced	0.00	0.00
1-Fluoropropane	3860	[120]	0.000	[68]	Not yet sourced	0.00	0.00
2-Fluoropropane	3660	[120]	0.000	[68]	Not yet sourced	0.00	0.00
2-Iodopropane	1400	[111]	0.000	[68]	Not yet sourced	0.00	0.00
1-Nitropropane	15000	[111]	0.000	[68]	131.15	0.00	0.00
2-Nitropropane	17100	[111]	0.000	[68]	120.25	0.00	0.00



TABLE 9.6 CONTINUED

Name	Solubility in water (ppm)	Ref	Hc	Ref	Boiling temperature (C)	K	$K.G_m/L_m @$ $L=120 \text{ m}^3/\text{m}^2/\text{h}$ $+F=0.5$
Dimethoxymethane	244000	[111]	0.000	[68]	Not yet sourced	0.00	0.00
Perfluorocyclobutane	140	[120]	0.000	[68]	Not yet sourced	0.00	0.00
Succinonitrile	115000	[111]	0.000	[68]	Not yet sourced	0.00	0.00
Methylacrylonitrile	25700	[111]	0.000	[68]	Not yet sourced	0.00	0.00
Pyrrole	45000	[111]	0.000	[68]	129.75	0.00	0.00
trans-Crotonic acid	90000	[111]	0.000	[68]	Not yet sourced	0.00	0.00
Methyl acrylate	49400	[111]	0.000	[68]	80.25	0.00	0.00
Butanenitrile	33000	[111]	0.000	[68]	Not yet sourced	0.00	0.00
cis-Crotonyl alcohol	166000	[111]	0.000	[68]	Not yet sourced	0.00	0.00
Ethyl vinyl ether	9000	[111]	0.000	[68]	35.55	0.00	0.00
Isobutanal	91000	[111]	0.000	[68]	Not yet sourced	0.00	0.00
2-Butanone	259000	[116]	0.000	[68]	79.60	0.00	0.00
Ethyl acetate	80800	[111]	0.000	[68]	77.05	0.00	0.00
1-Chloro-2-methylpropane	920	[111]	0.000	[68]	Not yet sourced	0.00	0.00
1-Butanol	74000	[122]	0.000	[68]	117.65	0.00	0.00
2-Butanol	181000	[122]	0.000	[68]	99.55	0.00	0.00
2-Methyl-1-propanol	81000	[122]	0.000	[68]	107.65	0.00	0.00
Diethanolamine	954000	[111]	0.000	[68]	Not yet sourced	0.00	0.00
Tetramethylsilane	19.6	[111]	0.000	[68]	Not yet sourced	0.00	0.00

### 9.1.5. PACKED COLUMN DESIGN: MECHANICAL DESIGN

The design of the packed column stripping unit was centred around increasing the size of the testing column section, while taking various precautionary measures to assure easy assembly and operation. As previously stated, this report will refrain from providing the mechanical sketches, in favour of presenting them in the attached CD. Consequently, a short discussing of the most notable consideration is provided as follows.

#### 9.1.5.1. CHIMNEY VAPOUR DISTRIBUTOR:

The chimney vapour distributor was designed according to similar considerations to those presented by Lamprecht on the hydrodynamic plant. Alterations to the original design included additional flow restrictors to limit liquid leaking into the humidification section. The original design used bended stainless hoods, to capture and direct the falling liquid. This was found to induce liquid leakage into the succeeding section at aqueous surface tensions, as the liquid bended with the perceived slope. An illustration of this behaviour, based on visual interpretation, is presented in Figure 9.1.

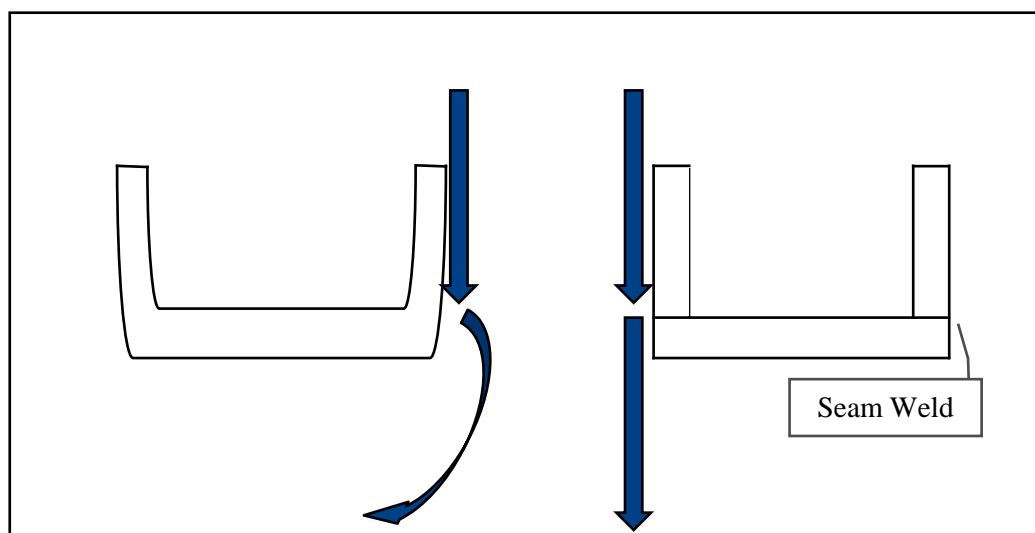
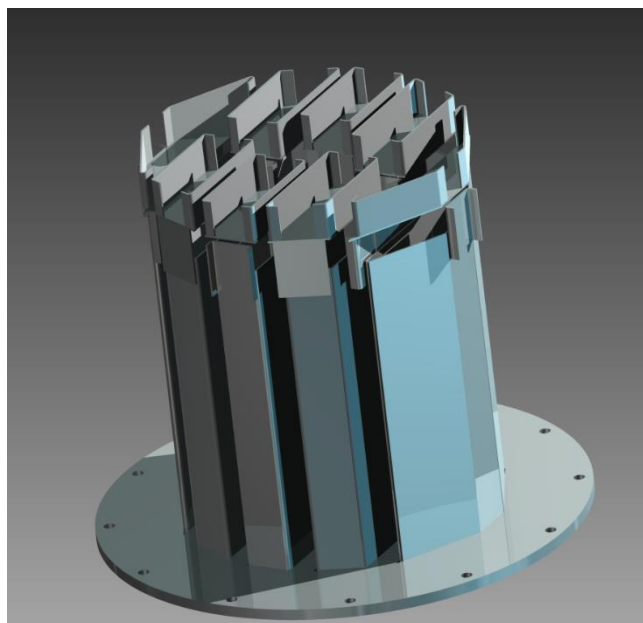


FIGURE 9.1: AQUEOUS HOOD BEHAVIOUR.

A solution was found in producing two-piece seam welded hoods. The seams were grinded down to a smooth finish, to inhibit the bending of liquid. This limited the stripping solution from leaking into the humidification column. The improved design also sported an 40% increased liquid capacity, to act as buffer in the event of a downstream disruption. An illustration of the chimney distributor is presented in Figure 9.2



**FIGURE 9.2: CHIMNEY VAPOUR DISTRIBUTOR.**

#### *9.1.5.2. LIQUID SAMPLING SECTION.*

Liquid sampling was done by way of a 1' stainless halfpipe, drawing and recirculating liquid 50mm from the bottom of the packing. This allowed for constant replenishment of liquid at the inlet of the sampling pump. Although not included in the graphic (Figure 9.3), the inlet was situated at the lowest point of the flexible circulating tube in the form of a deaerating water trap. The subsequent trap allowed sufficient time for any bubbles captured in the sampling pipe, to be removed before UV-Quantification.

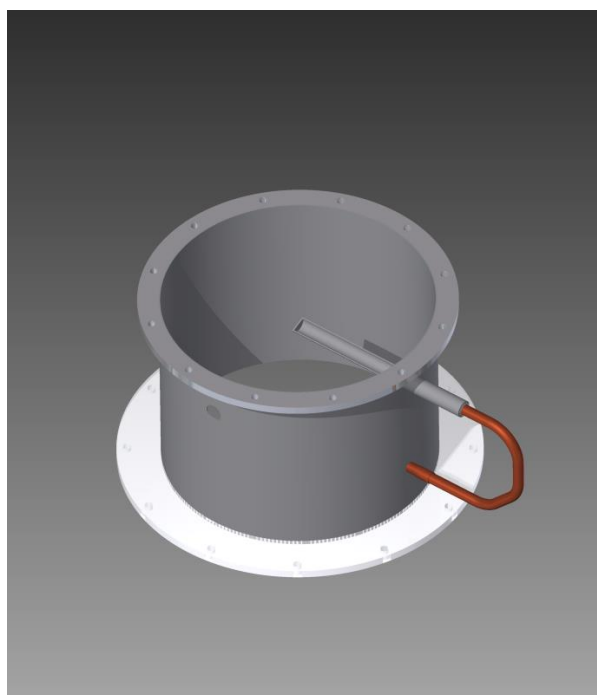


**FIGURE 9.3: LIQUID SAMPLING.**

The proceeding sampling technique, provided an average liquid composition, as the sample was averaged across the radial distance. Various radial lengths were evaluated, from 280 to 120mm, providing comparative results. This led this report to believe that the liquid was well distributed, mitigating any radial concentration profiles.

A slightly smaller flange was used on the top half of sample section, for attachment to the succeeding holdup grid. This was done in designing for easy disassembly, so as to limit the need for unpacking atop the rig. The variable flange size design, offered the user the option of removing the testing section of the column (with a crane), without having to empty the packing. The benefits of this design consideration, sizably improved the turnaround times, decreasing this to within 1hour.

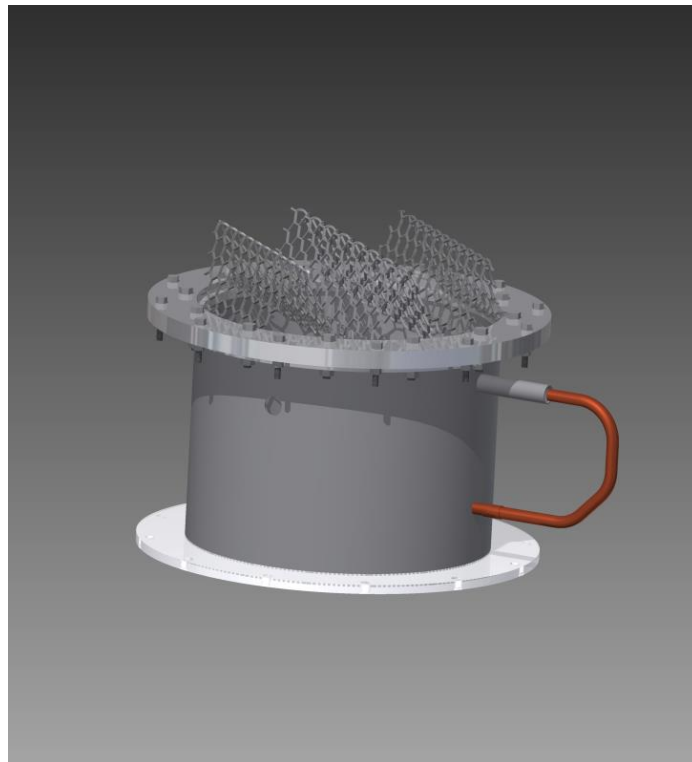


**FIGURE 9.4: HOLDUP-GRID.**

### 9.1.5.3. HOLDUP GRID DESIGN

Various hold-grid designs were investigated for use in the packed column configuration at Stellenbosch University. The designs were constructed on Autodesk Inventor 2013 and modelled in terms of their open area. A summary of the open area of the various designs are presented in Table 9.7 .

**TABLE 9.7: OPEN AREA GRID MODELLING.**

<b>Perforation plates</b>	<b>Mesh Area(m<sup>2</sup>)</b>	<b>Open Area(m<sup>2</sup>)</b>	<b>% Open Area</b>
20mm Square Perforated Plate	0.0076	0.0324	81.0%
20mm Round Perforated Plate	0.0146	0.0254	63.6%
20mm Hexagonal Perforated Plate	0.0079	0.0321	80.3%
25mm Square Perforated Plate	0.0061	0.0339	84.6%
25 Hexagonal Perforated Plate	0.0059	0.0341	85.2%
30mm Square Perforated Plate	0.0054	0.0346	86.5%
30mm Round Perforated Plate	0.0133	0.0267	66.6%
30 mm Hex Perforated Plate	0.0054	0.0346	86.5%
40 mm Square Perforated Plate	0.0039	0.0361	90.3%
40mm Round Perforated Plate	0.0110	0.0290	72.5%
40mm Hexagonal Perforated Plate	0.0041	0.0359	89.6%
45 mm Square Perforated Plate	0.0039	0.0361	90.3%
50mm Square Perforated Plate	0.0031	0.0369	92.2%

Based on low mechanical strength requirements of the shallow bed, it was decided to continue with the design of a woven mesh hold-up grid. The subsequent design was fabricated for 1/8 of the cost of the hexagonal equivalent, sacrificing only 0.7% of the open area.

### 9.1.5.4. PLC DESIGN

The PLC inherited from the carbon monoxide capturing plant, was indicative of various fundamental mistakes. These mistakes included, incorrectly connected pressure transmitting units and notable mathematician error's in Ladder logic of the vapour mass flow quantification. The combination resulted in the author quoting calibrated venturi friction coefficients in excess of 2. This led to a complete overhaul of the PLC design, reprogramming all of the plant functions from Kritzinger, backdating to the work done by Erasmus in 2002.

The overhaul involved:

- [1] Reprogramming the faulty ladder logic.
- [2] Rescaling of all sensors.
- [3] Adding various safety interlocks.
- [4] Restoring operability to the Erasmus plants.
- [5] Rewiring of the electrical DV board to match SABS standards.

As a result of the size of the coding, the body of this report will refrain from including any of the human machine interface(HMI) and ladder logic data. This is in turn presented in full in the attached CD Appendix. A graphical representation of the plant control screen (one of seventy-two) is presented in Figure 9.5.

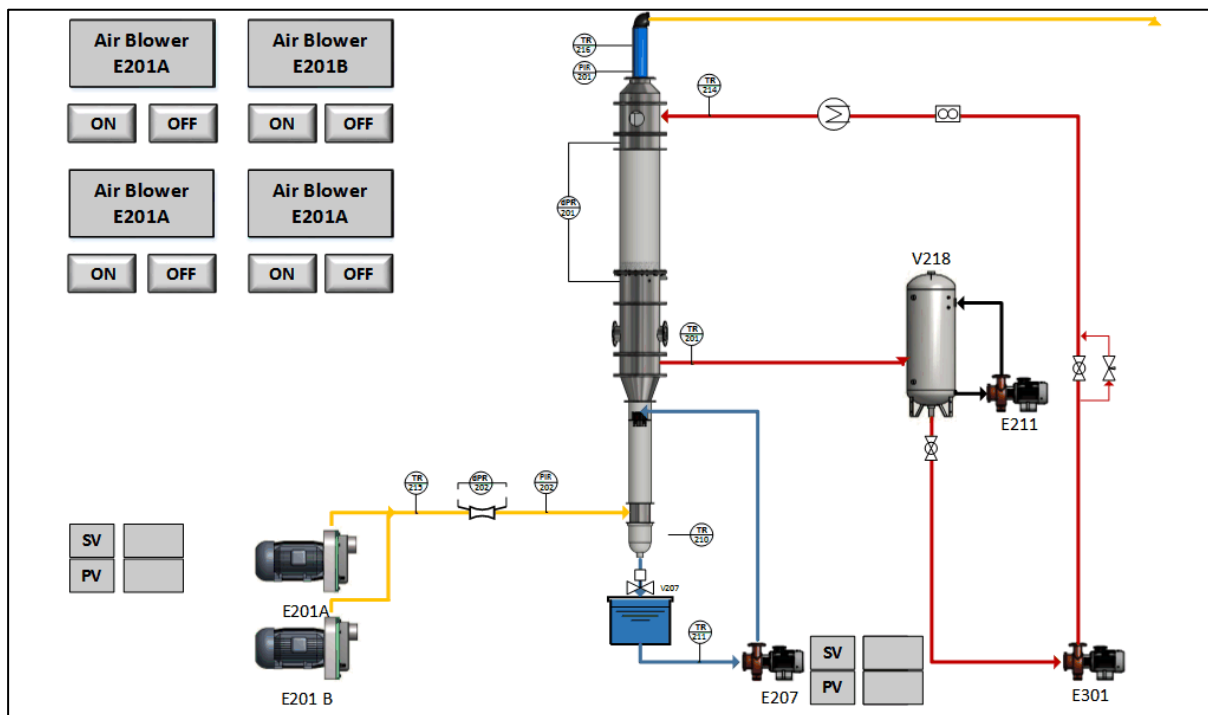


FIGURE 9.5: PLC MAIN SCREEN.

### 9.1.6. PACKED VENTURI CALIBRATION

The venturi used, was calibrated according to method dictated by ISO-5167-1;1991. This was done as discrepancies were found in the mathematical coding used by Kritzinger [20]. Questions were raised as quoted values of friction coefficients unconventionally exceeded 2. The problem was found embedded in the coding, as an arbitrary computation value was used as the reference temperature.

This led to the recalibration by way of pitot tube. Differential pressure readings were collected at variable increments across the flowpath and translated to velocities. This was done for incremental flow rates. Validation of the Pitot-tube was done by way of visual observations from a water manometer. This comparison is presented in Figure 9.6. Deviations were considered to be within the viable ranges as blowers are known to have oscillating pressures.

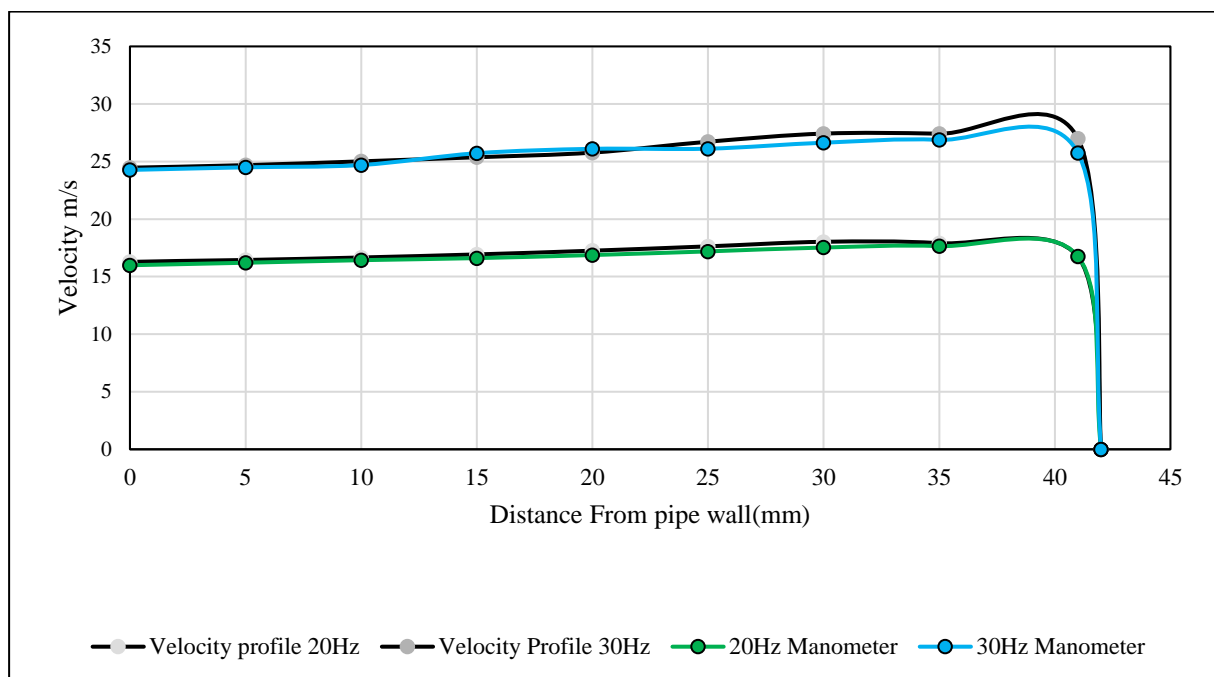


FIGURE 9.6: PITOT TUBE PRESSURE DROP VALIDATION BY WAY OF WATER MANOMETER.

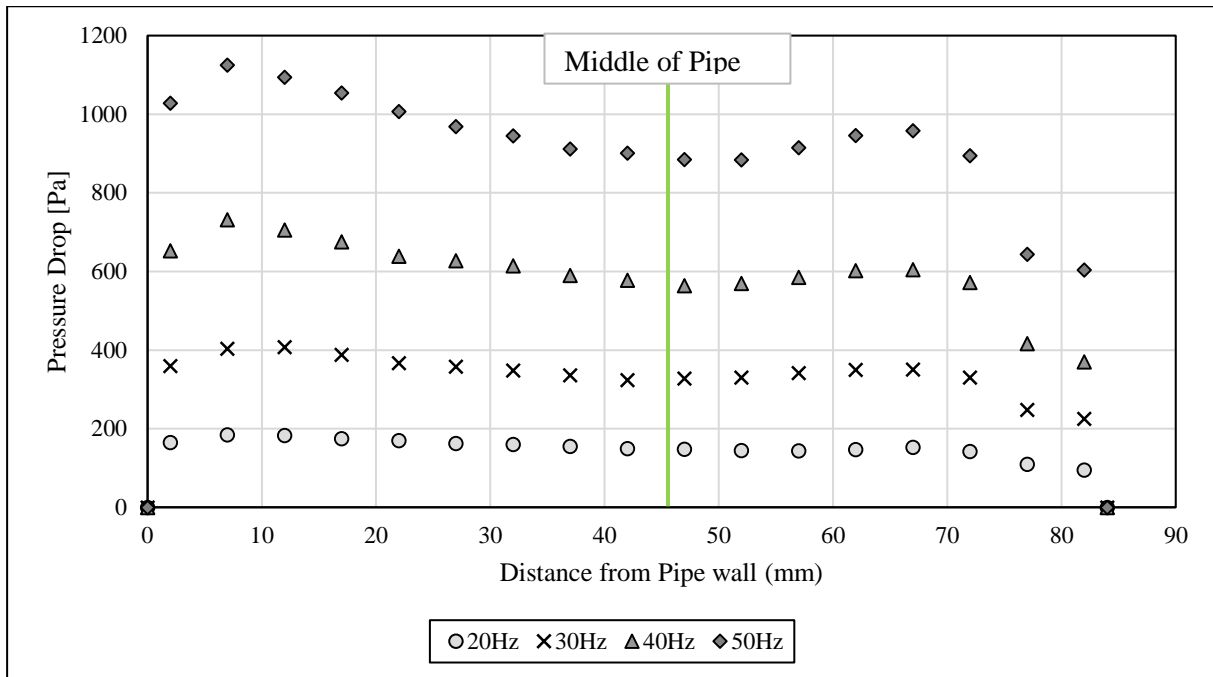


FIGURE 9.7: PRESSURE DROP READINGS ACROSS A FULL PIPE SECTION.

The report will refrain from going into full detail on the procedure of calibration, as it is presented in the ISO standards. However broadly, it was as opted to integrate across the flow rates of the full pipe-diameter (Figure 9.7), obtaining a volume flow rates and solving Equations 9.3 to 9.8 for the friction coefficient (Cd).

$$\dot{m} = \frac{C_d}{\sqrt{1-\beta^4}} * \varepsilon_2 * \left(\frac{\pi}{4} * d_{throat}^2\right) * \sqrt{2 * (P_2 - P_1) * \rho_{fluid}} \quad 9.3$$

where

$$\varepsilon_2 = \varepsilon_1 * \sqrt{1 + \frac{P_2 - P_1}{P_1}} \quad 9.4$$

$$Q_{fluid} = \frac{\dot{m}}{\rho_{fluid}} \quad 9.5$$

$$\varepsilon_1 = \left[ \left( \kappa * \frac{\tau^{\frac{2}{\kappa}}}{\kappa - 1} \right) * \left( \frac{1 - \beta^4}{1 - \beta^4 \tau^{\frac{2}{\kappa}}} \right) * \left( \frac{1 - \tau^{(\kappa-1)/\kappa}}{1 - \tau} \right) \right]^{0.5} \quad 9.6$$

and where

$$\tau = \frac{P_2}{P_1} \quad 9.7$$

$$\beta = \frac{d_{throat}}{d_{pipe}} \quad 9.8$$

$\kappa = \text{sientropic exponent ; Air} = 1.4$



TABLE 9.8: VENTURI FRICTION COEFFICIENT.

Hz	Volume Flow rate according to Pitot $\text{m}^3.\text{s}^{-1}$	Density $\text{kg}.\text{m}^{-3}$	Mass Flow Pitot $\text{kg}.\text{h}^{-1}$	PLC $\text{kg}.\text{h}^{-1}$	$\Delta$	Cd
20.00	0.09	1.16	366.64	366.64	0.00	0.98
30.00	0.13	1.17	558.56	558.56	0.00	0.98
40.00	0.17	1.18	738.11	738.11	0.00	0.97
50.00	0.22	1.19	930.37	930.37	0.00	0.96

The result of the solver algorithm is presented in Table 9.8. All values considered, it was decided to use a Cd of 0.98.

### 9.1.7. BED PRESSURE DROP VALIDATION

As all the sensors were rescaled to the correct ranges, it was decided to validate the pressure measurement equipment against a water manometer. The results are presented in Figure 9.8. The illustrated error bars are used to indicate the oscillations seen in the manometer.

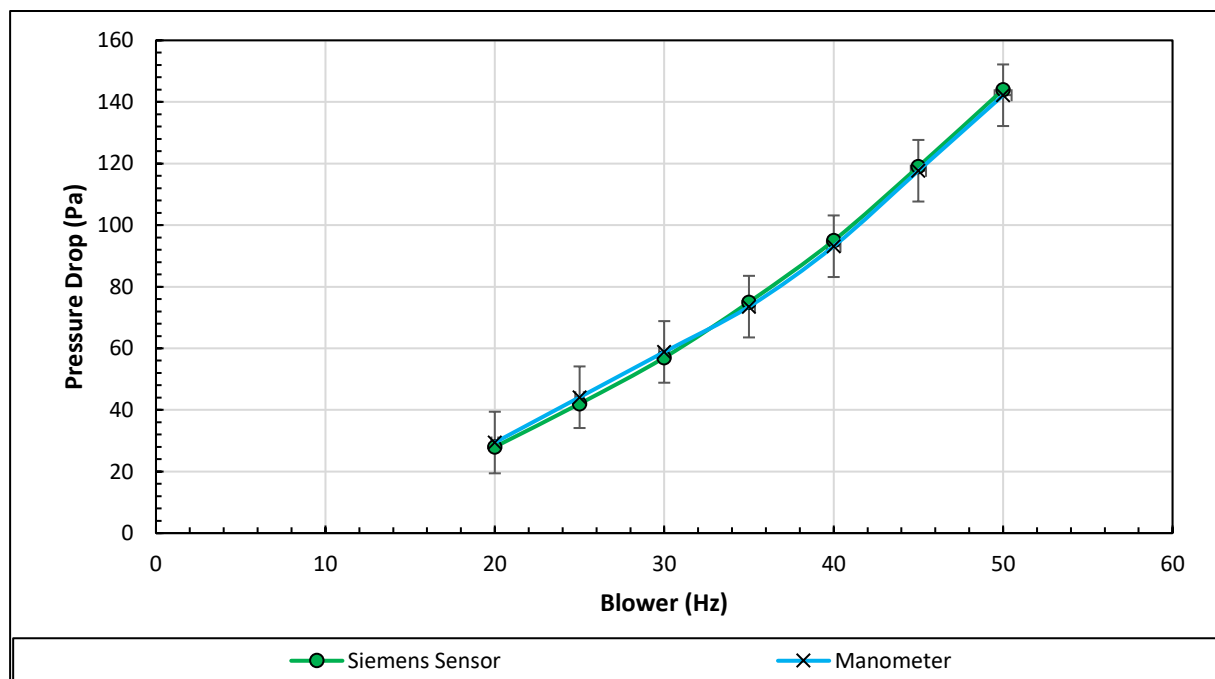


FIGURE 9.8: BED PRESSURE DROP VALIDATION.

## 9.1.8. UV QUANTIFICATION

### 9.1.8.1. CALIBRATION

The UV-spectrophotometer was calibrated by way of serial dilution. Two independent serial dilutions were conducted for each flow cell, to mitigate scatter. The acceptable accuracy limit was set as 98%. The aforementioned procedure was repeated 12 times, once every fortnight to account for experimental drift. Due to the large number of the graphs, the exact combination of experimental data and calibration curves, are presented in the attached CD Appendix. An example of the calibration curves generated on 29 May 2016, is presented in Figures 9.9 and 9.10.

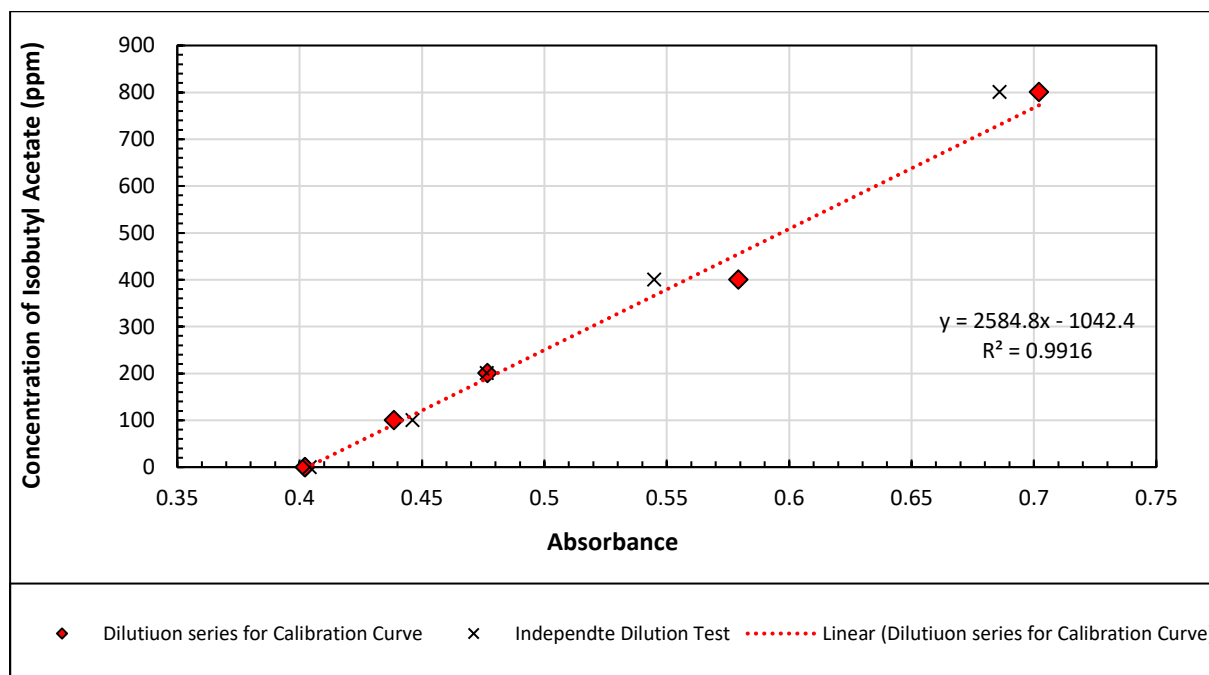


FIGURE 9.9: CALIBRATION CURVE FOR CELL 1.

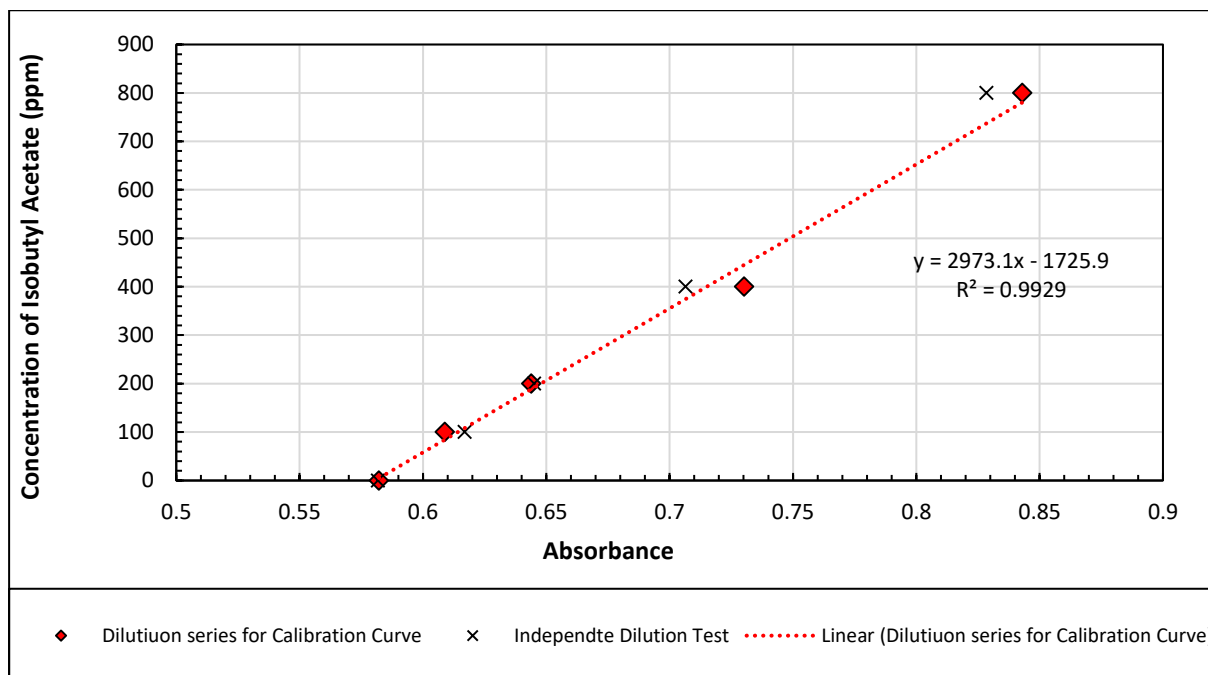


FIGURE 9.10: CALIBRATION CURVE FOR CELL 2.

An alternative quartz cuvette was used in setting the offset of the curves. This was done so that once every hour, the curves could be readjusted.

#### 9.1.8.2. TEMPERATURE CALIBRATION

Temperature variations in the solvent solution was found to attribute to addition compositional errors. This was migrated through the use of temperature compensation curves presented below. The adjustments were made prior to quantification on the absorbance measurement form the instrument.

9.1.8.2.1. INLET CONCENTRATION FLOW CELL MEASURED IN THE SUMP

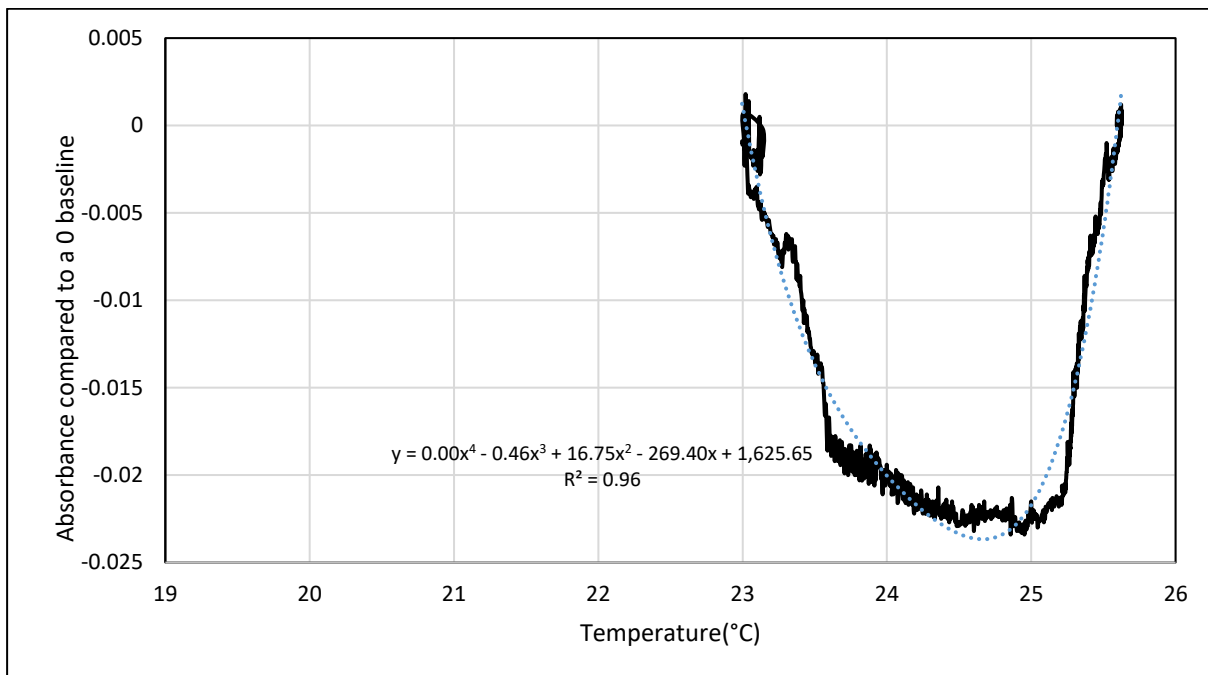


FIGURE 9.11: INLET CONCENTRATION; WATER BASELINE CORRECTION FOR 25.6°C-23°C.

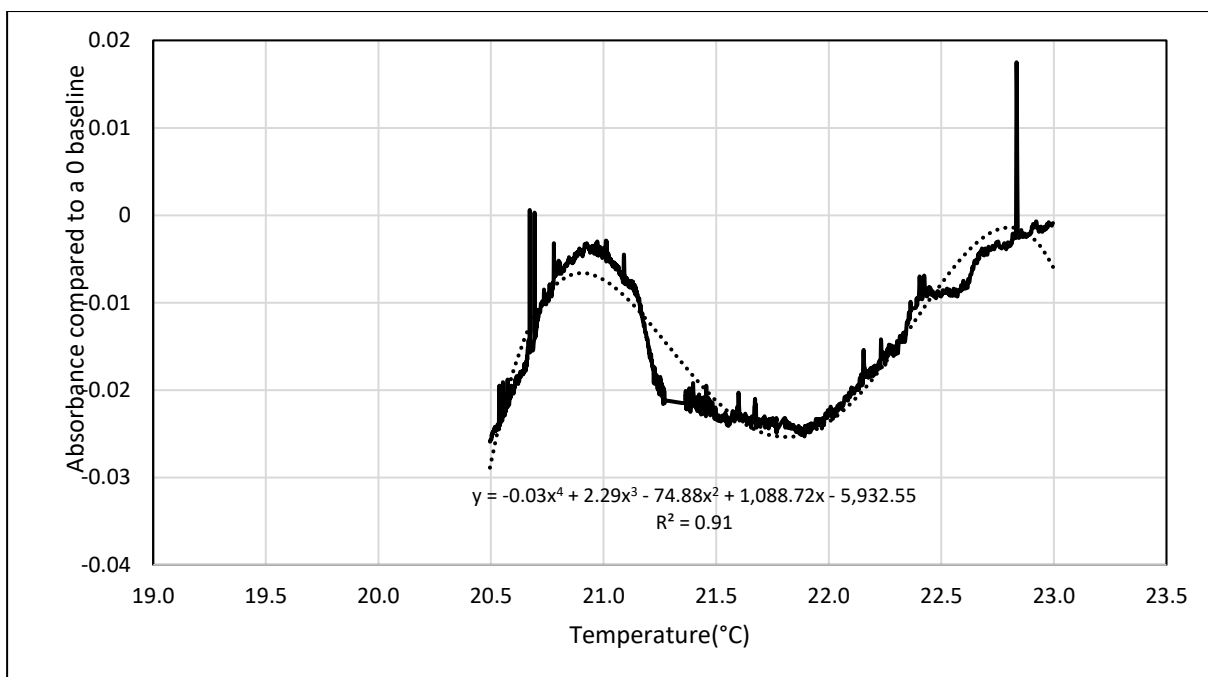


FIGURE 9.12: INLET CONCENTRATION: WATER BASELINE CORRECTION FOR 23°C-20.5°C.

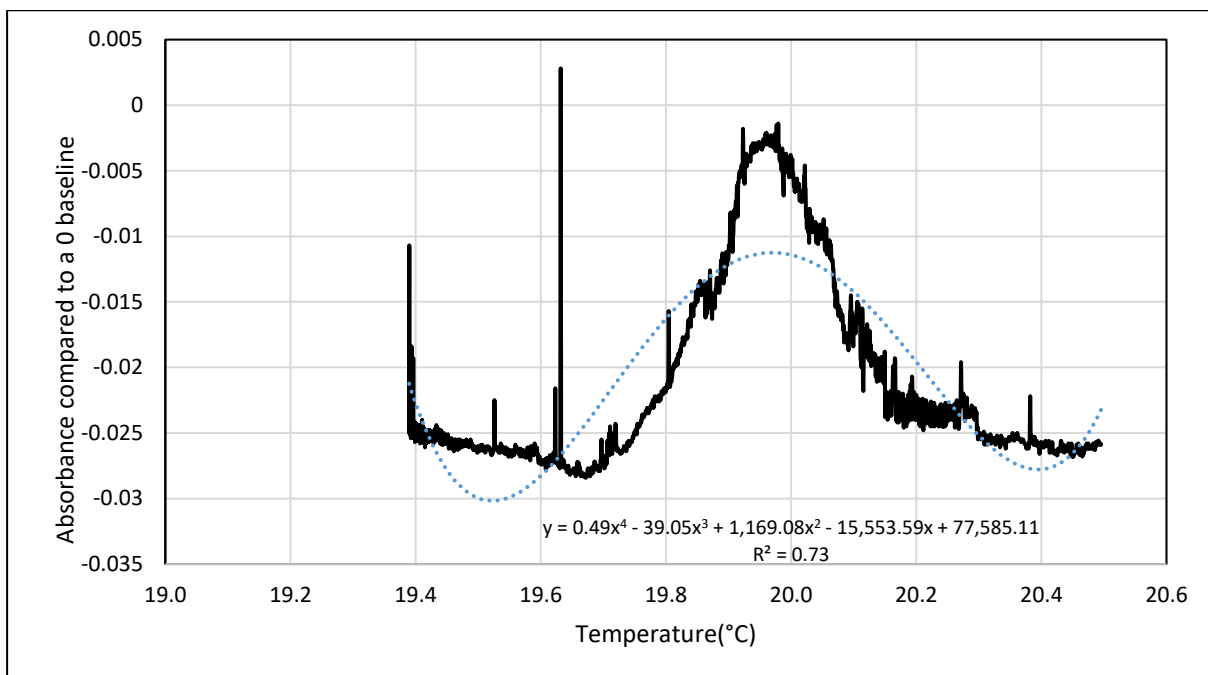


Figure 9.13: Inlet concentration: water baseline correction for 20.5°C-19°C.

#### 9.1.8.2.2. OUTLET CONCENTRATION FLOW CELL MEASURED 50MM BELOW THE PACKED BED

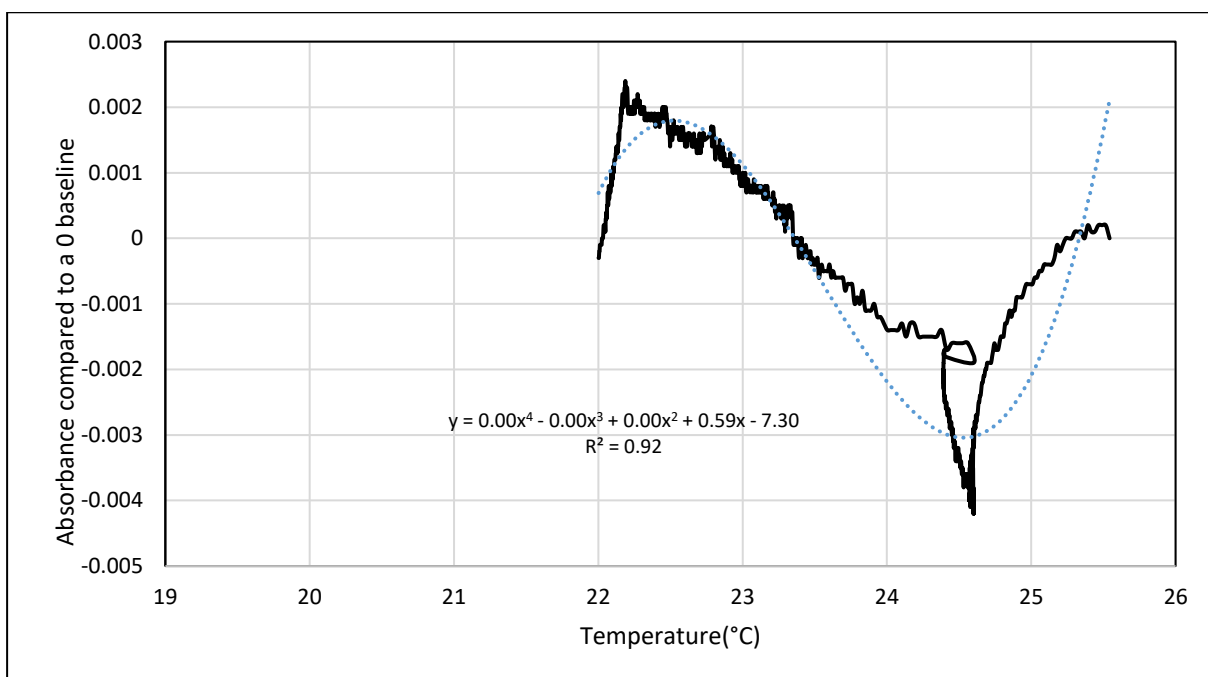


FIGURE 9.14: OUTLET CONCENTRATION: WATER BASELINE CORRECTION FOR 25°C-22°C.

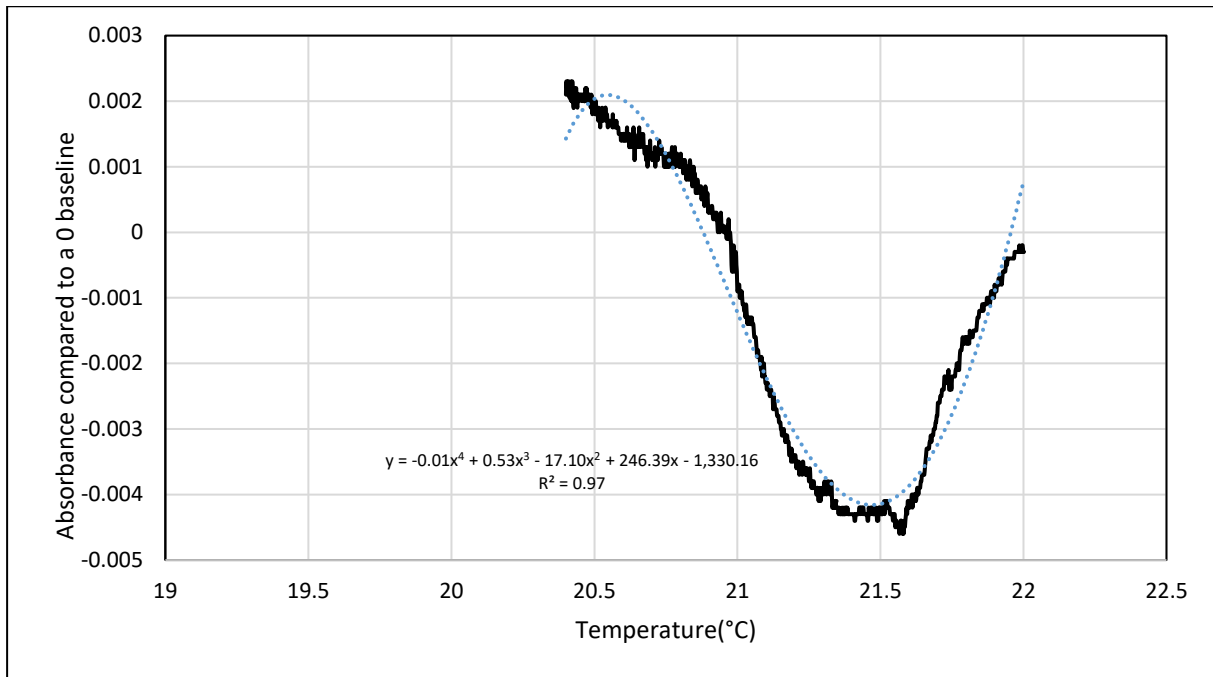


FIGURE 9.15: OUTLET CONCENTRATION: WATER BASELINE CORRECTION FOR 22°C-20.4°C.

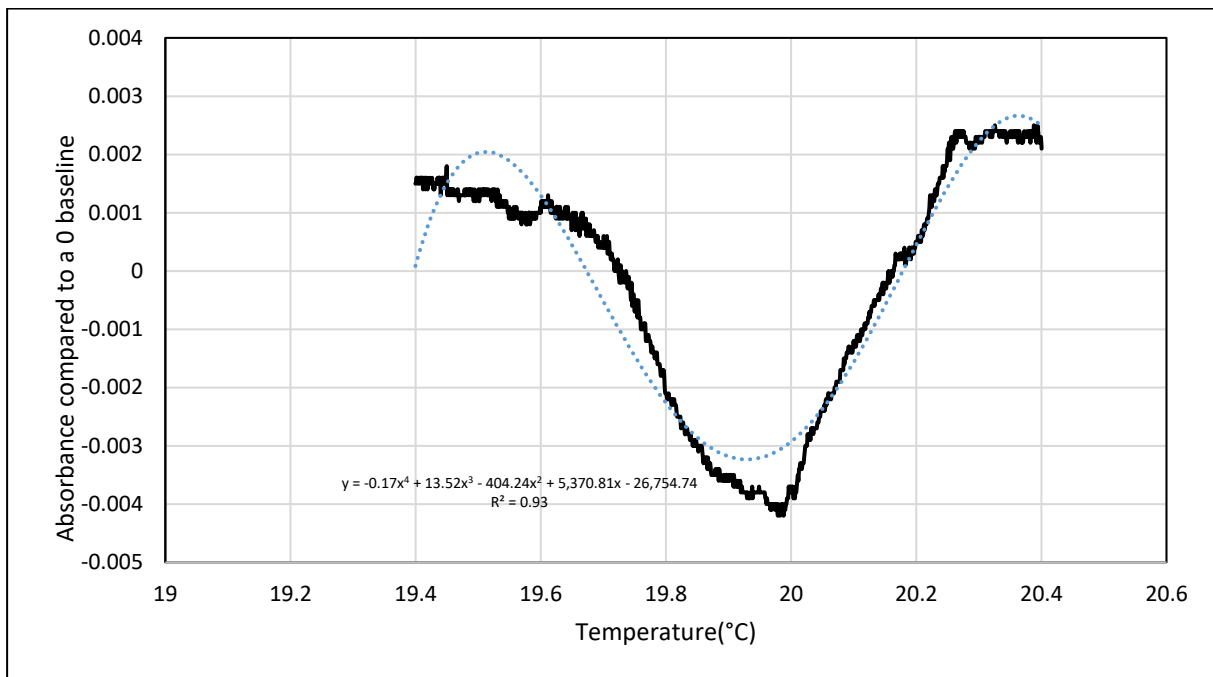


FIGURE 9.16: OUTLET CONCENTRATION: WATER BASELINE CORRECTION FOR 20.4°C-19.4°C.

### 9.1.9. PACKED COLUMN RESULTS IN VAPOUR FLOW FACTORS

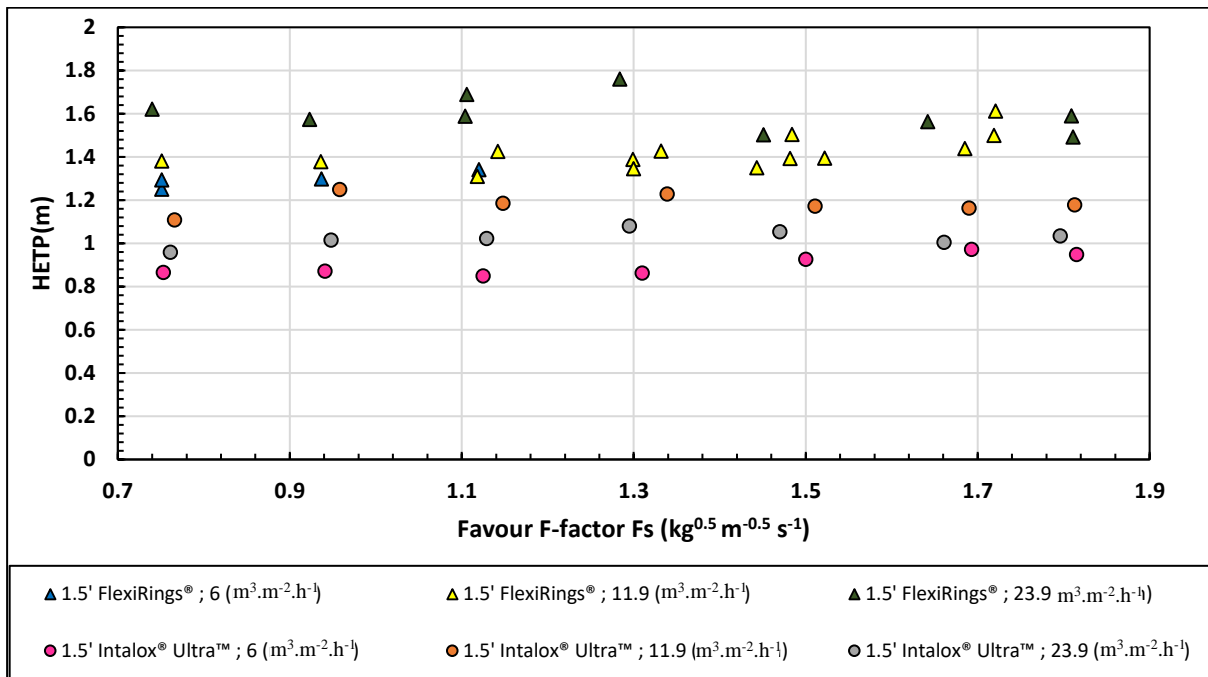


FIGURE 9.17: FIGURE 7.4 IN TERMS OF VAPOUR FLOW FACTORS

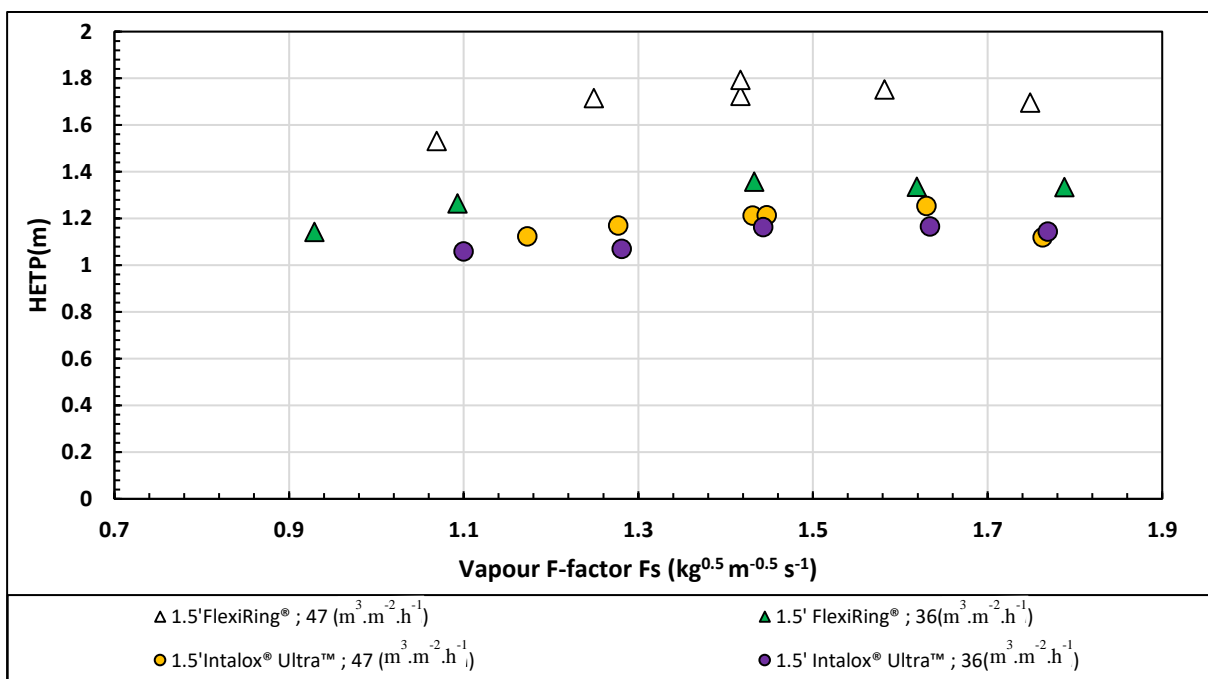


FIGURE 9.18: FIGURE 7.5 IN TERMS OF VAPOUR FLOW FACTORS

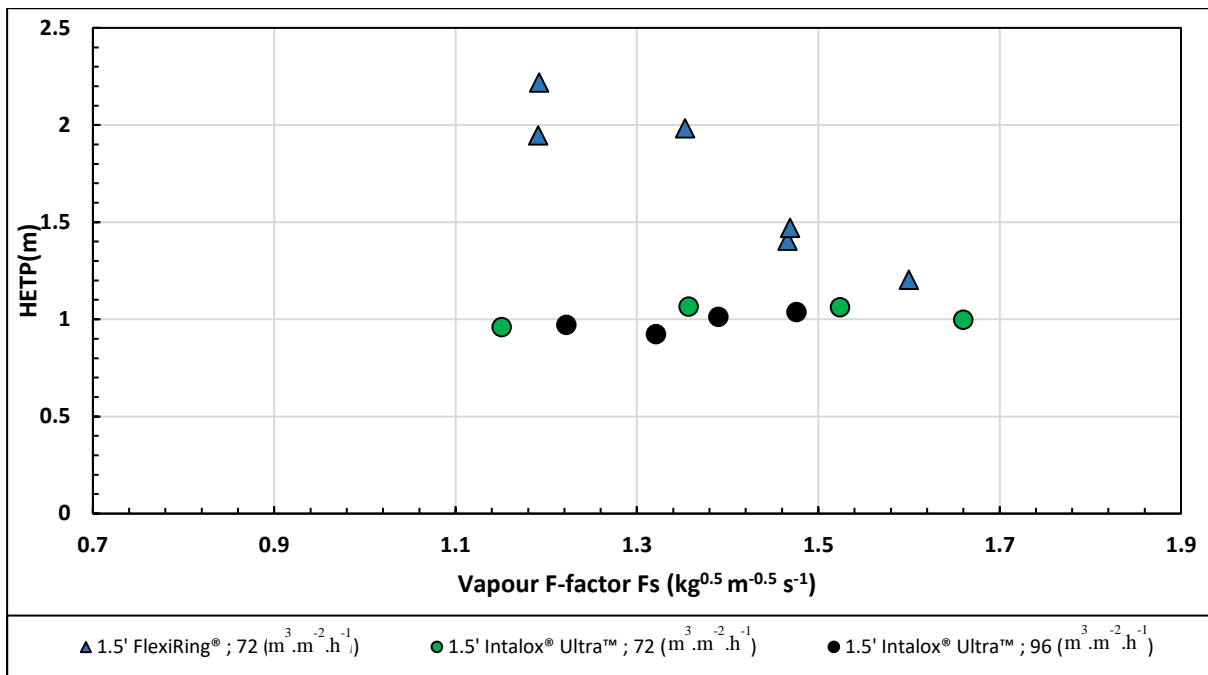


FIGURE 9.19: FIGURE 7.6 IN TERMS OF VAPOUR FLOW FACTORS

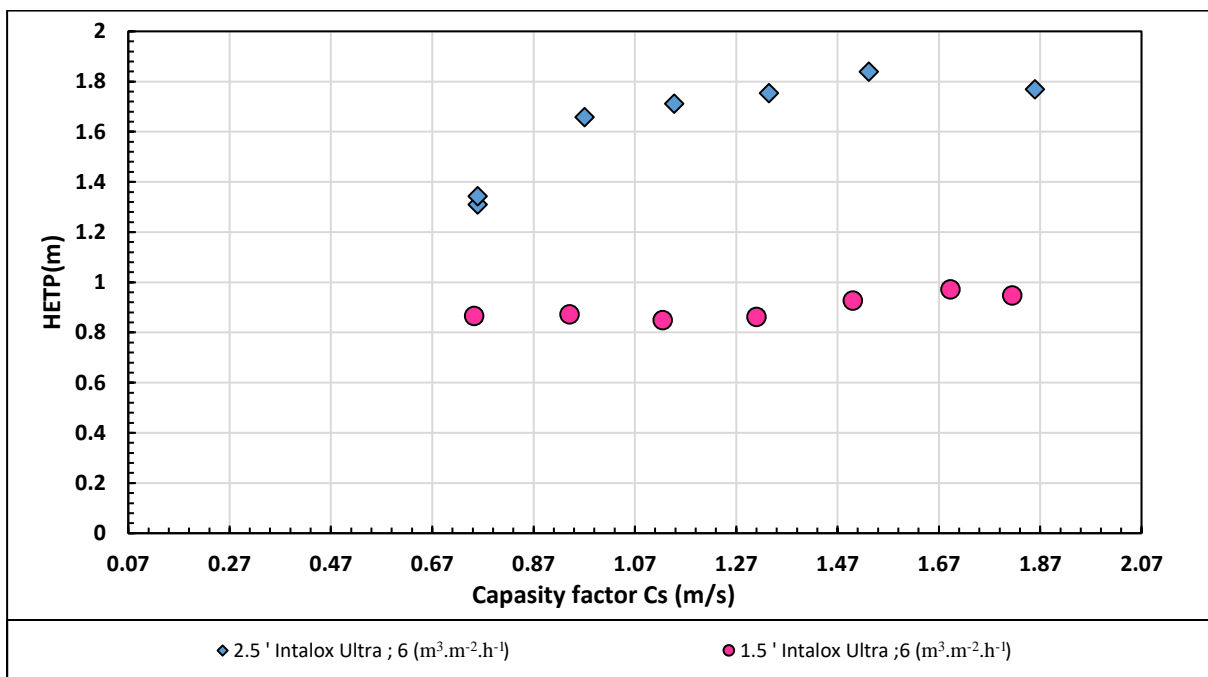


FIGURE 9.20: FIGURE 7.7 IN TERMS OF VAPOUR FLOW FACTORS



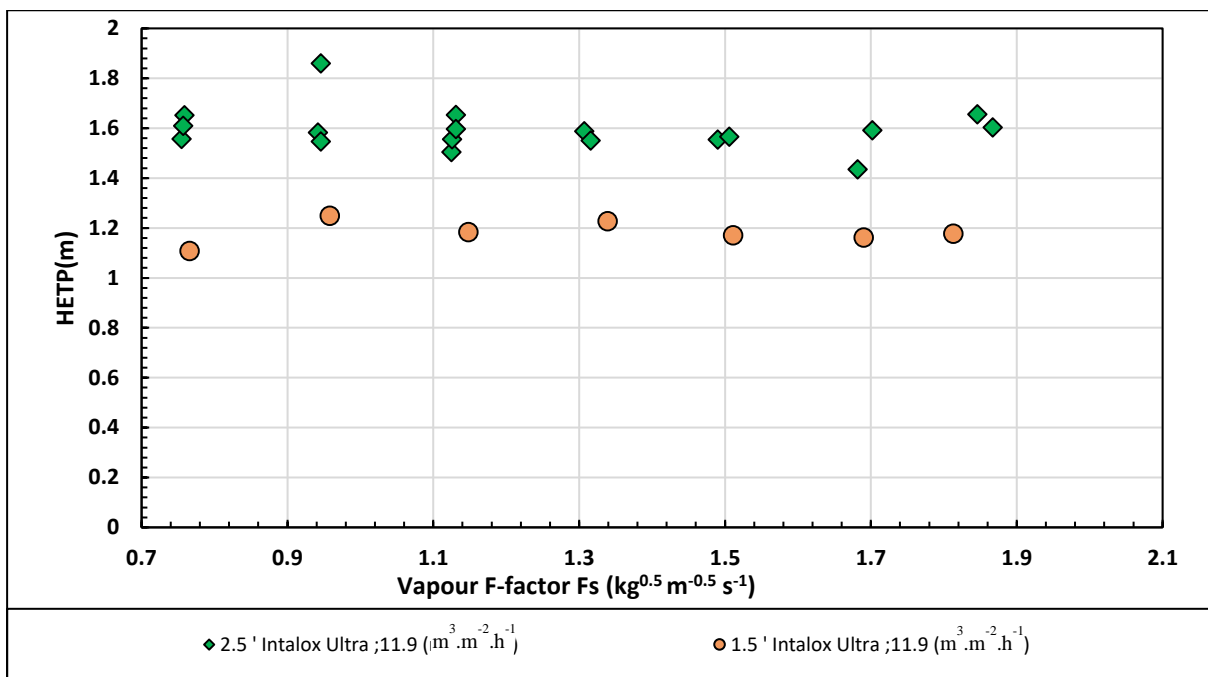


FIGURE 9.21: FIGURE 7.8 IN TERMS OF VAPOUR FLOW FACTORS

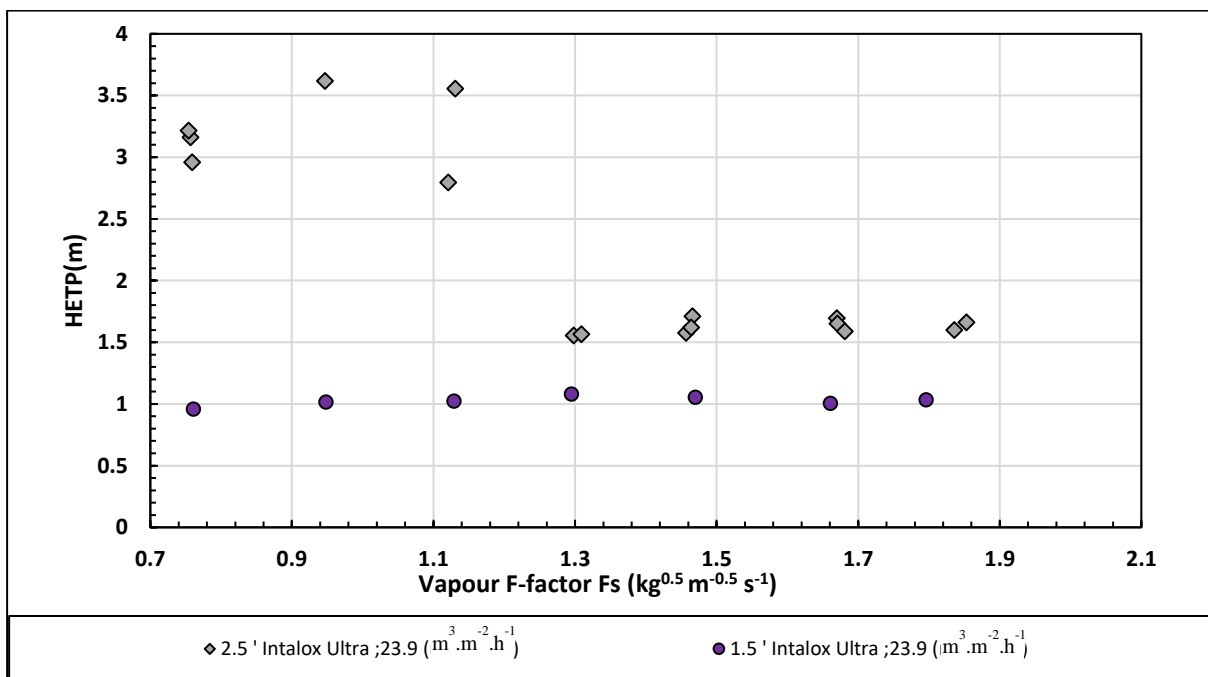


FIGURE 9.22: FIGURE 7.9 IN TERMS OF VAPOUR FLOW FACTORS

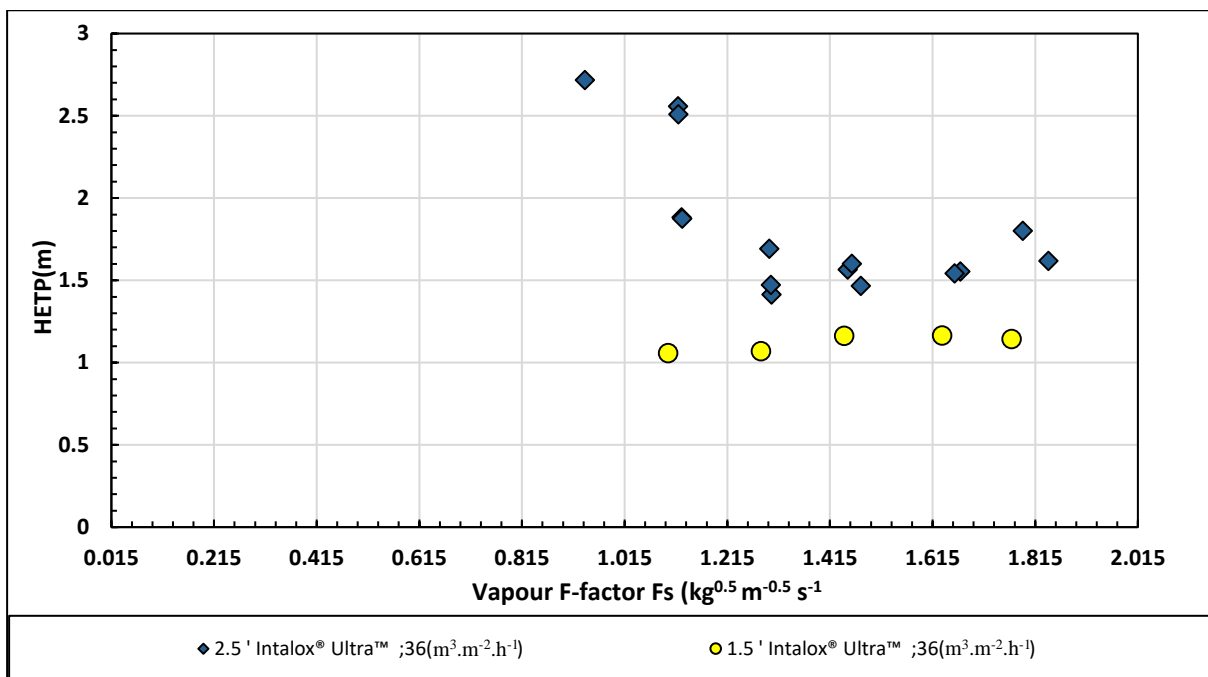


FIGURE 9.23: FIGURE 7.10 IN TERMS OF VAPOUR FLOW FACTORS

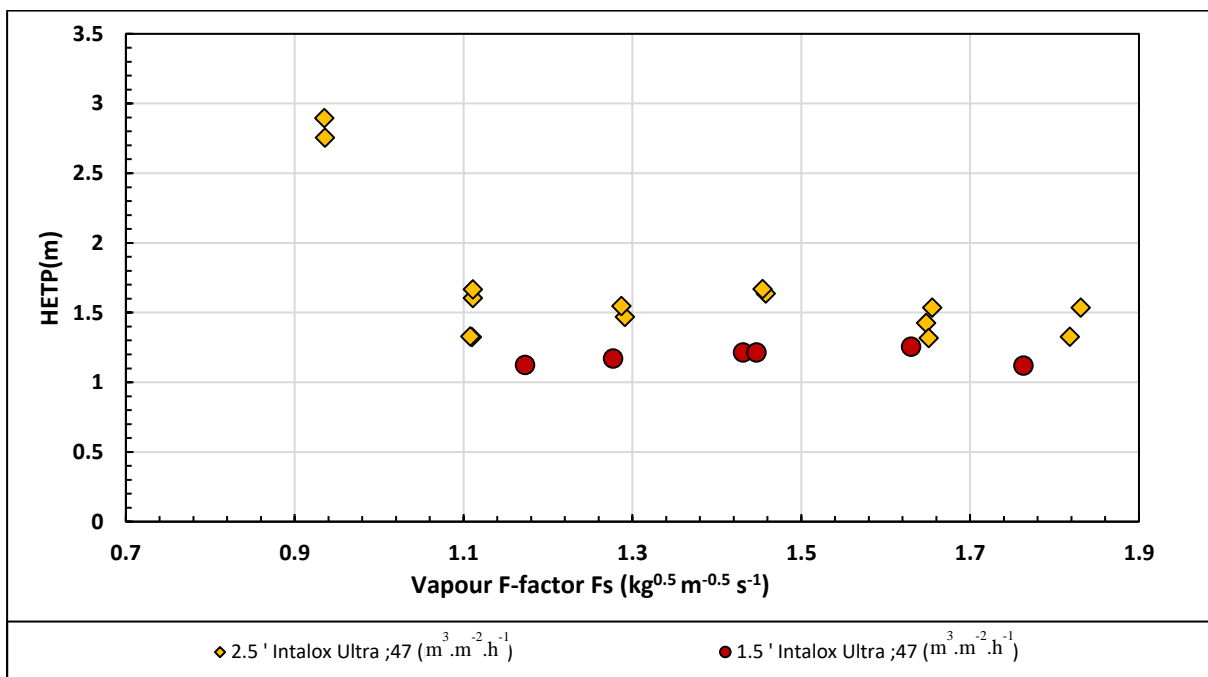


FIGURE 9.24: FIGURE 7.11 IN TERMS OF VAPOUR FLOW FACTORS

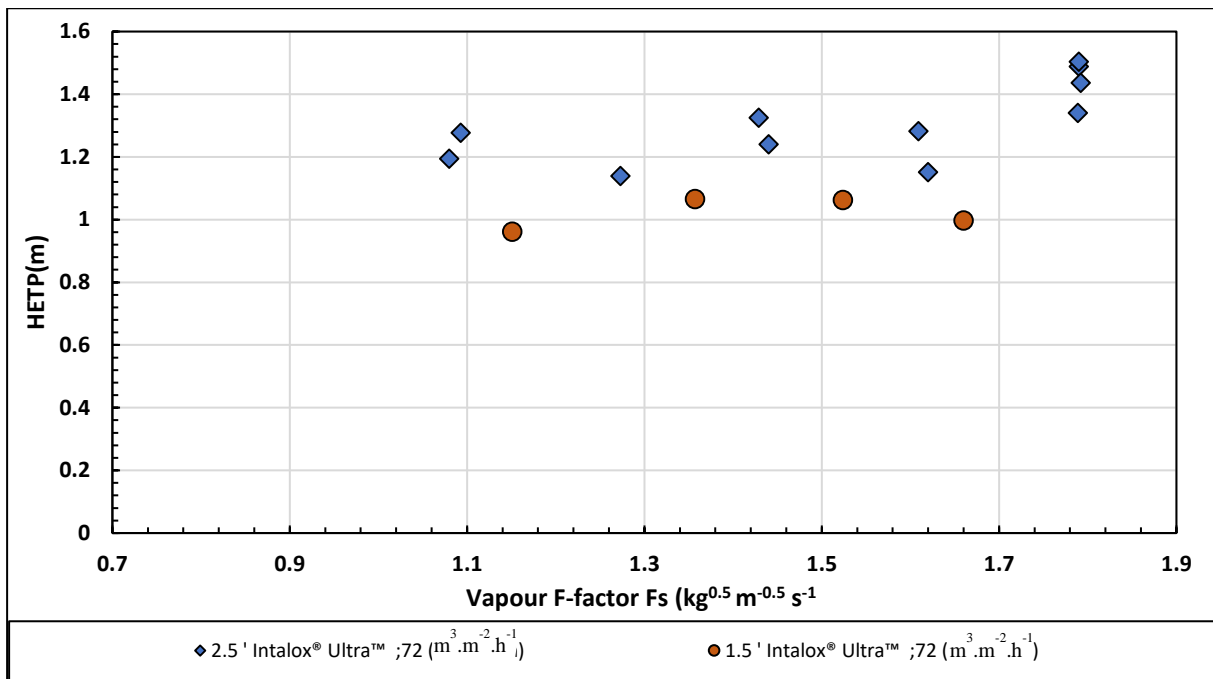


FIGURE 9.25: FIGURE 7.12 IN TERMS OF VAPOUR FLOW FACTORS

## 9.2. APPENDIX B: TRAY COLUMNS

### 9.2.1. CONCENTRATION PROFILES BELOW THE TEST TRAY

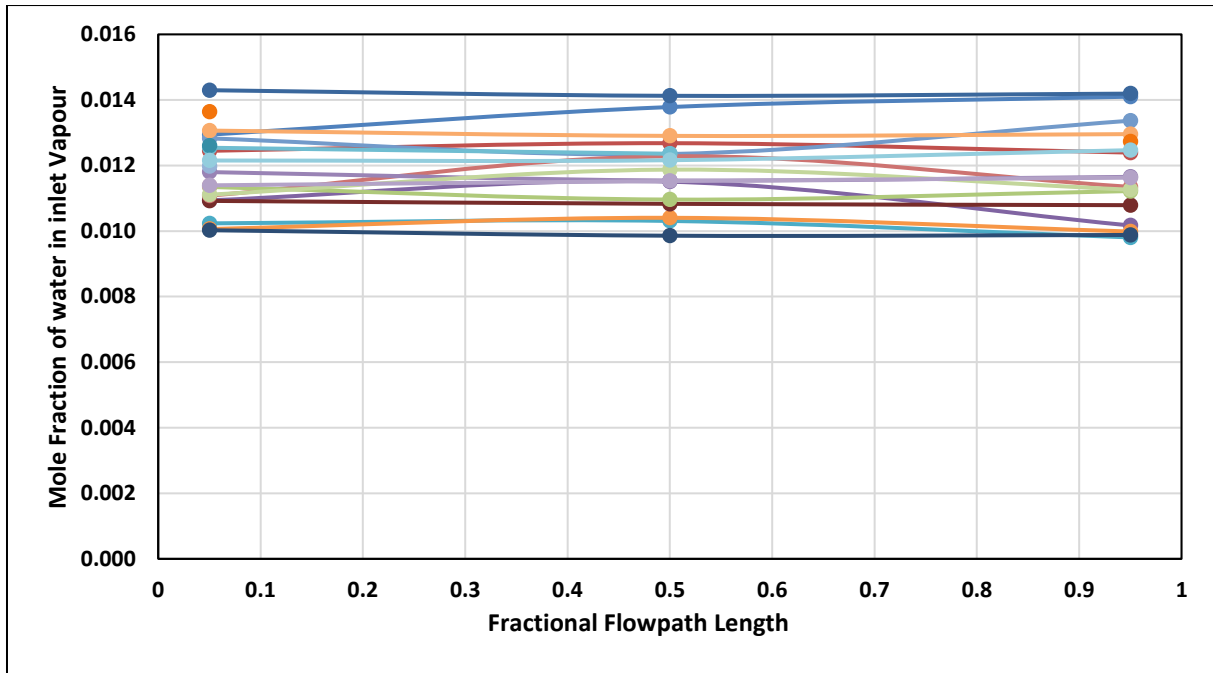


FIGURE 9.26: CONCENTRATION PROFILE BELOW THE TEST TRAY

### 9.2.2. TRAY COLUMN DESIGN: BUBBLE PROMOTOR SCHEMATIC

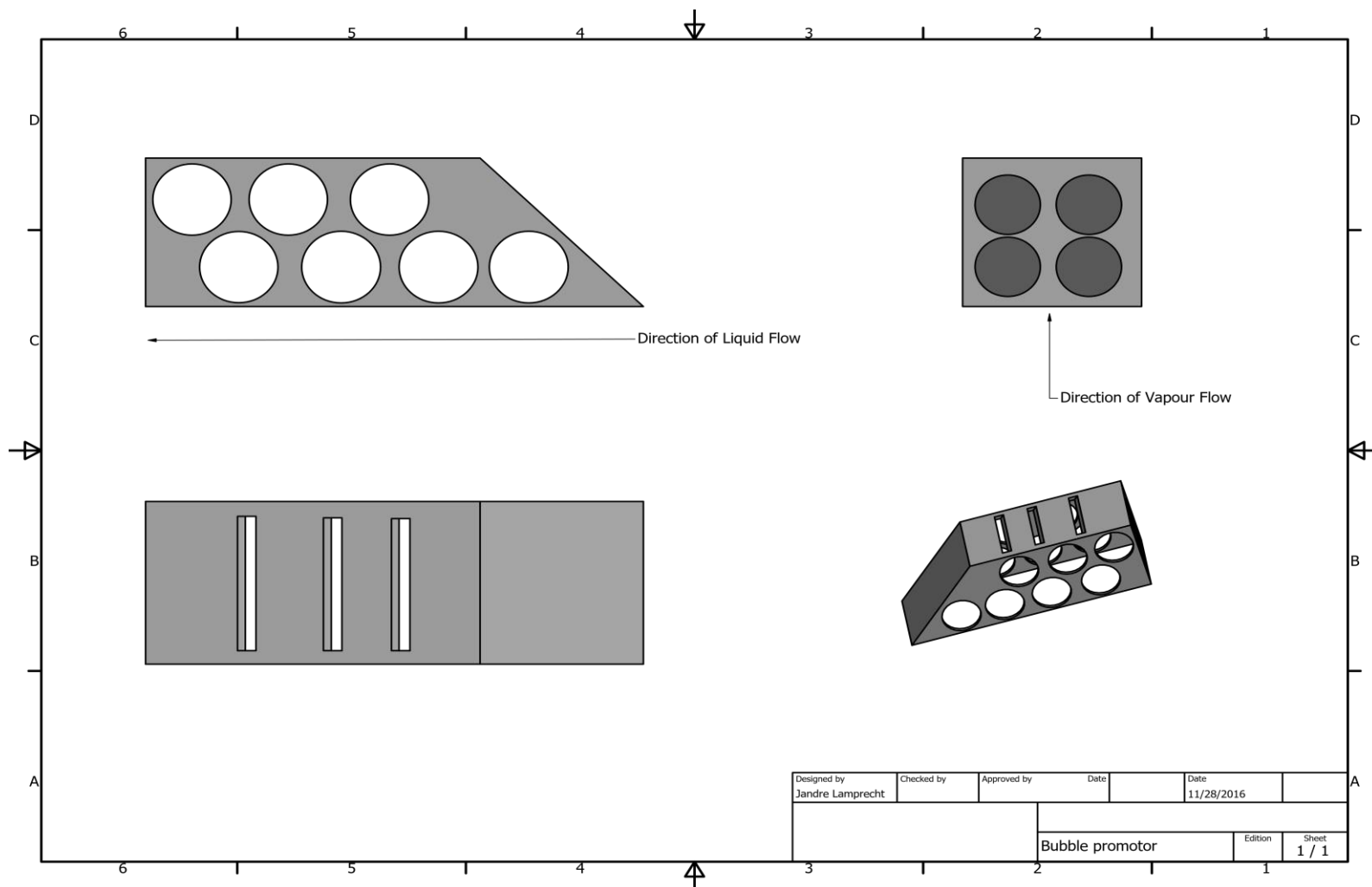


FIGURE 9.27: EXAMPLE OF A BUBBLE PROMOTOR

### 9.3. APPENDIX C: SUPPLEMENTARY CONSIDERATIONS

#### 9.3.1. HOFHUIS AND ZUIDERWEG [6] GRAPHICAL ILLUSTRATION (REDRAWN FROM ORIGINAL PAPER)

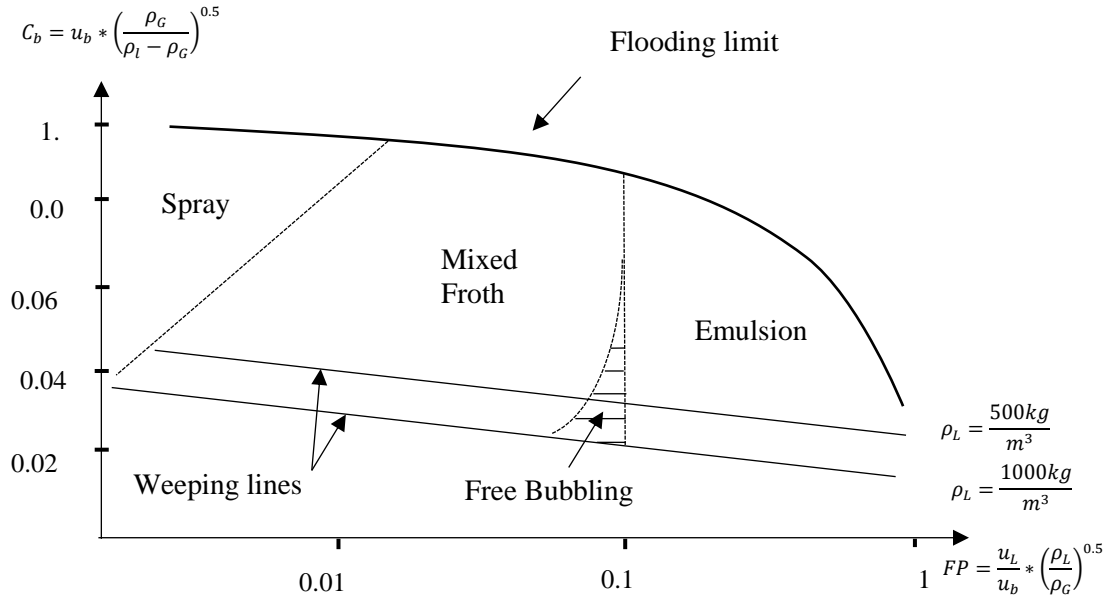


FIGURE 9.28: TRAY FLOW REGIMES (REDRAWN HOFHUIS AND ZUIDERWEG [6])

### 9.3.2. THEORETICAL CONSIDERATIONS RELATED TO THE MASS TRANSFER COEFFICIENT

TABLE 9.9: THEORETICAL EVALUATION OF THE LIQUID PHASE MASS TRANSFER COEFFICIENT.

Theory	Basis	Approximation	Liquid phase mass transfer coefficient	Reference
<b>Two film</b>	Molecular diffusion through a stagnant boundary layer	$D_{i,L} \frac{d^2 C_i}{dx^2} = 0$	$D_{i,L} \frac{d^2 C_i}{dx^2} = 0$	[10, 22]
<b>Penetration</b>	Non-steady state approximation. Diffusion into an infinite depth of fluid. Elements are expected to spend equal amounts of time at the phase boundary.	$D_{i,L} \frac{d^2 C_i}{dx^2} = 0$	$k_L = 2 \sqrt{\frac{D_{i,L}}{\pi * t_c}}$	[78, 22]
<b>Surface renewal</b>	This approach rejects the theory that all elements spend equal time at the phase boundary. Provided a more realistic model as it rejects perfect mixing in the bulk liquid		$k_L = \sqrt{D_{i,L} * s}$ $s = 0.115 Re_L^{1.678}$	[10, 22]
<b>Eddie diffusivity</b>	Molecular diffusion is expected to dominate with Eddie back mixing implemented in the bulk phase	$\frac{d}{dx} [(D_{i,L} + e_d x^2) \frac{dC_i}{dt}] = 0$	$k_L = \frac{2}{\pi} \sqrt{D_{i,L} e_d}$	[51, 10, 22]

### 9.3.3. TRAY COLUMN $K_{LA}$ CORRELATIONS

TABLE 9.10: CORRELATIONS FOR THE PREDICTION OF  $K_{LA}$  IN TRAY COLUMNS.

Source	Date	Equations	Equation ID
AIChE [16]	1958	Sieve Tray $k_L a = 197 * D_{iL}^{0.5} * (0.4 * F + 0.17)$	9.9
		<b>Bubble Caps</b> $NTU_L' = 2.03 * 10^4 (0.15 + 0.213 * F) * t_L * L * D_{iL}^{0.5}$ Where $t_L = 1.2 * h_{cl} * W/Z$	
Krishnamurthy and Taylor [16]	1984	$h_{cl} = 0.0254(1.65 + 7.48H_w + 80.5L_F - 0.533F)$	9.10

With similar reasoning, as provided in the case of packed columns, the above-mentioned correlations are expected to provide doubtful predictive accuracy. This opinion is further substantiated, as no provisions are included to distinguish between the relevant flow regimes, as discussed in Chapter 1. Following a similar thought patterns as presented earlier, it was opted to evaluate the respective interfacial area and liquid phase mass transfer coefficients separately, in a bid to enhance extrapolated predictive performance.